

IAEA TECDOC SERIES

IAEA-TECDOC-1722

Review of Seismic Evaluation Methodologies for Nuclear Power Plants Based on a Benchmark Exercise



IAEA

International Atomic Energy Agency

IAEA SAFETY STANDARDS AND RELATED PUBLICATIONS

IAEA SAFETY STANDARDS

Under the terms of Article III of its Statute, the IAEA is authorized to establish or adopt standards of safety for protection of health and minimization of danger to life and property, and to provide for the application of these standards.

The publications by means of which the IAEA establishes standards are issued in the **IAEA Safety Standards Series**. This series covers nuclear safety, radiation safety, transport safety and waste safety. The publication categories in the series are **Safety Fundamentals**, **Safety Requirements** and **Safety Guides**.

Information on the IAEA's safety standards programme is available at the IAEA Internet site

<http://www-ns.iaea.org/standards/>

The site provides the texts in English of published and draft safety standards. The texts of safety standards issued in Arabic, Chinese, French, Russian and Spanish, the IAEA Safety Glossary and a status report for safety standards under development are also available. For further information, please contact the IAEA at PO Box 100, 1400 Vienna, Austria.

All users of IAEA safety standards are invited to inform the IAEA of experience in their use (e.g. as a basis for national regulations, for safety reviews and for training courses) for the purpose of ensuring that they continue to meet users' needs. Information may be provided via the IAEA Internet site or by post, as above, or by email to Official.Mail@iaea.org.

RELATED PUBLICATIONS

The IAEA provides for the application of the standards and, under the terms of Articles III and VIII.C of its Statute, makes available and fosters the exchange of information relating to peaceful nuclear activities and serves as an intermediary among its Member States for this purpose.

Reports on safety and protection in nuclear activities are issued as **Safety Reports**, which provide practical examples and detailed methods that can be used in support of the safety standards.

Other safety related IAEA publications are issued as **Radiological Assessment Reports**, the International Nuclear Safety Group's **INSAG Reports**, **Technical Reports** and **TECDOCs**. The IAEA also issues reports on radiological accidents, training manuals and practical manuals, and other special safety related publications.

Security related publications are issued in the **IAEA Nuclear Security Series**.

The **IAEA Nuclear Energy Series** consists of reports designed to encourage and assist research on, and development and practical application of, nuclear energy for peaceful uses. The information is presented in guides, reports on the status of technology and advances, and best practices for peaceful uses of nuclear energy. The series complements the IAEA's safety standards, and provides detailed guidance, experience, good practices and examples in the areas of nuclear power, the nuclear fuel cycle, radioactive waste management and decommissioning.

REVIEW OF
SEISMIC EVALUATION METHODOLOGIES FOR
NUCLEAR POWER PLANTS
BASED ON A BENCHMARK EXERCISE

The following States are Members of the International Atomic Energy Agency:

AFGHANISTAN	GUATEMALA	PANAMA
ALBANIA	HAITI	PAPUA NEW GUINEA
ALGERIA	HOLY SEE	PARAGUAY
ANGOLA	HONDURAS	PERU
ARGENTINA	HUNGARY	PHILIPPINES
ARMENIA	ICELAND	POLAND
AUSTRALIA	INDIA	PORTUGAL
AUSTRIA	INDONESIA	QATAR
AZERBAIJAN	IRAN, ISLAMIC REPUBLIC OF	REPUBLIC OF MOLDOVA
BAHRAIN	IRAQ	ROMANIA
BANGLADESH	IRELAND	RUSSIAN FEDERATION
BELARUS	ISRAEL	RWANDA
BELGIUM	ITALY	SAN MARINO
BELIZE	JAMAICA	SAUDI ARABIA
BENIN	JAPAN	SENEGAL
BOLIVIA	JORDAN	SERBIA
BOSNIA AND HERZEGOVINA	KAZAKHSTAN	SEYCHELLES
BOTSWANA	KENYA	SIERRA LEONE
BRAZIL	KOREA, REPUBLIC OF	SINGAPORE
BULGARIA	KUWAIT	SLOVAKIA
BURKINA FASO	KYRGYZSTAN	SLOVENIA
BURUNDI	LAO PEOPLE'S DEMOCRATIC REPUBLIC	SOUTH AFRICA
CAMBODIA	LATVIA	SPAIN
CAMEROON	LEBANON	SRI LANKA
CANADA	LESOTHO	SUDAN
CENTRAL AFRICAN REPUBLIC	LIBERIA	SWAZILAND
CHAD	LIBYA	SWEDEN
CHILE	LIECHTENSTEIN	SWITZERLAND
CHINA	LITHUANIA	SYRIAN ARAB REPUBLIC
COLOMBIA	LUXEMBOURG	TAJIKISTAN
CONGO	MADAGASCAR	THAILAND
COSTA RICA	MALAWI	THE FORMER YUGOSLAV REPUBLIC OF MACEDONIA
CÔTE D'IVOIRE	MALAYSIA	TOGO
CROATIA	MALI	TRINIDAD AND TOBAGO
CUBA	MALTA	TUNISIA
CYPRUS	MARSHALL ISLANDS	TURKEY
CZECH REPUBLIC	MAURITANIA	UGANDA
DEMOCRATIC REPUBLIC OF THE CONGO	MAURITIUS	UKRAINE
DENMARK	MEXICO	UNITED ARAB EMIRATES
DOMINICA	MONACO	UNITED KINGDOM OF GREAT BRITAIN AND NORTHERN IRELAND
DOMINICAN REPUBLIC	MONGOLIA	UNITED REPUBLIC OF TANZANIA
ECUADOR	MONTENEGRO	UNITED STATES OF AMERICA
EGYPT	MOROCCO	URUGUAY
EL SALVADOR	MOZAMBIQUE	UZBEKISTAN
ERITREA	MYANMAR	VENEZUELA
ESTONIA	NAMIBIA	VIET NAM
ETHIOPIA	NEPAL	YEMEN
FIJI	NETHERLANDS	ZAMBIA
FINLAND	NEW ZEALAND	ZIMBABWE
FRANCE	NICARAGUA	
GABON	NIGER	
GEORGIA	NIGERIA	
GERMANY	NORWAY	
GHANA	OMAN	
GREECE	PAKISTAN	
	PALAU	

The Agency's Statute was approved on 23 October 1956 by the Conference on the Statute of the IAEA held at United Nations Headquarters, New York; it entered into force on 29 July 1957. The Headquarters of the Agency are situated in Vienna. Its principal objective is "to accelerate and enlarge the contribution of atomic energy to peace, health and prosperity throughout the world".

**REVIEW OF
SEISMIC EVALUATION METHODOLOGIES
FOR NUCLEAR POWER PLANTS
BASED ON A BENCHMARK EXERCISE**

COPYRIGHT NOTICE

All IAEA scientific and technical publications are protected by the terms of the Universal Copyright Convention as adopted in 1952 (Berne) and as revised in 1972 (Paris). The copyright has since been extended by the World Intellectual Property Organization (Geneva) to include electronic and virtual intellectual property. Permission to use whole or parts of texts contained in IAEA publications in printed or electronic form must be obtained and is usually subject to royalty agreements. Proposals for non-commercial reproductions and translations are welcomed and considered on a case-by-case basis. Enquiries should be addressed to the IAEA Publishing Section at:

Marketing and Sales Unit, Publishing Section
International Atomic Energy Agency
Vienna International Centre
PO Box 100
1400 Vienna, Austria
fax: +43 1 2600 29302
tel.: +43 1 2600 22417
email: sales.publications@iaea.org
<http://www.iaea.org/books>

For further information on this publication, please contact:

International Seismic Safety Centre
International Atomic Energy Agency
Vienna International Centre
PO Box 100
1400 Vienna, Austria
Email: Official.Mail@iaea.org

© IAEA, 2013
Printed by the IAEA in Austria
November 2013

IAEA Library Cataloguing in Publication Data

Review of seismic evaluation methodologies for nuclear power plants based on a benchmark exercise. — Vienna : International Atomic Energy Agency, 2013.
p. ; 30 cm. — (IAEA-TECDOC series, ISSN 1011-4289 ; no. 1722)
ISBN 978-92-0-114913-8
Includes bibliographical references.

1. Earthquake hazard analysis. 2. Earthquake resistant design.
3. Nuclear power plants — Safety measures. I. International Atomic Energy Agency. II. Series.

FOREWORD

Niigataken-chuetsu-oki (NCO) earthquake ($M_w = 6.6$) occurred on 16 July 2007 and affected the Kashiwazaki-Kariwa (K-K) NPP in Japan. Although there was significant loss of main shock data due to transmission problems, a significant number of instruments were still able to measure the acceleration at different locations in soil (boreholes) and in structures at the K-K NPP during the main shock and the aftershocks. The availability of all these instrumental data provided an excellent background for initiating a benchmarking exercise known as the Kashiwazaki-Kariwa Research Initiative for Seismic Margin Assessment (KARISMA).

The main objective of the KARISMA benchmark exercise is to study a comparison between analytical seismic response versus real response of selected structure, system and components (SSCs) of K-K NPP Unit 7. The KARISMA benchmark exercise includes benchmarking the analytical tools and numerical simulation techniques used for predicting seismic response of NPP structures (in linear and non-linear ranges), site response, soil-structure interaction phenomena, seismic response of piping systems, 'sloshing' in the spent fuel pool and buckling of tanks. The benchmark is primarily based on data provided by Tokyo Electric Power Company (TEPCO). It is not linked to the seismic re-evaluation of K-K NPP carried out by TEPCO.

Twenty-one organizations, comprising researchers, operating organizations, regulatory authorities, vendors and technical support organizations from 14 countries, participated in the benchmarking exercises.

This publication, including a CD-ROM, summarizes the analyses of the main results of the benchmarking exercise for the K-K NPP reactor building (including static and modal analyses of the fixed base model, soil column analyses, analyses of the soil-structure models and margin assessment of the K-K NPP reactor building), the analyses of the main results of the benchmarking exercise for the residual heat removal piping system (including quantification of the effect of different analytical approaches on the response of the piping system under single and multi-support input motions), the spent fuel pool (to estimate the sloshing frequencies, maximum wave height and spilled water amount, and predict free surface evolution), and the pure water tank (to predict the observed buckling modes of the pure water tank). Analyses of the main results include comparison between different computational models, variability of results among participants, and comparison of analysis results with recorded ones.

This publication addresses state of the practice for seismic evaluation and margin assessment methodologies for SSCs in NPPs based on the KARISMA benchmark exercise. As such, it supports and complements other IAEA publications with respect to seismic safety of new and existing nuclear installations. It was developed within the framework of International Seismic Safety Centre activities. It provides detailed guidance on seismic analysis, seismic design and seismic safety re-evaluation of nuclear installations and will be of value to researchers, operating organizations, regulatory authorities, vendors and technical support organizations.

The contributions of all those who were involved in the drafting and review of this report are greatly appreciated. The IAEA officer responsible for this publication was A. Altinyollar of the Division of Nuclear Installation Safety.

EDITORIAL NOTE

This report has been prepared from the original material as submitted for publication and has not been edited by the editorial staff of the IAEA. The views expressed do not necessarily reflect those of the IAEA or the governments of its Member States.

It does not address questions of responsibility, legal or otherwise, for acts or omissions on the part of any person.

The use of particular designations of countries or territories does not imply any judgement by the publisher, the IAEA, as to the legal status of such countries or territories, of their authorities and institutions or of the delimitation of their boundaries.

The mention of names of specific companies or products (whether or not indicated as registered) does not imply any intention to infringe proprietary rights, nor should it be construed as an endorsement or recommendation on the part of the IAEA.

The depiction and use of boundaries, geographical names and related data shown on maps do not necessarily imply official endorsement or acceptance by the IAEA.

The IAEA has no responsibility for the persistence or accuracy of URLs for external or third party Internet web sites referred to in this report and does not guarantee that any content on such web sites is, or will remain, accurate or appropriate.

CONTENTS

1.	INTRODUCTION	1
1.1.	BACKGROUND	1
1.2.	OBJECTIVES OF THE PUBLICATION	9
1.3.	SCOPE OF THE PUBLICATION	10
1.4.	STRUCTURE OF THE PUBLICATION	10
2.	ESTABLISHING THE BENCHMARKING EXERCISE	11
2.1.	OBJECTIVE OF THE BENCHMARK	11
2.2.	SCOPE OF THE BENCHMARK	11
2.3.	ORGANIZATION OF THE BENCHMARK	12
2.3.1.	Guidance Documents and results templates.....	12
2.3.2.	ISSC Database.....	13
2.3.3.	Participants	13
2.3.4.	Organizing Committee (OC).....	13
2.3.5.	Review Meetings (RM).....	13
2.4.	INPUT DATA FOR THE BENCHMARKING EXERCISE.....	14
2.4.1.	Description of Structure and Equipment.....	14
2.4.2.	Recorded NCO earthquake signals	20
2.4.3.	Soil properties for site response and soil-structure interaction analyses of the reactor building	25
2.5.	BENCHMARK REQUESTED ANALYSIS.....	33
2.5.1.	Part 1 Structure.....	33
2.5.2.	Part 2 Equipment.....	36
3.	ANALYSES OF THE MAIN RESULTS OF THE BENCHMARKING EXERCISE FOR PART 1 STRUCTURE	39
3.1.	MAIN RESULTS FOR TASK 1.1 OF PHASE I: CONSTRUCTION AND VALIDATION OF THE SOIL AND STRUCTURE MODELS.....	39
3.1.1.	Subtask 1.1.1 Static and modal analyses of the fixed- base model.....	39
3.1.2.	Subtask 1.1.2 Soil Column Analyses	45
3.1.3.	Subtask 1.1.3 Analysis of the complete model	52
3.2.	MAIN RESULTS FOR TASK 1.2 OF PHASE II: MAIN SHOCK RESPONSE.....	53
3.2.1.	Subtask 1.2.1 “Reference analyses” in frequency or time domain.....	53
3.2.2.	Subtask 1.2.2 “Best estimate analysis”	58

3.3.	MAIN RESULTS OF TASK 1.3 FOR PHASE III: MARGIN ASSESSMENT	63
3.3.1.	Model presentation	63
3.3.2.	Pushover Analysis	68
3.3.3.	Dynamic Response Analysis	71
3.3.4.	Comparison of pushover analysis and dynamic analysis results	82
4.	ANALYSES OF THE MAIN RESULTS OF THE BENCHMARKING EXERCISE FOR PART 2 EQUIPMENT	85
4.1.	MAIN RESULTS FOR TASK 2.1 RHR PIPING SYSTEM	85
4.1.1.	Phase I and Phase II: Initial Analyses and Analyses with modified support conditions	85
4.1.2.	Phase III: Multi-support Analysis	95
4.2.	MAIN RESULTS FOR THE TASK 2.2 SLOSHING OF THE SPENT FUEL POOL	101
4.2.1.	Phase I and Phase II: Initial and Complete Analyses	101
4.3.	MAIN RESULTS FOR TASK 2.3 PURE WATER TANK BUCKLING	104
4.3.1.	Phase I: Initial Analyses	104
5.	OBSERVATIONS AND CONCLUSIONS	109
5.1.	OBSERVATIONS	109
5.1.1.	Part 1 Structure	109
5.1.2.	Part 2 Equipment	115
5.2.	CONCLUSIONS	116
5.2.1.	Part 1 Structure	116
5.2.2.	Part 2 Equipment	118
6.	OUTLOOK AND SUGGESTIONS	120
6.1.	GENERAL OUTLOOK AND SUGGESTIONS	120
6.2.	SPECIFIC SUGGESTIONS	120
	APPENDIX	123
	SUMMARY OF PARTICIPANTS' MODELLING ASSUMPTIONS	123
	REFERENCES	138
	ABBREVIATIONS	139
	LIST OF THE KARISMA BENCHMARK PARTICIPANTS	141
	CONTRIBUTORS TO DRAFTING AND REVIEW	143

1. INTRODUCTION

1.1. BACKGROUND

Niigataken-chuetsu-oki (NCO) earthquake occurred at 10:13 local time on 16 July 2007 with a moment magnitude of 6.6 and at a depth of 10 km near the West Coast of Honshu (37.576°N, 138.469°E), in Japan. The hypocentre of the earthquake was below the seabed of the Jo-chuetsu area in Niigata prefecture. The epicentre was 70 km away from Niigata, Honshu, Japan. Nine people died, at least 1,088 injured, 875 houses damaged, roads and bridges damaged and landslides occurred in Nagano, Niigata and Toyama Prefectures. A two-car train derailed on the JR Echigo Line at Kashiwazaki. A minor tsunami was observed on Sadoga-shima [1]. Japan Meteorological Agency (JMA) intensity map for the NCO earthquake published by the Headquarters for Earthquake Research Promotion is presented in Fig. 1. Peak acceleration contour map for the NCO earthquake is presented in Fig. 2 (K-NET and KiK-net, Japan National Research Institute for Earth Science and Disaster Prevention: NIED).

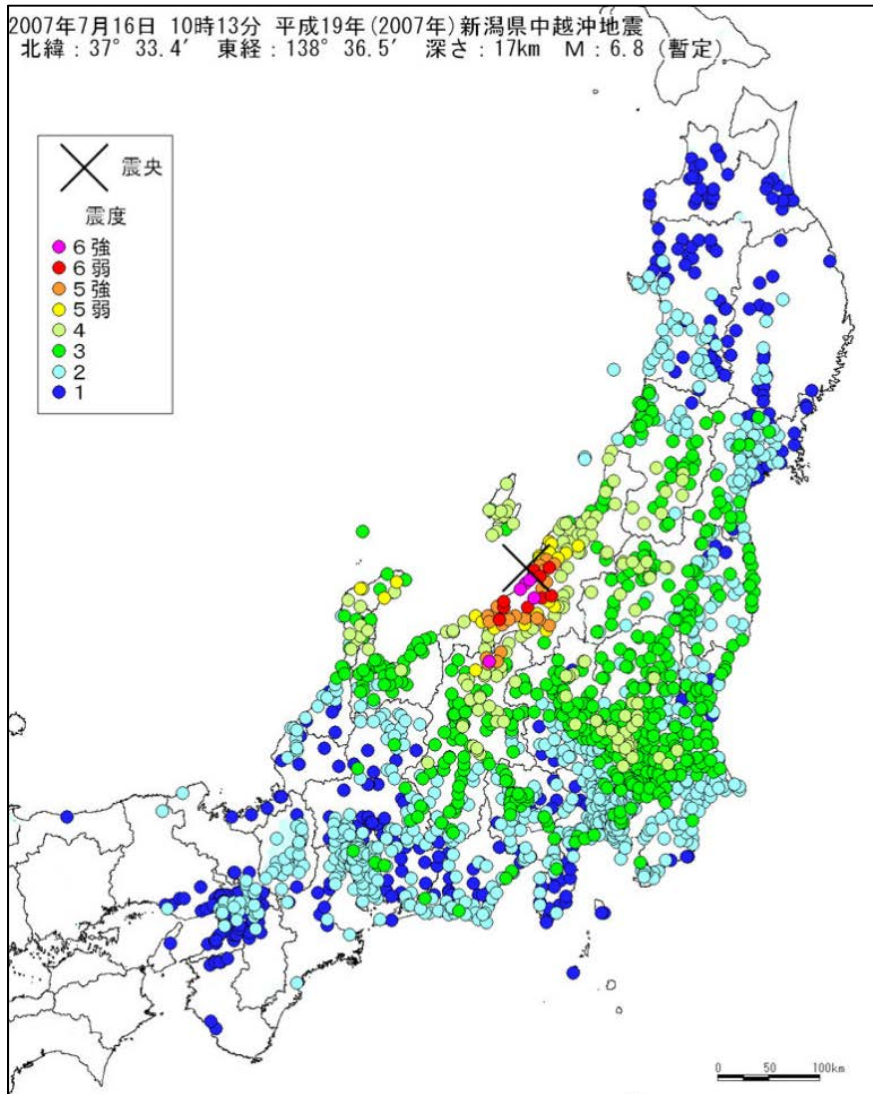


FIG. 1. JMA intensity map published by the Headquarters for Earthquake Research Promotion (Source: http://www.jishin.go.jp/main/oshirase/20070716_chuetsu_oki.htm).

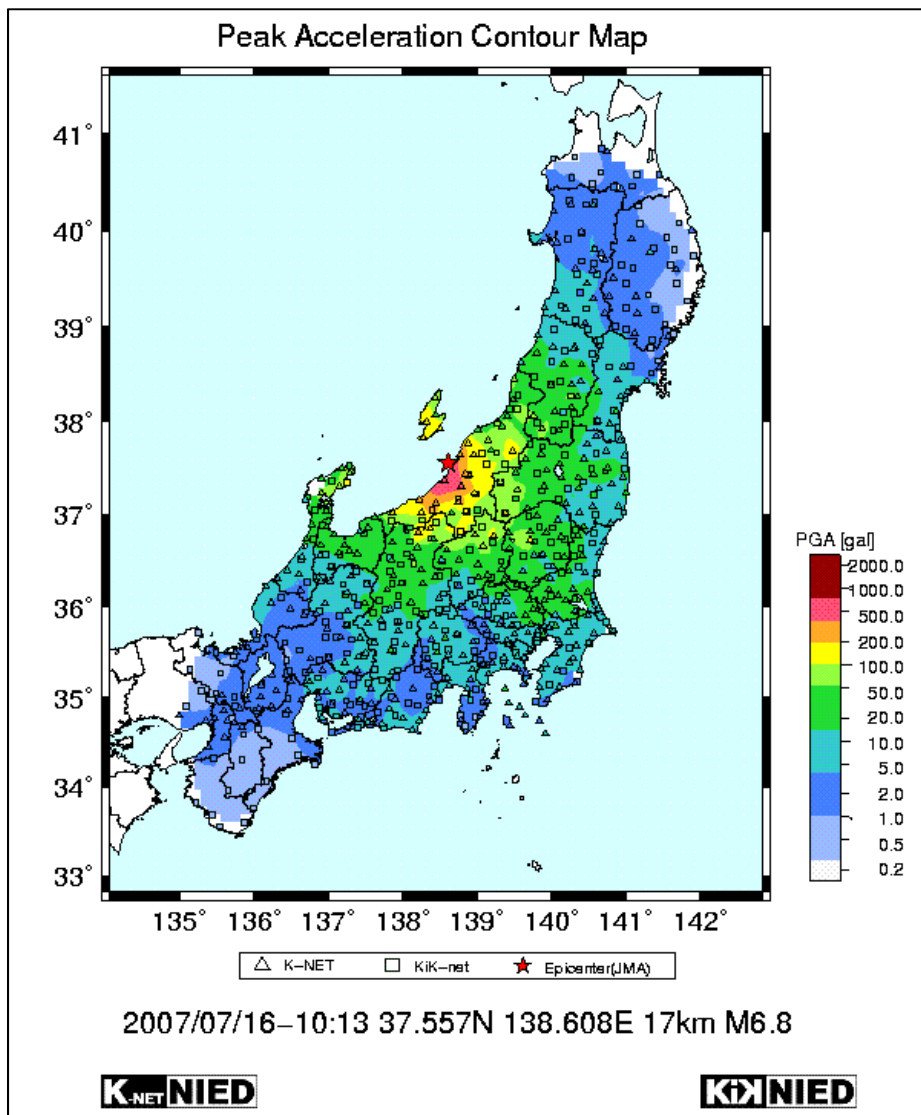


FIG. 2. NCO earthquake peak acceleration counter map.

The epicentre was 16 km away from the Kashiwazaki- Kariwa (K-K) Nuclear Power Plant (NPP) site and the NCO earthquake affected K-K NPP. K-K NPP is located in Kashiwazaki city and Kariwa town in Niigata Prefecture, approximately 217 km north-west of Tokyo, on the west coast of Japan (Fig. 3). The site covers an area of about 4.2 square-kilometers including land in Kashiwazaki city and Kariwa town. K-K NPP is owned and operated by TEPCO.

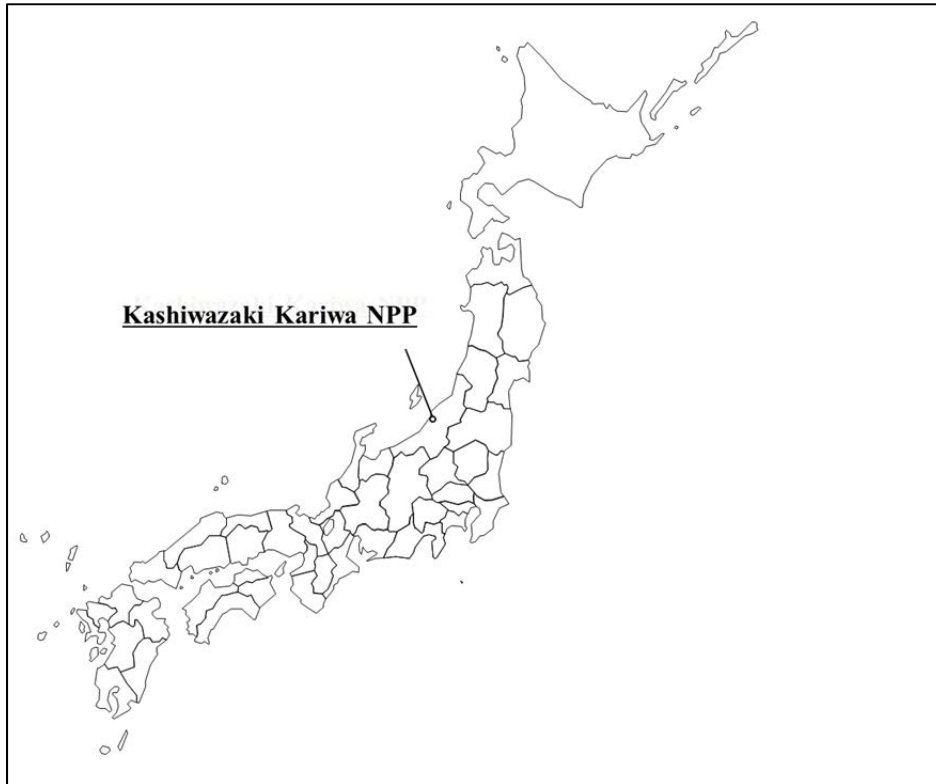


FIG. 3. Location of K-K NPP site.

The K-K NPP site has seven units with a total of 7965 MW installed capacity (Figs 4 and 5). Five reactors are of Boiling Water Reactor (BWR) type with a net installed capacity of 1067 MW each. Two reactors are of Advanced Boiling Water Reactor (ABWR) type with 1315 MW installed capacity each. The five BWR units entered commercial operation between 1985 and 1994 and the two ABWRs in 1996 and 1997 respectively. At the time of the earthquake, four reactors were in operation: Units 2, 3 and 4 (BWRs) and Unit 7 (ABWR). The other three reactors were in shutdown conditions for planned outages.



FIG. 4. Picture of the K-K NPP site (TEPCO).

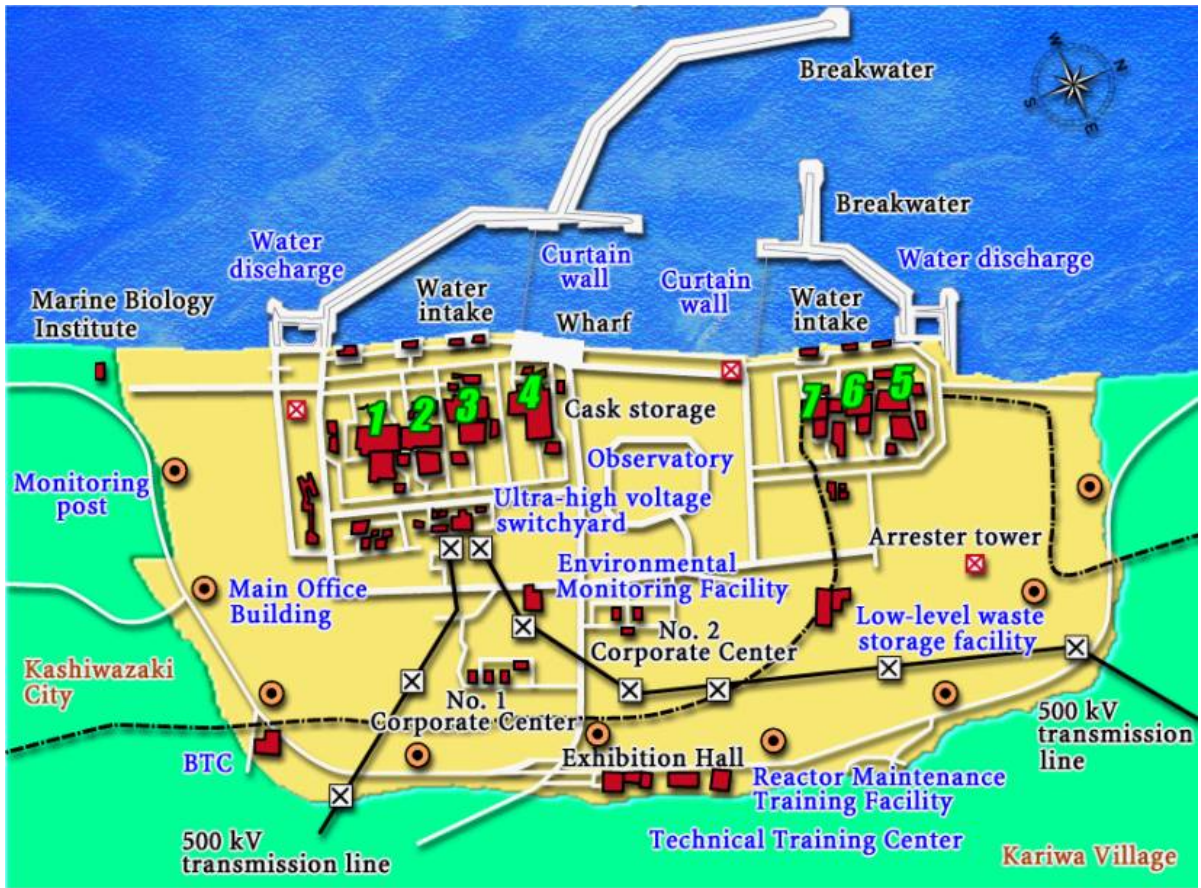


FIG. 5. Plan view of the K-K NPP site (TEPCO).

The largest peak ground acceleration at free field surface in the horizontal direction was 1.25g (E-W) as measured at the seismic observation shed for Unit 5 (5-G1) and in the vertical direction was 0.73 g as measured at the seismic observation shed for Unit 1 (1-G1). Comparison of response spectra obtained from the observed records and simulated motions (The Design Base Earthquake Ground Motion (DBEGM) was defined at the engineering bed rock level¹. In order to compare with the recorded motion on the base mat, the motion was simulated at the base mat level as the response using the DBEGM by TEPCO.) at the Unit 7 reactor building basemat is given in Fig. 6. The response spectra obtained from simulated motions were exceeded by the response spectra obtained from observed records for a very wide range of spectral frequencies. The earthquake caused automatic shutdown of the operating reactors.

Following the NCO earthquake, few IAEA expert missions were conducted at the Kashiwazaki-Kariwa NPP to identify the findings and lessons learned from that seismic event and for sharing them with the international nuclear community. From the TEPCO expert presentations, the regulatory authority (NISA) reports, and the plant walkdowns performed by the IAEA team, despite the exceedance of the seismic design bases, it is indicated that the safety related structures, systems and components (SSCs) of all seven units of the plant (in operating, start-up and shut down conditions) demonstrated good apparent performance in ensuring the basic safety functions concerning control of reactivity, cooling and confinement [3].

¹ The rock outcrop (free surface of the base stratum) is a nearly flat surface of the base stratum expanding over a significant area, and above which neither surface layers nor structures are present. The base stratum is firm bedrock with a shear wave velocity, V_s higher than 0.7 km/s (2300 fps), which was formed in the Tertiary or earlier era and which is not significantly weathered [2].

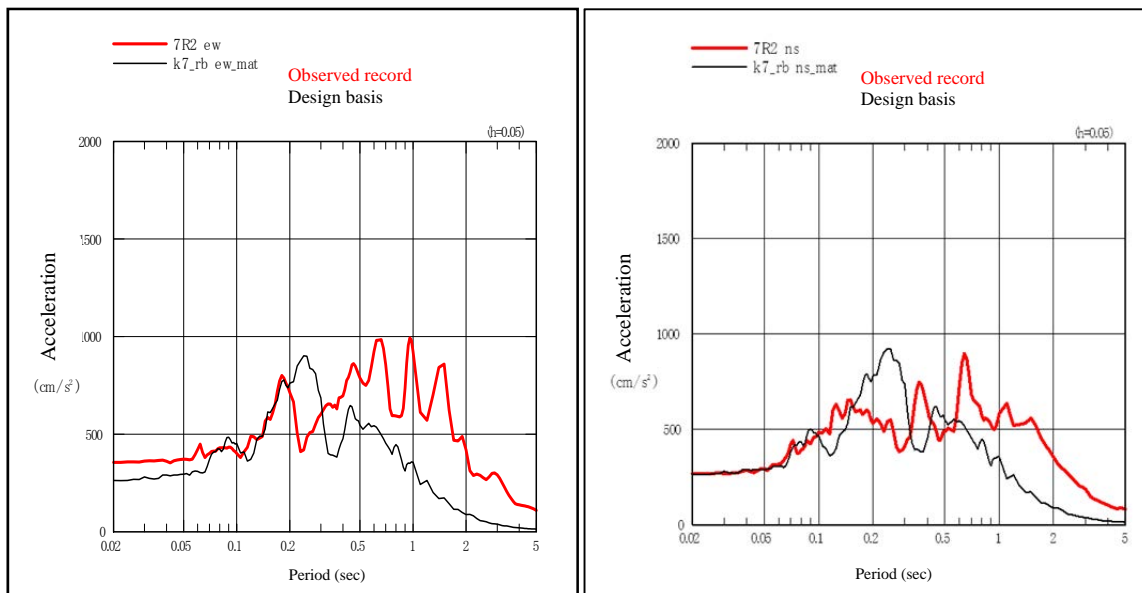


FIG. 6. Comparison of response spectra obtained from the observed records and simulated motions at the Unit 7 reactor building basemat in East-West (E-W) and North-South (N-S) directions.

There was no visible significant damage to safety related SSCs. On the other hand, non-safety related SSCs were affected by significant damage such as soil and anchor failures and oil leakages (Fig. 7).

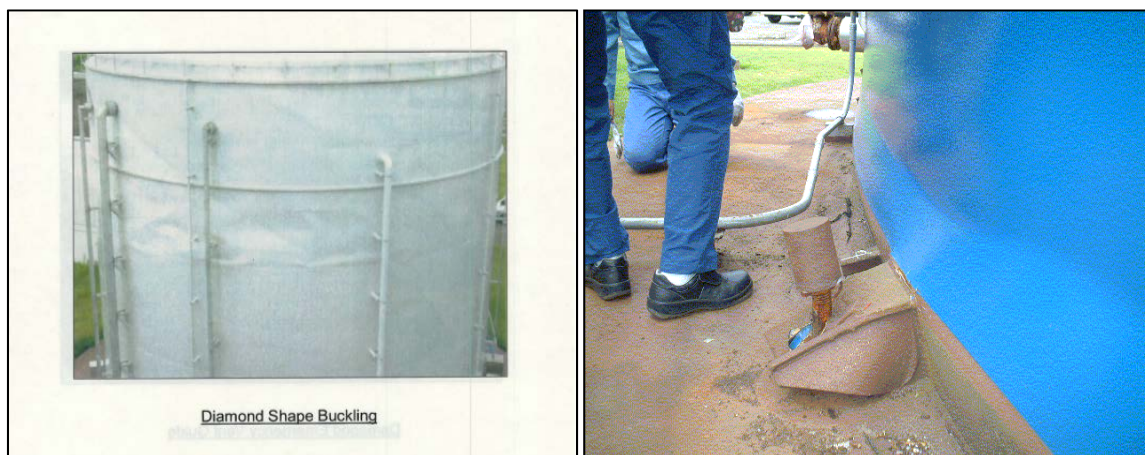


FIG. 7. Non safety related pure water tank buckling.

According to the IAEA mission report [3], some of the findings are summarized hereafter:

Examples of flooding hazards:

- Sloshing of the spent fuel pool water into the reactor building operating floor of Unit 6 and leakage through cable penetrations into the radiological non-controlled area and subsequently discharged into the sea (Fig. 8);
- Failure of the rubber flexible connection of the condenser B seawater box and connecting valve in Unit 4 leaking sea water onto the turbine building floor at lower elevations. The flexible connection that failed had originally been installed 13 years ago –plant personnel stated that the normal replacement schedule was 10 to 15 years – and so ageing of the flexible connection was probably a factor in its failure;

- Localized soil failure caused failure of fire suppression piping at a cable penetration to the Unit 1 reactor building. Water (about 2000 m³) and soil entered the reactor building at grade elevation and flowed through floor penetrations and stairwells to lower levels, finally reaching the B5 level at about 38 m below the plant grade level. A 40 cm deep puddle of water formed at the B5 level. It seems that this water and soil did not produce adverse consequences to SSCs.



FIG. 8. Sloshing spent fuel pool in Unit 3.

Soil deformation at NPP site:

- Although not of particular safety significance, the large ground deformations blocked the road to the plant at a critical moment when any delay in help and access was of importance;
- The ground failures caused a common failure of the outdoor fire extinguishing system, which prevented quick and immediate response to the fire in the in-house electrical transformer of Unit 3;
- The large ground settlements caused the oil leak of several transformers on the site, as well as the fire in the in-house electrical transformer of Unit 3;
- The large ground deformations around the safety related buildings most probably have caused damage in non-safety related buried piping penetrating the buildings (Fig. 9).



FIG. 9. Road damage near water discharge and switch yard (non-safety related facilities) indicating the high seismic demand at the site.

A significant number of instruments measured acceleration at different locations in soil (boreholes) and in structures in K-K NPP during the main shock and the aftershocks of the NCO earthquake. During the main shock, time history data in the borehole and free field data at all units were lost. Because the aftershocks time histories were overwritten due to limited memory of the seismometers, only the maximum accelerations are available for these. The maximum acceleration value of each signal and recording time for the main shock are presented in Table 1.

TABLE 1. MAXIMUM ACCELERATION VALUES AND RECORDING TIME (MAIN SHOCK: 10:13 ON JULY 16, 2007)

Observation point				Maximum acceleration value observed (Gal)			Recording time		Remark
				NS	EW	UD	Recording start time	Recording period (Sec)	
Service hall	Free field	SG1	T.M.S.L.+65.1m	347	437	590	10:12:57:00	600.00	The seismometer of the basic system
		SG2	T.M.S.L.+16.7m	340	411	179			
		SG3	T.M.S.L.-31.9m	403	647	174			
		SG4	T.M.S.L.-182.3m	430	728	160			
Ground surface	Unit 1	1-G1	Seismic observation shed for Reactor No.1	890	890	715	10:12:46.00	600.00	The new additional seismometer
	Unit 5	5-G1	Seismic observation shed for Reactor No.5	964	1223	539	10:12:45.00	600.00	
Unit 1	Reactor building	1-R1	2 nd floor	599	884	394	10:12:45:00	493.26	
		1-R2	Basement 5 (on foundation)	311	680	408	10:12:46:00	498.20	
	Turbine building	1-T2	1 st floor (pedestal)	1862	1459	741	10:12:46:00	186.29	
Unit 2	Reactor building	2-R1	2 nd floor	517	718	412	10:12:45:00	493.92	
		2-R2	Basement 5 (on foundation)	304	606	282	10:12:45:00	498.79	
	Turbine building	2-T1	1 st floor	431	764	594	10:12:45:00	493.17	
		2-T2	1 st floor (pedestal)	642	1159	650	10:12:46:00	181.75	
		2-T3	Basement 3 (on foundation)	387	681	470	10:12:45:00	497.95	
Unit 3	Reactor building	3-R1	2 nd floor	525	650	518	10:12:44:00	494.84	
		3-R2	Basement 5 (on foundation)	308	384	311	10:12:46:00	498.15	
	Turbine building	3-T2	1 st floor (pedestal)	1350	2058	619	10:12:46:00	183.01	
		3-T3	Basement 3 (on foundation)	581	549	513	10:12:44:00	600.00	
Unit 4	Reactor building	4-R1	2 nd floor	606	713	548	10:12:45:00	492.74	
		4-R2	Basement 5 (on foundation)	310	492	337	10:12:45:00	494.02	
	Turbine building	4-T1	1 st floor	411	560	549	10:12:46:00	492.61	
		4-T2	1 st floor (pedestal)	614	763	526	10:12:45:00	326.96	
		4-T3	Basement 3 (on foundation)	348	442	443	10:12:45:00	600.00	
Unit 5	Reactor building	5-R1	3 rd floor	472	697	331	10:12:45:00	493.21	
		5-R2	Basement 4 (on foundation)	277	442	205	10:12:45:00	493.69	
	Turbine building	5-T2	2 nd floor (pedestal)	1166	1157	533	10:12:45:00	187.26	
Unit 6	Reactor building	6-R1	3 rd floor	554	545	578	10:12:45:00	498.67	
		6-R2	Basement 3 (on foundation)	271	322	488	10:12:45:00	600.00	
Unit 7	Reactor building	7-R1	3 rd floor	367	435	464	10:12:45:00	493.92	
		7-R2	Basement 3 (on foundation)	267	356	355	10:12:44:00	600.00	
	Turbine building	7-T1	2 nd floor	418	506	342	10:12:44:00	600.00	
		7-T2	2 nd floor (pedestal)	673	1007	362	10:12:45:00	266.77	
		7-T3	Basement 2 (on foundation)	318	322	336	10:12:45:00	600.00	

Cross-section view showing the location of seismometers at K-K Unit 7 and in borehole and recorded maximum accelerations in the N-S, E-W and Up-Down (U-D) directions respectively are shown in Fig. 10.

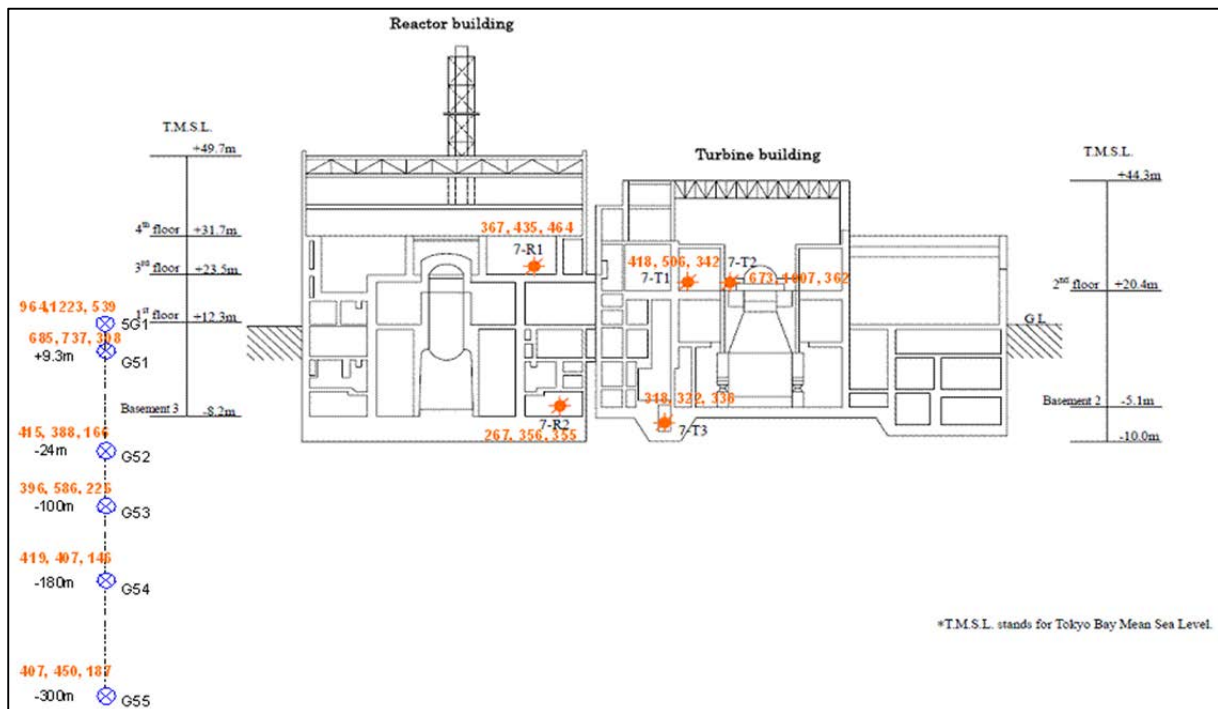


FIG. 10. Cross-section view showing the location map of seismometers in K-K Unit 7 and recorded maximum accelerations in the N-S, E-W and U-D directions respectively (in gal).

In addition, equipment behaviour during the NCO earthquake constitutes a very extensive and unique database which must be processed. From an analytical point of view, there is no measurement (acceleration or displacement sensor) directly on equipment; consequently, simulation with quantitative comparison of time-histories is not possible. However, it could be possible to reproduce some qualitative observations, such as a specific type of failure for thin walled tanks or the generic water spill from spent fuel pools. From another point of view, it may be interesting to analyse a piping system, whose behaviour is usually good during earthquake through different teams using different approaches. The system is supported by the structure at different supports; it would be possible to apply different analytical approaches to the piping system, using a complete set of input data at supports.

The NCO earthquake had unusual effects at the K-K site not only because of the very high accelerations it caused at the seven NPP units but also because of the significant variability between the recorded accelerations at these units. In particular, the first four units experienced considerably higher accelerations (both peak and spectral) compared to Units 5, 6 and 7. TEPCO and Japan Nuclear Energy Safety Organization (JNES) have spent a great deal of time and resources to explain these differences and eventually to model the subsurface formations in order to re-evaluate the hazard for the seismic backfit program. In fact, JNES started the deep borehole project at the K-K site largely to address these issues. The modelling emerging from these considerations includes the effects of the source and the travel path (including site response) together.

The relative location of the newer units is more favourable for the conventional soil modelling (which includes the assumption of vertically propagating shear waves) to be included in the

benchmark exercise. The fact that both the Unit 5 observation point and Unit 7 are in a similar part of the site has been considered as a positive attribute within this context.

IAEA launched the Extrabudgetary Programme (EBP) on the “Seismic safety of existing NPPs” in September 2007, to investigate available methods and practices for resolving current seismic safety issues concerning design and operational aspects of existing NPPs, and to provide advice for Member States (MSs) in the application of the solutions.

Availability of all these information on the performance of SSCs (Structure, System and Component) from walkdowns and correlation with instrumental data provided an excellent background to initiate a benchmarking exercise which is called KAshiwazaki-Kariwa Research Initiative for Seismic Margin Assessment (KARISMA) within the framework of above-mentioned EBP.

An expert meeting held in May 2008, elaborated the main characteristics of the KARISMA exercise which were documented in the general specification document [4].

The first announcement was made in July 2008 concerning the launching of a benchmarking exercise related to the structural behaviour of the reactor building structure including the soil and equipment response of the K-K NPP during the NCO earthquake. This benchmarking exercise was proposed in order to compare the analytical response to the real one and to understand the margin – this was important because accelerations significantly exceeded ‘design’ with no effect on safety related SSCs.

Available data which was provided by TEPCO was assembled and Guidance documents [5, 6, 7 and 8] and result templates were developed for Phase I and KARISMA benchmarking exercise was launched for Phase I in July 2009. The Guidance document was modified for Phase II including standard soil profile and control motion. New result templates were developed for Phase II and Phase II was launched in January 2011. The Guidance document was modified including standard soil profiles for 1*NCOE, 2*NCOE, 4*NCOE and 6*NCOE² and control motions for Phase III. New results templates were developed for Phase III and Phase III was launched in August 2011.

The benchmarking exercise was based both on data provided by TEPCO and a set of assumptions in order to be able to define the characteristics of the structure with the manageable amount of data. The KARISMA benchmark is not linked to the seismic re-evaluation of the Kashiwazaki-Kariwa NPP which was carried out by TEPCO.

1.2. OBJECTIVES OF THE PUBLICATION

The objective of this publication is to present the results of the KARISMA benchmarking exercise, to estimate how well the analytical results can predict the actual response and performance of SSCs and to identify the areas that may need reinforcement or highlight those areas where analytical results are not an accurate predictor of SSC performance. Findings are presented based on KARISMA benchmarking exercise results.

On the basis of the lessons learned, this publication contributes to the development, revision and implementation of IAEA safety standards related to seismic safety re-evaluation of nuclear installations such as the Safety Guide NS-G-2.13 on Evaluation of Seismic Safety of Existing Nuclear Installations [9], and the Safety Guide NS-G-1.6, Seismic Design and Qualification for Nuclear Power Plants [10] of which revision is starting.

² 1*NCOE, 2*NCOE, 4*NCOE and 6*NCOE are free field time-histories input motions defined at the Outcrop of the Raft Elevation (ORE) and at the Outcrop of the Engineering Bedrock elevation (OEB).

1.3. SCOPE OF THE PUBLICATION

This publication addresses state of the practice for seismic evaluation and margin assessment methodologies for SSCs in NPPs based on the KARISMA benchmark exercise.

The KARISMA exercise includes benchmarking on the analytical tools and numerical simulation techniques for predicting seismic response of NPP structures (in linear and non-linear range), site response, soil-structure interaction (SSI) phenomena, seismic response of piping systems, sloshing in the spent fuel pool and buckling of tank.

Analyses of the main results of the benchmarking exercise for the K-K NPP reactor building including static and modal analyses of the fixed-base model, soil column analyses, analyses of the soil-structure models under the NCO earthquake, margin assessment of the K-K NPP reactor building are summarized. Analyses of the main results include comparison between different computational models, variability of results among participants, and comparison of analysis results with recorded ones.

Analyses of the main results of the benchmarking exercise for the RHR Piping system (including quantification of the effect of different analytical approaches on the response of the piping system under single and multi support input motions), the spent fuel pool (to estimate the sloshing frequencies, maximum wave height and spilled water amount, and predict free surface evolution), and pure water tank (to predict the observed buckling modes of the pure water tank) are presented.

Recommendations on comparison between different analytical approaches, effect of soil and its role in K-K NPP response, modelling approaches for SSI and embedment, margins analysis and criteria to define "ultimate" behaviour, piping analyses, spent fuel pool sloshing and tank analysis based on KARISMA benchmark results are proposed.

The basis for this publication consists of the guidance documents [5, 6, 7 and 8], participants' results and minutes of the review meetings [11, 12 and 13].

1.4. STRUCTURE OF THE PUBLICATION

Following this introduction, Section 2 provides information on objective and scope of the benchmark and organization of the benchmark. Input data for the benchmarking exercise and benchmarking requested analysis are also presented in Section 2.

Section 3 is dedicated to analyses of the main results of the benchmarking exercise for Part 1 Structure for Phase I, II and III as they were provided by the participants and processed in order to present mean values, standard deviations and coefficient of variations of these outputs.

Section 4 includes analyses of the main results of the benchmarking exercise for Part 2 Equipment for Phase I, II and III as they were provided by the participants and processed in order to present mean values, standard deviations and coefficient of variations of these outputs.

Section 5 presents observations and conclusions on KARISMA benchmark results for Part 1 Structure and Part 2 Equipment.

Section 6 summarizes the recommendations.

Appendix includes summary of participants' modelling assumptions.

On an attached CD-ROM, the following information is organized in 5 Annexes:

Annex I	List of Participants and Organizing Committee (OC) Members
Annex II	Minutes of the Review Meetings (RM)
Annex III	Guidance Documents for the Benchmark
Annex IV	Participants' Results for Part 1 Structure for Phase I, II and III
Annex V	Participants' Results for Part 2 Equipment for Phase I, II and III

2. ESTABLISHING THE BENCHMARKING EXERCISE

2.1. OBJECTIVE OF THE BENCHMARK

It is important to understand all the elements involved in the derivation of the seismic design basis and identify the sources of conservatism as well as sources that contributed to the exceedance of the seismic design basis by the observations from the earthquake.

The Benchmark exercise has been designed to address two major aspects. The first involves the use of the main shock and aftershock records collected at the free field, downhole, basemat and in-structure locations. In this regard, the benchmarking involves the predictive capabilities of the methods used by the participants in terms of soil/structure modelling and the chosen input parameters. The second major element of the Benchmark exercise is related to the ensemble of the participants' findings when a recorded target value is not available. In this case, it is possible to make observations regarding the overall methodologies (e.g. pushover analysis versus dynamic modelling) and the variability involved between the participants. The latter provides a useful indication of the epistemic uncertainties that may be encountered in seismic structural analyses in general.

General objectives of the KARISMA benchmarking exercise were based on the following question items discussed in the expert meeting held in May 2008;

- To understand what happened to soil and structures during the NCO earthquake: are we able to capture the main characteristics of the response?;
- Understanding of margins: quantifying what happens both in soil and in structure, when the input is increased;
- Calibration of different simulation methodologies for soil, structures and soil-structure interaction;
- Identification of main parameters influencing the response, by collecting and analysing the results from different teams;
- Understanding of epistemic uncertainties i.e. difference caused by modelling soil and structure;
- Understanding of equipment behaviour for some selected equipment and approaches to margins evaluation.

2.2. SCOPE OF THE BENCHMARK

The scope of the benchmark was to analyse the seismic behaviour of the following SSCs of the K-K Unit 7 under the NCO earthquake loading:

- Reactor building;

- RHR (Residual Heat Removal) piping system;
- Spent fuel pool;
- Pure water tank.

The benchmark exercise included static analysis of the reactor building, soil column analysis and modal analysis of the soil-structure model of the reactor building, pushover analysis and dynamic response analysis of the reactor building under input motions corresponding to 1*NCOE, 2*NCOE, 4*NCOE and 6*NCOE.

It comprised static analysis under vertical loads (weight) and pressure, modal analysis, response spectrum analysis and time history analysis of the RHR piping system under single input motion and multi-support input motion which represent NCO earthquake.

Regarding spent fuel pool, it included the modal analysis of the sloshing, estimation of the maximum wave height assuming no water spill from spent fuel pool, estimation of spilled water amount from the spent fuel pool during the NCO earthquake.

The benchmark exercise also comprised modal analysis, response spectrum analysis, time history analysis and buckling estimation of the pure water tank under NCO earthquake motion.

All of the above work was based on data (description of SSCs, soil properties, input motions etc.) provided by TEPCO [5, 6, 7 and 8] and a set of assumptions in order to be able to define the characteristics of the structure with the manageable amount of data.

2.3. ORGANIZATION OF THE BENCHMARK

There were two main parts of the KARISMA benchmarking exercise:

Part 1- Structure;

- Task 1 Seismic analysis of the K-K Unit 7 reactor building.

Part 2- Equipment;

- Task 2.1 Seismic analysis of RHR piping system;
- Task 2.2 Seismic analysis of spent fuel pool (sloshing);
- Task 2.3 Seismic analysis of pure water tank (buckling).

The exercise was accomplished in three phases (See Section 2.7 for more details).

2.3.1. Guidance Documents and results templates

Guidance documents were developed for all tasks and phases [5, 6, 7, and 8]. Guidance documents present all necessary information including assumptions for analytical modelling, input signals and requested analyses. They provided the freedom to the participants to use their state of the practice analysis procedure and tools to develop their own analytical model.

For the reactor building structure model, the necessary input data was extracted from the real K-K Unit7 structure and simplified in order to reduce the modelling effort to a reasonable level of detail. Thus, structural models of the different participants represent in a generic way the real K-K Unit7 reactor building.

Result templates have been developed for each task and phase to collect participants' results. For each task and phase, the expected outputs were in the form of curves and tables of results and pictures. Outputs in terms of global parameters (displacements, accelerations, forces and

moments) at key locations were requested to validate the models, to compare analysis results with observations and to compare results from the participants

2.3.2. ISSC Database

A database created at the ISSC was used as a tool to effectively exchange data between participants, Organizing Committee (OC) and the ISSC secretariat. Data packages including guidance documents, results templates, input signals and other complementary data files were uploaded to the ISSC database (<http://issc.iaea.org/db/>) for each phase. This database was used by participants for downloading input data and templates for requested outputs, uploading their outputs and reports, etc. Announcements, general documents and OC and RM meeting documents were made available in the ISSC database. There was one folder for each participant as a repository of the results.

2.3.3. Participants

21 organizations expressed their intention to participate in the KARISMA benchmarking exercise as of September 2008.

18 organizations from 11 countries participated in Part 1 Structure. 6 organizations from 5 countries participated in Task 2.1 RHR piping system analysis. 7 organizations from 6 countries participated in Task 2.2 Sloshing of the spent fuel pool. 6 organizations from 6 countries participated in Task 2.3 Pure water tank buckling. List of the KARISMA benchmark participants is presented in Annex I.

2.3.4. Organizing Committee (OC)

The kick-off meeting was held in October 2008 and an Organizing Committee (OC) was established for the benchmarking exercise. The first OC meeting held in January 2009 identified the necessary data [14].

The benchmark was managed by the ISSC following the advice of the OC, which included representatives from ISSC, TEPCO, external experts and representatives from participating organizations. OC meetings were held before and after each Review Meeting to discuss and advise the phases of the benchmarking exercise, to review available data (Guidance documents and Results templates) and to advice on organizational matters for conducting of the benchmark. OC member list is given in Annex II.

2.3.5. Review Meetings (RM)

RMs involved all participants. Three RMs were held after collecting participants' results for each phase. The results obtained by participants were shared and reviewed. Suggestions for further phases of the benchmarking exercise were discussed.

The first review meeting was held in May 2010 in Vienna to share the results obtained by different participants during Phase I, to review the participants' results and to discuss suggestions for further phases of the benchmark [11].

The second review meeting was held in May 2011 in Vienna to share the results obtained by different participants during Phase II of the benchmarking exercise, to review the participants' results and to discuss suggestions for Phase III [12].

The third review meeting was held in December 2011 in Vienna to share the results obtained by different participants during Phase III of the benchmarking exercise and to discuss general lessons learned from the benchmarking exercise and suggestions for content of TECDOC [13].

2.4. INPUT DATA FOR THE BENCHMARKING EXERCISE

2.4.1. Description of Structure and Equipment

2.4.1.1. Part 1- Structure

Geometric description of the Unit 7 reactor building is presented in Guidance Document [5]. The Unit 7 reactor building is a 56.7m x 59.3m reinforced concrete structure. It has eight main floors: composed of mainly reinforced concrete slabs and beams, locally a few steel beams at the same elevations. It has a steel roof structure.

The main structural parts of the reactor building are:

- Basemat;
- Exterior walls;
- Reinforced Concrete Containment Vessel (RCCV);
- Interior walls and auxiliary walls;
- 8 main floors: composed of mainly reinforced concrete slabs and beams, locally a few steel beams at the same elevations;
- Intermediate reinforced concrete columns;
- Steel roof structure.

Floor elevations are given in term of Tokyo Mean Sea Level (T.M.S.L) (Table 2).

TABLE 2. REACTOR BUILDING FLOOR ELEVATIONS

Elevation	T.M.S.L (m) (Z direction)
Bottom of Basement	-13.7
3 rd Basement	-8.2
2 nd Basement	-1.7
1 st Basement	4.8
1 st Floor	12.3
2 nd Floor	18.1
3 rd Floor	23.5
4 th Floor	31.7
Crane Floor	38.2
Roof	49.7

Thickness of basemat is 5.5m. Embedment depth of the building is 26m. Height of the building from grade level is about 37.4m. The concrete layer thickness 10cm on the top of the roof is connected to steel beams by shear keys, inducing a composite behaviour. Reinforcement ratio and rebar diameters of main and auxiliary structural walls, pool walls, RCCV, floors, raft, beams and columns are presented in Guidance Document [5]. Concrete and reinforcement steel properties are also presented. Additional loads corresponding to piping loads, equipment loads and live load, (all temporary equipment and storage and other equipment and piping loads) exist on different floors.

Constitutive laws for concrete and reinforcing steel and structural material damping for Phase III were also presented in Guidance Document [5].

All relevant data are described in the plant coordinate system, including input signals. The axes of the plant coordinate system for the description of structures (Figs 11 and 12) are as follows:

- X axis is Plant North (PN, N-S);
- Y axis is perpendicular to X axis (E-W);
- Z axis is vertical upwards, in the RPV centreline.

All elevations are given in terms of T.M.S.L.

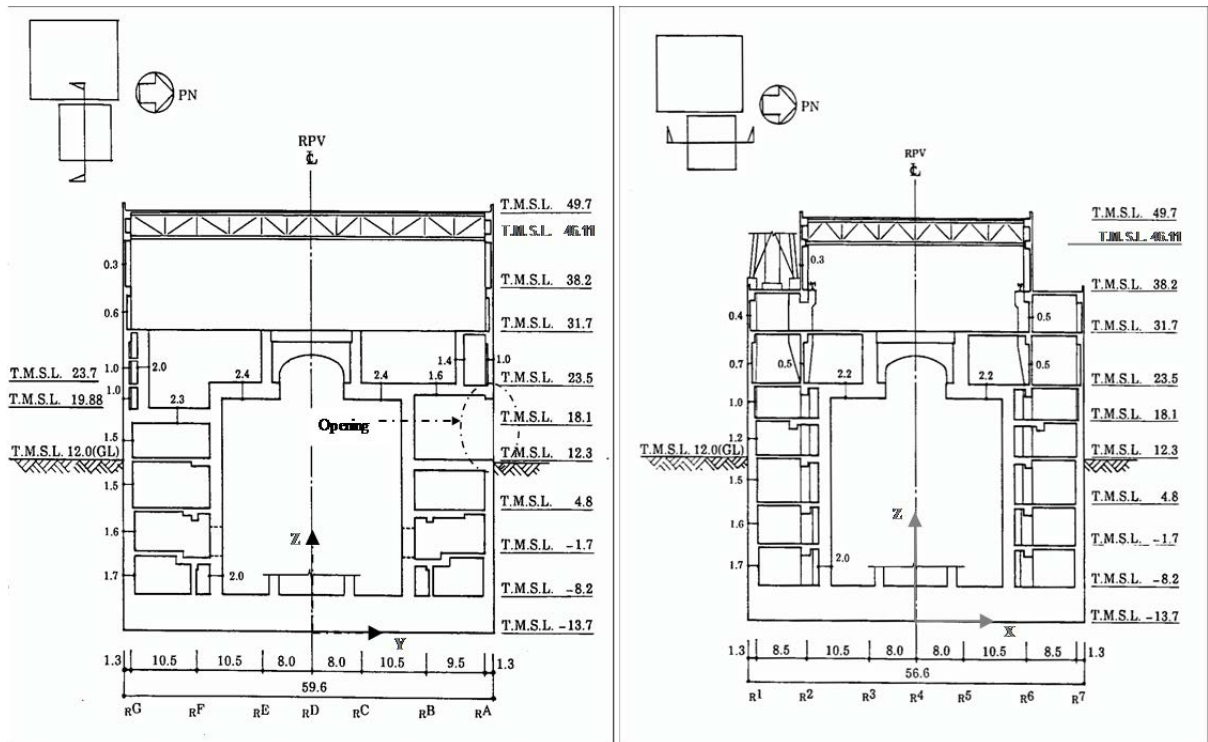


FIG. 11. K-K Unit 7 Reactor Building: Cross Section view.

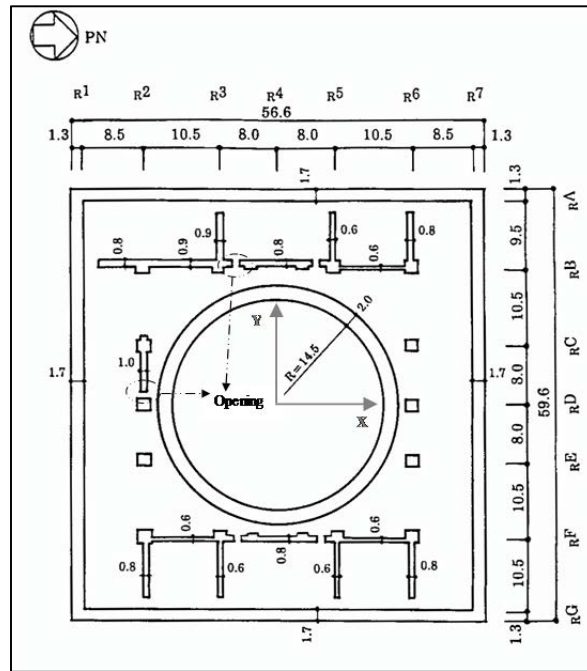


FIG. 12 Floor plan: 3rd Basement (T.M.S.L. -8.2m).

2.4.1.2. RHR piping system

General view of the RHR piping system is given in Fig. 13. Supports for the RHR piping system are shown in Fig. 54. The following information was provided:

- Description of the RHR piping system, including valves, reducers, nozzles, penetrations and tees: geometry (length, outside diameter, thickness etc.), material description (composition of the material, Young's modulus), additional weight from e.g. insulation;
- Description of supporting structures: geometry, restricted support directions, spring constants (translation and rotation) at supports and penetration points;
- Design condition of the RHR piping system: maximum design pressure, maximum design temperature and operating temperature.

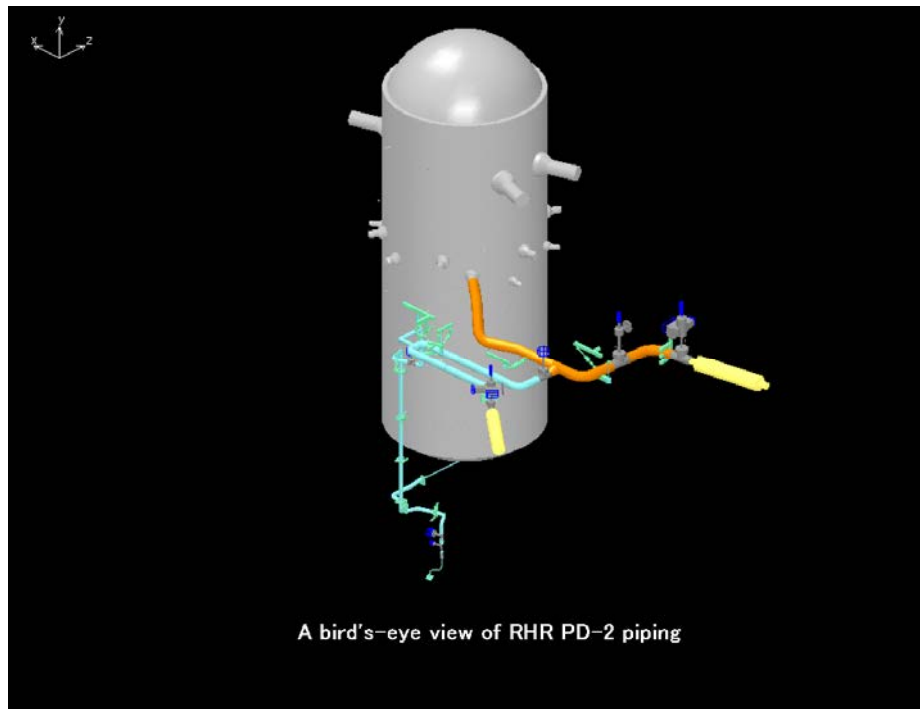


FIG. 13. General view of the RHR piping system.

The coordinate system for description of the RHR piping system in data files is different from the one for “Part 1-Structure”. The axes of the coordinate system for the description of the RHR piping system are as follows:

- X axis is Plant North (PN);
- Z axis is perpendicular to X axis;
- Y axis is vertical upwards.

2.4.1.3. Spent fuel pool

The Spent fuel pool is located in the reactor building between TMSL +17.58m and TMSL +31.70m (Fig. 11). Plan dimension of the spent fuel pool is 14.0m x 17.90m (Fig. 14). The water level is 31cm below operating floor (TMSL +31.70m). Depth of the pool from operation floor to bottom is 11.82m at the spent fuel storage rack area and 8m at other parts of the pool.

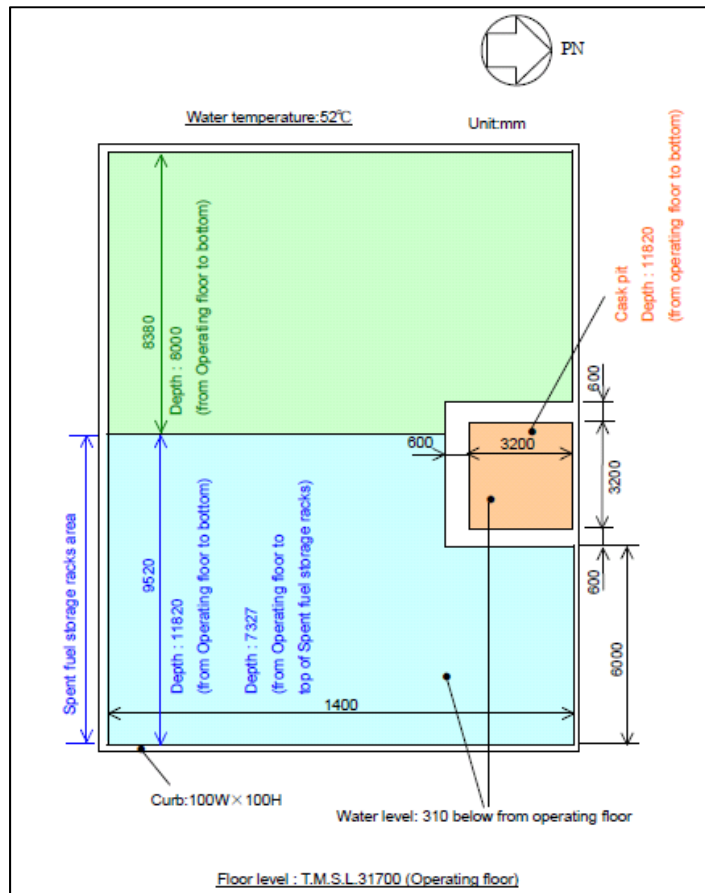


FIG. 14. Plan dimension of spent fuel pool.

2.4.1.4. Pure water tank

The pure water tank is located near the Unit 1 as shown in Fig. 15 (The pure water system is installed to supply pure water for equipments not to be radioactively-contaminated at the stage of reactor start-up, shutdown and operation.). Dimension of the pure water tank is shown in Fig. 16. Shell height (L) is 12.8m. Roof height is 2.02m. Radius of the tank (R) is 7.5m. L/R ratio is 1.707. Material thickness is 9mm at the bottom and 4.5mm at the top of the tank. Water level at the NCO earthquake was 8.6m.

The coordinate system for the pure water tank is the same as the one for “Part 1-Structure”.

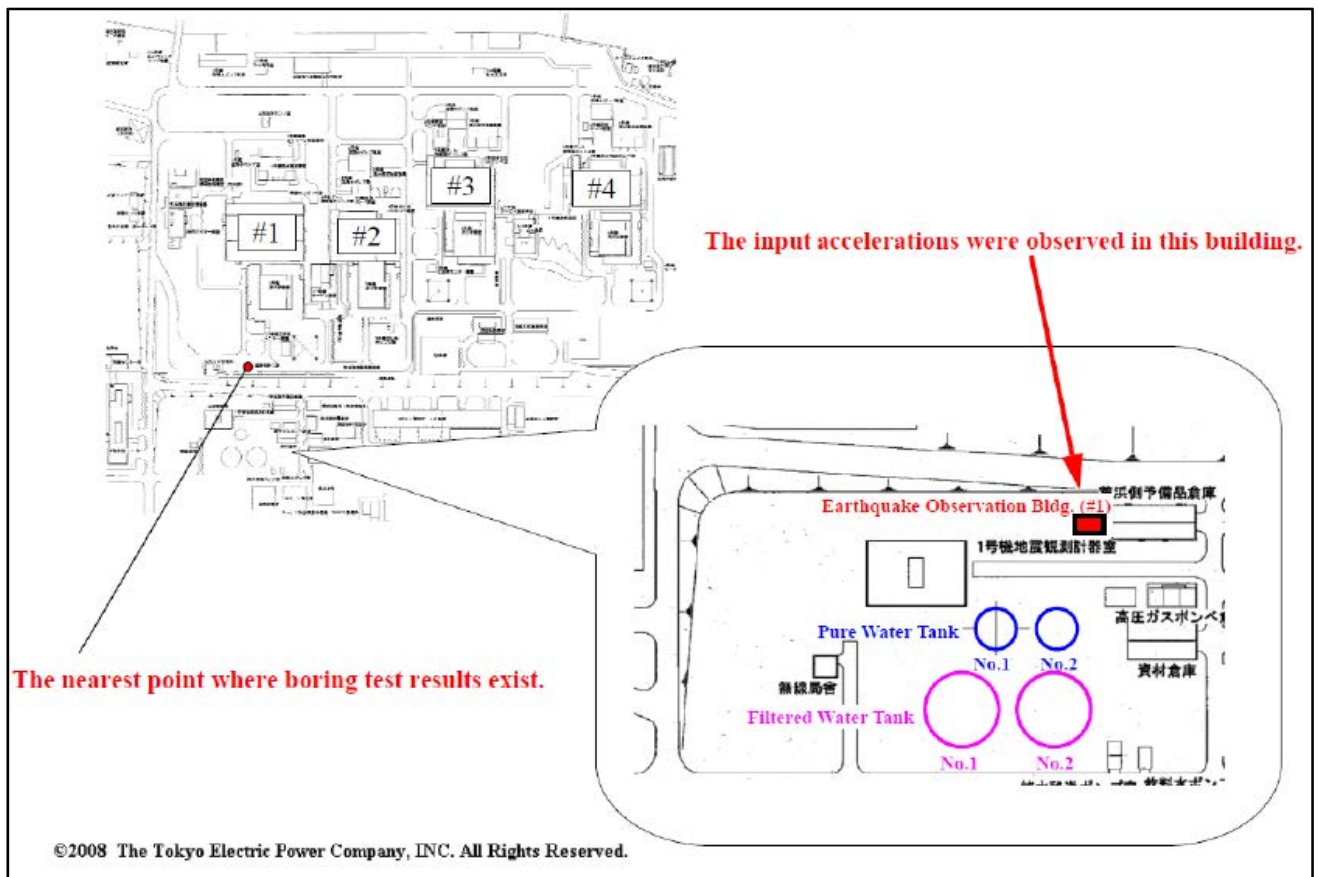


FIG. 15. Location of pure water tank

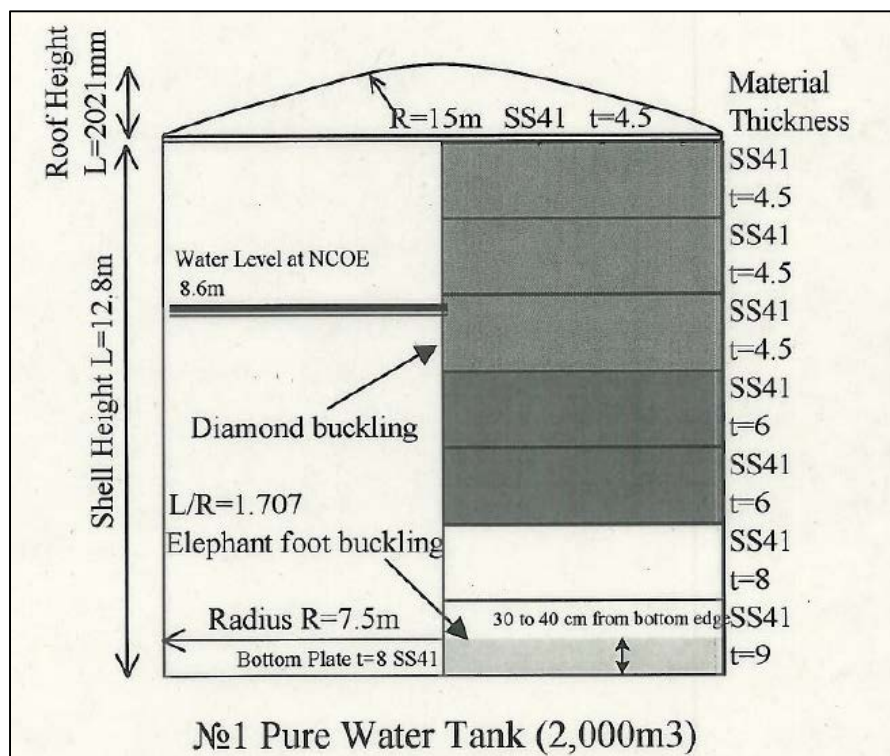


FIG. 16. Dimension of pure water tank.

2.4.2. Recorded NCO earthquake signals

2.4.2.1. Structure

The NCO earthquake signals recorded by the seismic instrumentation installed in the free field at K-K NPP site and in the reactor building structure of Unit 7 were used as input for the benchmark exercise. Locations of seismometers on free field and boreholes are shown in Fig. 17. Positions of seismometers in Unit 7 on the 3rd basemat (TMSL -8.2m) and the 3rd Floor (TMSL +23.5m) are shown in Fig. 18.

i. Phase I

The following recorded signals at the free field (5-G1) and in borehole 5 (G51-G55) were used:

- Main shock: 16th July 2007, 10:13 (Mw=6.6, Mj=6.8, R=16 km)³;
- Aftershock I: 16th July 2007, 15:37 (Mj=5.8, R=8.7 km);
- Aftershock II: 16th July 2007, 17:42 (Mj=4.2, R=4.2 km);

The first aftershock corresponds to the strongest recorded aftershock. The second aftershock is one of the low level aftershocks during which the soil behaviour is expected to be linear. The maximum accelerations of the recorded signals are presented Table 3.

Acceleration time histories are available for the main shock at the free field surface station, 5-G1. The time histories of accelerations in the borehole G5 have been lost for the main shock while only the peak ground accelerations are available.

The free field station 5-G1 is located near Unit 5; borehole G5 is located close to 5-G1 and is equipped with 5 in-hole seismometers G51, G52, G53, G54 and G55, respectively at depths 2.7m, 36.0m, 112.0m, 192.0m and 312.0m below the surface.

Since original recorded signals cover longer duration, relevant segment of 20 sec of each signal has been selected to be used for the analyses. For the main shock and aftershock I, data from 29 sec to 49 sec of the original signals were used. For aftershock II, data from 27 sec to 47 sec of the original signals were used. For the benchmark purpose, all input signals were provided in the global plant system as defined in Section 2.4.1.1 (See Figs 11 and 12).

³ R: Distance from epicentre of the earthquake to K-K NPP site

Mj: Local magnitude defined and calculated by Japan Meteorological Agency (JMA).

Mw: Moment magnitude

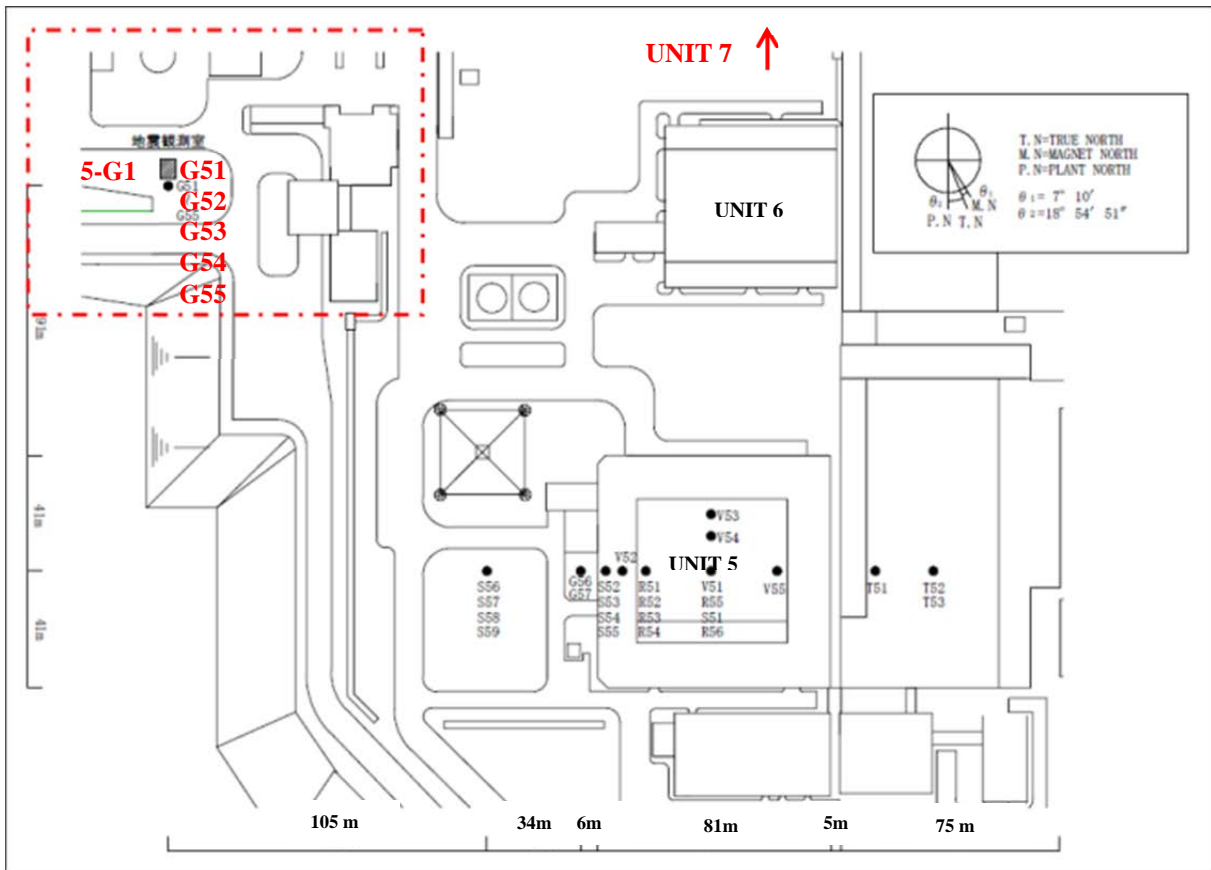


FIG. 17. Locations of seismometers: on free field (5-G1) and borehole (G51-G55).

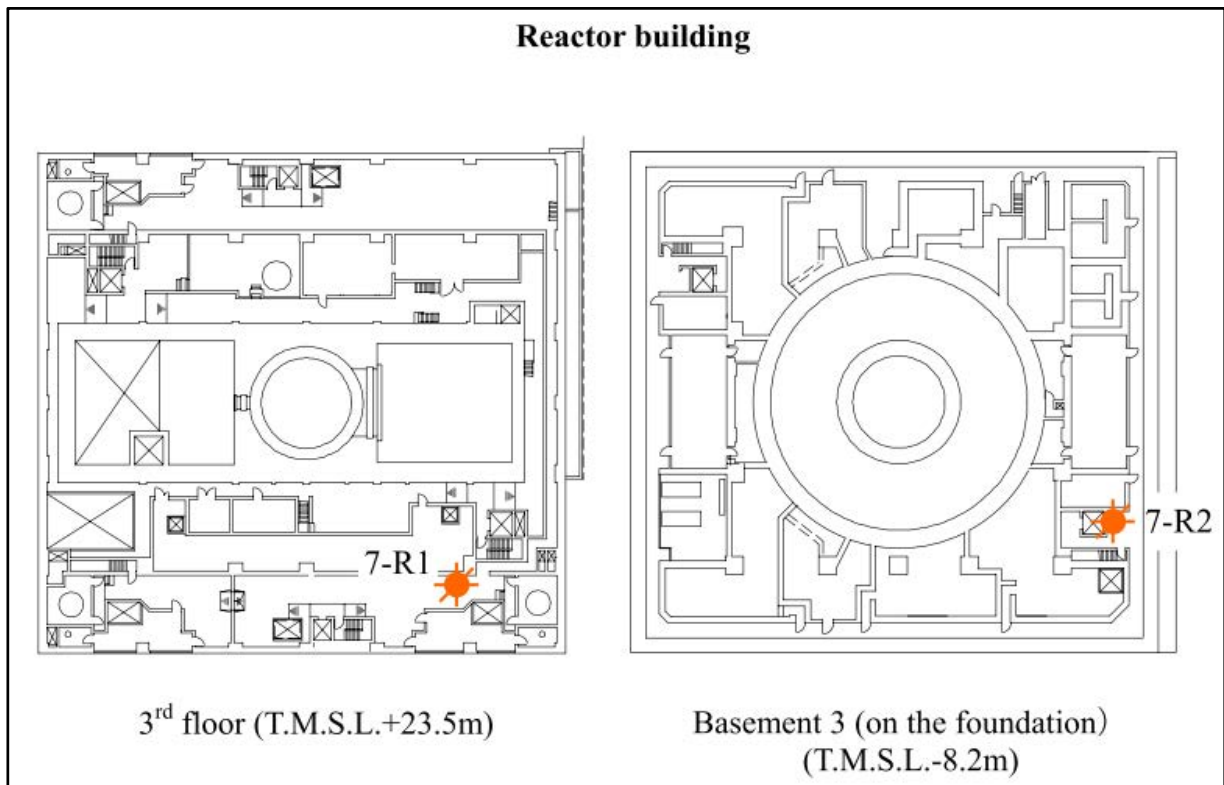


FIG. 18 Locations of seismometers in the reactor building of Unit 7 on 3rd Basemat and 3rd Floor.

TABLE 3. MAXIMUM ACCELERATION OF SIGNALS USED IN ANALYSES

		Maximum acceleration value observed (Gal)		
		N-S	E-W	UD
Mains shock NCOE signals	FreeField_5-G1 (TMSL+12.3m)	963.83	1222.75	538.72
	RB7 3rd Basement (TMSL-8.2m) (on foundation)	267.00	356.00	355.00
	RB7 3rd Floor (TMSL+23.5m)	367.00	435.00	464.00
Aftershock signals I (16th July, 15:37)	FreeField_5-G1 (TMSL+12.3m)	386.00	362.00	108.00
	RB7 3rd Basement (TMSL-8.2m) (on foundation)	170.16	134.50	73.63
	RB7 3rd Floor (TMSL+23.5m)	208.00	167.00	103.00
	Borehole 5 - G51 (T.M.S.L. +9.3m)	217.00	275.00	97.40
	Borehole 5 - G52 (T.M.S.L. -24.0m)	152.98	105.38	53.10
	Borehole 5 - G53 (T.M.S.L. -100.0m)	119.19	92.91	32.00
	Borehole 5 - G54 (T.M.S.L. -180.0m)	131.63	92.13	32.50
	Borehole 5 - G55 (T.M.S.L. -300.0m)	122.11	108.77	51.20
Aftershock signals II (16th July, 17:42)	FreeField_5-G1 (TMSL+12.3m)	106.00	82.00	36.00
	RB7 3rd Basement (TMSL-8.2m) (on foundation)	15.00	13.00	10.00
	RB7 3rd Floor (TMSL+23.5m)	15.33	15.08	15.35
	Borehole 5 - G51 (T.M.S.L. +9.3m)	39.00	43.00	25.00
	Borehole 5 - G52 (T.M.S.L. -24.0m)	31.01	24.98	10.00
	Borehole 5 - G53 (T.M.S.L. -100.0m)	21.64	27.00	9.00
	Borehole 5 - G54 (T.M.S.L. -180.0m)	14.29	22.59	11.00
	Borehole 5 - G55 (T.M.S.L. -300.0m)	13.58	18.58	6.00

ii. Phase II

Signals derived at the outcrop of engineering bedrock (TMSL -155m) compatible with NCOE main shock records in the X, Y and Z directions were used as shown in Fig. 19. Engineering bedrock outcrop level is the one at which the design basis ground motion was derived for the design of Unit 7. Corresponding time histories were provided. Response spectra of the signals are given in Fig. 20.

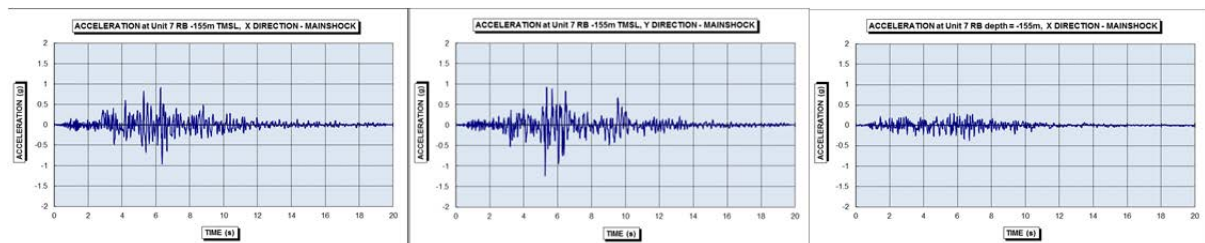


FIG. 19. Signals derived at the outcrop of engineering bedrock (TMSL -155m) compatible with NCOE main shock records in the X, Y and Z directions.

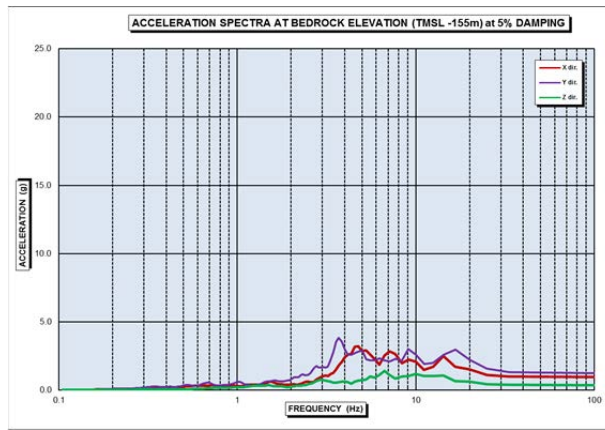


FIG. 20. Response spectra of the signals derived at the outcrop of engineering bedrock (TMSL - 155m).

iii. Phase III

Signals derived at the Outcrop of the Raft Elevation (ORE) and at the Outcrop of the Engineering Bedrock elevation (OEB) corresponding to 1*NCOE, 2*NCOE, 4*NCOE and 6*NCOE were provided to the participants. Corresponding time histories and response spectra were provided (Figs 21 and 22).

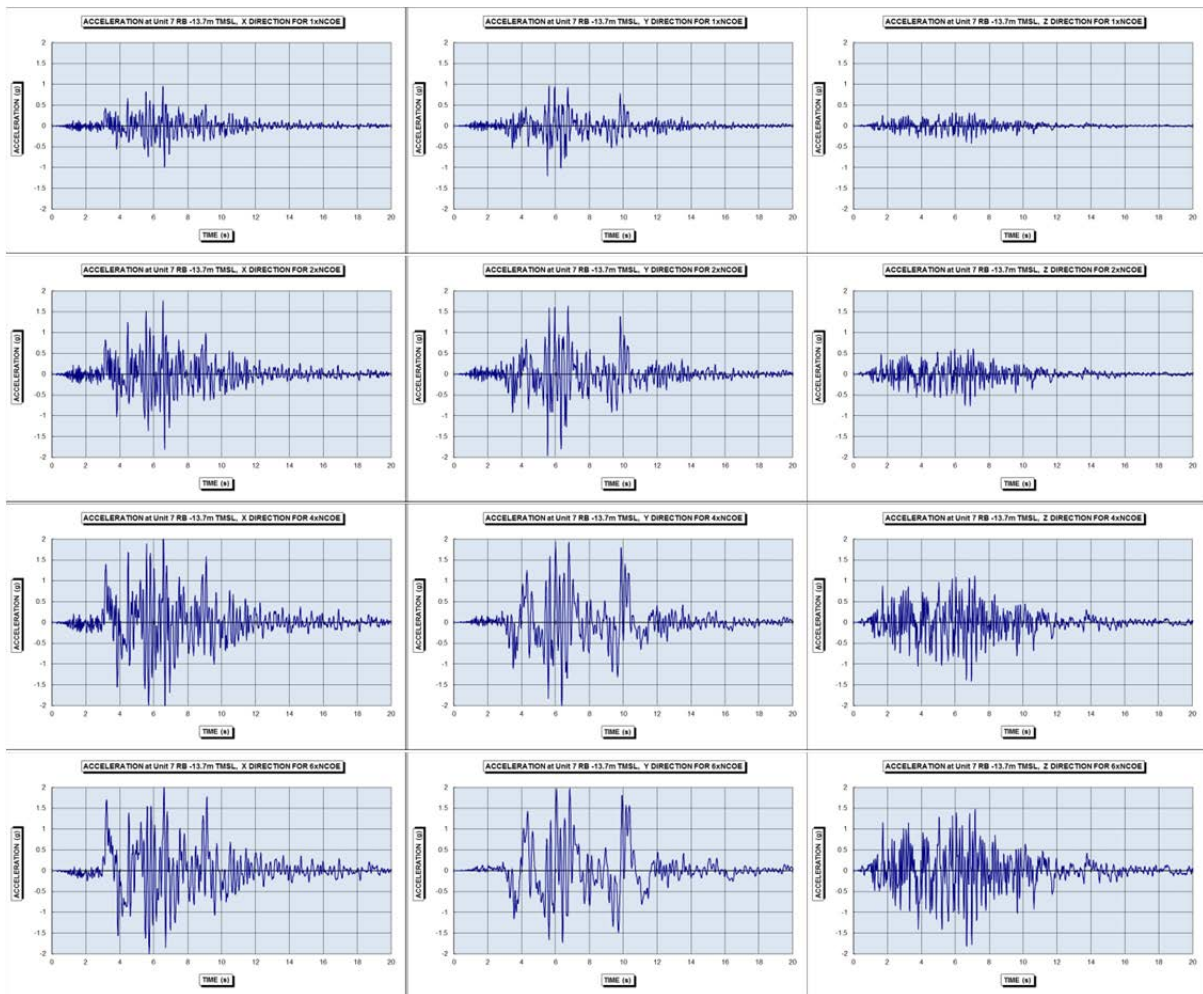


FIG. 21. Signals derived at the Outcrop of the Raft Elevation (TMSL -13.7m) compatible with 1*NCOE, 2*NCOE, 4*NCOE and 6*NCOE in the X, Y and Z directions.

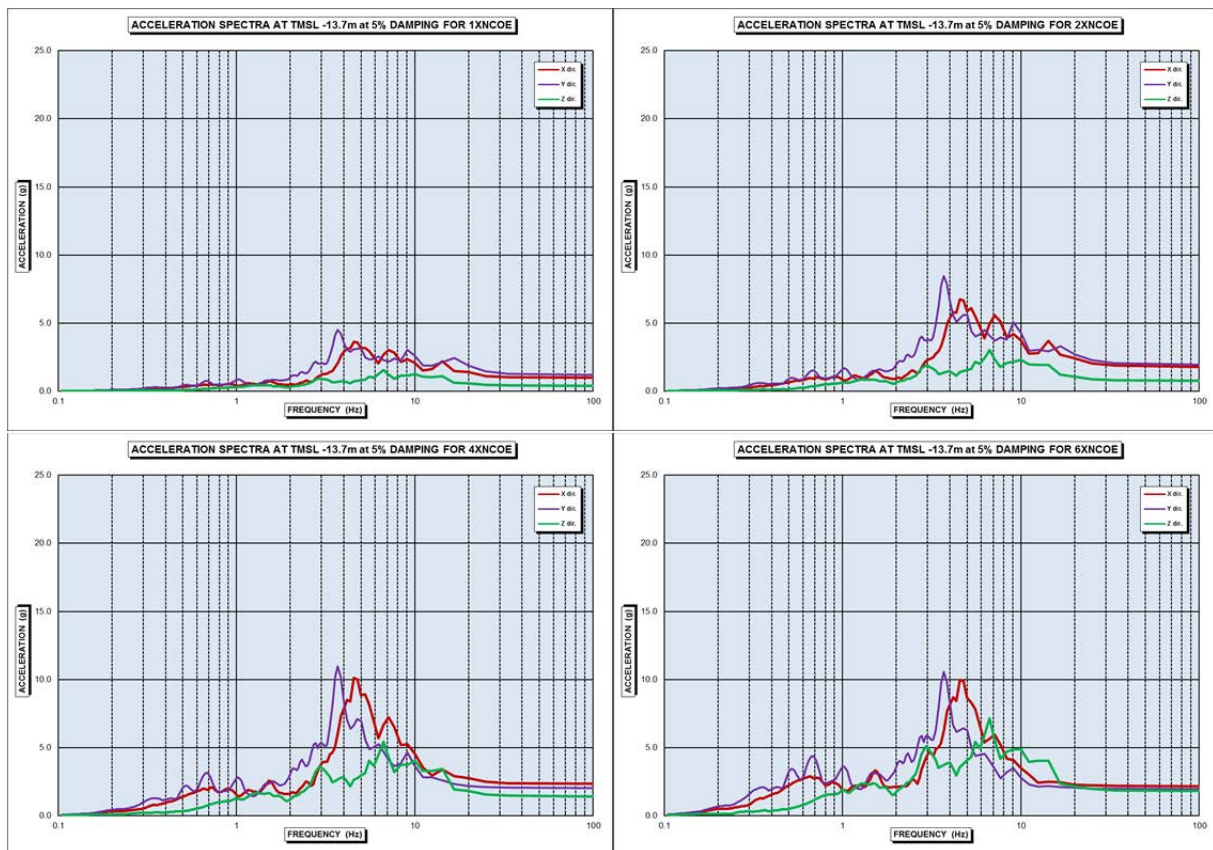


FIG. 22. Response spectra of the signals derived at the Outcrop of the Raft Elevation (TMSL -13.7m) compatible with 1*NCOE, 2*NCOE, 4*NCOE and 6*NCOE in the X, Y and Z directions.

2.4.2.2. RHR Piping system

i. Phase I and II

Data from 5 sec to 25 sec (20 sec duration) of acceleration time histories obtained by simulation provided by TEPCO (at TMSL 12.3m, 3 directions, NS (X direction), EW (Z direction) and UD (Y direction)) were used.

ii. Phase III

RHR piping system supports are attached to the following structures and components: RPV, RPV pedestal, RCCV, DEPSS and RSW. DEPSS and RSW are assumed to have the same movement. All the supports are included in four groups according to the structures and components they are attached to; all supports in one group are assumed to have identical movement for the multi-support analysis. Four points, N1, 31N, 37 and 84 represent Group 1 (RPV), Group 2 (RCCV), Group 3 (DEPSS and RSW) and Group 4 (RPV pedestal) respectively.

Input signals at four points (N1, 31N, 37, 84) (in the X, Y, and Z directions) in terms of acceleration obtained from best estimate analyses⁴ of the structure (See Section 2.5.1.2) were provided to the participants.

⁴ In this document, best estimate analysis refers to the soil column calculated by individual participants.

2.4.2.3. Spent fuel pool

i. Phase I and II

Recorded acceleration time histories at TMSL 23.5 m during the NCOE (3 directions, NS, EW and UD) and simulated acceleration time histories provided by TEPCO at TMSL 18.1 m and TMSL 31.7 m were used. Data from 30 sec to 60 sec (30 sec duration) of these signals (3 directions, NS (X direction), EW (Y direction) and UD (Z direction)) were used.

2.4.2.4. Pure water tank

i. Phase I

Recorded acceleration time histories, at the station 1-G1 which is the closest one, during the NCOE (3 directions, NS, EW and UD) were used. They are considered as free field signals. Data from 30 sec to 60 sec (30 sec duration) of these recorded signals (3 directions, NS (X direction), EW (Y direction) and UD (Z direction)) were used.

2.4.3. Soil properties for site response and soil-structure interaction analyses of the reactor building

i. Phase I

Soil properties near K-K Unit 7, i.e. geological conditions, initial shear wave velocity, unit weight, Poisson ratio and initial shear modulus, is presented in Table 4.

The soil properties along Unit 5 free field (borehole G5) are given in Table 5 and Fig. 23. The borehole is 312m deep. The surface is located at TMSL 12.0m and the water table at TMSL 7.0m. The Yasuda layer extends from the surface down to TMSL -16.6m. It mainly consists of clay with a shear wave velocity (V_s) ranging from 160m/s to 390m/s. Further down, the Nishiyama layer is made of soft rock with a shear wave velocity of the order of 500m/s. Finally, the substratum, called the Shiiya layer, consists of rock. The shear wave velocity exceeds 660 m/s and reaches 870m/s at the bottom of the borehole (TMSL -300m). In addition positions of seismometers in the borehole are presented in Fig. 23.

Strain dependent G/G_0 and damping ratio for sand, clay and rock were also provided to participants (Fig. 24).

TABLE 4. SOIL PROPERTIES (NCOE) NEAR UNIT 7 REACTOR BUILDING⁵

Attitude T.M.S.L. (m)	Geological Layer	Soil type (Sand, clay or rock)	Shear Wave Velocity Vs (m/s)	Shear wave damping (%)	Primary Wave Velocity Vp (m/s)	Primary wave damping (%)	Unit Weight γ (kN/m ³)	Poisson's Ratio ν	Initial Shear Modulus G0 (kN/m ²)
Grade Level (+12.0)	Sand	Sand	150		310		16.1	0.347	36,000
+8.0		Sand	200		380		16.1	0.308	65,700
+4.0	Yasuda	Clay	330		1240		17.3	0.462	192,000
-6.0	Nishiyama	Rock	490		1640		17.0	0.451	416,000
-33.0		Rock	530		1700		16.6	0.446	475,000
-90.0		Rock	590		1710		17.3	0.432	614,000
-136.0		Rock	650		1790		19.3	0.424	832,000
-155.0		Rock	720		1900		19.9	0.416	1,050,000
The free surface of the ∞	Nishiyama	Rock	720		1900		19.9	0.416	1,050,000

⁵ "Rock" designation is coming from Japanese terminology and is not consistent with IAEA safety standard.

TABLE 5. SOIL PROPERTIES (NCOE) – UNIT 5 FREE FIELD

Attitude T.M.S.L. (m)	Geological Layer	Soil type (Sand, clay or rock)	Shear Wave Velocity Vs (m/s)	Shear wave damping (%)	Primary Wave Velocity Vp (m/s)	Primary wave damping (%)	Unit Weight γ (kN/m ³)	Poisson's Ratio ν	Initial Shear Modulus G0 (kN/m ²)
Grade Level (+12.0) +2.0	Yasuda stratum	Clay	160		1380		17.3	0.462	50,000
		Clay	390		1520		17.3	0.462	260,000
-16.6	Nishiyama stratum	Rock	500		1730		17.0	0.451	420,000
-33.0		Rock	540		1750		16.6	0.446	475,000
-66.0		Rock	550		1780		16.9	0.440	510,000
-89.2	Shiïya stratum	Rock	660		1930		19.3	0.416	900,000
-120.0		Rock	770		2000		19.9	0.416	1,100,000
-149.0		Rock	840		2020		19.9	0.416	1,400,000
-231.0		Rock	860		2120		19.9	0.416	1,470,000
-266.0		Rock	870		2290		19.9	0.416	1,500,000
-300.0									

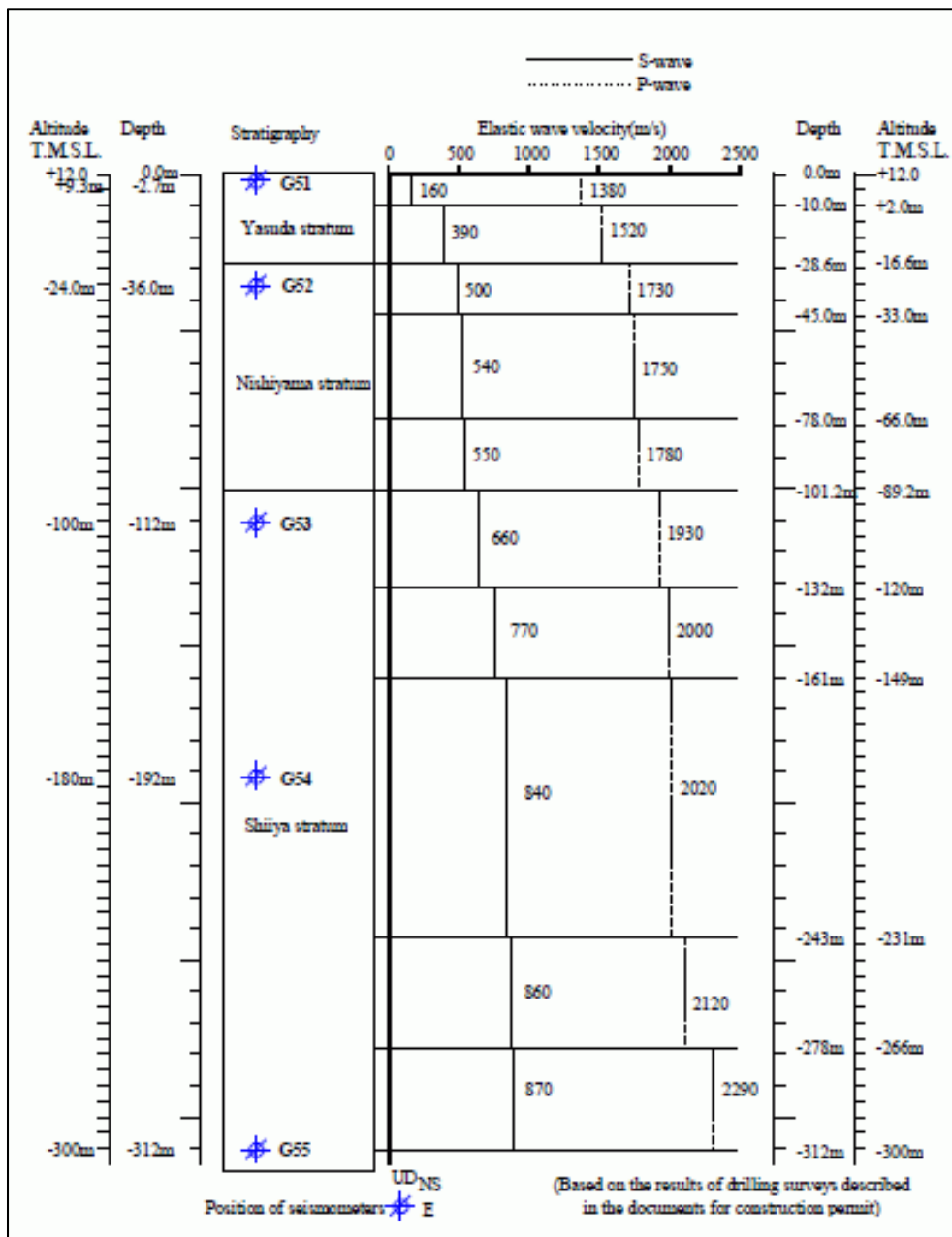


FIG. 23. Outline of Unit 5 free field vertical array.

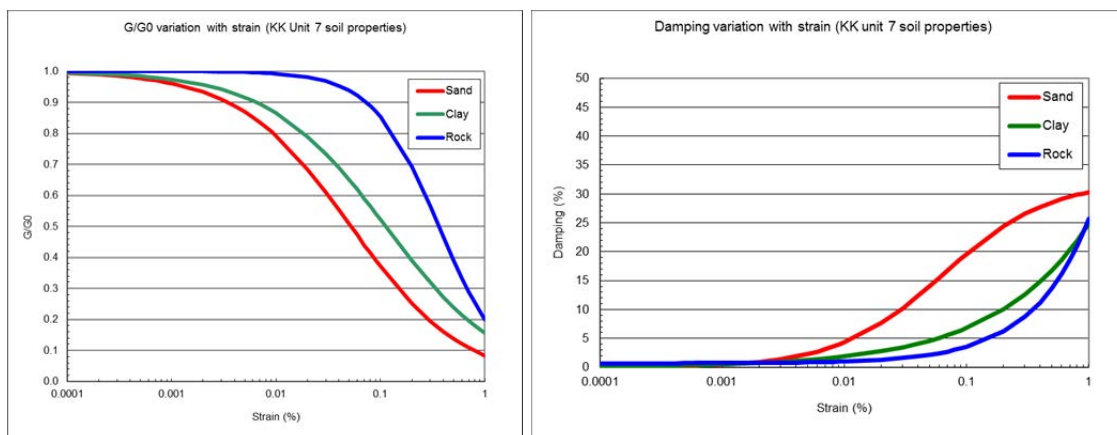


FIG. 24. Strain dependent G/G_0 and damping ratio for soil properties.

ii. Phase II

For “reference analysis”, soil profile under the Unit 7 was used as standard soil profile at low strain. Modified nonlinear curves of sand and clay were provided to participants (Fig. 25). Two types of soil data, strain compatible shear modulus (G) values and damping ratios during the NCOE, were provided: “Baseline1” and “Baseline 2”. These data had to be used directly in a model with linear soil behaviour. These data have been defined from specific soil analyses by external expert. Strain dependence of G/G_0 and damping was modified from TEPCO data in order to take into account the effect of confining pressure. “Baseline 2” soil data are more representative of soil profile under the Unit 7. Strain compatible G/G_0 , damping, and strain values along the depth for the soil profile under Unit 7 during the NCOE are presented in Fig. 26.

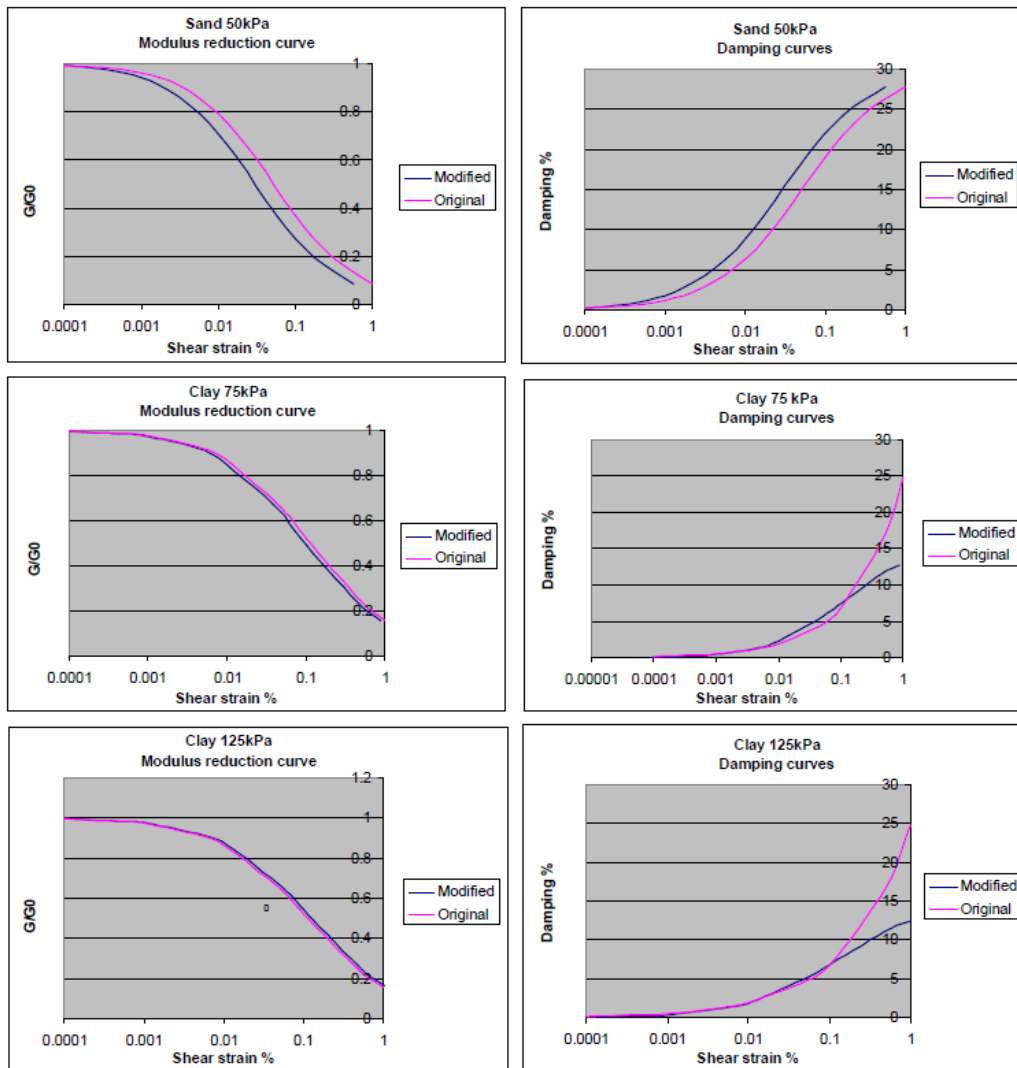


FIG. 25. Modified nonlinear curves of sand and clay.

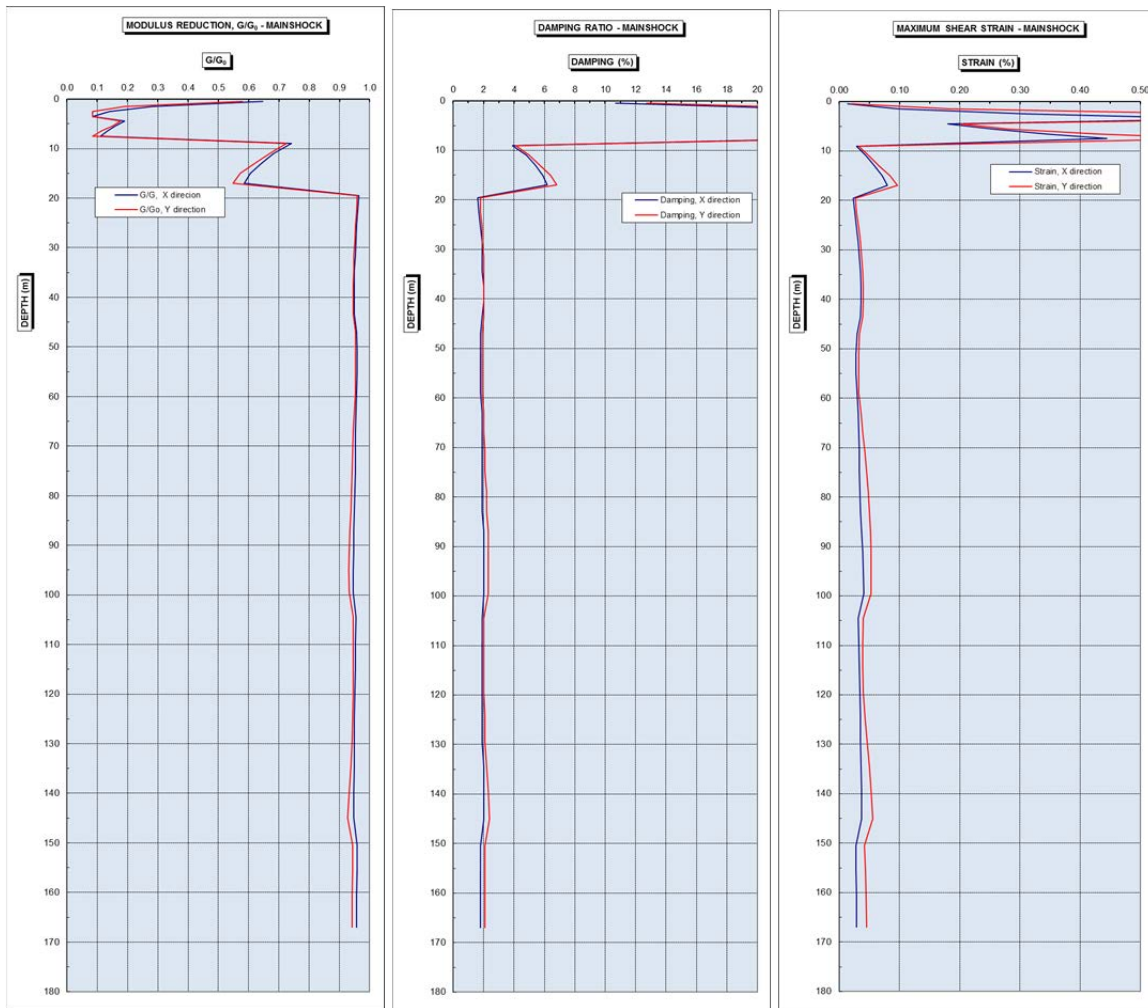


FIG. 26. Strain compatible G/G_0 , damping and strain values along the depth for the soil profile under Unit 7 during the NCOE.

iii. Phase III

Soil column analyses under increased input signal (2*NCOE, 4*NCOE and 6*NCOE) were performed by an external expert. For each input level, strain compatible G values and damping ratios were derived. These data were used in different subtasks of Phase III; they can be used directly in a model with linear soil behaviour.

Resulting strain compatible G/G_0 , damping and strain values along the depth for the soil profile under Unit 7 for 2*NCOE, 4*NCOE and 6*NCOE are presented in Figs 27, 28 and 29, respectively.

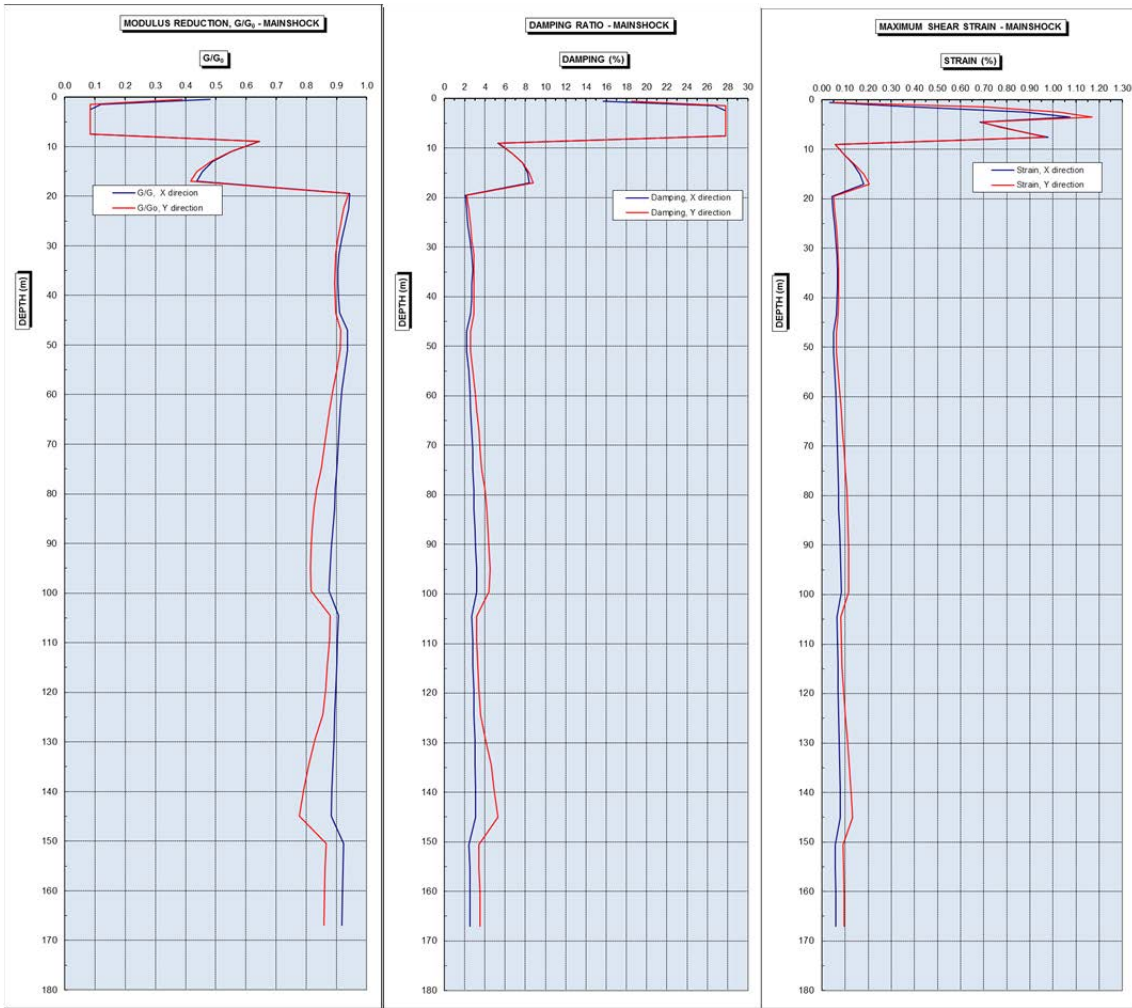


FIG. 27. Strain compatible G/G_0 , damping and strain values along the depth for the soil profile under the Unit 7 for $2 \cdot NCOE$.

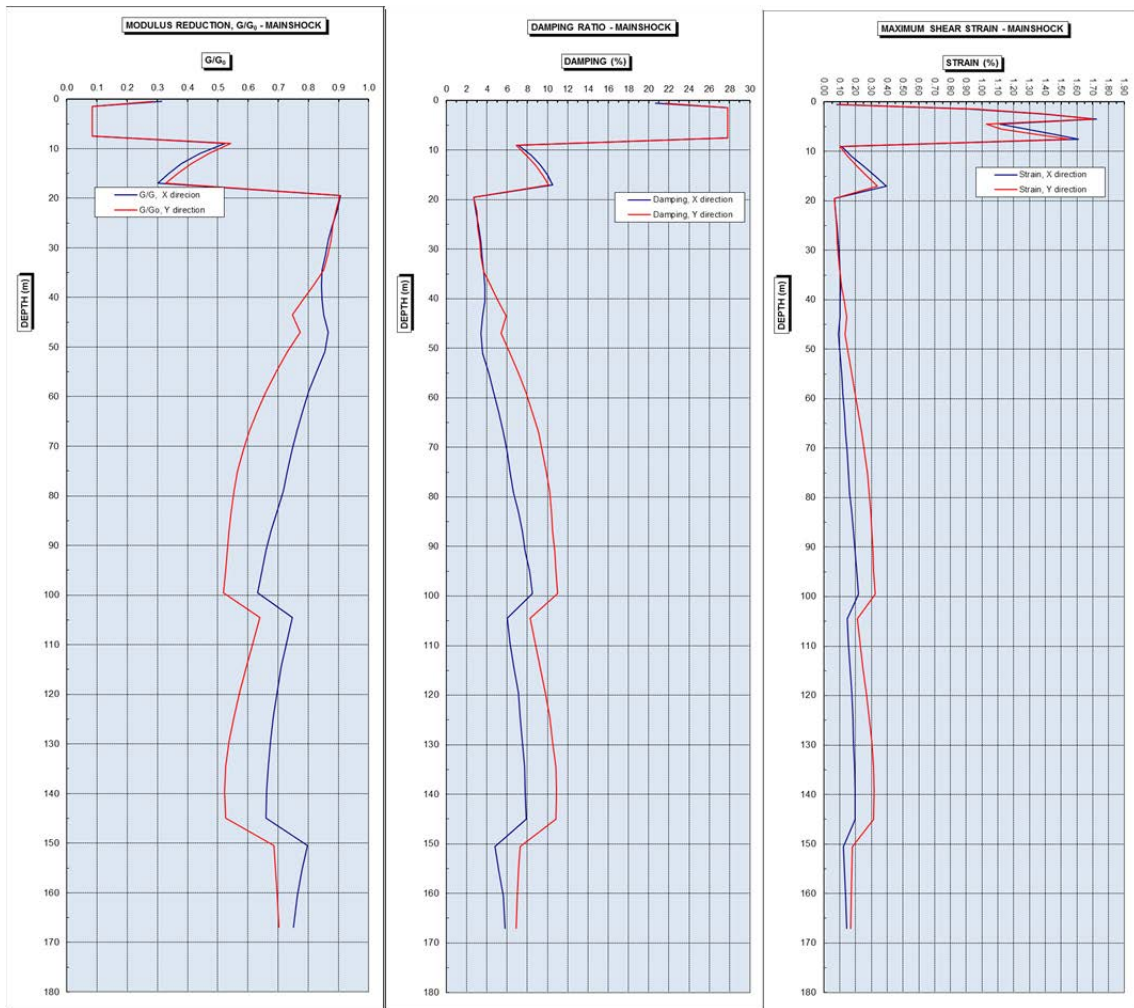


FIG. 28. Strain compatible G/G_0 , damping and strain values along the depth for the soil profile under the Unit 7 for $4 \cdot NCOE$.

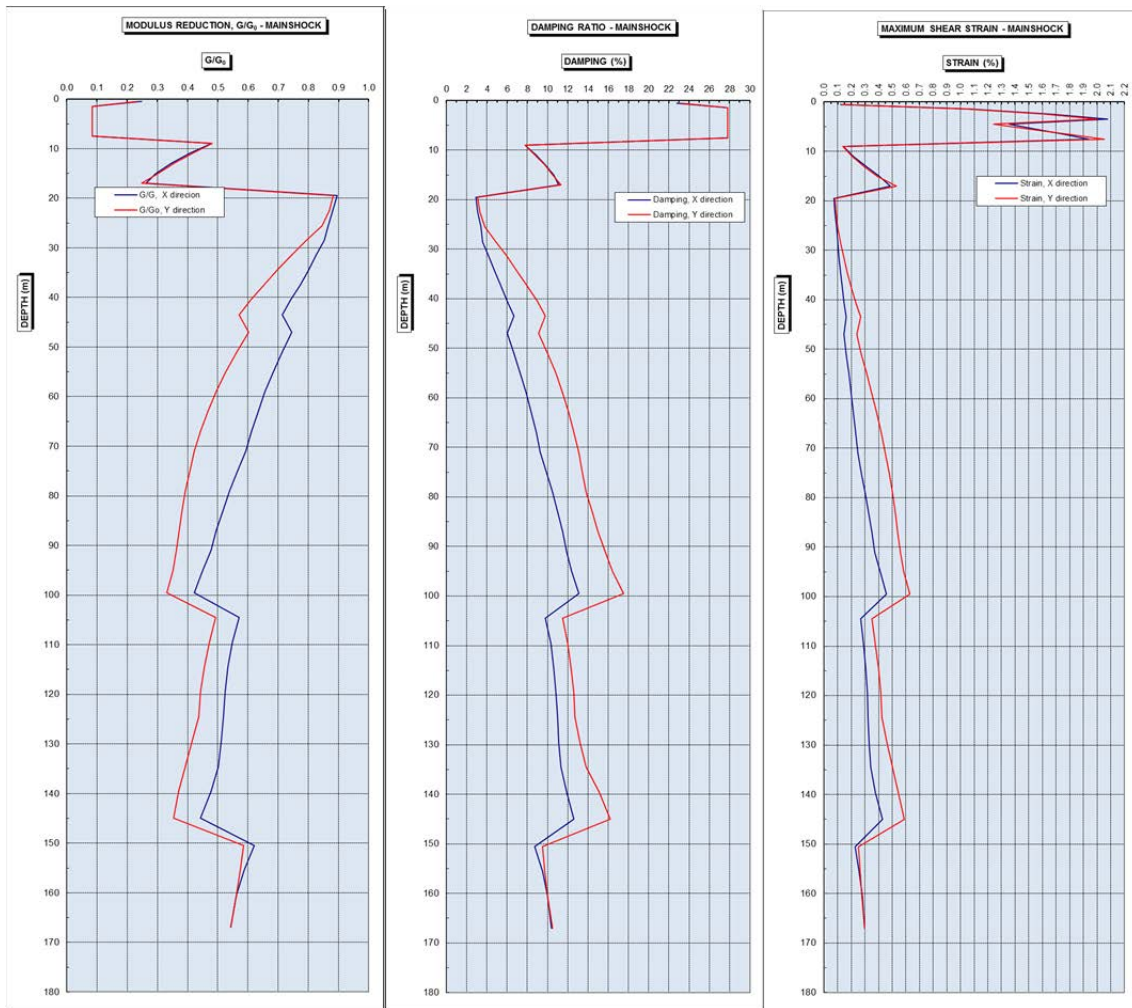


FIG. 29. Strain compatible G/G_0 , damping and strain values along the depth for the soil profile under the Unit 7 for $6*NCOE$.

2.5. BENCHMARK REQUESTED ANALYSIS

The analyses results from each participant needed for performing the benchmark are obtained in three phases, see Table 6. More detailed presentation of the scope of the three phases is given in the following sub-sections.

Results templates have been developed for each task and phase to collect participants' results, see section 2.3.1.

Input data (signals, soil properties, characteristics of the structures etc.) required to perform the requested seismic analyses is specified in Section 2.4.

Locations where the global parameters results are requested are given in Appendix H of the Guidance Document [5].

2.5.1. Part 1 Structure

2.5.1.1. Phase I: Task 1.1 Construction and validation of the soil and structure models

The following analyses have been requested:

- Subtask 1.1.1- Static and modal analyses of the fixed base model;
 - A. Static analysis of the fixed base model under vertical loads (weight);
 - B. Static analysis of the fixed base model under horizontal forces;
 - C. Modal analysis of the fixed base model;
- Subtask 1.1.2- Soil Column Analysis;
 - A. Soil Column Analysis under After-shock I (16th July, 15:37);
 - B. Soil Column Analysis under After-shock II (16th July, 17:42);
 - C. Soil Column Analysis under Main shock;
- Subtask 1.1.3- Analysis of the complete model;
 - A. Modal Analysis;
 - B. Frequency Domain Analysis;

Participants were free to construct the model and to choose the control point and type of analysis (linear or non-linear soil behaviour). For soil column analysis, the participants used data from the free field station 5-G1 and from borehole G5.

2.5.1.2. Phase II: Task 1.2 Main shock response

The objective of this task was to simulate the response of K-K reactor building under the NCO earthquake using the model developed in Phase I. The following analyses have been requested:

- Subtask 1.2.1- “Reference Analysis” of the Soil-Structure Model;
 - A. Modal analysis of the soil-structure model;
 - B. Frequency domain/Time domain analysis of the soil-structure model;
- Subtask 1.2.2- “Best estimate analysis” of the soil-structure model;
 - A. Modal analysis of the soil-structure model;
 - B. Frequency domain/Time domain of the soil-structure model;
- Subtask 1.2.A NCOE response data for RHR piping system;

“Reference analysis” consists of the analysis of the soil-structure model under signals defined at outcrop of engineering bedrock (-155m TMSL) compatible with NCOE main shock records using calculated strain compatible G values and damping ratios compatible with the NCOE ground motion and provided by the secretariat.

Analysis of the soil-structure model under signals defined at outcrop of engineering bedrock (-155m TMSL) compatible with NCOE main shock records using standard soil characteristics were requested. Reference analysis was carried out for “Baseline 1” and “Baseline 2” soil conditions.

In the “Best estimate analysis”, participants were free to use any provided data, specially input signals or soil profile.

Requested analysis results are: relative displacement of the centre of the bottom of the basemat, absolute acceleration and corresponding response spectrum at key locations in the structure.

The Subtask 1.2.A was related to equipment behaviour; some complementary results from the structural analysis under the NCOE were needed. They constituted the NCOE response data for the RHR piping system:

- Task 1.2.A NCOE response data for RHR piping system: it was planned to calculate the response of the pipe subjected to movements of supports deduced from the

analysis of the R/B during the NCOE. The movements in different supports vary according to the supporting structure and the position of support; a comparison with uniform excitation applied during Phase I of the RHR piping case, as performed routinely for design.

2.5.1.3. Phase III: Task 1.3 Margin Assessment

The following analyses have been requested;

- Subtask 1.3.1. Pushover Analysis;
 - A. Fixed-base structure model;
 - B. Soil-structure interaction model;
- Subtask 1.3.2. Dynamic response analysis;
 - A. Fixed-base structure model;
 - B. Soil-Structure interaction model with reference soil properties;
 - C. Soil-Structure interaction model with best-estimate conditions.

For Subtask 1.3.1 Pushover Analysis, non-linear behaviour must be captured by models. The load function was generated by uniform distribution of horizontal accelerations. Uniform horizontal load should have been applied from lower level of the raft elevation to the roof (top). The following analyses would be performed:

- Subtask 1.3.1.A. Fixed-base structure model: definition of capacity curves under the uniform horizontal load function. In addition, determination of performance points corresponding to free field time-histories input motion defined at an outcrop of the raft elevation (ORE) corresponding to 1*NCOE, 2*NCOE, 4*NCOE and 6*NCOE. Corresponding time histories and response spectra were provided to the participants. In this part, it was expected that the structure would have non-linear behaviour;
- Subtask 1.3.1.B. Soil-structure interaction model: definition of capacity curves under the uniform horizontal load function. In addition, determination of performance points corresponding to free field time-histories input motion defined at an outcrop of the raft elevation (ORE) corresponding to 1*NCOE, 2*NCOE, 4*NCOE and 6*NCOE. Corresponding time histories and response spectra were provided to the participants. In this part, it was expected that the structure and soil would have non-linear behaviour.

Two separate analyses in the two horizontal directions would be performed.

For Subtask 1.3.2 Dynamic response analysis, the following cases were considered:

- Subtask 1.3.2.A. Fixed-base structure model, with the free field time-histories input motion defined at an outcrop of the raft elevation (ORE) corresponding to 1*NCOE, 2*NCOE, 4*NCOE and 6*NCOE. Corresponding time histories were provided to the participants. In this part, it was expected that the structure would have non-linear behaviour. The input corresponding to three directions would be applied simultaneously;
- Subtask 1.3.2.B. Soil-Structure interaction model, with the free field time-histories input motion defined at an outcrop of the engineering bedrock elevation (OEB) corresponding to 1*NCOE, 2*NCOE, 4*NCOE and 6*NCOE. The soil properties were the standard values determined by the geotechnical consultant for the defined input levels. The input corresponding to three directions would be applied simultaneously;

- Subtask 1.3.2.C. Soil-Structure interaction model as above with best-estimate conditions defined by participants. The input corresponding to three directions would be applied simultaneously.

Story drift would be used as a damage indicator, as it is global and simple. However, each participant might propose their own damage indicators.

2.5.2. Part 2 Equipment

2.5.2.1. Task 2.1 RHR piping system analyses

The objective of this task was to carry out an exercise in order to quantify the effects of different analytical approaches on the response of the RHR piping system.

i. Phase I: Subtask 2.1.1 Initial analyses

Phase I of the RHR piping system analyses were modelling, modal analysis and response analysis to uniform excitation under given input signal; permanent loads would be added. The following analyses have been requested:

- A. Static analysis under vertical loads (weight) + pressure;
- B. Modal analysis of the RHR piping system;
- C. Response spectrum analysis;
- D. Time history analysis.

ii. Phase II: Subtask 2.1.2 Analyses with modified support conditions

It was requested to carry out the same analyses as the ones in Phase I with modified support conditions. Clarifications for three support points were provided to participants and the following analyses have been requested:

- A. Static analysis under vertical loads (weight) + pressure;
- B. Modal analysis of the RHR piping system;
- C. Response spectrum analysis;
- D. Time history analysis.

iii. Phase III: Subtask 2.1.3 Multi-support motion analysis

The following analyses have been requested:

- A. Response spectrum analysis using enveloped response spectra developed from the four input motions;
- B. Multi-support motion response spectrum analysis using four input motions;
- C. Multi-support motion time history analysis using four input motions;
- D. Assessment of seismic margin of the RHR piping system.

2.5.2.2. Task 2.2 Sloshing of the Spent Fuel Pool

i. Phase I: Subtask 2.2.1 Initial analyses

The objective was to estimate the sloshing frequencies, maximum wave height and spilled water amount, and to predict free surface evolution. The following analyses have been requested:

- A. Modal analysis of the sloshing;
- B. Estimation of the maximum wave height assuming no water spill;
- C. Estimation of spilled water amount during the NCOE;
- D. Free surface evolution.

ii. Phase II: Subtask 2.2.2 Complete analysis of spilled water

It was requested to re-upload results with complete analysis of spilled water. Detailed descriptions of fluid model and of the methodology used for the determination of the spilled water amount were requested. The following analyses have been requested:

- A. Modal analysis of the sloshing;
- B. Estimation of the maximum wave height assuming no water spill;
- C. Estimation of spilled water amount during the NCOE;
- D. Free surface evolution (if available).

2.5.2.3. Task 2.3 Pure water tank buckling

i. Phase I: Subtask 2.3.1 Initial analyses

The objective was to predict the observed buckling modes of the pure water tank. The following analyses have been requested:

- A. Modal analysis of the tank;
- B. Response spectrum analysis of the pure water tank;
- C. Time history analysis of the pure water tank;
- D. Buckling estimation.

TABLE 6. TASK MATRIX OF THE KARISMA BENCHMARK

Parts	Phase I	Phase II	Phase III
Part 1 Structure	<p>Task 1.1 Construction and validation of the soil and structure models</p> <p>1) Subtask 1.1.1. Static and modal analyses of the fixed base model</p> <p>A. Static analysis of the fixed base under vertical loads (weight)</p> <p>B. Static analysis of the fixed base model under horizontal forces</p> <p>C. Modal analysis of the fixed base model</p> <p>2) Subtask 1.1.2. Soil column analyses</p> <p>A. Soil Column Analyses under Aftershock I (16th July, 15:37)</p> <p>B. Soil Column Analyses under Aftershock II (16th July, 17:42)</p> <p>C. Soil Column Analyses under Mainshock</p> <p>3) Subtask 1.1.3. Analysis of the complete model</p> <p>A. Modal Analysis</p> <p>B. Frequency Domain Analyses</p>	<p>Task 1.2 Main shock response</p> <p>1) Subtask 1.2.1 Reference Analysis of the Soil-Structure Model</p> <p>A. Modal analysis of the soil-structure model</p> <p>B. Frequency domain/Time domain analysis of the soil-structure model</p> <p>2) Subtask 1.2.2 Best estimate analysis of the soil-structure model</p> <p>A. Modal analysis of the soil-structure model</p> <p>B. Frequency domain/time domain analysis of the soil-structure model</p> <p>3) Subtask 1.2.3 Direct processing of the in-structure signals</p> <p>4) Subtask 1.2.A NCOE Response data for RHR Piping System Analysis</p>	<p>Task 1.3 Margin assessment</p> <p>1) Subtask 1.3.1. Pushover Analysis</p> <p>Subtask 1.3.1.A. Fixed base structure model</p> <p>Subtask 1.3.1.B. Soil-structure interaction model</p> <p>2) Subtask 1.3.2. Dynamic response analysis</p> <p>Subtask 1.3.2.A. Fixed base structure model</p> <p>Subtask 1.3.2.B. Soil-Structure interaction model</p> <p>Subtask 1.3.2.C. Soil-Structure interaction model as above with best-estimate conditions defined by participants (Optional).</p>
Task 2.1 RHR Piping System	<p>Subtask 2.1.1 Initial analyses</p> <p>A. Static analysis under vertical loads (weight) + pressure</p> <p>B. Modal analysis of the RHR piping system</p> <p>C. Response spectrum analysis</p> <p>D. Time history analysis</p>	<p>Subtask 2.1.2- Analyses with modified support conditions</p> <p>A. Static analysis under vertical loads (weight) + pressure</p> <p>B. Modal analysis of the RHR piping system</p> <p>C. Response spectrum analysis</p> <p>D. Time history analysis</p>	<p>Subtask 2.1.3 Multisupport analysis</p> <p>A. Response spectrum analysis using envelope response spectra developed from the four input motions.</p> <p>B. Multi-support response spectrum analysis using four input motion</p> <p>C. Multi-support time history analysis using four input motions</p>
Task 2.2 Sloshing of the Spent Fuel Pool	<p>Subtask 2.2.1 Initial analyses</p> <p>A. Modal analysis of the sloshing</p> <p>B. Estimation of maximum wave height assuming no water spill</p> <p>C. Estimation of spilled water amount during NCOE</p> <p>D. Free surface evolution</p>	<p>Subtask 2.2.2 Complete analysis of spilled water</p> <p>A. Modal analysis of the sloshing</p> <p>B. Estimation of maximum wave height assuming no water spill</p> <p>C. Estimation of spilled water amount during NCOE</p> <p>D. Free surface evolution (if available)</p>	-
TASK 2.3 Pure Water Tank Buckling	<p>Subtask 2.3.1 Initial analyses</p> <p>A. Modal analysis of the tank</p> <p>B. Response spectrum analysis of the pure water tank</p> <p>C. Time history analysis of the pure water tank</p> <p>D. Buckling estimation</p>	-	-
Part 2 Equipment			

3. ANALYSES OF THE MAIN RESULTS OF THE BENCHMARKING EXERCISE FOR PART 1 STRUCTURE

Benchmarking results for Part 1 “Structure” for Phases I, II and III are presented in tables and figures with corresponding evaluation and comments. Representative comparisons are presented in the body of the document; all results are presented in Annex V.

Statistical processing of the results was performed when it was appropriate: mean, standard deviation and COV (Coefficient of Variation) are presented in the tables. Maximum and minimum results were not included in mean, standard deviation and COV calculations in the tables with enough number of results.

3.1. MAIN RESULTS FOR TASK 1.1 OF PHASE I: CONSTRUCTION AND VALIDATION OF THE SOIL AND STRUCTURE MODELS

3.1.1. Subtask 1.1.1 Static and modal analyses of the fixed-base model

3.1.1.1. Model presentation

Types of models, model characteristics and calculation codes used by participants are presented in Table 7. Out of 18 participants, 15 participants used 3D finite element models and 4 participants used stick models (one used both 3D and stick model). Most of the used computer codes were commercial. The number of nodes for 3D models ranged from 2603 to 74780 with an average of 20000 nodes. Stick models have naturally a small number of nodes. Some typical models are shown in Fig. 30.

TABLE 7. PARTICIPANT MODEL PRESENTATION

PART 1 STRUCTURE: TASK 1.1- Construction and validation of the soil and structure models Subtask 1.1.1. Static and modal analysis of the fixed base model - Model Presentation					
No	Participant Organization	Type of model	Model characteristics (Number of nodes, elements)	Concrete Young's Modulus (MPa)	Calculation code
1	CNEA, Argentina	3D FEM	46274 nodes, 52371 elements	31300	ANSYS 12.1
2	CNPDC, China	Stick model	10 nodes, 9 beam elements	31300	Super-sap/ansys11.0
3	NNSA, China	3D FEM	9037 nodes, 5829 elements	31300	ANSYS 11.0
4	SNERDI-SNPTC, China	3D FEM	2603 nodes, 4406 elements	31300	ANSYS 11.0
5	FNS, Finland	3D FEM	5400 nodes, 6200 elements	30000	Abaqus/Standard-6.9
6	CEA&IRSN, France	3D FEM	4546 nodes, 6265 elements	31300	Finite Element code CAST3M (Version 2010)
7	EdF, France	3D FEM	12600 nodes, 14500 elements	31300	Code_Aster (STA9.6)
8	AREVA, Germany	3D FEM	19000 nodes	31300	Sofistik 25
9	VGB, Germany	3D FEM	12560 nodes, 15288 elements	31300	Femap with NX Nastran 10.1
10	SPI, Germany	Stick model	123 nodes, 120 elements	31300	SOFiStiK, Version 23
11	AERB, India Model 1	3D FEM	16297 nodes, 16686 elements	30000	ANSYS
	AERB, India Model 2	Stick model	44 nodes,	31300	ANSYS
12	BARC, India	3D FEM	41901 nodes, 47834 elements	31300	COSMOS/M version 2.0
13	ITER, Italy	3D FEM	74780 nodes, 57316 elements	31300	COSMOS/M 2.5
14	KINS, Korea	3D FEM	7571 nodes, 9440 elements	31300	SAP 2000 Ver 11.0
15	KOPEC, Korea	Stick model		31300	SAP2000 Version 7.42
16	CSN & IDOM, Spain	3D FEM			
17	ENSI, Switzerland	3D FEM	10596 nodes, 10745 elements		SAP2000 v.14.1.0 Advanced
18	NRC, USA	3D FEM	11278 nodes, 15626 elements	38500	SAP2000 Version 14

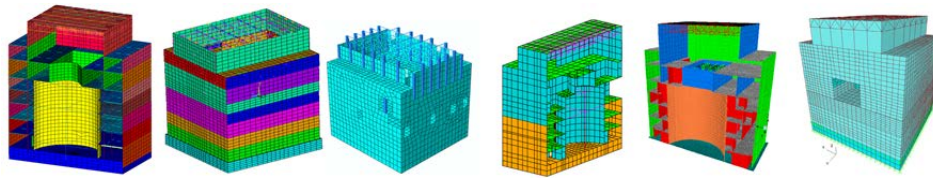


FIG. 30. Schematic example of participants' K-K Unit 7 reactor building models.

3.1.1.2. Resultant Forces

The first set of analyses is static analyses under vertical loads (dead load) and uniform 1g acceleration in the X and Y directions, independently. This was a good check for, first, the completeness and coherence of input data and, second, for the soundness of models. Participants' results for resultant forces at the centre of the bottom of the basemat, exterior shear walls and RCCV (Reinforced Concrete Containment Vault) under static loading (i.e. dead load, uniformly distributed load due to 1 g acceleration applied in the X and Y directions) for the fixed-base model are given in Tables 8, 9 and 10, respectively.

The total self-weight of the structure - including permanent loads which are assumed to be present during the NCOE - is given in the first column of Table 8. The total self-weight values obtained by the participants are well comparable: i.e. COV is 8%. Two participants gave lower values (1474 and 1424 MN compared to the mean of 1931MN), probably due to omitting the self-weight of the raft (about 455MN). As expected, for the load cases in the two horizontal directions, the resultant forces are equal to the vertical one, with small differences in amplitude for a few participants.

Concerning the resulting moments due to the loads in the vertical direction, the eccentricities of the self-weight (given by the "lever arms" a_x and a_y) are very small, less than one meter for almost all the presented results, but the COV is high (e.g. 50% for M_y). For the load cases in the horizontal direction, the ratio of M/F indicates the level of the centre of gravity. The calculated M/F values are coherent for the X and Y directions except the results of one participant. After suppressing the "outlier", most of the values lie between 18m and 25m which correspond approximately to one-third of the total height (63.4m). Due to the concentration of masses at the lower levels and to the relative slenderness of upper 20m of the structure, this result seems plausible.

The next sets of results summarized in Tables 9 and 10, are devoted to the repartition of horizontal loads just above the raft (TMSL -8.2m) among the main horizontal load-bearing structural members: i.e. RCCV and main shear walls. Generally, results in the X and Y directions are comparable and coherent. Most of the participants' results indicate that the RCCV will bear close to 40% of the total horizontal load. This value is in accordance with the ratio of shear areas. As expected, loads on main shear walls which are perpendicular to the applied load direction are much lower than the loads on walls in the load direction. The last columns in Tables 9 and 10 give the total horizontal load just above the raft, calculated by subtracting the weight of the raft (455MN) from the total load at the centre of the basemat bottom.

It appears that there are some incoherent results: most of the forces in the last column are significantly higher than the total forces. The difference in the values between the last column and the "Total" column represents the forces balanced by other structural members, e.g. the auxiliary walls (those already included in the design model plus those added in the NCOE re-evaluation model – see Figure C16 of the Guidance Document [5]). The calculation of section

forces in structural members is not straightforward in commercial FEM codes. This may lead to inconsistent results.

TABLE 8. TOTAL RESULTANT FORCES AT THE CENTRE OF THE BASEMAT BOTTOM

PART 1 STRUCTURE: TASK 1.1- Construction and validation of the soil and structure models Subtask 1.1.1. Static and modal analysis of the fixed base model													
No	Participant Organization	General resultant of forces at the centre of the basemat (T.M.S.L. -13.7 m) at BP1											
		Under vertical loads (weight)						Uniform distribution of 1 g acceleration, applied in X			Uniform distribution of 1 g acceleration, applied in Y		
		Force (MN) Fz	Moment (MNm)		ay=Ratio Mx/Fz	ax=Ratio My/Fz	Force (MN) Fx	Moment (MNm) My	My/Fx (m)	Force (MN) Fy	Moment (MNm) Mx	My/Fx (m)	
			Mx	My									
1	CNEA, Argentina	1474							1474				
2	CNPDC, China	1903							1903				
3	NNSA, China	2018						8	2128	16187	8		
4	SNERDI-SNPTC, China	2011	1925	351	0.96	0.17	2011	37956	19	2011	37956	19	
5	FNS, Finland	1421					1421			1421			
6	CEA&IRSN, France	1971	1728	132	0.88	0.07	1971	44749	23	1971	44749	23	
7	EdF, France	1956	1279	141	0.65	0.07	1956	37843	19	1956	37846	19	
8	AREVA, Germany	2051	289	622	0.14	0.30	2044	36412	18	2047	36514	18	
9	VGB, Germany	1874	1441	263	0.77	0.14	1872	41853	22	1872	42217	23	
10	SPI, Germany	1992					1992	44963	23	1992	44956	23	
11	AERB, India Model 1	2017	1578	323	0.78	0.16	2028	47803	24	2013	47389	24	
	AERB, India Model 2	1772					1736	44054	25	1736	44054	25	
12	BARC, India	1638					1757			1764			
13	ITER, Italy	1941	1882	19	0.97	0.01	1942	42860	22	1942	42883	22	
14	KINS, Korea	2019	947	567	0.47	0.28	2019	45650	23	2019	45650	23	
15	KOPEC, Korea	1992					1992	39393	20	1992	39400	20	
16	CSN & IDOM, Spain	2208	858	3502	0.39	1.59	2208	43838	20	2208	42920	19	
17	ENSI, Switzerland	1865	794	480	0.43	0.26	1876	41069	22	1876	41059	22	
18	NRC, USA	2097	1823	579	0.87	0.28	2098	45694	22	2098	45694	22	
	Mean	1917	1370	384	0.69	0.19	1929	42026	21	1929	41992	21	
	Standard deviation	159	422	187	0.21	0.09	158	3217	2	157	3169	2	
	Coefficient of variation	0.08	0.31	0.49	0.31	0.47	0.08	0.08	0.08	0.08	0.08	0.09	

TABLE 9. RESULTANT FORCES AT THE BOTTOM CENTRE OF THE EXTERIOR SHEAR WALLS AND RCCV; UNIFORMLY DISTRIBUTED LOAD DUE TO 1g ACCELERATION APPLIED IN THE X DIRECTION

PART 1 STRUCTURE: TASK 1.1- Construction and validation of the soil and structure models Subtask 1.1.1. Static and modal analysis of the fixed base model										
No	Participant Organization	Resultant forces at the center of the exterior shear walls and center of RCCV, 3rd basement, T.M.S.L. -8.2m								
		Uniform distribution of 1 g acceleration, applied in X								
		Fx (MN)								
		EW 1	EW 2	EW 3	EW 4	RCCV	Total	RCCV/ Total	Fxat BP1	Fx- 455
1	CNEA, Argentina	247	35	219	36	324	860	0.38	1474	1019
2	CNPDC, China								1903	1448
3	NNSA, China								2128	1673
4	SNERDI-SNPTC, China								2011	1556
5	FNS, Finland								1421	966
6	CEA&IRSN, France	356	35	319	32	436	1179	0.37	1971	1516
7	EdF, France								1956	1501
8	AREVA, Germany	321	33	272	31	413	1070	0.39	2044	1589
9	VGB, Germany	342	21	317	19	488	1187	0.41	1872	1417
10	SPI, Germany								1992	1537
11	AERB, India Model 1	372	52	343	49	1572	2389	0.66	2028	1573
	AERB, India Model 2								1736	1281
12	BARC, India								1757	1302
13	ITER, Italy	365	48	338	48	135	935	0.14	1942	1487
14	KINS, Korea	323	9	263	11	439	1045	0.42	2019	1564
15	KOPEC, Korea								1992	1537
16	CSN & IDOM, Spain								2208	1753
17	ENSI, Switzerland	267	35	227	34	374	937	0.40	1876	1421
18	NRC, USA	339	16	287	32	435	1110	0.39	2103	1648
	Mean	330	32	289	33	416	1066	0.39	1930	1475
	Standard deviation	32	11	39	9	53	103	0.02	158	158
	Coefficient of variation	0.10	0.33	0.13	0.26	0.13	0.10	0.05	0.08	0.11

TABLE 10. RESULTANT FORCES AT THE BOTTOM CENTRE OF THE EXTERIOR SHEAR WALLS AND RCCV; UNIFORMLY DISTRIBUTED LOAD DUE TO 1g ACCELERATION APPLIED IN THE Y DIRECTION

PART 1 STRUCTURE: TASK 1.1- Construction and validation of the soil and structure models										
Subtask 1.1.1. Static and modal analysis of the fixed base model										
No	Participant Organization	Resultant forces at the center of the exterior shear walls and center of RCCV, 3rd basement, T.M.S.L. -8.2m								
		Uniform distribution of 1 g acceleration, applied in Y								
		Fy (MN)								
		EW1	EW2	EW3	EW4	RCCV	Total	RCCV / Total	Fy at BP1	Fy - 455
1	CNEA, Argentina	39	245	39	245	337	905	0.37	1474	1019
2	CNPDC, China								1903	1448
3	NNSA, China								2128	1673
4	SNERDI-SNPTC, China								2011	1556
5	FNS, Finland								1421	966
6	CEA&IRSN, France	25	350	26	349	460	1209	0.38	1971	1516
7	EdF, France								1956	1501
8	AREVA, Germany	22	287	28	298	410	1045	0.39	2047	1592
9	VGB, Germany	18	347	18	352	529	1265	0.42	1872	1417
10	SPI, Germany								1992	1537
11	AERB, India Model 1	48	359	46	348	1558	2358	0.66	2013	1558
	AERB, India Model 2								1736	1281
12	BARC, India								1764	1309
13	ITER, Italy	46	357	43	357	336	1138	0.30	1942	1487
14	KINS, Korea	9	282	10	300	434	1034	0.42	2019	1564
15	KOPEC, Korea								1992	1537
16	CSN & IDOM, Spain								2208	1753
17	ENSI, Switzerland	31	241	32	249	384	937	0.41	1876	1421
18	NRC, USA	27	296	34	301	441	1098	0.40	2103	1648
	Mean	30	309	31	314	428	1104	0.39	1929	1474
	Standard deviation	10	43	8	38	60	111	0.04	157	157
	Coefficient of variation	0.33	0.14	0.26	0.12	0.14	0.10	0.11	0.08	0.11

3.1.1.3. Displacement

Participants' displacement results at the top of the RCCV and roof level under static loading (i.e. vertical loads (dead load), uniformly distributed load due to 1 g acceleration applied in the X and Y directions) for the fixed-base model are given in Tables 11, 12 and 13.

For displacement results under static loadings, the following observations are made:

- One calculation point (CP1) is located at the top of the RCCV, which is a major structural member contributing to the overall stiffness of the structure; two other calculation points (FP2 and WP1) are located on the steel space truss roof where results are probably influenced by reduced modelling precision. It is observed that under the vertical loads all results in the vertical direction are well comparable with a COV of 21%; 3D and stick models give comparable values for global displacements. For the case of horizontal loads (in the X and Y directions), results of displacements in the direction of the applied loads scatter with COVs of 22% and 21% in the X and Y directions, respectively. Results from stick models are comparable to those from 3D models;
- Concerning the central point of the roof (FP2), the calculated vertical displacement under the dead load indicates a mean of 11.2mm with a COV of 63%. Stick model results are lower (1.8mm, 1.9mm, 1.8 mm and 2.2 mm for the 4 stick models). Eliminating the 4 results from the 4 stick models decreases the COV to 44%, indicating the effect of modelling uncertainty in the roof structure. For the horizontal loads, results scatter significantly (COV \approx 100%). Obviously, participants did not spend much effort on modelling the roof structure;

- For the calculation point WP1, located at the roof corner above a shear wall, differences are smaller: i.e. COV of 15% and 16% for displacements in the X and Y directions due to loading in the X and Y directions, respectively.

TABLE 11. DISPLACEMENT AT THE TOP OF RCCV (AT T.M.S.L. +23.5m), CP1

PART 1 STRUCTURE: TASK 1.1- Construction and validation of the soil and structure models Subtask 1.1.1. Static and modal analysis of the fixed base model										
No	Participant Organization	Displacement (T.M.S.L. +23.5m) at CP1								
		Under Vertical loads (weight)			Uniform distribution of 1 g acceleration, applied in X			Uniform distribution of 1 g acceleration, applied in Y		
		Δx (mm)	Δy (mm)	Δz (mm)	Δx (mm)	Δy (mm)	Δz (mm)	Δx (mm)	Δy (mm)	Δz (mm)
1	CNEA, Argentina	0.04	0.24	1.25	9.32	0.04	0.01	0.00	9.14	1.62
2	CNPDC, China			1.33	10.49				10.71	
3	NNSA, China	0.41	0.63	3.21	11.60	0.14	0.02	0.08	8.46	1.59
4	SNERDI-SNPTC, China	0.03	0.34	2.10	14.09	0.26	0.01	0.13	13.28	2.54
5	FNS, Finland									
6	CEA&IRSN, France	0.03	0.19	1.99	14.80	0.10	0.02	0.03	13.97	2.47
7	EdF, France	0.00	0.19	1.98	13.73	0.12	0.02	0.06	13.02	2.17
8	AREVA, Germany	0.07	0.15	1.97	11.21	0.04	0.01	0.05	10.56	1.77
9	VGB, Germany		0.10	2.50	14.40	0.30		0.10	13.30	2.10
10	SPI, Germany			1.49	34.20				49.60	
11	AERB, India Model 1	0.02	0.12	2.34	15.23	0.23	0.00	0.09	13.59	2.31
	AERB, India Model 2			1.77	2.49				2.15	
12	BARC, India	0.00	0.05	1.17	8.18	0.01	0.00	0.03	7.79	1.24
13	ITER, Italy	0.00	0.02	2.02	12.42	0.00	0.00	0.00	11.82	1.99
14	KINS, Korea	0.06	0.13	1.95	8.87	0.03	0.00	0.04	11.57	1.67
15	KOPEC, Korea			1.71	8.87		0.00		7.84	1.34
16	CSN & IDOM, Spain	0.16	0.03	2.01	13.78	0.55	0.10	0.01	13.57	2.88
17	ENSI, Switzerland	0.03	0.24	1.25	9.30	0.02	0.13	0.01	9.09	1.30
18	NRC, USA	0.03	0.13	1.40	8.88	0.09	0.04	0.12	8.09	1.30
	Mean			1.82	11.57				10.99	
	Standard deviation			0.38	2.49				2.31	
	Coefficient of variation			0.21	0.22				0.21	

TABLE 12. ROOF DISPLACEMENT (AT T.M.S.L. +49.7m), FP2 (ROOF CENTRE)

PART 1 STRUCTURE: TASK 1.1- Construction and validation of the soil and structure models Subtask 1.1.1. Static and modal analysis of the fixed base model										
No	Participant Organization	Roof Displacement (T.M.S.L. +49.7m) at FP2								
		Under vertical loads (weight)			Uniform distribution of 1 g acceleration, applied in X			Uniform distribution of 1 g acceleration, applied in Y		
		Δx (mm)	Δy (mm)	Δz (mm)	Δx (mm)	Δy (mm)	Δz (mm)	Δx (mm)	Δy (mm)	Δz (mm)
1	CNEA, Argentina	0.01	0.11	8.64	25.19	0.01	0.00	0.01	17.48	0.62
2	CNPDC, China			1.84	19.73				19.37	0.00
3	NNSA, China	0.44	0.73	9.70	23.58	0.45	0.07	0.16	19.27	0.14
4	SNERDI-SNPTC, China	0.05	0.53	31.76	22.08	0.16	0.50	0.03	17.15	0.42
5	FNS, Finland									
6	CEA&IRSN, France	0.03	0.30	17.46	23.74	0.13	0.32	0.02	18.66	0.06
7	EdF, France	0.13	0.29	19.25	31.79	0.19	0.65	0.15	22.20	0.16
8	AREVA, Germany	0.27	0.26	3.74	28.77	0.13	0.03	0.19	18.05	0.09
9	VGB, Germany		0.30	18.20	22.80		0.20		17.90	0.20
10	SPI, Germany			1.91	104.60				120.40	
11	AERB, India Model 1	0.13	0.23	23.16	69.20	0.44	0.56	0.55	132.59	0.05
	AERB, India Model 2			1.78	5.98					0.01
12	BARC, India	0.06	0.37	17.30	18.48	0.19	0.09	0.09	14.18	0.03
13	ITER, Italy	0.00	0.14	17.38	19.94	0.00	0.27	0.00	17.11	0.10
14	KINS, Korea									
15	KOPEC, Korea			2.20	13.70		0.51		11.90	0.00
16	CSN & IDOM, Spain	0.83	0.23	9.28	23.97	0.48	0.39	0.78	19.96	0.11
17	ENSI, Switzerland	0.08	0.10	8.45	18.83	0.02	0.17	0.07	14.17	0.11
18	NRC, USA	0.13	0.36	9.76	24.01	0.12	0.50	0.08	15.20	0.05
	Mean			11.22	25.72				25.08	
	Standard deviation			7.09	23.27				27.52	
	Coefficient of variation			0.63	0.90				1.10	

TABLE 13. ROOF DISPLACEMENT (AT T.M.S.L. +49.7m), WP1 (ROOF CORNER)

PART 1 STRUCTURE: TASK 1.1- Construction and validation of the soil and structure models										
Subtask 1.1.1. Static and modal analysis of the fixed base model										
No	Participant Organization	Roof Displacement (T.M.S.L. +49.7m) at WP1								
		Under vertical loads (weight)			Uniform distribution of 1 g acceleration, applied in X			Uniform distribution of 1 g acceleration, applied in Y		
		Δx (mm)	Δy (mm)	Δz (mm)	Δx (mm)	Δy (mm)	Δz (mm)	Δx (mm)	Δy (mm)	Δz (mm)
1	CNEA, Argentina	0.03	0.28	1.97	14.06	0.52	2.09	0.29	12.59	1.75
2	CNPDC, China			1.84	19.73				19.37	
3	NNSA, China	0.51	0.00	3.61	21.96	0.72	3.29	0.36	18.69	2.31
4	SNERDI-SNPTC, China	0.15	0.33	2.30	17.97	0.38	2.54	0.39	16.31	1.83
5	FNS, Finland									
6	CEA&IRSN, France	0.04	0.41	2.57	19.43	0.63	2.97	0.39	17.72	2.55
7	EdF, France	0.07	0.41	2.44	17.92	0.35	2.60	0.56	16.77	2.21
8	AREVA, Germany	0.08	0.04	2.07	15.61	0.12	2.47	0.64	13.84	1.92
9	VGB, Germany	0.10	0.50	2.40	18.60	0.70	2.80	0.40	17.00	2.30
10	SPI, Germany									
11	AERB, India Model 1	0.24	0.37	2.91	19.51	1.14	3.74	0.16	18.12	3.03
	AERB, India Model 2			1.78	5.98					0.01
12	BARC, India	0.05	0.04	1.61	14.97	0.78	1.37	0.10	13.56	1.65
13	ITER, Italy	0.07	0.52	2.36	16.56	0.86	2.74	0.39	15.95	2.56
14	KINS, Korea	0.21	0.10	2.10	18.50	0.29	2.68	0.06	16.73	1.99
15	KOPEC, Korea			2.20	14.90		1.95		11.90	2.74
16	CSN & IDOM, Spain	0.94	0.54	2.02	20.40	2.25	3.42	1.92	18.93	2.43
17	ENSI, Switzerland	0.10	0.19	1.74	13.93	0.90	2.46	0.67	12.03	1.82
18	NRC, USA	0.03	0.03	1.71	12.59	0.17	1.76	0.49	10.90	1.53
	Mean			2.16	16.98				15.72	
	Standard deviation			0.34	2.48				2.47	
	Coefficient of variation			0.16	0.15				0.16	

3.1.1.4. Modal Analysis of the Fixed-Base Model

Participants’ results for modal analysis of the fixed-base model are given in Table 14. The mean of the fundamental frequencies are 4.56 Hz and 4.96 Hz in the X and Y directions, respectively. An important thing is that the modal analysis results show very small scatter in the frequency values of the fundamental horizontal modes (COV of 9%).

It is recalled that the COV of the calculated fundamental frequencies was 10% for a simple test structure in the CAMUS benchmark within the framework of the IAEA Coordinated Research Project on the “Safety Significance of Near- Field Earthquakes” [15].

TABLE 14. MODAL ANALYSES RESULTS FOR FIXED BASE MODEL

PART 1 STRUCTURE: TASK 1.1- Construction and validation of the soil and structure models											
Subtask 1.1.1. Static and modal analysis of the fixed base model - C. Modal analysis of the fixed base model											
No	Participant Organization	Natural Frequency (Hz)			Modal participating mass ratios (%)			Total mass (ton)	Total mass in each direction (%)		
		in X	in Y	in Z	UX	UY	UZ		M _{total}	M _x	M _y
1	CNEA, Argentina	4.89	5.32	9.72	60.0	64.9	22.2	150230	81.8	75.2	46.1
2	CNPDC, China	4.43	4.45	14.21	52.2	53.6	76.4	193969	99.9	99.9	94.1
3	NNSA, China	4.58	5.08	8.00	31.6	41.9	64.4	201760	95.2	96.0	90.4
4	SNERDI-SNPTC, China	4.24	4.63	8.86	49.5	40.8	12.8	204950	71.5	71.6	66.4
5	FNS, Finland	4.88	4.85	8.35	33.1	46.9	11.7	144899	87.0	87.2	73.2
6	CEA&IRSN, France	4.04	4.43	8.31	70.4	76.7	15.2	151000	94.6	94.6	86.5
7	EdF, France	4.08	4.54	8.49	42.7	53.3	3.7	199411	68.0	68.0	57.0
8	AREVA, Germany	4.40	5.10	7.20	40.0	54.0	3.0	150000	93.0	92.0	75.0
9	VGB, Germany	3.93	4.33	6.84	53.5	57.9	4.9	187400	86.9	90.4	74.7
10	SPI, Germany	4.84	5.24	13.85	55.8	57.6	69.9	199170	83.1	83.5	90.7
11	AERB, India Model 1	4.29	4.59	7.76	48.2	49.0	3.9	205780	76.1	75.7	70.6
	AERB, India Model 2	7.03	7.59	8.25	24.0	24.0	3.5	200380	41.6	40.5	73.8
12	BARC, India	5.21	5.62	7.70	36.3	49.7	3.8	183869	58.4	59.1	45.6
13	ITER, Italy	4.48	4.77	8.55	53.8	55.7	12.9	197916	66.8	66.8	53.2
14	KINS, Korea	4.42	4.87	8.03	56.5	59.3	3.9	205915	78.1	78.5	69.7
15	KOPEC, Korea	5.31	5.63	3.11	67.8	68.4	1.2	203235	94.4	93.9	84.3
16	CSN & IDOM, Spain	3.50	4.07	5.10	61.8	70.8	27.0	218930	89.0	89.4	71.8
17	ENSI, Switzerland	4.74	5.42	7.31	42.0	41.9	1.6	190152	56.9	58.1	25.0
18	NRC, USA	4.85	5.42	7.48	43.7	62.1	2.4	214410	92.2	92.8	81.9
	Mean	4.56	4.96	8.22	48.7	54.6	15.7	190562	80.8	80.7	71.2
	Standard deviation	0.40	0.43	1.75	10.3	9.0	20.7	20518	12.6	12.7	14.0
	Coefficient of variation	0.09	0.09	0.21	0.21	0.16	1.32	0.11	0.16	0.16	0.20

3.1.2. Subtask 1.1.2 Soil Column Analyses

3.1.2.1. Soil Column Model Presentation

Soil column analysis types, calculation codes, the number and thickness of layers, input motions and control points used by participants are given in Table 15.

All participants used one-dimensional models with vertically propagating shear waves. This is a reasonable assumption considering the data available for the benchmark.

SHAKE91 was used by most of the participants. EERA, which is a SHAKE version implemented in EXCEL, was used by 3 out of the 14 participants. CYBERQUAKE is software which can deal with both equivalent linear and elasto-plastic models in 1D; thereby the equivalent linear model is similar to the one utilized in SHAKE91. All these software solve analytically the wave equation in a given (sub) layer; therefore for elastic materials the exact solution is obtained with no numerical errors arising from the mesh discretization. With an equivalent linear model, for which properties are adjusted in each layer to the average induced shear strain, mesh discretization may influence the results. Depending on the sub-layer thickness, different characteristics may be calculated at different depths after iterations. This is the reason for listing the sub-layer thicknesses in Table 15. This indication is only provided for the clay layer because the underlying strains are more uniform across the layer due to the larger wave length, and the rock is believed to behave almost elastically; it is therefore less sensitive to the geometric discretization.

Two participants used ACS-SASSI. Unlike the previous codes, ACS-SASSI is based on a finite element solution of the wave equation. As any finite element code it is sensitive to the element mesh size (here the layer thickness). Experience has shown that, for frequency

domain solutions, the element thickness should not be larger than one-eighth of the smallest wave length of interest.

One participant used a proprietary code called “DEC” and 4 participants did not indicate their codes.

TABLE 15. SOIL COLUMN MODEL PRESENTATION

PART 1 STRUCTURE: TASK 1.1- Construction and validation of the soil and structure models									
Subtask 1.1.2. Soil Column Analyses - Soil Column Model Presentation									
No	Participant Organization	Model	Code	Number of layers in clay	Layer thickness in Clay (m)		Input motion		
					Minimum	Maximum		Outcrop	Within
1	CNEA, Argentina	1D - VE							
2	CNPDC, China	1D - VE	SHAKE (1991)	6	5.00	5.00	5G1	Yes	No
3	NNSA, China	1D - VE	EERA	5	2.00	17.00			
4	SNERDI-SNPTC, China	1D - VE	ACS SASSI 2.3	14	0.60	3.20	5G1	Yes	No
5	FNS, Finland	1D - VE							
6	CEA&IRSN, France	1D - VE	EERA	6	5.00	5.00	5G1	Yes	No
7	EdF, France	1D - VE	CYBERQUAKE 2.0	14	2.00	2.00	5G1	Yes	No
8	AREVA, Germany	1D - VE	SHAKE (AREVA)	6	5.00	5.00	G55	No	Yes
9	VGB, Germany	1D - VE	SHAKE (1991),	10	0.65	3.70	5G1	Yes	No
10	SPI, Germany	1D - VE	SHAKE (1991)	12	0.70	3.20	5G1	Yes	No
11	AERB, India	1D - VE	SHAKE (1991)	30	0.35	1.00	G55	Yes	No
12	BARC, India	1D - VE							
13	ITER, Italy	1D - VE	DEC	6	5.00	5.00	G55	No	Yes
14	KINS, Korea	1D - VE	EERA (2000)	18	0.50	3.10	5G1	Yes	No
15	KOPEC, Korea	1D - VE	SHAKE (1991)	5	4.00	5.00	5G1	Yes	No
16	CSN & IDOM, Spain	1D - VE							
17	ENSI, Switzerland	1D - VE	ACS SASSI 2.2	6	5.00	5.00	G55	Yes	No
18	NRC, USA	1D - VE	SHAKE	9	0.64	5.40	5G1	Yes	No

VE : Visco Elastic
1D : One dimeational

All participants assumed a viscoelastic equivalent linear constitutive model. The input data to this model are the shear wave velocity profile (Table 5) and the variation of the shear modulus and equivalent damping ratio with shear strain (Fig. 24).

SHAKE91, EERA, CYBERQUAKE and ACS-SASSI perform successive iterations on the soil characteristics until convergence is achieved within each sub-layer between the average induced shear strain, shear modulus and damping ratio.

3.1.2.2. Soil Column Analyses: Aftershock I (16th July, 15:37)

Participants’ soil column analyses results for the maximum acceleration at observation levels in the X direction for Aftershock I are presented in Table 16.

For Aftershock I, COV varies from 9 to 19% for the maximum accelerations at observation points in the X direction. Nine participants used observation point 5-G1 and four participants used G55 as control points in their analysis. At 5-G1 and G55, COV is 2%: and 9%, respectively. Measured values and the mean values of analysis results are very close for 3 observation points, namely 5G-1, G54 and G55.

TABLE 16. SOIL COLUMN ANALYSES UNDER AFTERSHOCK I: MAXIMUM ACCELERATION AT OBSERVATION LEVELS IN THE X DIRECTION

PART I STRUCTURE: TASK 1.1- Construction and validation of the soil and structure models							
Subtask 1.1.2. Soil Column Analyses - A. Soil Column Analyses under Aftershock I (16th July, 15:37)							
No	Participant Organization	A.1.1.a. Maximum Acceleration at observation levels in X direction - Aftershock I (16th July, 15:37)					
		Maximum Acceleration (g)					
		5G-1 (T.M.S.L. +12.3)	G51 (T.M.S.L. +9.3)	G52 (T.M.S.L. -24.0)	G53 (T.M.S.L. -100.0)	G54 (T.M.S.L. -180.0)	G55 (T.M.S.L. -300.0)
1	CNEA, Argentina						
2	CNPDC, China	0.398	0.317	0.162	0.146	0.110	0.112
3	NNSA, China	0.401	0.276	0.216	0.196	0.132	0.132
4	SNERDI-SNPTC, China	0.394	0.315	0.237	0.169	0.142	0.151
5	FNS, Finland						
6	CEA&IRSN, France	0.386	0.279	0.148	0.137	0.121	0.118
7	EdF, France	0.393	0.247	0.117	0.124	0.094	0.103
8	AREVA, Germany	0.381	0.239	0.146	0.127	0.116	0.122
9	VGB, Germany	0.386	0.307	0.201	0.166	0.136	0.143
10	SPI, Germany	0.386	0.311	0.215	0.168	0.135	0.144
11	AERB, India	0.405	0.241	0.131	0.135	0.115	0.124
12	BARC, India	0.601	0.504	0.379	0.202	0.240	0.122
13	ITER, Italy	0.402	0.268	0.185	0.172	0.137	0.124
14	KINS, Korea	0.393	0.300	0.230	0.179	0.155	0.158
15	KOPEC, Korea	0.394	0.221	0.156	0.122	0.134	0.125
16	CSN & IDOM, Spain						
17	ENSI, Switzerland	0.387	0.260	0.184	0.141	0.132	0.124
18	NRC, USA	0.394	0.305	0.225	0.171	0.138	0.146
Measured		0.393	0.221	0.156	0.121	0.134	0.124
Mean		0.394	0.282	0.187	0.156	0.131	0.130
Standard deviation		0.006	0.029	0.036	0.022	0.012	0.012
Coefficient of variation		0.02	0.10	0.19	0.14	0.10	0.09

Recorded response spectra and participants' results for different observation levels in the soil (5G1, G11, G22, G33, G44 and G55) are compared in Fig. 31. Most of the participants almost correctly predicted the resonant frequencies of the soil profile with a slight shift towards the lower frequencies.

Figure 32 presents participants' results for soil shear modulus reduction, damping ratio and maximum shear strain along the depth. Results are more consistent for maximum shear strain than for shear modulus reduction and damping ratio.

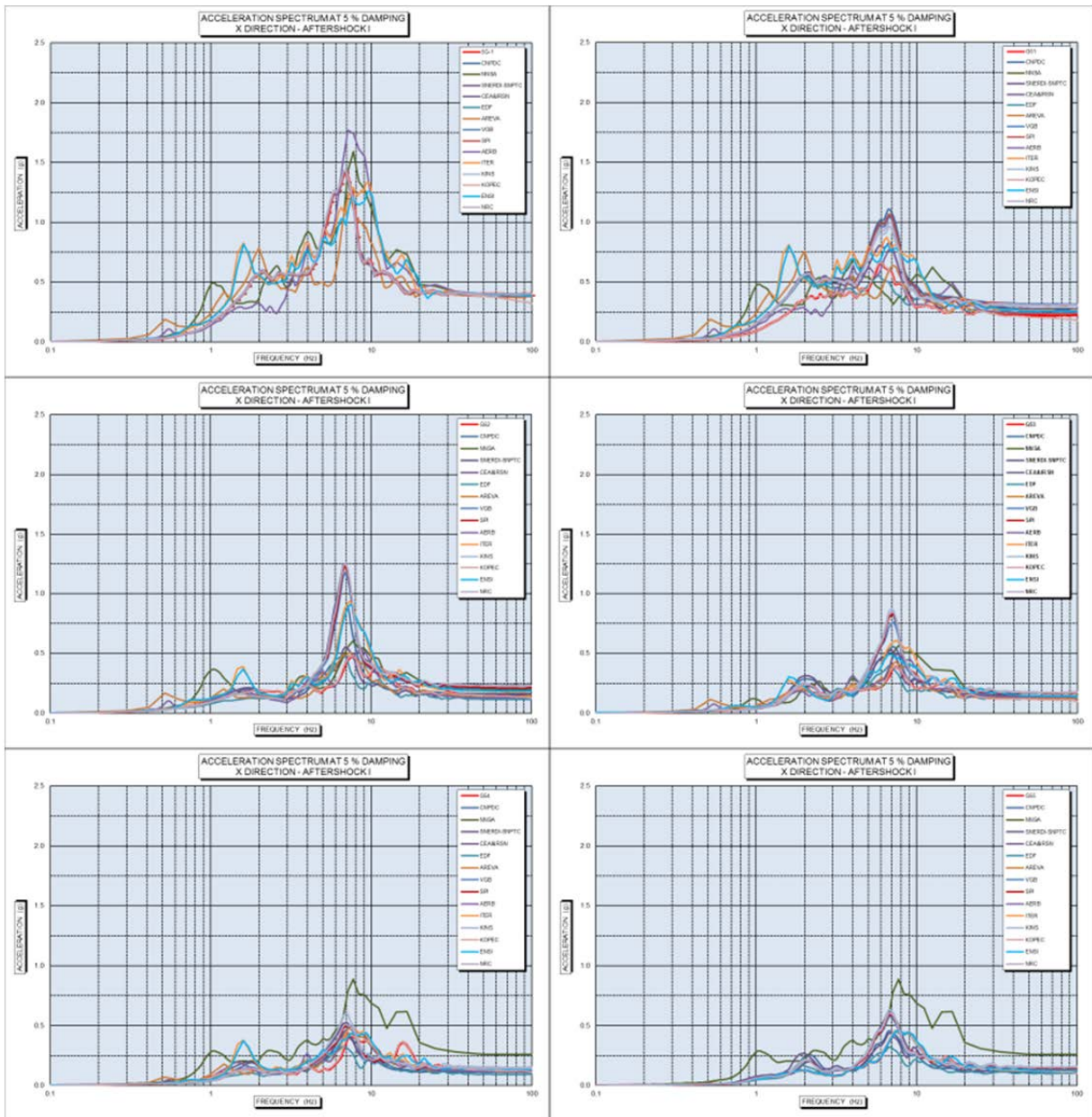


FIG. 31. Participants' results for acceleration response spectra (damping 5%) at different observation levels in the soil (5G1, G11, G22, G33, G44 and G55) in the X direction for Aftershock I.

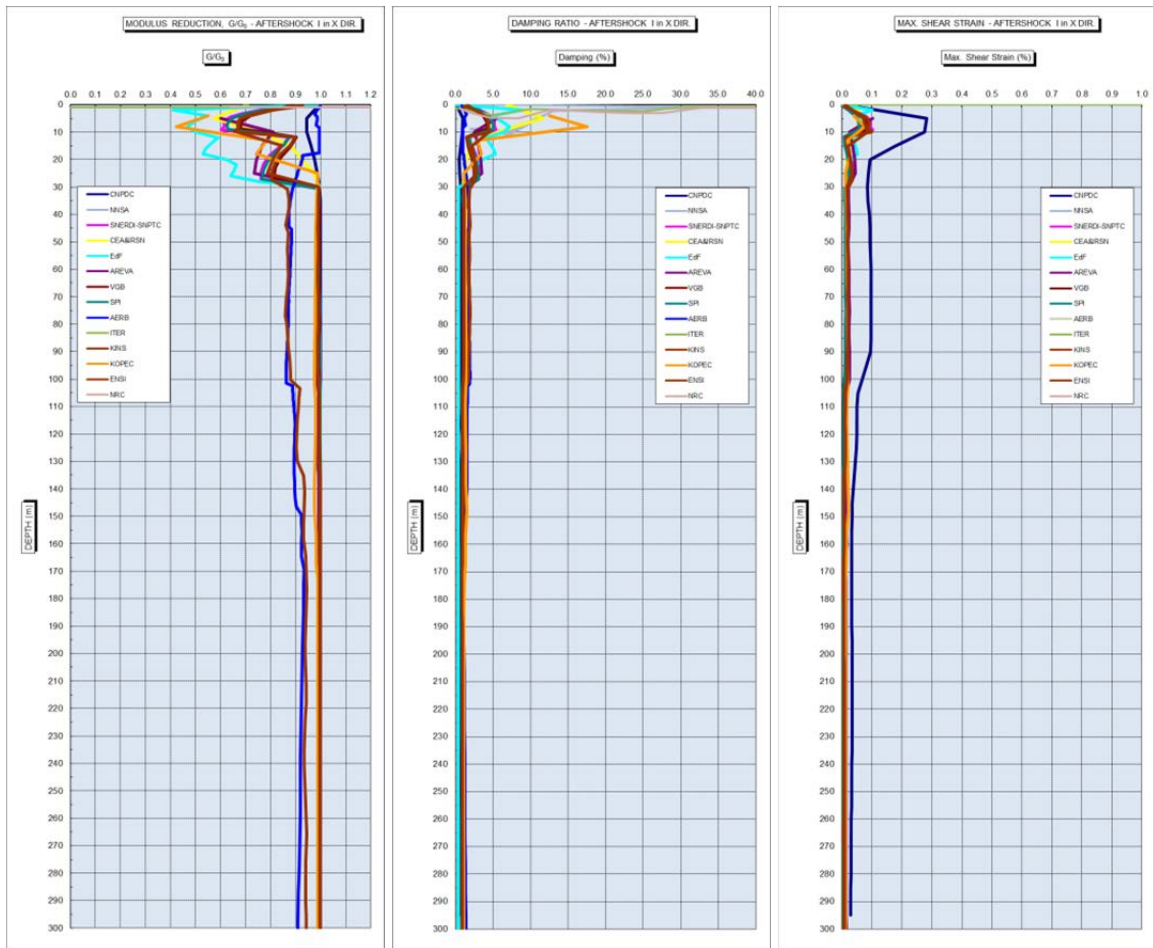


FIG. 32. Participants' soil column analysis results for G/G_0 , damping ratio and maximum shear strain in the X direction along the bore hole depth for Aftershock I.

3.1.2.3. Soil Column Analyses: Main shock

Participants' maximum acceleration results (from soil column analyses) at different observation levels in the X direction for the Main shock are given in Table 17. According to this, COV of the maximum accelerations at different observations points varies between 11 to 38%. COVs for the Main shock are higher than those for Aftershock I due to the stronger non-linear response of the softer top soil.

TABLE 17. SOIL COLUMN ANALYSES UNDER MAIN SHOCK: MAXIMUM ACCELERATION AT DIFFERENT OBSERVATION LEVELS IN THE X DIRECTION

PART 1 STRUCTURE: TASK 1.1- Construction and validation of the soil and structure models Subtask 1.1.2. Soil Column Analyses - C. Soil Column Analyses under Mainshock							
No	Participant Organization	C.1.1.a. Maximum Acceleration at observation levels in X direction - Mainshock					
		Maximum Acceleration (g)					
		5G-1 (T.M.S.L. +12.3)	G51 (T.M.S.L. +9.3)	G52 (T.M.S.L. -24.0)	G53 (T.M.S.L. -100.0)	G54 (T.M.S.L. -180.0)	G55 (T.M.S.L. -300.0)
1	CNEA, Argentina						
2	CNPDC, China	0.983	0.781	0.552	0.374	0.396	0.280
3	NNSA, China	0.974	0.969	1.117	1.238	1.090	1.090
4	SNERDI-SNPTC, China	0.984	0.785	0.658	0.449	0.426	0.339
5	FNS, Finland						
6	CEA&IRSN, France	0.964	0.707	0.603	0.724	0.589	0.865
7	EdF, France	0.944	0.748	0.841	0.680	0.649	0.519
8	AREVA, Germany	0.963	0.812	0.597	0.351	0.310	0.366
9	VGB, Germany	0.964	0.720	0.562	0.466	0.445	0.632
10	Stangenberg, Germany	0.974	0.717	0.486	0.516	0.404	0.588
11	AERB, India	0.982	0.645	0.489	0.517	0.436	1.303
12	BARC, India	1.571	1.569	1.540	1.408	1.240	0.961
13	ITER, Italy	0.887	0.640	0.480	0.403	0.441	0.366
14	KINS, Korea	0.980	0.701	0.450	0.543	0.561	0.795
15	KOPEC, Korea	0.983	0.837	0.880	0.675	0.627	0.723
16	CSN & IDOM, Spain						
17	ENSI, Switzerland	0.990	0.723	0.500	0.506	0.458	0.547
18	NRC, USA	0.980	0.710	0.501	0.505	0.432	0.567
Measured		0.983	0.698	0.423	0.404	0.427	0.415
Mean		0.974	0.758	0.636	0.584	0.535	0.643
Standard deviation		0.012	0.082	0.194	0.223	0.188	0.234
Coefficient of variation		0.01	0.11	0.31	0.38	0.35	0.36

Participants' results for acceleration response spectra at different observation levels in the soil (5G1, G11, G22, G33, G44 and G55) are compared in Fig. 33. Most of the participants predicted almost the same resonant frequencies of the soil profile. A few results show a shift towards higher frequencies with depth. Results at different soil depths cannot be compared with corresponding recorded motions in the borehole G5 since they were lost.

Figure 34 presents participants' results for the soil shear modulus reduction, damping ratio and maximum shear strain along the soil depth. Similar to the Aftershock I results, calculated soil response exhibit the same trend. The only exceptions are data from one participant over-predicting the soil shear strain and data from two participants over-predicting the reduction of the soil shear modulus significantly.

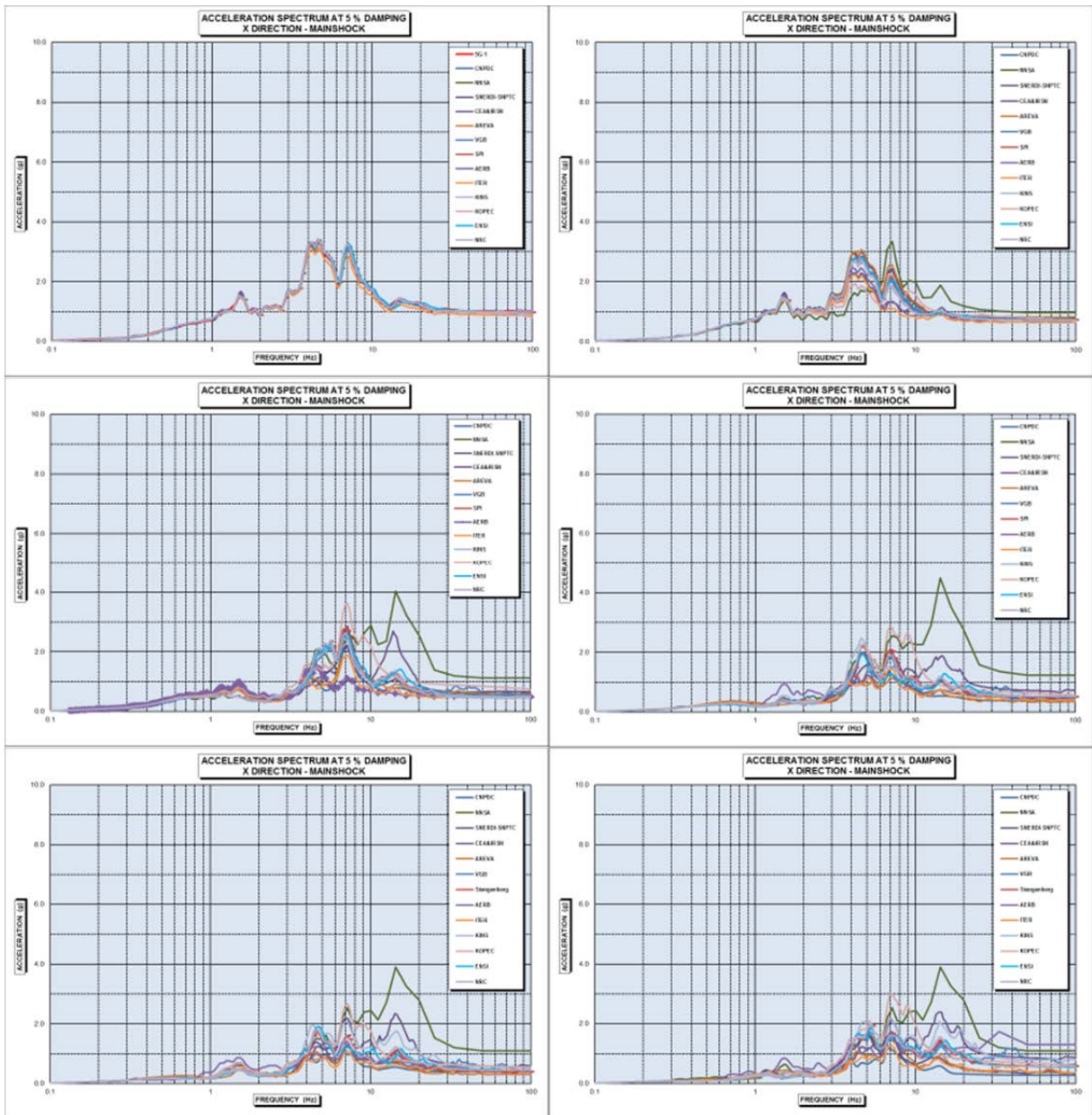


FIG. 33. Participants' results for acceleration response spectra (damping 5 %) at different observation levels in the soil (5G1, G11, G22, G33, G44 and G55) in the X direction for the Main shock.

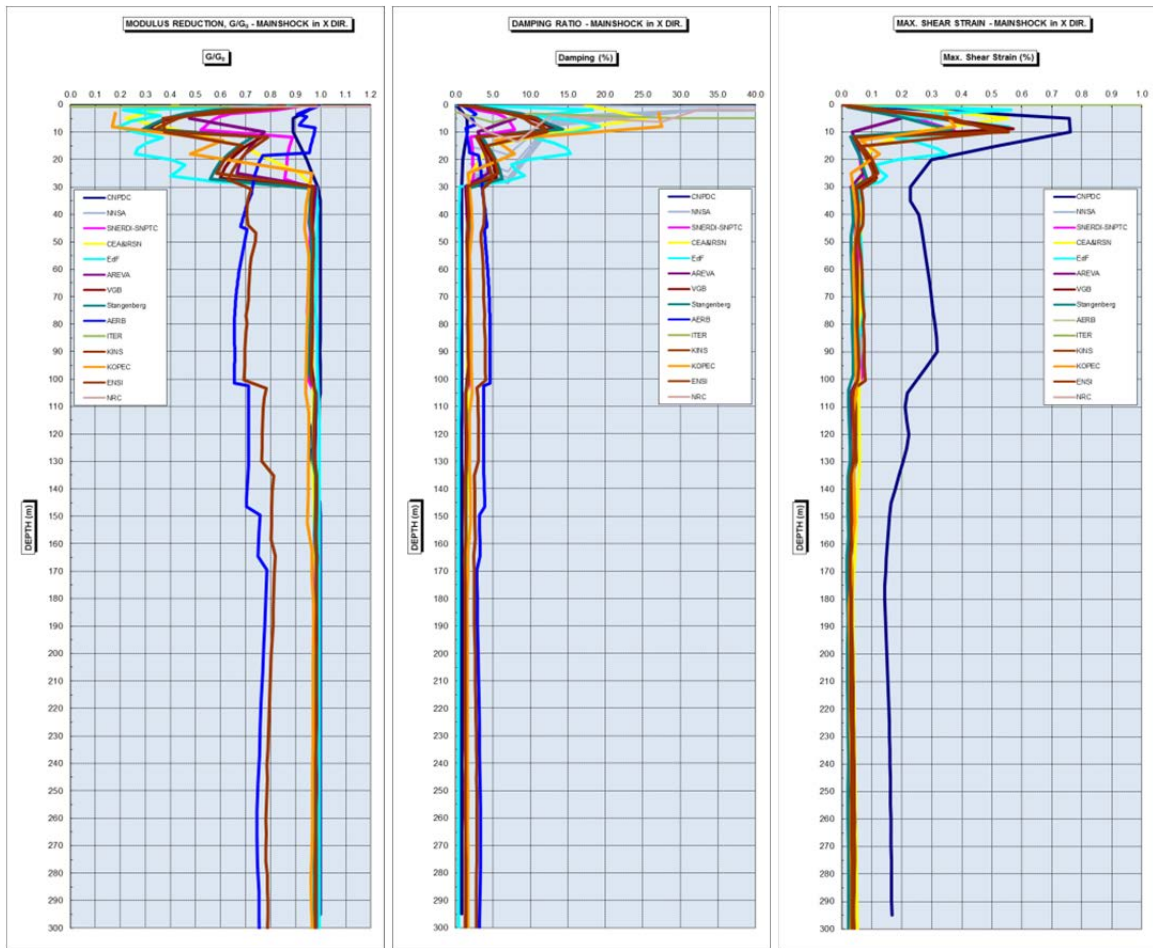


FIG. 34. Participants’ soil column analyses results for G/G_0 , damping ratio and maximum shear strain in the X direction along the borehole depth for Main shock.

3.1.3. Subtask 1.1.3 Analysis of the complete model

Participants applied two different types of analyses: either in the frequency domain with codes of the CLASSI or SASSI family, or in the time domain with “conventional” finite element commercial codes. In the time domain analysis, soil is modelled either by distributed spring and dampers or by finite elements with special absorbing boundaries.

Comparison of modal analysis results for the fixed-base and coupled soil-structure interaction (SSI) models is presented in Table 18. Only 7 out of 18 participants provided results. Results for the fixed-base model show a COV of 9 % in both directions. COVs of the results for the coupled SSI model are 9% in the X direction and 12% in the Y direction, respectively, despite different approaches considered in the analyses.

As expected, SSI has a significant effect on the response by decreasing the fundamental frequency. In the horizontal direction the decrease was by a factor of about 2 and about 2.5 in the vertical direction.

TABLE 18. COMPARISON OF MODAL ANALYSIS RESULTS FOR FIXED-BASE MODEL AND COMPLETE MODELS

No	Participant Organization	Fixed base Model Natural Frequency (Hz)			Complete Model Natural Frequency (Hz)		
		in X	in Y	in Z	in X	in Y	in Z
1	CNEA, Argentina	4.89	5.32	9.72			
2	CNPDC, China	4.43	4.45	14.21			
3	NNSA, China	4.58	5.08	8.00			
4	SNERDI-SNPTC, China	4.24	4.63	8.86			
5	FNS, Finland	4.88	4.85	8.35			
6	CEA&IRSN, France	4.04	4.43	8.31			
7	EdF, France	4.08	4.54	8.49			
8	AREVA, Germany	4.40	5.10	7.20	2.55	2.60	3.77
9	VGB, Germany	3.93	4.33	6.84	2.11	2.08	3.46
10	SPI, Germany	4.84	5.24	13.85	2.27	2.33	3.03
11	AERB, India Model 1	4.29	4.59	7.76	1.97	2.46	3.55
	AERB, India Model 2	7.03	7.59	8.25			
12	BARC, India	5.21	5.62	7.70			
13	ITER, Italy	4.48	4.77	8.55	1.91	1.96	2.80
14	KINS, Korea	4.42	4.87	8.03	1.74	1.79	2.93
15	KOPEC, Korea	5.31	5.63	3.11			
16	CSN & IDOM, Spain	3.50	4.07	5.10			
17	ENSI, Switzerland	4.74	5.42	7.31	2.35	2.96	3.64
18	NRC, USA	4.85	5.64	7.48			
	Mean	4.56	4.97	8.22	2.12	2.29	3.32
	Standard deviation	0.40	0.45	1.75	0.19	0.26	0.32
	Coefficient of variation	0.09	0.09	0.21	0.09	0.12	0.10

As a conclusion of Phase I, the analytical models developed by the participants give coherent global results and they are suitable for the next phases of the benchmark.

3.2. MAIN RESULTS FOR TASK 1.2 OF PHASE II: MAIN SHOCK RESPONSE

3.2.1. Subtask 1.2.1 “Reference analyses” in frequency or time domain

Participants’ maximum relative displacement results at the 3rd floor (TMSL +23.5m) and at roof top (TMSL +49.7m) for “Baseline 1” and “Baseline 2” soil conditions from the “reference analysis” with a coupled SSI model are given in Table 19. After exclusion of the two outlier results, COVs of the results vary between 50 and 120%.

Participants’ maximum absolute acceleration results at basemat bottom (TMSL -13.7m) and the 3rd basement (TMSL -8.2m) for “Baseline 1” and “Baseline 2” soil conditions from the “reference analysis” with a coupled SSI model are given in Table 20. After exclusion of two outlier results, COVs of the results vary between 4 and 32%. The calculated maximum acceleration mean values at the 3rd basement are higher than the recorded peak acceleration of the NCOE.

TABLE 19. MAXIMUM RELATIVE DISPLACEMENT AT THE 3rd FLOOR AND ROOF TOP FOR THE COUPLED SSI MODEL

PART 1 STRUCTURE: TASK 1.2- NCOE Response (Phase II)														
Subtask 1.2.1 Reference Analysis of the Soil-Structure Model														
B. Frequency domain/time domain analysis of the soil-structure model														
No	Participant Organization	B.1. Maximum relative displacement due to loading Combination												
		"Baseline 1" soil condition						"Baseline 2" soil condition						
		RCCV Displacement (T.M.S.L. +23.5m) at FP2 (mm)			Roof Displacement (T.M.S.L. +49.7m) at WP1 (mm)			RCCV Displacement (T.M.S.L. +23.5m) at FP2 (mm)			Roof Displacement (T.M.S.L. +49.7m) at WP1 (mm)			
		Δx	Δy	Δz	Δx	Δy	Δz	Δx	Δy	Δz	Δx	Δy	Δz	
1	CNPDC, China	For Δx max												
		For Δy max												
		For Δz max												
2	SNERDI-SNPTC, China	For Δx max	30.1			38.7								
		For Δy max		146.8			200.5							
		For Δz max			82.5			89.6						
3	CEA&IRSN, France	For Δx max							11.2			16.5		
		For Δy max							15.3			24.3		
		For Δz max								6.9				10.9
4	EdF, France	For Δx max												
		For Δy max												
		For Δz max												
5	AREVA, Germany	For Δx max							108.3			114.7		
		For Δy max							123.4			117.7		
		For Δz max								17.0				24.4
6	VGB, Germany	For Δx max	15.5			22.8			16.4			24.2		
		For Δy max		24.2			39.1			24.0			38.7	
		For Δz max			10.3			15.6			10.2			15.7
7	SPI, Germany	For Δx max	113.8			119.8								
		For Δy max		78.9			88.0							
		For Δz max			70.0			64.5						
8	AERB, India	For Δx max	45.5			63.8								
		For Δy max		25.4			25.1							
		For Δz max			50.9			69.6						
9	BARC, India	For Δx max												
		For Δy max												
		For Δz max												
10	ITER, Italy	For Δx max	18.0			25.2								
		For Δy max		26.2			38.6							
		For Δz max			28.3			31.7						
11	KINS, Korea	For Δx max							46.8			53.5		
		For Δy max							59.9			91.4		
		For Δz max								48.2			50.3	
12	ENSI, Switzerland	For Δx max							13.3			39.4		
		For Δy max							12.2			171.3		
		For Δz max								5.2				6.3
13	NRC, USA	For Δx max	3.7			6.2			3.6			5.9		
		For Δy max		4.7			8.6			5.0			8.9	
		For Δz max			2.1			2.5			2.0			2.9
Mean			27.3	55.6	43.0	37.6	75.8	51.6	21.9	27.9	17.6	33.4	81.4	20.8
SD			13.7	60.8	31.1	18.8	83.4	34.0	16.7	22.0	20.5	16.4	66.5	20.1
COV			0.5	1.1	0.7	0.5	1.1	0.7	0.8	0.8	1.2	0.5	0.8	1.0

TABLE 20. MAXIMUM ACCELERATION AT BASEMAT AND THE 3rd BASEMENT FOR THE COUPLED SSI MODEL

PART 1 STRUCTURE: TASK 1.2- NCOE Response (Phase II) - Baseline 1 & 2														
Subtask 1.2.1 Reference Analysis of the Soil-Structure Model														
B. Frequency domain/time domain analysis of the soil-structure model														
No	Participant Organization		B.2.1 Maximum absolute acceleration due to Combination											
			"Baseline 1" soil condition						"Baseline 2" soil condition					
			Absolute acceleration (T.M.S.L. -13.7m) at BP1 (g)			Absolute acceleration (T.M.S.L. -8.2m) at FP2 (g)			Absolute acceleration (T.M.S.L. -13.7m) at BP1 (g)			Absolute acceleration (T.M.S.L. -8.2m) at FP2 (g)		
			ax	ay	az	ax	ay	az	ax	ay	az	ax	ay	az
1	CNPDC, China	For ax max								0.45			0.40	
		For ay max									0.58			0.69
		For az max										0.30		
2	SNERDI-SNPTC, China	For ax max	0.53			0.52								
		For ay max		0.72			0.67							
		For az max			0.42			0.49						
3	CEA&IRSN, France	For ax max							0.35				0.32	
		For ay max								0.37				0.36
		For az max										0.31		
4	EdF, France	For ax max												
		For ay max												
		For az max												
5	AREVA, Germany	For ax max							0.49				0.49	
		For ay max								0.46				0.46
		For az max										0.30		
6	VGB, Germany	For ax max	0.61			0.53				0.60			0.52	
		For ay max		0.61			0.55				0.69			0.62
		For az max			0.28			0.50				0.28		
7	SPI, Germany	For ax max	0.69			0.61								
		For ay max		0.67			0.58							
		For az max			0.56			0.54						
8	AERB, India	For ax max	1.56			1.56								
		For ay max		1.31			1.75							
		For az max			1.21			1.26						
9	BARC, India	For ax max												
		For ay max												
		For az max												
10	ITER, Italy	For ax max	0.56			0.58								
		For ay max		0.73			0.77							
		For az max			0.45			0.49						
11	KINS, Korea	For ax max							1.73				1.60	
		For ay max								2.29			2.25	
		For az max									0.73			1.80
12	ENSI, Switzerland	For ax max							0.61				0.61	
		For ay max								0.43				0.43
		For az max									0.30			0.30
13	NRC, USA	For ax max	0.46			0.44				0.50			0.48	
		For ay max		0.50			0.46				0.55			0.51
		For az max			0.25			0.49				0.25		
Mean			0.57	0.65	0.39	0.53	0.61	0.50	0.50	0.51	0.29	0.47	0.51	0.42
SD			0.09	0.09	0.13	0.06	0.12	0.02	0.10	0.12	0.02	0.10	0.12	0.11
COV			0.15	0.14	0.32	0.12	0.19	0.04	0.20	0.23	0.07	0.21	0.24	0.27
Recorded												0.27	0.36	0.36

Similarly, participants’ “reference analyses” results analysis of the soil-structure model for “Baseline 1” and “Baseline 2” soil conditions for the maximum acceleration at the 3rd floor and the top of the roof are given in Table 21. The COVs of the results vary from 13 to 42%. The means of the analyses results are comparable with the recorded value in the X direction. The means of the analyses results are higher than peak accelerations recorded in the Y and Z directions.

In general, the maximum acceleration values at two recording points (the 3rd basement and 3rd floor) are overly estimated by analyses comparing to recorded ones.

Participants’ floor response spectrum (FRS) results (5% damping) at the 3rd basement (TMSL -8.2m) and the 3rd floor for “Baseline 2” soil condition from “reference analyses” with a coupled SSI model are presented in Figs 35 and 36 respectively. The figures include the observed NCOE response spectra at the same locations as well.

TABLE 21. MAXIMUM ACCELERATION AT THE 3rd FLOOR AND ROOF TOP FOR THE COUPLED SSI MODEL

PART I STRUCTURE: TASK 1.2- NCOE Response (Phase II) - Baseline 1 & 2														
Subtask 1.2.1 Reference Analysis of the Soil-Structure Model														
B. Frequency domain/time domain analysis of the soil-structure model														
No	Participant Organization	B.2.1 Maximum absolute acceleration due to Combination												
		"Baseline 1" soil condition						"Baseline 2" soil condition						
		Absolute acceleration (TMSL +23.5m) at FP2 (g)			Absolute acceleration (T.M.S.L. +49.7m) at WP1 (g)			Absolute acceleration (TMSL +23.5m) at FP2 (g)			Absolute acceleration (T.M.S.L. +49.7m) at WP1 (g)			
		ax	ay	az	ax	ay	az	ax	ay	az	ax	ay	az	
1	CNPDC, China	For ax max							0.44			0.49		
		For ay max								0.49			0.88	
		For az max									0.34			0.35
2	SNERDI-SNPTC, China	For ax max	0.55			0.82								
		For ay max		1.08			1.65							
		For az max			0.45			0.96						
3	CEA&IRSN, France	For ax max						0.34				0.69		
		For ay max							0.62				1.15	
		For az max									0.67		0.59	
4	EdF, France	For ax max												
		For ay max												
		For az max												
5	AREVA, Germany	For ax max						0.49				0.67		
		For ay max							0.71				1.21	
		For az max									0.91		0.32	
6	VCB, Germany	For ax max	0.45			0.87			0.42			0.83		
		For ay max		0.76			1.29			0.71			1.20	
		For az max			0.86			0.98			0.81		0.98	
7	SPL, Germany	For ax max	0.48			0.62								
		For ay max		0.79			0.96							
		For az max			0.71			1.00						
8	AERB, India	For ax max	2.58			3.63								
		For ay max		1.74			2.23							
		For az max			2.17			2.97						
9	BARC, India	For ax max												
		For ay max												
		For az max												
10	ITER, Italy	For ax max	0.88			1.31								
		For ay max		1.13			1.45							
		For az max			0.68			0.81						
11	KINS, Korea	For ax max						1.70				1.75		
		For ay max							1.46				3.22	
		For az max									1.90		2.39	
12	ENSI, Switzerland	For ax max						0.62				1.33		
		For ay max							0.59				1.84	
		For az max									0.43		0.52	
13	NRC, USA	For ax max	0.41			0.74			0.41			0.75		
		For ay max		0.63			1.07			0.65			1.10	
		For az max			0.94			0.71			0.82		0.73	
Mean			0.55	0.88	0.73	0.87	1.28	0.89	0.45	0.63	0.66	0.79	1.23	0.58
SD			0.19	0.22	0.19	0.26	0.28	0.13	0.10	0.08	0.23	0.28	0.32	0.25
COV			0.35	0.25	0.26	0.30	0.22	0.14	0.22	0.13	0.35	0.36	0.26	0.42
Recorded									0.37	0.44	0.47			

Calculated floor response spectral amplitudes and peaks at the location (FP2) of the installed accelerometer on the 3rd basement do not fit well to the observed response spectra. For example, most of the calculated response spectra have peaks at around 4 Hz in the X and Y directions. By contrast, the peaks in the observed response spectra are at around 1.5 Hz. The calculated peak at 4 Hz could be due to a rocking mode frequency affected by over-estimation of soil stiffness and under-estimation of the soil radiation damping. Most of participants' results show significant over-estimation of the spectral acceleration in the vertical direction throughout the whole frequency range.

Except for a few, FRS provided by the participants for the location (FP2) of the installed accelerometer on the 3rd floor is comparable with the observed response spectrum in the X direction. Most participants predicted well the location of the first peak in the observed response spectrum at about 1.3 Hz. However, all participants failed to predict the second spectral peak at about 2.7 Hz. Spectral values beyond the second peak frequency are over-predicted by most participants. Most of participants' results show significant over-estimation of the spectral acceleration beyond 2 Hz in the horizontal Y direction and throughout the whole frequency range in the vertical direction.

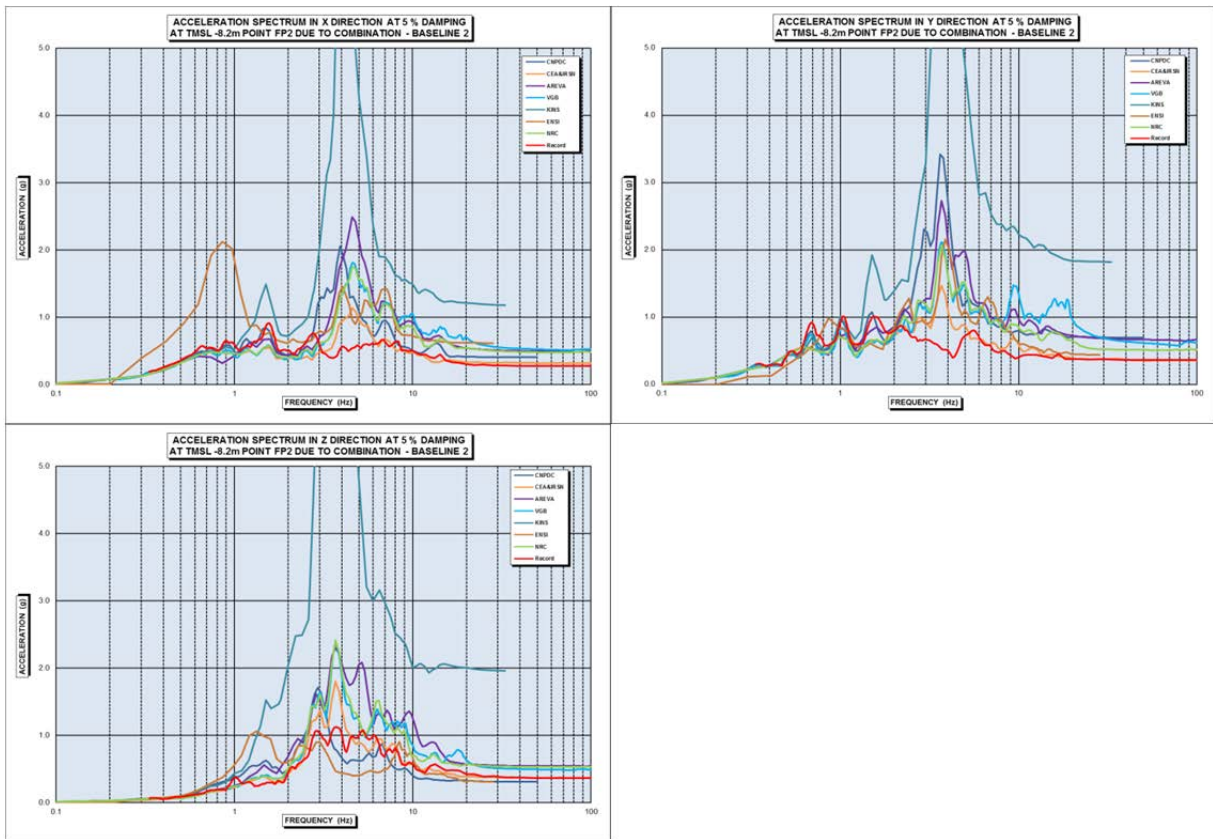


FIG. 35. Calculated and observed floor response spectra (damping 5 %) at the location (FP2) of the accelerometer on the 3rd basement (TMSL -8.2m).

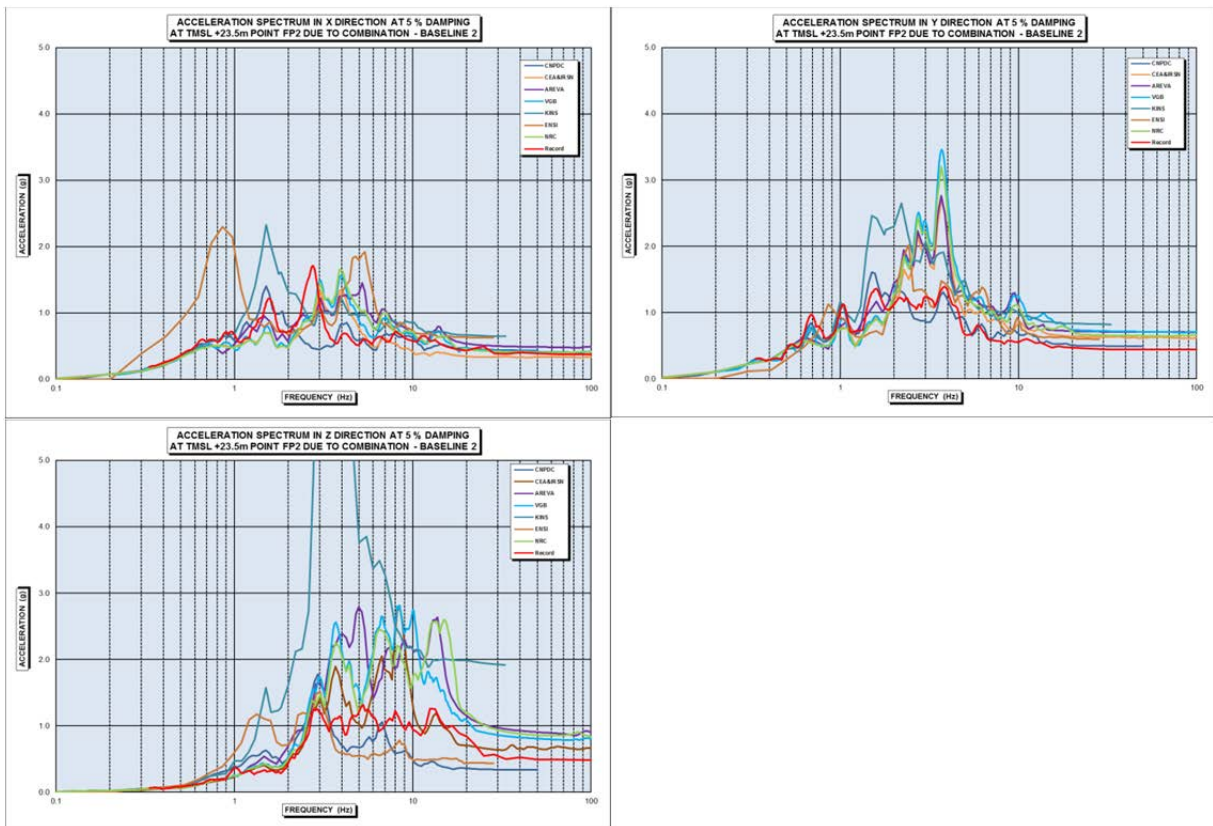


FIG. 36. Calculated and observed floor response spectra (damping 5 %) at the location (FP2) of the accelerometer on the 3rd floor (TMSL +23.5m).

3.2.2. Subtask 1.2.2 “Best estimate analysis”

Participants’ “best estimate analysis” results of the coupled SSI model under the NCOE main shock include modification of the “reference analyses” parameters in order to obtain the best possible fit to the observed records. Each participant was free to use any provided data (e.g. input seismic signals, soil profile etc.) and the best engineering practice to achieve the goal.

Participants’ “best estimate analysis” results of the coupled SSI model for the maximum displacement at the 3rd floor (T.M.S.L. +23.5 m) and at the roof top (T.M.S.L. +49.7 m) are given in Table

22. COVs of the results vary from 67 to 84 %. "Best estimate analysis" displacement results show lower COVs comparing to the “reference analysis”.

Participants’ “best estimate analysis” results of the coupled SSI model for the maximum acceleration at bottom and top (3rd basement) of basemat are given in Table 23. The maximum acceleration values in three directions recorded during the NCOE at the 3rd basement (T.M.S.L. -8.2 m) are also presented in Table 22. COVs of the results vary from 20 to 32 %. It is observed that COVs of acceleration results are smaller than COVs of displacement results. The mean values of the analyses results are higher than peak accelerations recorded at the 3rd basement. In this sense, “best estimate analysis” results in term of acceleration are better than “reference analysis” results.

Similarly, participants’ acceleration results for “best estimate analysis” of the coupled SSI model at the 3rd floor and roof top are presented in Table 24. COVs of the results vary from 20 to 35 %. The mean values are comparable with the recorded values. The mean values of the analysis results are higher than the recorded peak accelerations.

In general, similar to the “reference analyses” results, maximum acceleration values at the two recording locations (on the 3rd basement and on the 3rd floor) are over-estimated by analysis comparing to the recorded values.

TABLE 22. MAXIMUM RELATIVE DISPLACEMENT AT THE 3rd FLOOR AND ROOF TOP FOR THE COUPLED SSI MODEL

PART 1 STRUCTURE: TASK 1.2- NCOE Response (Phase II)								
Subtask 1.2.2 Best estimate analysis of the soil-structure model								
B. Frequency domain/time domain analysis of the soil-structure model								
No	Participant Organization		B.1. Maximum relative displacement due to loading Combination					
			RCCV Displacement (T.M.S.L. +23.5m) at FP2 (mm)			Roof Displacement (T.M.S.L. +49.7m) at WP1 (mm)		
			Δx	Δy	Δz	Δx	Δy	Δz
1	CNPDC, China	For Δx max						
		For Δy max						
		For Δz max						
2	SNERDI-SNPTC, China	For Δx max	35.0			44.3		
		For Δy max		78.6			90.4	
		For Δz max			23.6			21.2
3	CEA&IRSN, France	For Δx max	14.8			21.5		
		For Δy max		16.3			25.9	
		For Δz max			6.3			10.4
4	EdF, France	For Δx max	15.7			9.3		
		For Δy max		25.6			17.4	
		For Δz max			7.7			10.1
5	AREVA, Germany	For Δx max	83.3			89.7		
		For Δy max		101.6			111.6	
		For Δz max			11.7			13.8
6	VGB, Germany	For Δx max	15.2			22.6		
		For Δy max		15.1			23.0	
		For Δz max			5.8			8.6
7	SPI, Germany	For Δx max	123.5			127.0		
		For Δy max		84.4			91.1	
		For Δz max			71.3			68.4
8	AERB, India	For Δx max	34.5			50.1		
		For Δy max		21.8			18.8	
		For Δz max			17.1			22.3
9	BARC, India	For Δx max						
		For Δy max						
		For Δz max						
10	ITER, Italy	For Δx max	17.1			23.7		
		For Δy max		26.2			38.7	
		For Δz max			28.5			30.9
11	KINS, Korea	For Δx max	37.8			52.8		
		For Δy max		60.3			84.5	
		For Δz max			48.1			49.8
12	ENSI, Switzerland	For Δx max	6.7			19.4		
		For Δy max		5.2			27.8	
		For Δz max			5.2			6.3
13	NRC, USA	For Δx max	3.3			5.0		
		For Δy max		3.7			5.5	
		For Δz max			1.6			1.5
Mean			28.9	37.1	17.1	37.1	46.4	19.3
SD			23.2	29.4	14.3	24.9	32.3	14.0
COV			0.80	0.79	0.84	0.67	0.70	0.72

TABLE 23. MAXIMUM ACCELERATION AT BASEMAT AND THE 3rd BASEMENT FOR THE COUPLED SSI MODEL

PART 1 STRUCTURE: TASK 1.2- NCOE Response (Phase II)								
Subtask 1.2.2 Best estimate analysis of the soil-structure model								
B. Frequency domain/time domain analysis of the soil-structure model								
No	Participant Organization		B.2.1 Maximum absolute acceleration due to Combination					
			Absolute acceleration (T.M.S.L. -13.7m) at BP1 (g)			Absolute acceleration (T.M.S.L. -8.2m) at FP2 (g)		
			ax	ay	az	ax	ay	az
1	CNPDC, China	For ax max						
		For ay max						
		For az max						
2	SNERDI-SNPTC, China	For ax max	0.27			0.27		
		For ay max		0.37			0.39	
		For az max			0.30			0.31
3	CEA&IRSN, France	For ax max	0.49			0.46		
		For ay max		0.58			0.56	
		For az max			0.22			0.34
4	EdF, France	For ax max	0.48			0.48		
		For ay max		0.54			0.54	
		For az max			0.19			0.40
5	AREVA, Germany	For ax max	0.29			0.29		
		For ay max		0.35			0.35	
		For az max			0.34			0.38
6	VGB, Germany	For ax max	0.29			0.29		
		For ay max		0.37			0.38	
		For az max			0.39			0.36
7	SPI, Germany	For ax max	0.41			0.41		
		For ay max		0.46			0.42	
		For az max			0.45			0.42
8	AERB, India	For ax max	0.63			0.67		
		For ay max		0.56			0.67	
		For az max			0.62			0.64
9	BARC, India	For ax max						
		For ay max						
		For az max						
10	ITER, Italy	For ax max	0.32			0.33		
		For ay max		0.52			0.58	
		For az max			0.45			0.49
11	KINS, Korea	For ax max	1.30			1.16		
		For ay max		2.00			1.81	
		For az max			0.55			1.74
12	ENSI, Switzerland	For ax max	0.31			0.31		
		For ay max		0.32			0.32	
		For az max			0.30			0.30
13	NRC, USA	For ax max	0.33			0.32		
		For ay max		0.38			0.39	
		For az max			0.37			0.37
Mean			0.39	0.46	0.37	0.39	0.49	0.41
SD			0.12	0.09	0.10	0.13	0.12	0.10
COV			0.30	0.20	0.27	0.32	0.24	0.24
Recorded						0.27	0.36	0.36

TABLE 24. MAXIMUM ACCELERATION AT THE 3rd FLOOR AND ROOF TOP FOR THE COUPLED SSI MODEL

PPART 1 STRUCTURE: TASK 1.2- NCOE Response (Phase II)								
Subtask 1.2.2 Best estimate analysis of the soil-structure model								
B. Frequency domain/time domain analysis of the soil-structure model								
No	Participant Organization		B.2.1 Maximum absolute acceleration due to Combination					
			Absolute acceleration (TMSL+23.5m) at FP2 (g)			Absolute acceleration (T.M.S.L. +49.7m) at WP1 (g)		
			ax	ay	az	ax	ay	az
1	CNPDC, China	For ax max						
		For ay max						
		For az max						
2	SNERDI-SNPTC, China	For ax max	0.30			0.39		
		For ay max		0.45			0.50	
		For az max			0.33			0.28
3	CEA&IRSN, France	For ax max	0.48			0.77		
		For ay max		0.62			0.98	
		For az max			0.56			0.72
4	EdF, France	For ax max	0.44			0.60		
		For ay max		0.61			1.15	
		For az max			0.66			0.80
5	AREVA, Germany	For ax max	0.38			0.45		
		For ay max		0.50			0.64	
		For az max			0.30			0.35
6	VGB, Germany	For ax max	0.35			0.55		
		For ay max		0.48			0.61	
		For az max			0.52			0.43
7	SPI, Germany	For ax max	0.37			0.61		
		For ay max		0.50			0.73	
		For az max			0.54			0.62
8	AERB, India	For ax max	0.98			1.25		
		For ay max		0.78			0.67	
		For az max			0.86			1.06
9	BARC, India	For ax max						
		For ay max						
		For az max						
10	ITER, Italy	For ax max	0.56			0.81		
		For ay max		0.98			1.35	
		For az max			0.62			0.79
11	KINS, Korea	For ax max	0.65			1.34		
		For ay max		0.69			2.46	
		For az max			1.67			2.37
12	ENSI, Switzerland	For ax max	0.33			0.72		
		For ay max		0.32			0.92	
		For az max			0.43			0.52
13	NRC, USA	For ax max	0.38			0.59		
		For ay max		0.49			0.63	
		For az max			0.71			0.46
Mean			0.44	0.57	0.58	0.70	0.85	0.64
SD			0.11	0.11	0.16	0.23	0.27	0.22
COV			0.25	0.20	0.27	0.33	0.31	0.35
Recorded			0.37	0.44	0.47			

Participants' FRS results from "best estimate analysis" of the coupled soil-structure model under the NCOE main shock at 3rd basement and 3rd floor for 5% damping are presented in Figs 37 and 38, respectively. The figures include also the observed response spectra at the same locations.

Peaks of the FRS provided by the participants at the location (FP2) of the accelerometer installed on the 3rd basement do not fit well to the observed response spectra. Most of the

calculated response spectra have peaks at 4 Hz - 5 Hz in the X direction and at 3Hz - 4Hz in the Y direction which differ from the peaks in the observed response spectra. Most of participants' results show significant over-estimation of the spectral acceleration for frequencies beyond 3 Hz.

A few participants provided FRS at the location (FP2) of the accelerometer installed on the 3rd floor which are very comparable with the observed response spectra in all three directions. In general, most of participants' results show significant over-estimation of the spectral acceleration over the whole frequency range.

In general, variation among participants' FRS results is higher in comparison to the variation observed in the FRS of the “reference analyses”. However, a few participants predicted quite well the observed response spectra.

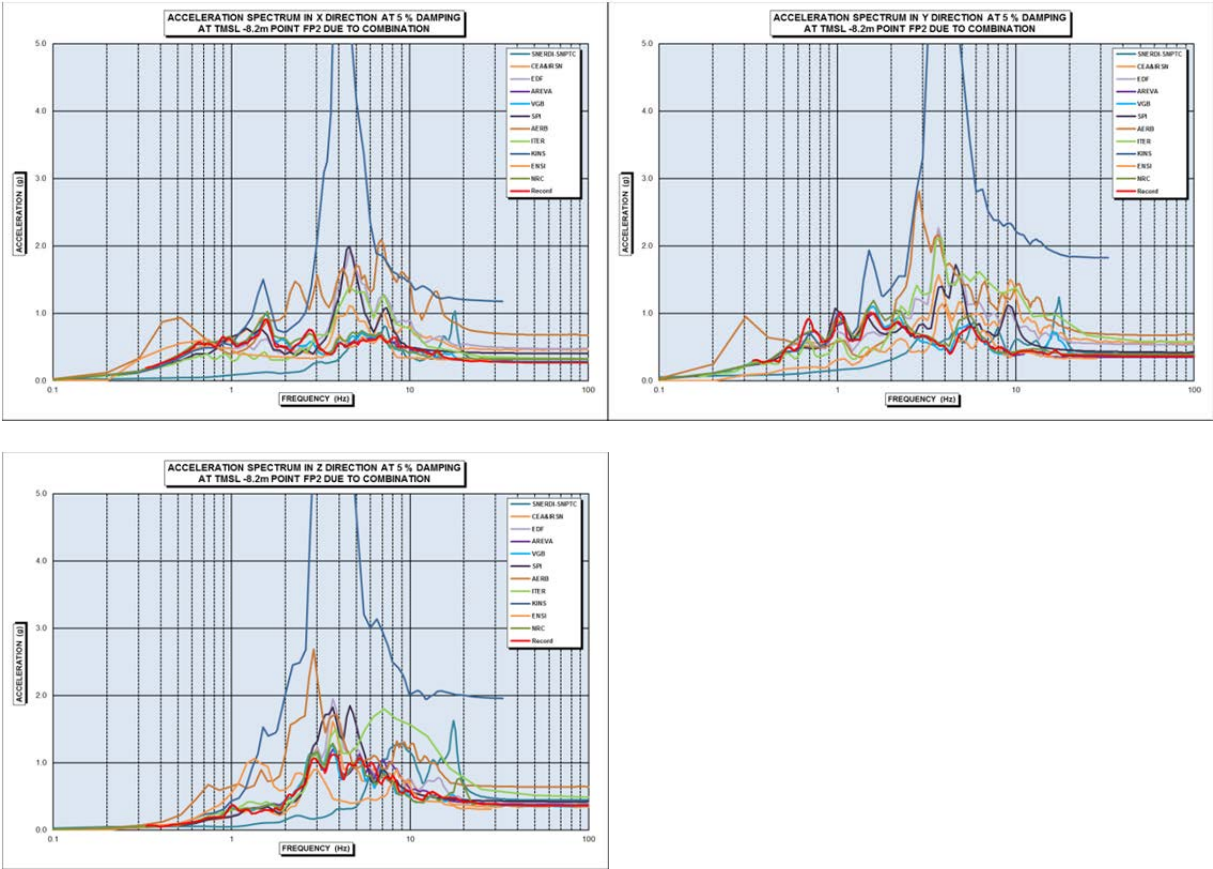


FIG. 37. Calculated and observed floor response spectra (damping 5 %) at the location (FP2) of the accelerometer on the 3rd basement (TMSL -8.2m).

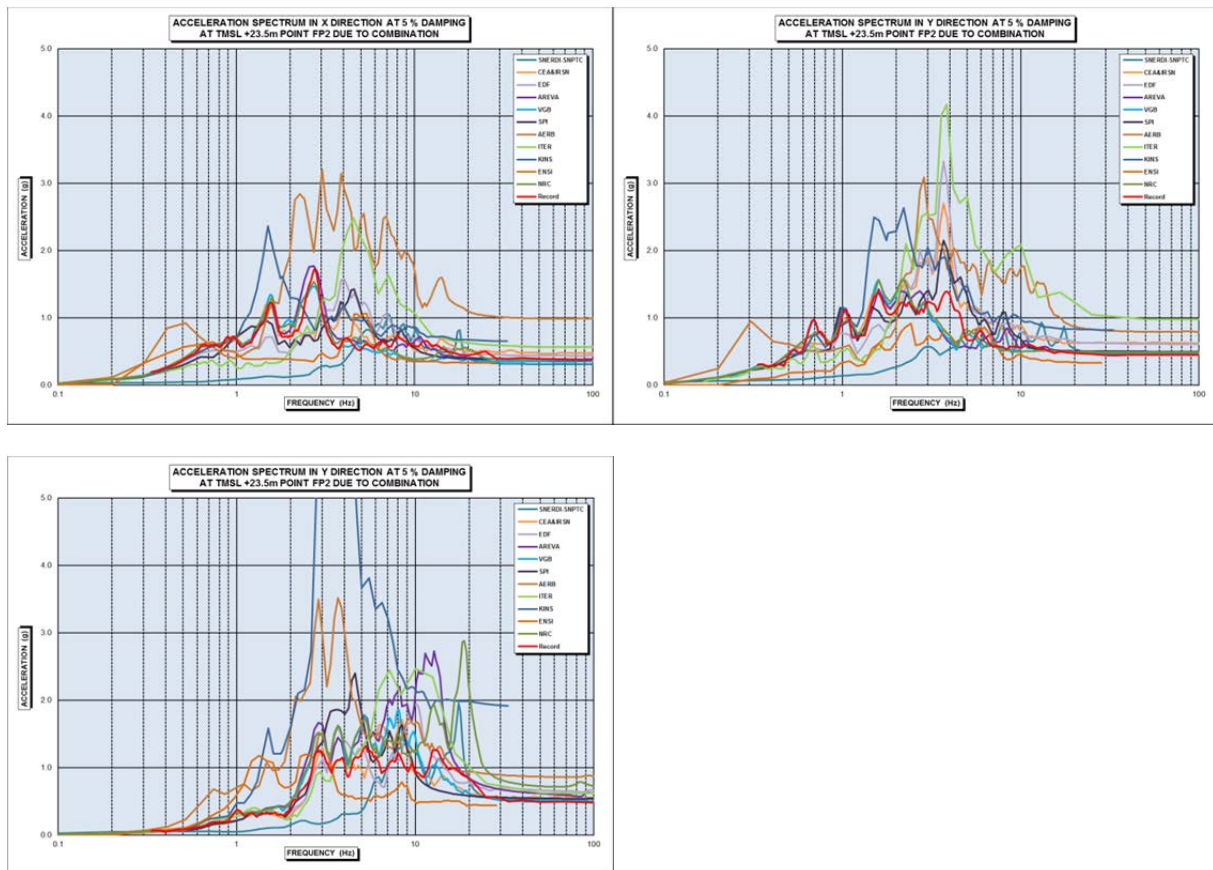


FIG. 38. Calculated and observed floor response spectra (damping 5 %) at the location (FP2) of the accelerometer on the 3rd floor (TMSL +23.5m).

As a general comment on Phase II, although some variation exists among the participants' results, the results show a general tendency towards over-prediction of the recorded data. Variation in the "best-estimate analysis" results is higher in comparison to the variation observed in the "reference analysis" results. Notably, some outlier results are observed. SSI plays a key role in the response of the structure and thus the freedom of choice of control point location for SSI analysis within the "best-estimate analysis" contributes to the scatter in the results (e.g. relative displacement) significantly. This effect is less pronounced on the calculated absolute accelerations which exhibit lower COVs and fit better the recorded data. In general, computed spectral acceleration at the basemat and at the top of RCCV are higher than the recorded data throughout the whole frequency range. However, a few participants predicted quite well the observed response spectra at both levels.

3.3. MAIN RESULTS OF TASK 1.3 FOR PHASE III: MARGIN ASSESSMENT

3.3.1. Model presentation

Types of models, model characteristics (number of nodes, type and number of elements, etc.) and calculation codes used by participants for Phase III are presented in Tables 25, 26 and 27, respectively.

TABLE 25. MODEL PRESENTATION: TYPES OF MODELS

PART 1. STRUCTURE: TASK 1.3- Margin Assessment : Model Presentation	
No	Participant Organization
	Type of model (lumped mass, shell elements, etc.)
1	SNERDI-SNPTC, China Shell Elements Model
2	CEA & IRSN, France Detailed 3D model with several types of finite elements for the reactor building, stick model for the NSSS.
3	EdF, France Shell and beam elements
4	AREVA, Germany 3D shell model with additional beam elements. Inner containment as lumped masses model as per benchmark specification.
5	VGB, Germany The model is generated with shell-elements for walls and floors, beam-elements for beams and columns, rod-elements for roof-trusses and solid-elements for the basemat. In addition mass-elements and springs
6	SPI, Germany A 3D model was used (see pictures of the model).
7	AERB, India Shell-beam 3D model
8	ITER, Italy The structure has been analysed using a 3D Finite Element model. 8-noded 3D solid elements have been used to model reinforced concrete structures. 3D TRUSS elements have been adopted to model the steel roof structure.
9	KINS, Korea Soil-Structure Impedance analysis Model (ACS-SASSI) : A 3-dimensional finite element model has been used. In the model, the basemat was modeled with 8-node brick elements, and the superstructure including RCCV were modeled with 2-node frame elements which have lumped mass. Pushover and Dynamic Response Analysis (RCAHEST) : Shell elements for wall, floor, and RCCV Frame elements for column and girder Solid elements for basemat Spring elements for soil medium, obtained from the impedance analysis by ACS-SASSI
10	NRC, USA CLASSI substructuring approach uses the fixed-base structure model modal characteristics to define structure dynamic properties Structure model same as described under "Fixed-Base Model" and Subtask 1.1.1 Structure model 3D Finite Element model using beam, shell and solid elements.

TABLE 26. MODEL PRESENTATION: MODEL CHARACTERISTICS

PART 1. STRUCTURE: TASK 1.3- Margin Assessment : Model Presentation	
No	Participant Organization
	Model characteristics (Number of nodes, type of elements, number of elements, etc)
1	SNERDI-SNPTC, China There are 4259 nodes and 6315 elements in this model. Layered shell elements are used to simulate floor slabs and walls. Beam elements are used to simulate beams and columns. Link elements are used to simulate steel truss of the steel roof. Piping, equipment and other loads are converted to equivalent masses. They participate in the seismic calculation. 1202 spring elements are added in soil-structure model to simulate the soil under and surround the embedded structure.
2	CEA&IRSN, France Solid elements for the basemat, shell elements for the walls and floors, beam elements for the beams and columns, bar elements for the roof truss elements. Beam elements for the stick model of NSSS, bar elements for the links between RB and NSSS. Number of nodes:10700.
3	EdF, France Shell elements: "Love-Kirchhoff models" based on quadrangular and triangular surface mesh Number of elements: Quadrangular 9700, Triangular 2600, Edges 3300 Beam elements: Euler beam (R/C beams and columns) Timochenko beam (stick model of R/B)
4	AREVA, Germany ca. 50000 nodes; ca. 62000 elements (shell and beam elements). 3D isoparametric shell elements with bending and axial forces.
5	VGB, Germany Number of elements: 15288, Number of nodes: 12560, Number of shell-elements: 9567, Number of solid-elements : 3072, Number of Beams: 1901, Number of Rods: 569, Number of lumped masses: 165, Number of springs: 14
6	SPI, Germany Number of nodes : 32,050 Number of plate/shell elements: 13,897 Number of beam elements: 2,698 Number of lumped masses: 6,854 Number of coupling spring: 10 Number of soil springs (in case of SSI model): 5,142

7	AERB, India	Total no. of Nodes = 7904, 2-noded beam element=1899, 2-noded truss element=578, 4-noded shell element=10752
8	ITER, Italy	Number of nodes= 74780, number of finite elements = 57316 (55594 Solid 3D, 978 QUAD, 669 Truss3D, 75 Mass ID). Total DOF=216168
9	KINS, Korea	<p>Soil-Structure Impedance analysis Model (ACS-SASSI) :</p> <p>Total number of nodes is 1463. (for the superstructure including the basemat)</p> <p>Total number of interaction nodes is 483.</p> <p>Total number of elements is 900.</p> <p>The number of Solid(brick) elements for the basemat of the superstructure is 880.</p> <p>The number of Frame elements for the superstructure is 20.</p> <p>The total number of lumped mass for the superstructure is 14.</p> <p>The soil medium is modelled by 45 horizontal layers.</p> <p>Pushover and Dynamic Response Analysis (RCAHEST) :</p> <p>Total number of nodes : 1,859</p> <p>Total number of elements : 2,407</p> <p>8-nodes Solid elements for basemat : 144 elements</p> <p>4-nodes Shell elements for walls, raft, floor : 1446 elements</p> <p>2-nodes Frame elements for beam columns : 817 elements</p> <p>Soil springs, obtained from the impedance analysis by ACS-SASSI, are attached at 169 nodes of the basemat.</p>
10	NRC, USA	<p>Structure model same as described under "Fixed-Base Model" and Subtask 1.1.1</p> <p>Number of Nodes = 11278, Number of Shell Element=11953, Number of Beam Elements=2367, Number of Solid Elements=1306</p>

TABLE 27. MODEL PRESENTATION: CALCULATION CODES

PART 1. STRUCTURE: TASK 1.3- Margin Assessment : Model Presentation		
No	Participant Organization	Calculation Code or Software used (including Version Number)
1	SNERDI-SNPTC, China	ANSYS 12.1
2	CEA&IRSN, France	Finite Element code CAST3M (Version 2011) developed by CEA
3	EdF, France	Code_Aster (STA10.5) ProMISS3D (v1.4)
4	AREVA, Germany	SOFiSTiK 25
5	VGB, Germany	SOFiSTiK 2010
6	SPI, Germany	SOFiSTiK, Version 25
7	AERB, India	Abaqus-6.9-1 & 6.11-1
8	ITER, Italy	ADINA 8.7
9	KINS, Korea,	ACS SASSI (An Advanced Computational Software for 3D Dynamic Analysis Including Soil-Structure Interaction) Version 2.3.0 : Soil-Structure Impedance Analysis RCA HEST(developed by H.M. Shin, et. al, Sungkyunkwan Univ., Korea) : Pushover and Dynamic Responce Analysis
10	NRC, USA	SAP2000 version 14

3.3.2. Pushover Analysis

Pushover analysis is based on nonlinear static assessment of the behaviour of the structure under an increasing pattern of lateral loads simulating the inertia forces due to an earthquake. This procedure accounts for the nonlinear load-deformation characteristics of individual components and elements of the structure, and provides an integral load–displacement curve representative of the structure capacity [15].

Pushover analyses of the K-K Unit 7 reactor building have been carried out for the fixed-base structural model and the couple soil-structure interaction model.

3.3.2.1. Fixed-base structural model

Participants’ pushover analysis results (top displacement versus applied base shear force and performance points corresponding to 1*NCOE, 2*NCOE, 4*NCOE and 6*NCOE) for the fixed-base model in the X and Y directions are plotted in Figs 39 and 40, respectively. In general, it is observed that the results are not in a good agreement. Some participants calculated performance points corresponding to free field time-histories input motion defined at an outcrop of the raft elevation (ORE) (see Fig. 21) corresponding to 1*NCOE, 2*NCOE, 4*NCOE and 6*NCOE; the correspond points are shown in Figs 39 and 40. Some curves indicate a significantly higher capacity. Some of the results show linear behaviour. However, it is expected that the structure will exhibit non-linear behaviour.

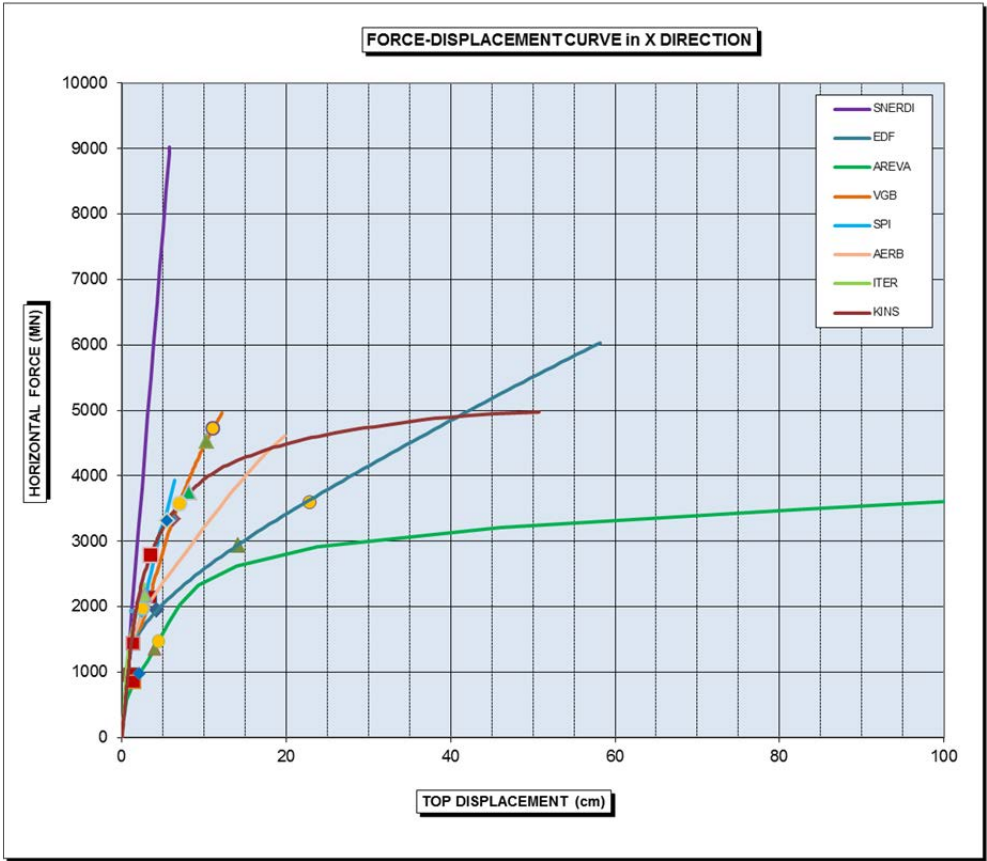


FIG. 39. Pushover curves in the X direction for the fixed-base structural model.

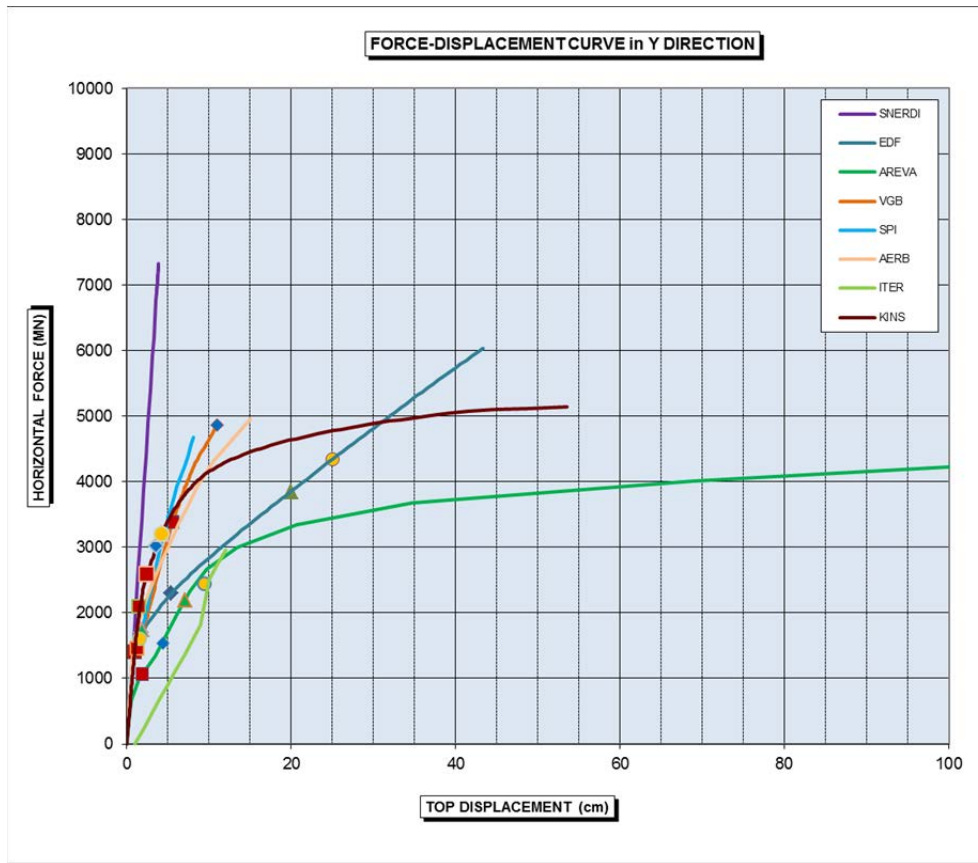


FIG. 40. Pushover curves in the Y direction for the fixed-base structural model.

3.3.2.2. Coupled Soil- Structure Interaction model

Participants’ pushover analysis results (top displacement versus applied base shear force and performance points corresponding to 1*NCOE, 2*NCOE, 4*NCOE, 6*NCOE) for the coupled soil-structure interaction model in the X and Y directions are plotted in Figs 41 and 42, respectively. As for the fixed-base case, it is observed that the results are not in a good agreement. Some participants calculated performance points corresponding to free field time-histories input motion defined at an outcrop of the raft elevation (ORE) (see Fig. 21) corresponding to 1*NCOE, 2*NCOE, 4*NCOE and 6*NCOE; the corresponding points are shown in Figs 41 and 42. Similar to the fixed-base model results, some of the models exhibit linear behaviour. However, it is expected that the structure will exhibit non-linear behaviour. Hence, some could “be applicable to interpretation of dynamic runs”, but not all.

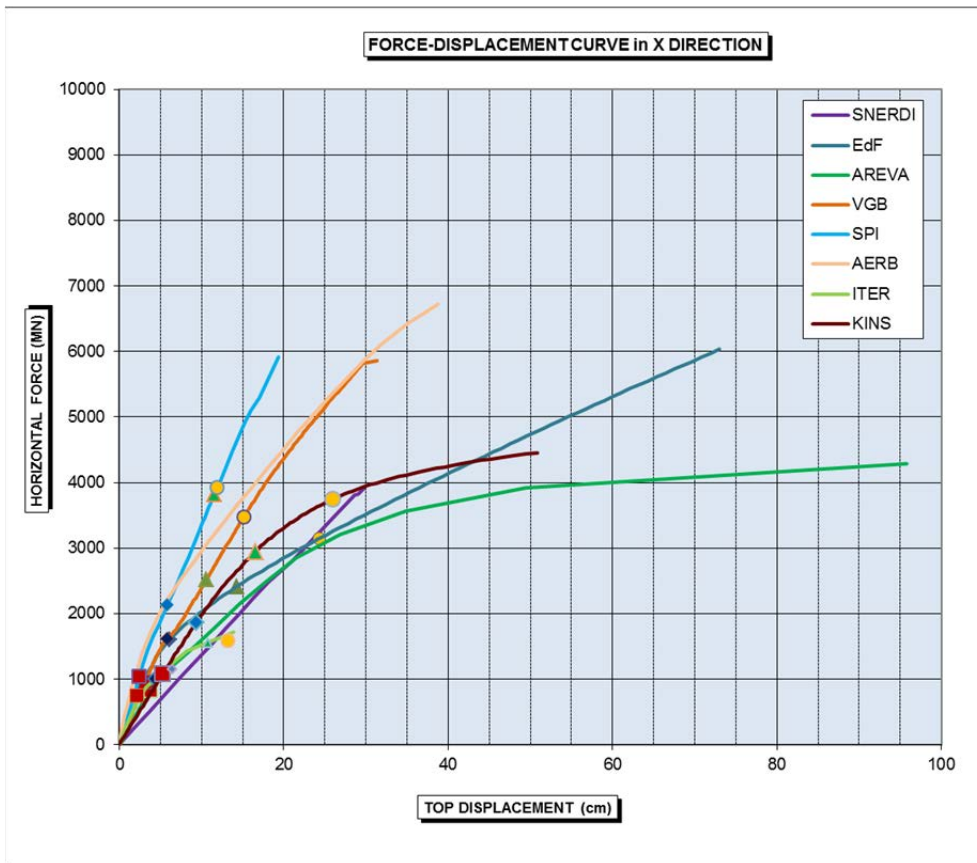


FIG. 41. Pushover curves in the X direction for the coupled soil-structural interaction model.

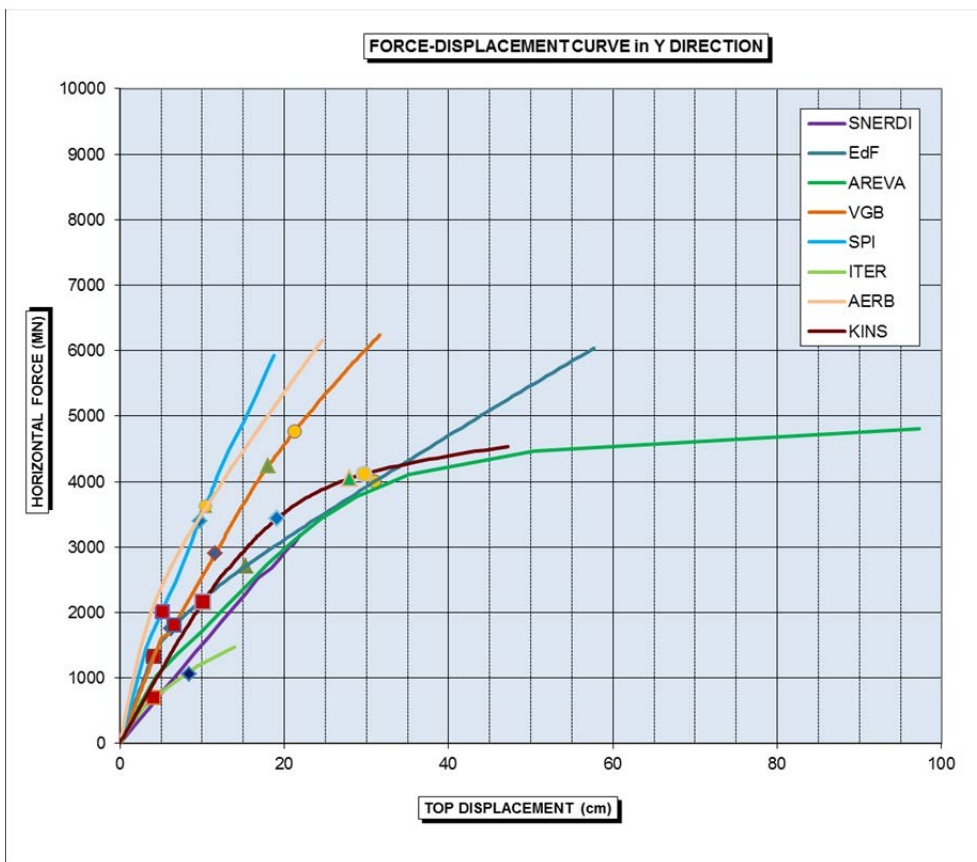


FIG. 42. Pushover curves in the Y direction for the coupled soil-structural interaction model.

3.3.3. Dynamic Response Analysis

3.3.3.1. Fixed-Base Structure Model: Displacement, Acceleration and Response Spectrum

Participants' maximum relative displacement results at the location (FP2) of the accelerometer device on the 3rd floor (TMSL +23.5M) due to seismic input time-histories scaled to 1*NCOE, 2*NCOE, 4*NCOE and 6*NCOE for the fixed-base structural model are given in Table 28. COVs of the relative displacement results vary from 11 to 52 %. COVs of the results in the X direction are significantly lower than in the Y and Z directions. The maximum relative displacement at the 3rd floor versus the scaling factor of the input time-histories (varied from 1*NCOE to 6*NCOE) in the X and Y directions are plotted in Fig. 43. Two result curves for a scaling factor of 6.0 show negative slope suggesting displacement decrease with increasing seismic demand. This contradicts expectations and the results of the remaining 6 participants. In comparison to the results from pushover analyses (presented in section 3.3.2.1), dynamic analyses indicate a higher seismic capacity.

It should be noted that nonlinear dynamic analysis generally provides more realistic results of structural response to strong ground shaking than nonlinear static analysis. Nonlinear static analysis is limited in its ability to capture transient dynamic behaviour with cyclic loading and degradation. Nevertheless, nonlinear static analysis is a convenient procedure that provides reliable results for structures whose dynamic response is governed by the first-mode sway motions.

TABLE 28. DYNAMIC RESPONSE ANALYSES FOR THE FIXED-BASE STRUCTURE MODEL: MAXIMUM RELATIVE DISPLACEMENT AT THE 3rd FLOOR (TMSL +23.5m)

PART 1. STRUCTURE: TASK 1.3- Margin Assessment														
Subtask 1.3.2 Dynamic response analysis														
A. Fixed Base Structure Model														
No	Participant Organization		A.1.1. Maximum displacement due to loading Combination											
			Displacement (T.M.S.L. +23.5m) at FP2 (mm)											
			1xNCOE			2xNCOE			4xNCOE			6xNCOE		
			Δx	Δy	Δz	Δx	Δy	Δz	Δx	Δy	Δz	Δx	Δy	Δz
1	SNERDI-SNPTEC, China	For Δx max												
		For Δy max												
		For Δz max												
2	CEA&IRSN, France	For Δx max	38.3			60.1			97.4			107.9		
		For Δy max		48.2			90.2			137.4			158.0	
		For Δz max			14.8			37.3			53.3			57.4
3	EdF, France	For Δx max	22.9			45.6			87.0			135.5		
		For Δy max		38.7			96.6			143.3			175.0	
		For Δz max			19.8			31.8			49.0			42.8
4	AREVA, Germany	For Δx max	10.8			24.1			41.4			87.1		
		For Δy max		10.9			19.5			35.0			100.3	
		For Δz max			4.4			9.7			15.4			21.4
5	VGB, Germany	For Δx max	29.0			53.5			77.1			105.6		
		For Δy max		42.0			92.7			141.7			176.7	
		For Δz max			14.2			21.6			33.7			49.2
6	SPI, Germany	For Δx max	31.0			46.5			98.6			108.4		
		For Δy max		49.7			96.2			170.3			200.9	
		For Δz max			18.2			35.3			26.7			25.4
7	AERB, India	For Δx max	22.1			48.1			67.7			65.4		
		For Δy max		18.5			43.4			48.1			46.2	
		For Δz max			13.0			34.3			58.7			59.6
8	ITER, Italy	For Δx max												
		For Δy max												
		For Δz max												
9	KINS, Korea	For Δx max	24.3			44.3			60.7			61.2		
		For Δy max		20.8			76.1			110.1			120.7	
		For Δz max			10.2			32.9			54.4			47.0
10	NRC, USA	For Δx max	20.3			37.6			56.1			54.5		
		For Δy max		15.3			26.2			30.2			28.1	
		For Δz max			5.8			11.5			16.9			16.2
Mean			24.9	30.6	12.7	45.9	70.8	27.9	74.5	107.1	38.8	89.3	129.5	46.9
SD			4.2	14.0	4.3	5.2	29.2	9.4	16.2	55.8	16.0	21.6	51.0	15.6
COV			0.17	0.46	0.34	0.11	0.41	0.34	0.22	0.52	0.41	0.24	0.39	0.33

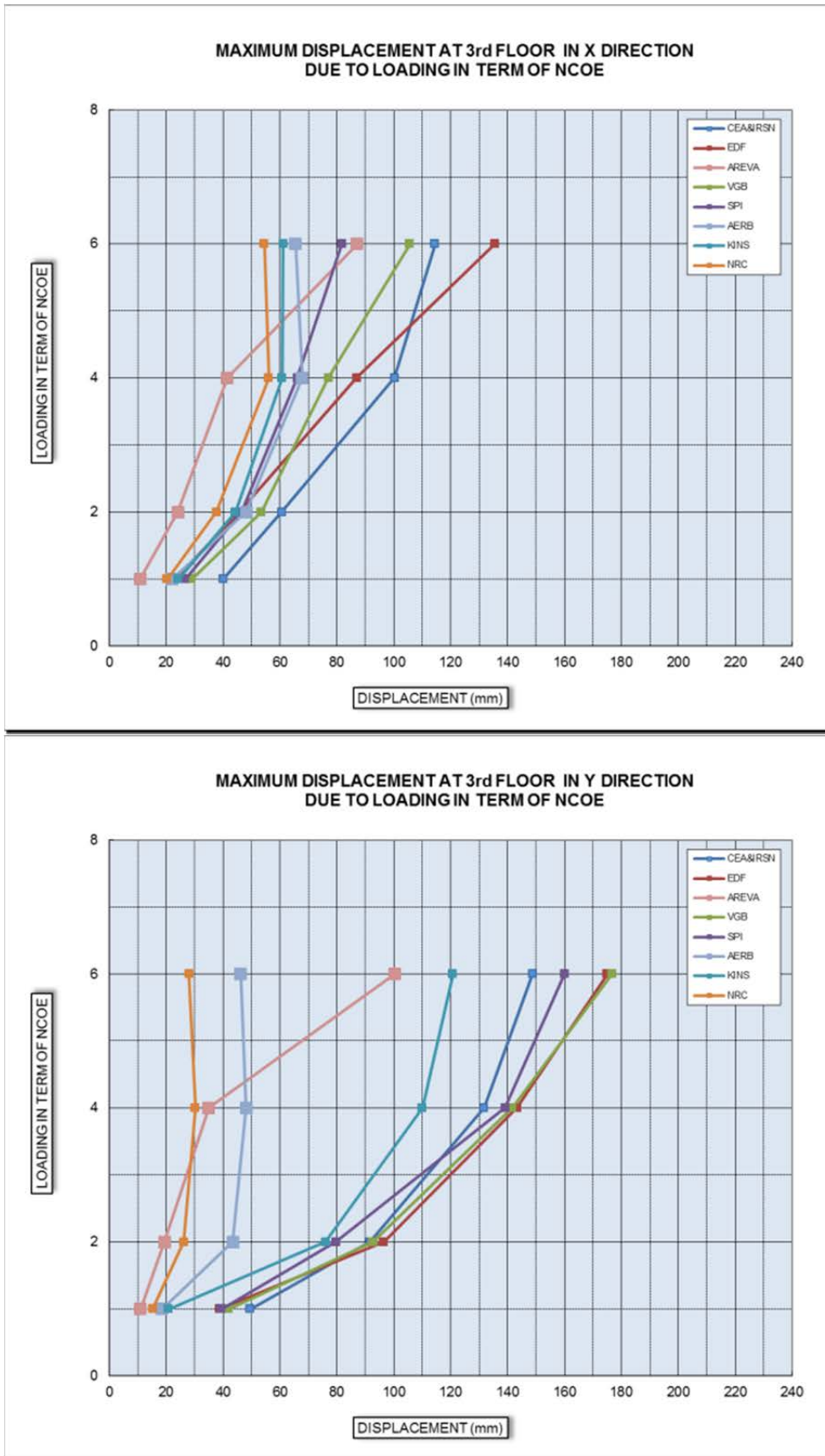


FIG. 43. Maximum relative displacement at the location (FP2) of the accelerometer device on the 3rd floor (TMSL +23.5m) in the X and Y directions as a function of the scaling factor of the seismic input time-history NCOE (with the fixed-base model).

Participants' maximum absolute acceleration results at point FP2 (location of the accelerometer device) on the 3rd floor (TMSL +23.5M) due to seismic input time-histories scaled to 1*NCOE, 2*NCOE, 4*NCOE and 6*NCOE for the fixed-base structural model are given in Table 29. The COVs of the results vary from 15 to 43 %. The maximum absolute acceleration results at the 3rd floor versus the scaling factor of the input time-histories (varied from 1*NCOE to 6*NCOE) in the X and Y directions are plotted in Fig. 44. Four result curves in the X direction and three in the Y direction for a scaling factor of 6.0 show negative slope suggesting accelerations decrease with increasing seismic demand.

TABLE 29 DYNAMIC RESPONSE ANALYSES FOR THE FIXED-BASE STRUCTURAL MODEL: MAXIMUM ABSOLUTE ACCELERATION AT THE 3rd FLOOR (TMSL +23.5m)

PART 1. STRUCTURE: TASK 1.3- Margin Assessment														
Subtask 1.3.2 Dynamic response analysis														
A. Fixed Base Structure Model														
No	Participant Organization	A.2.1. Maximum absolute acceleration due to loading Combination												
		Absolute acceleration (TMSL +23.5m) at FP2 (g)												
		1xNCOE			2xNCOE			4xNCOE			6xNCOE			
		ax	ay	az	ax	ay	az	ax	ay	az	ax	ay	az	
1	SNERDI-SNPTC, China	For Δx max												
		For Δy max												
		For Δz max												
2	CEA&IRSN, France	For Δx max	1.65			2.00			2.62			2.99		
		For Δy max		1.83			2.99			4.22			4.53	
		For Δz max			2.24			4.37			4.90			7.20
3	EdF, France	For Δx max	1.56			2.29			2.23			4.69		
		For Δy max		1.43			1.69			1.90			3.48	
		For Δz max			1.57			3.20			5.16			5.51
4	AREVA, Germany	For Δx max	0.97			2.02			2.63			2.17		
		For Δy max		0.92			1.94			2.69			2.72	
		For Δz max			0.46			1.15			2.05			2.23
5	VGB, Germany	For Δx max	1.47			2.34			3.62			3.26		
		For Δy max		1.66			3.00			2.98			2.79	
		For Δz max			1.69			2.31			4.02			3.88
6	SPI, Germany	For Δx max	4.80			11.48			8.06			13.37		
		For Δy max		6.12			11.48			5.68			2.93	
		For Δz max			4.80			11.48			8.06			13.37
7	AERB, India	For Δx max	2.64			4.47			5.11			5.09		
		For Δy max		2.02			3.36			3.35			3.60	
		For Δz max			3.53			5.56			6.35			6.10
8	ITER, Italy	For Δx max												
		For Δy max												
		For Δz max												
9	KINS, Korea	For Δx max	2.08			2.90			3.68			3.99		
		For Δy max		1.90			3.06			3.64			3.59	
		For Δz max			1.22			3.14			3.82			5.10
10	NRC, USA	For Δx max	2.07			3.80			5.72			5.63		
		For Δy max		2.24			3.71			3.95			3.56	
		For Δz max			1.54			2.92			4.50			5.01
Mean			1.91	1.85	1.96	2.97	2.97	3.58	3.83	3.34	4.79	4.28	3.59	5.47
SD			0.44	0.28	0.84	0.97	0.68	1.18	1.36	0.83	0.92	1.04	0.55	1.12
COV			0.23	0.15	0.43	0.33	0.23	0.33	0.36	0.25	0.19	0.24	0.15	0.20

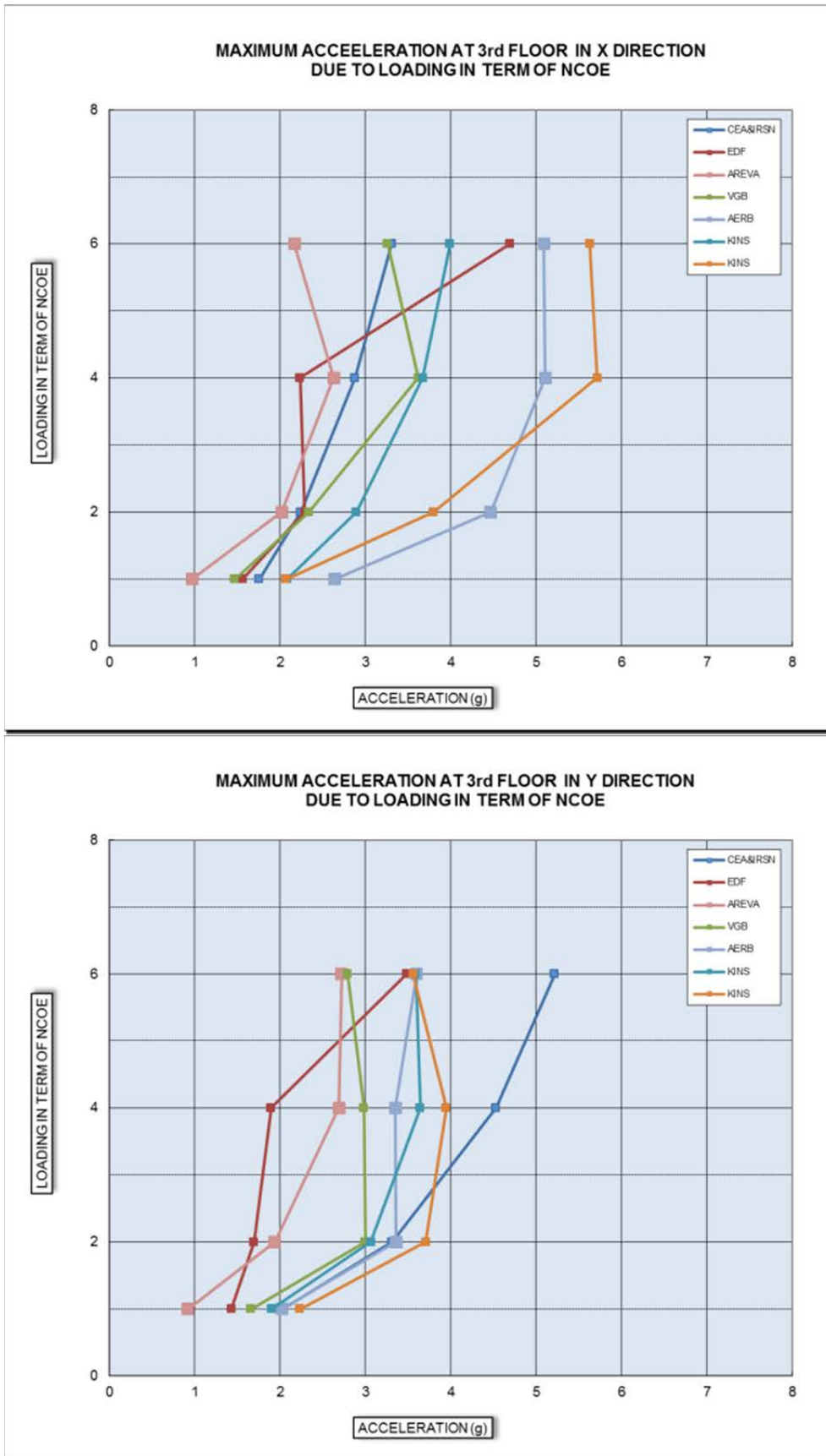


FIG. 44. Maximum absolute acceleration at the location (FP2) of the accelerometer device on the 3rd floor (TMSL +23.5m) in the X and Y directions as a function of the scaling factor of the seismic input time-history NCOE (with the fixed-base model).

Participants' floor response spectrum results in the X direction at point FP2 on the 3rd floor (TMSL +23.5m) for 5% damping due to seismic input time-histories scaled to 1*NCOE, 2*NCOE, 4*NCOE and 6*NCOE are shown in Fig. 45, respectively. The higher the scaling factor of the input time-histories the bigger the scatter of the results possibly due to strong nonlinear effects in the behaviour. The spectral peaks do not shift notably to lower frequencies due to anticipated stiffness degradation effects which may be due to the fact that the spectral peak frequency comes from the dominant frequency of the input seismic motion.

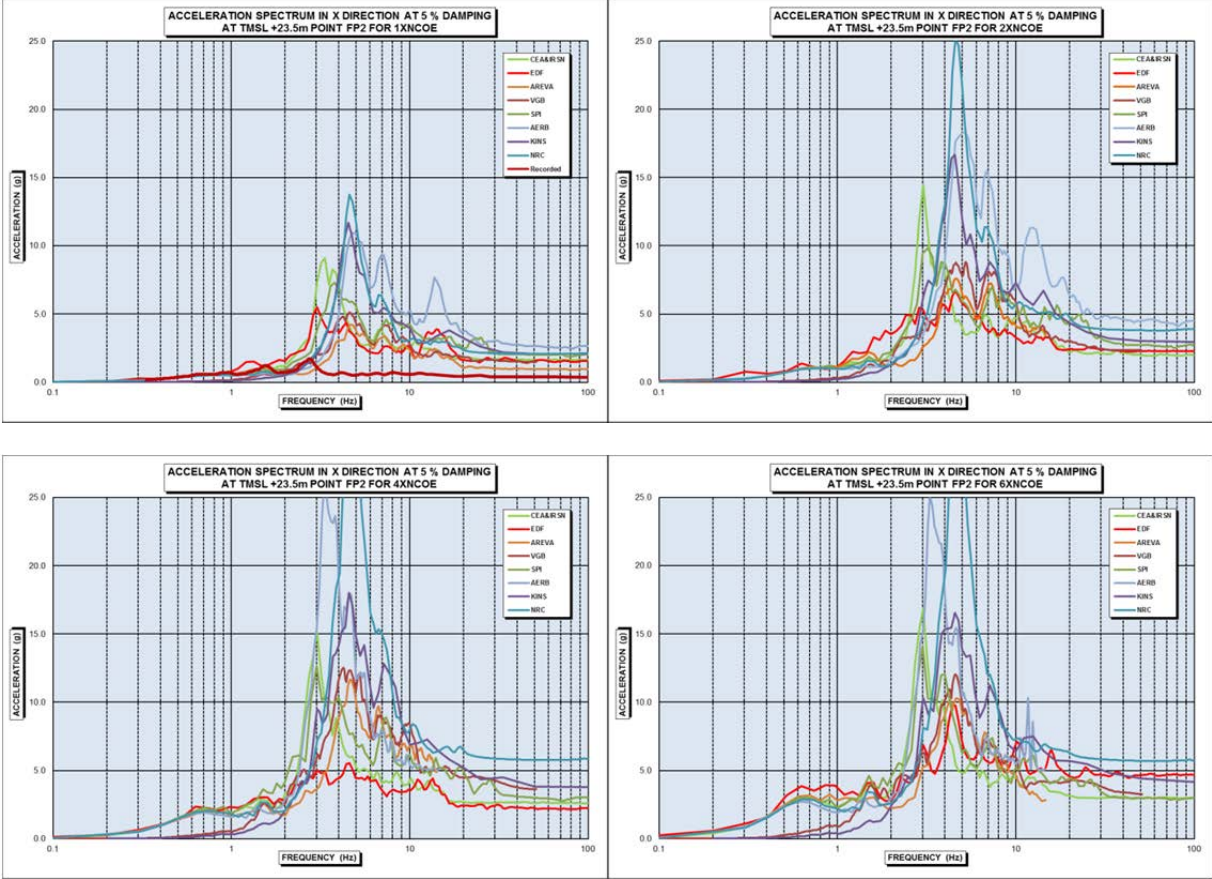
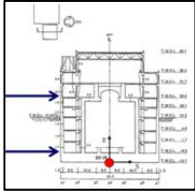


FIG. 45. Calculated and observed (1*NCOE) floor response spectra (damping 5 %) in the X direction at the location (FP2) of the accelerometer device on the 3rd floor (TMSL +23.5m) due to seismic input time-histories scaled to 1*NCOE, 2*NCOE, 4*NCOE and 6*NCOE, respectively (with the fixed-base model).

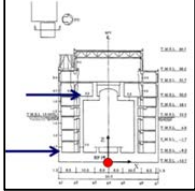
Participants' inter-story drift ratio results from nonlinear dynamic analysis of the coupled SSI models due to seismic input time-histories scaled to 1*NCOE, 2*NCOE, 4*NCOE and 6*NCOE are presented in Table 30.

TABLE 30. INTER-STORY DRIFT RATIO RESULTS FROM NONLINEAR DYNAMIC ANALYSIS OF THE FIXED-BASE MODEL

B.4. Drift determination								
(DW3 - DW1) / 3170								
	1xNCOE		2xNCOE		4xNCOE		6xNCOE	
	X dir.	Y dir.						
CEA&IRSN, France	0.0011	0.0014	0.0016	0.0029	0.0027	0.0041	0.0029	0.0048
EdF, France	0.0006	0.0013	0.0012	0.0028	0.0030	0.0039	0.0043	0.0055
AREVA, Germany	0.0008	0.0020	0.0014	0.0031	0.0021	0.0056	0.0072	0.0108
VGB, Germany	0.0009	0.0013	0.0015	0.0024	0.0024	0.0036	0.0035	0.0045
SPI, Germany	0.0010	0.0014	0.0016	0.0027	0.0030	0.0034	0.0035	0.0038
AERB, India	0.0082	0.0051	0.0156	0.0096	0.0232	0.0138	0.0240	0.0158
KINS, Korea	0.0007	0.0006	0.0015	0.0022	0.0021	0.0031	0.0020	0.0035
NRC, USA	0.0056	0.0045	0.0105	0.0077	0.0156	0.0106	0.0150	0.0101
Mean	0.0024	0.0022	0.0044	0.0042	0.0068	0.0060	0.0078	0.0073
SD	0.0029	0.0017	0.0055	0.0028	0.0081	0.0040	0.0078	0.0044
COV	1.23	0.75	1.27	0.67	1.19	0.66	1.00	0.60



B.4. Drift determination								
(DR3 - DW1) / 3170								
	1xNCOE		2xNCOE		4xNCOE		6xNCOE	
	X dir.	Y dir.						
CEA&IRSN, France	0.0012	0.0014	0.0017	0.0026	0.0028	0.0040	0.0030	0.0047
EdF, France	0.0007	0.0011	0.0014	0.0028	0.0030	0.0040	0.0043	0.0050
AREVA, Germany	0.0008	0.0018	0.0023	0.0031	0.0028	0.0054	0.0089	0.0124
VGB, Germany	0.0009	0.0013	0.0015	0.0029	0.0025	0.0044	0.0033	0.0055
SPI, Germany	0.0009	0.0016	0.0014	0.0031	0.0025	0.0052	0.0028	0.0061
AERB, India	0.0070	0.0063	0.0122	0.0154	0.0164	0.0186	0.0189	0.0192
KINS, Korea	0.0007	0.0006	0.0014	0.0023	0.0020	0.0033	0.0020	0.0036
NRC, USA	0.0063	0.0048	0.0117	0.0083	0.0174	0.0093	0.0170	0.0088
Mean	0.0023	0.0024	0.0042	0.0051	0.0062	0.0068	0.0075	0.0081
SD	0.0027	0.0020	0.0048	0.0046	0.0066	0.0051	0.0068	0.0053
COV	1.17	0.86	1.14	0.91	1.07	0.75	0.90	0.65



3.3.3.2. “Reference Analysis” of the Soil-Structure Interaction model: Displacement, Acceleration and Response Spectrum

Participants’ maximum relative displacement results at the location (FP2) of the accelerometer on the 3rd floor (TMSL +23.5M) due to seismic input time-histories scaled to 1*NCOE, 2*NCOE, 4*NCOE and 6*NCOE for the coupled soil-structure interaction model are shown in Table 31. COVs of the results vary from 27 to 55 %.The maximum relative displacement at the 3rd floor versus the scaling factor of the input time-histories (varied from 1*NCOE to 6*NCOE) in the X and Y directions are plotted in Fig. 46. Notably, there is an outlier in the results. In comparison to the results from pushover analyses (presented in section 3.3.2.2), dynamic analyses indicate a higher seismic capacity. As mentioned in the previous section, the ability of nonlinear static analysis is limited in capturing the transient dynamic behaviour with cyclic loading and corresponding degradation, and in taking into account high soil damping. In comparison to the results from the fixed-base model, the calculated displacements from the coupled soil-structure interaction model are larger.

TABLE 31. DYNAMIC RESPONSE ANALYSES FOR THE COUPLED SOIL-STRUCTURE INTERACTION MODEL: MAXIMUM RELATIVE DISPLACEMENT AT 3rd FLOOR (TMSL +23.5m)

PART 1. STRUCTURE: TASK 1.3- Margin Assessment													
Subtask 1.3.2 Dynamic response analysis													
B. Reference Analysis of the Soil-Structure Model													
No	Participant Organization	B.1.1. Maximum displacement due to loading Combination											
		Displacement (T.M.S.L. +23.5m) at FP2 (mm)											
		1xNCOE			2xNCOE			4xNCOE			6xNCOE		
		Δx	Δy	Δz	Δx	Δy	Δz	Δx	Δy	Δz	Δx	Δy	Δz
1	SNERDI-SNPTC, China	For Δx max											
		For Δy max											
		For Δz max											
2	CEA&IRSN, France	For Δx max	11.3			24.4			65.0			149.8	
		For Δy max		14.7			30.5			59.2			562.8
		For Δz max			7.7			14.8			25.7		
3	EdF, France	For Δx max	31.9			75.2							
		For Δy max		52.9			100.2						
		For Δz max			46.1			69.8					
4	AREVA, Germany	For Δx max	36.0			69.0			163.3			193.8	
		For Δy max		28.9			84.5			213.1			388.4
		For Δz max			27.4			41.9			54.0		
5	VGB, Germany	For Δx max	23.5			63.4			105.5			136.3	
		For Δy max		33.2			87.9			135.8			166.3
		For Δz max			12.3			33.5			62.3		
6	SPI, Germany	For Δx max	23.5			58.1			88.6			212.6	
		For Δy max		40.4			88.3			148.9			209.6
		For Δz max			38.4			45.8			52.4		
7	AERB, India	For Δx max	19.1			41.6			73.5			90.6	
		For Δy max		26.3			47.1			87.6			103.7
		For Δz max			27.5			37.6			39.3		
8	ITER, Italy	For Δx max											
		For Δy max											
		For Δz max											
9	KINS, Korea	For Δx max	44.5			83.8			140.2			208.5	
		For Δy max		46.6			82.2			134.4			229.8
		For Δz max			49.6			76.0			106.4		
10	NRC, USA	For Δx max	3.7			6.8			11.6			13.8	
		For Δy max		5.1			9.0			12.2			12.1
		For Δz max			2.4			4.0			6.5		
Mean		24.2	32.7	26.6	55.3	73.1	40.6	99.2	128.9	46.7	156.6	219.6	87.2
SD		8.9	13.0	14.7	19.0	27.6	17.9	39.0	59.4	14.4	48.3	106.0	23.6
COV		0.37	0.40	0.55	0.34	0.38	0.44	0.39	0.46	0.31	0.31	0.48	0.27

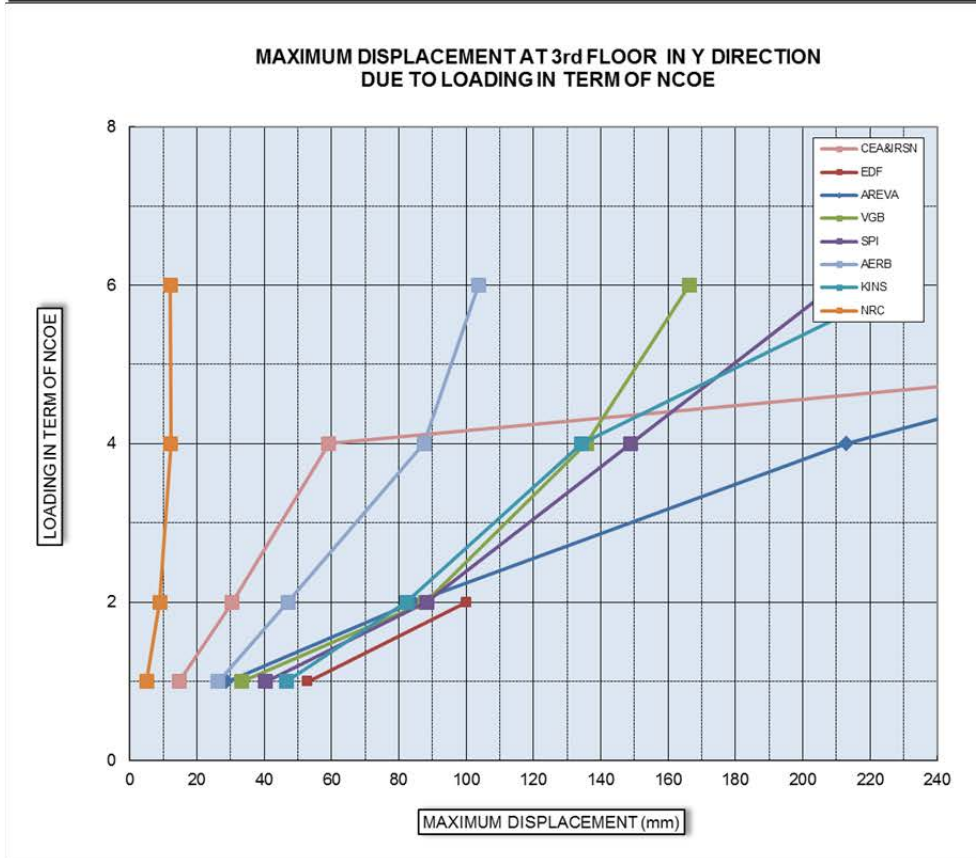
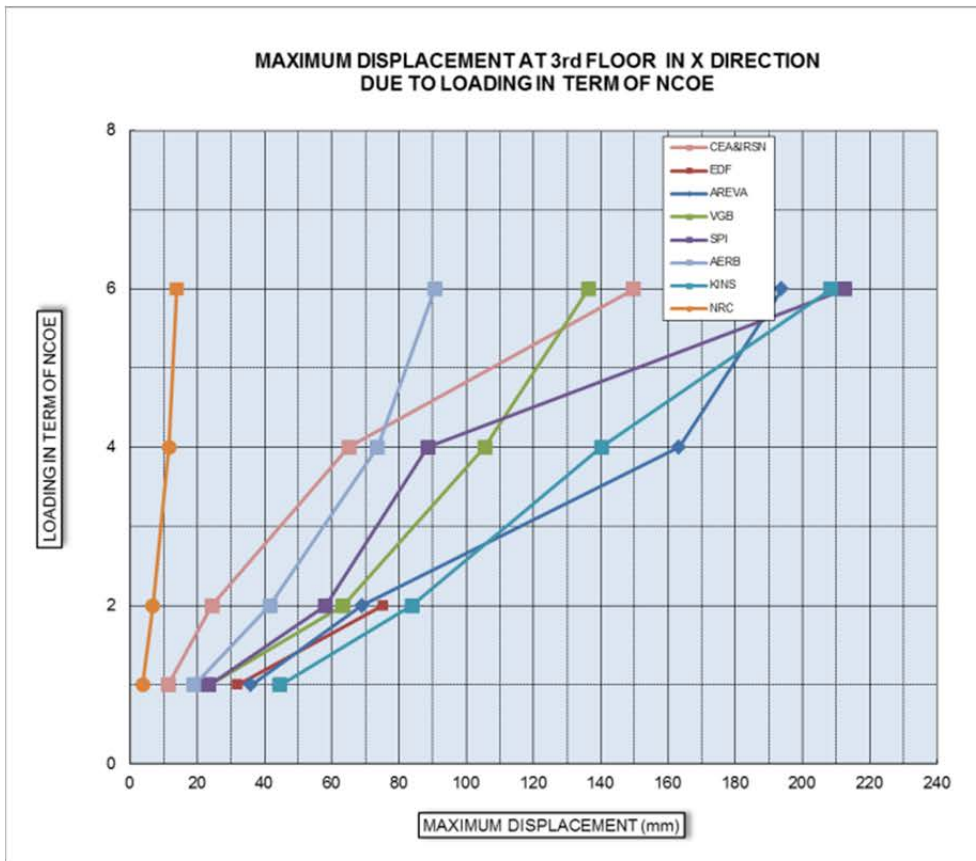


FIG. 46. Maximum relative displacement at the location (FP2) of the accelerometer device on the 3rd floor (TMSL +23.5m) in the X and Y directions as a function of the scaling factor of the seismic input time-history NCOE (with the SSI model).

Participants' maximum absolute acceleration results at point FP2 (location of the accelerometer device) on the 3rd floor due to seismic input time-histories scaled to 1*NCOE, 2*NCOE, 4*NCOE and 6*NCOE for the coupled soil-structure model are given in Table 32. COVs of the results vary from 19 to 42 %. COVs of the results in the horizontal direction for 1*NCOE, 2*NCOE and 4*NCOE are similar, and somewhat bigger than the ones for 6*NCOE. Maximum absolute acceleration results at the 3rd floor versus the scaling factor of the input time-histories (varied from 1*NCOE to 6*NCOE) in the X and Y directions are plotted in Fig. 47. Three result curves in the X direction and four in the Y direction for a scaling factor of 6.0 show negative slope suggesting accelerations decrease with increasing seismic demand. In comparison to the results from the fixed-base model, the calculated accelerations from the coupled soil-structure interaction model are smaller.

TABLE 32. DYNAMIC RESPONSE ANALYSES FOR THE COUPLED SOIL-STRUCTURE INTERACTION MODEL: MAXIMUM ABSOLUTE ACCELERATION AT THE 3rd FLOOR (TMSL +23.5m)

PART 1. STRUCTURE: TASK 1.3- Margin Assessment														
Subtask 1.3.2 Dynamic response analysis														
B. Reference Analysis of the Soil-Structure Model														
No	Participant Organization		B.2.1. Maximum absolute acceleration due to loading Combination											
			Absolute acceleration (TMSL +23.5m) at FP2 (g)											
			1xNCOE			2xNCOE			4xNCOE			6xNCOE		
			ax	ay	az	ax	ay	az	ax	ay	az	ax	ay	az
1	SNERDI-SNPTC, China	For ax max												
		For ay max												
		For az max												
2	CEA&IRSN, France	For ax max	0.68			1.20			2.29			3.11		
		For ay max		1.03			1.80			2.69			3.51	
		For az max			0.59			0.84			1.79			2.32
3	EdF, France	For ax max	0.57			1.00								
		For ay max		0.89			1.28							
		For az max			1.02			2.74						
4	AREVA, Germany	For ax max	1.32			2.59			3.14			3.16		
		For ay max		1.51			3.17			3.48			2.53	
		For az max			0.71			1.08			1.82			1.92
5	VGB, Germany	For ax max	1.12			2.46			3.04			2.93		
		For ay max		1.24			2.24			2.84			2.75	
		For az max			1.34			2.03			3.45			4.16
6	SPI, Germany	For ax max	0.78			1.33			1.88			3.03		
		For ay max		0.97			1.96			2.38			3.32	
		For az max			1.51			3.11			3.68			6.36
7	AERB, India	For ax max	2.03			2.74			4.63			4.44		
		For ay max		2.27			3.09			4.61			4.27	
		For az max			2.00			2.95			4.10			4.49
8	ITER, Italy	For ax max												
		For ay max												
		For az max												
9	KINS, Korea	For ax max	1.42			2.58			3.59			3.49		
		For ay max		1.35			2.20			2.35			2.48	
		For az max			1.14			1.85			3.42			3.74
10	NRC, USA	For ax max	0.41			0.78			1.31			1.49		
		For ay max		0.65			1.19			1.63			1.61	
		For az max			0.96			1.48			2.38			3.18
Mean			1.03	1.21	1.26	1.89	2.26	2.23	2.85	3.20	3.08	3.33	3.28	4.10
SD			0.43	0.29	0.46	0.79	0.75	0.83	0.79	0.89	0.95	0.62	0.69	1.52
COV			0.42	0.24	0.37	0.42	0.33	0.37	0.28	0.28	0.31	0.19	0.21	0.37

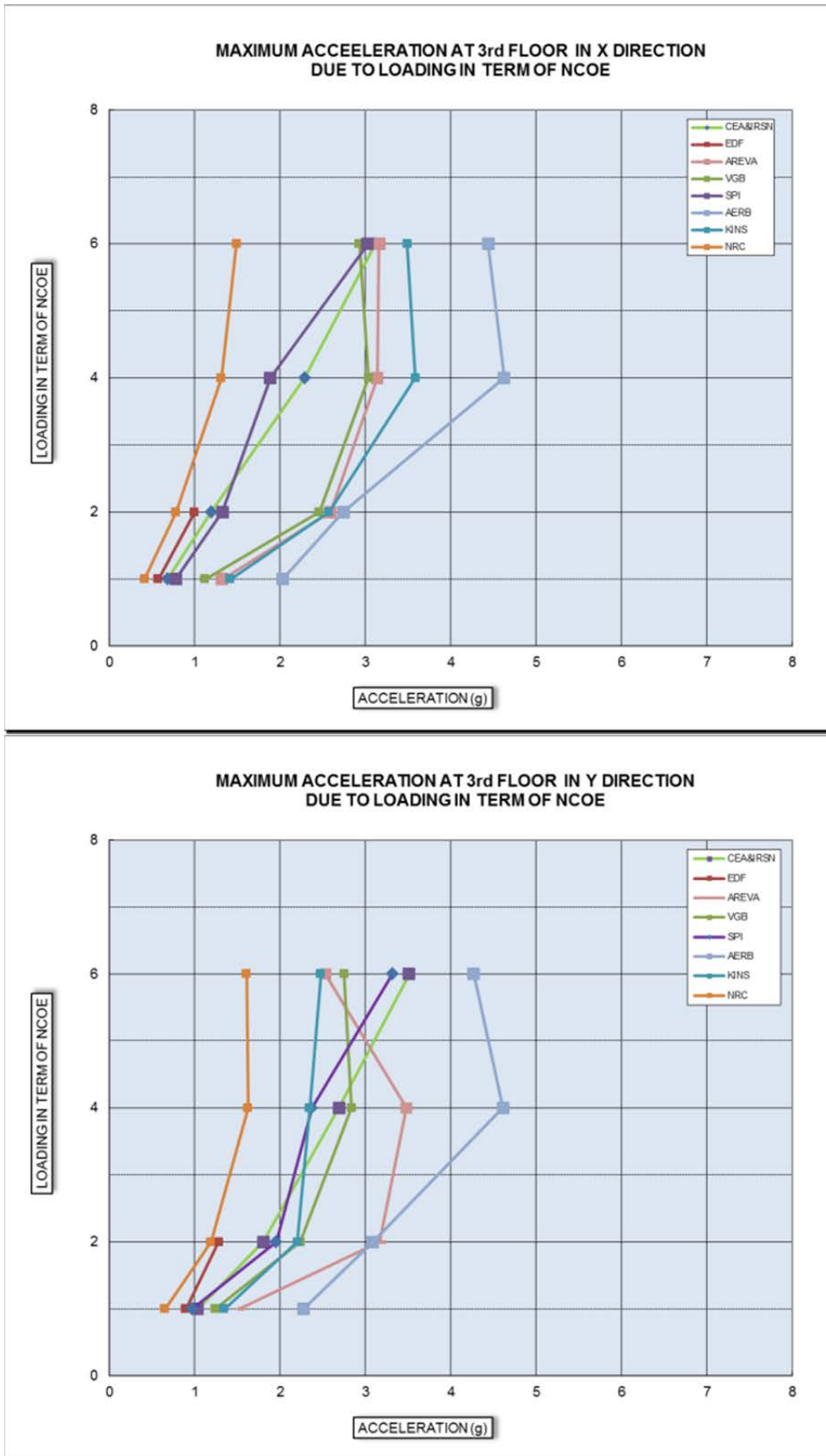


FIG. 47. Maximum absolute acceleration at the location (FP2) of the accelerometer device on the 3rd floor (TMSL +23.5m) in the X and Y directions as a function of the scaling factor of the seismic input time-history NCOE (with the SSI model).

Participants' floor response spectra results in the X direction at point FP2 on the 3rd floor (TMSL +23.5m) for 5% damping due to seismic input time-histories scaled to 1*NCOE, 2*NCOE, 4*NCOE and 6*NCOE are shown in Fig. 48, respectively. Calculated floor response spectral amplitudes and peaks for 1*NCOE do not fit well to the observed response spectra. For example, most of the calculated response spectra have peaks at around 4 - 5 Hz. By contrast, the peak in the observed response spectrum is at about 2.8 Hz. Most of participants' results show significant over-estimation of the spectral acceleration for frequencies beyond 3 Hz. The higher the scaling factor of the input time-histories the bigger the scatter of the results due to strong nonlinear effects in the behaviour. The spectral peaks do not shift notably to lower frequencies due to anticipated stiffness degradation effect, which may be due to the fact that the spectral peak frequency comes from the dominant frequency of the input seismic motion.

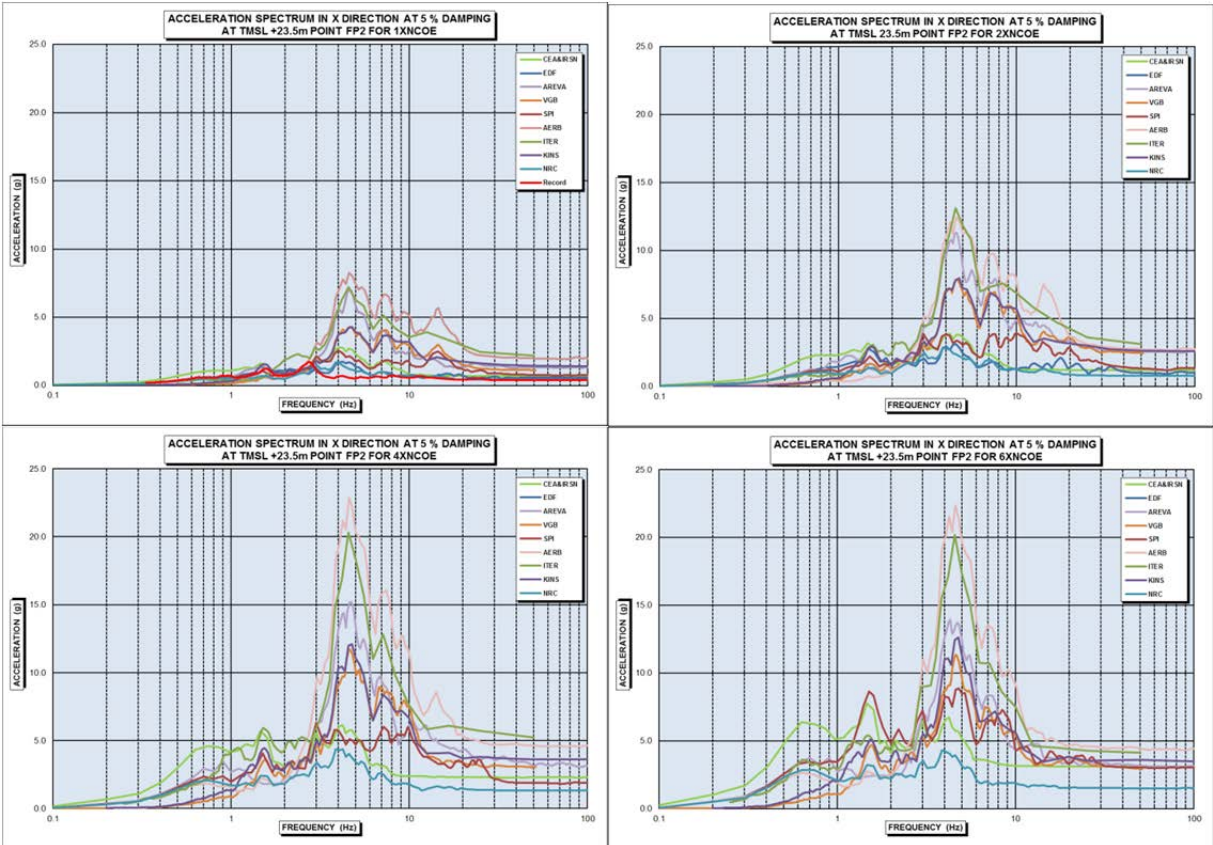
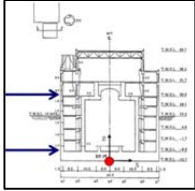


FIG. 48. Calculated and observed (1*NCOE) floor response spectra (damping 5 %) in the X direction at the location (FP2) of the accelerometer device on the 3rd floor (TMSL +23.5m) due to seismic input time-histories scaled to 1*NCOE, 2*NCOE, 4*NCOE and 6*NCOE, respectively.

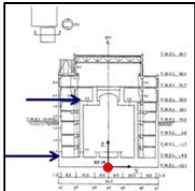
Participants' inter-story drift ratio results from nonlinear dynamic analysis of the coupled SSI models due to seismic input time-histories scaled to 1*NCOE, 2*NCOE, 4*NCOE and 6*NCOE are presented in Table 33.

TABLE 33. INTER-STORY DRIFT RATIO RESULTS FROM NONLINEAR DYNAMIC ANALYSIS OF THE COUPLED SSI MODELS

B.1.2. Maximum drift determination								
(DW3 - DW1) / 3170								
	1xNCOE		2xNCOE		4xNCOE		6xNCOE	
	X dir.	Y dir.						
CEA&IRSN, France	0.0003	0.0004	0.0006	0.0008	0.0017	0.0016	0.0039	0.0153
EdF, France	0.0007	0.0012	0.0019	0.0023				
AREVA, Germany	0.0021	0.0028	0.0054	0.0053	0.0091	0.0129	0.0107	0.0246
VGB, Germany	0.0005	0.0008	0.0016	0.0022	0.0031	0.0030	0.0039	0.0035
SPI, Germany	0.0004	0.0009	0.0013	0.0021	0.0023	0.0031	0.0049	0.0044
AERB, India	0.0058	0.0081	0.0113	0.0149	0.0194	0.0216	0.0272	0.0249
ITER, Italy								
KINS, Korea	0.0009	0.0010	0.0019	0.0018	0.0032	0.0033	0.0047	0.0052
NRC, USA	0.0010	0.0015	0.0019	0.0025	0.0032	0.0034	0.0037	0.0035
Mean	0.0015	0.0021	0.0032	0.0040	0.0060	0.0070	0.0084	0.0116
SD	0.0018	0.0025	0.0036	0.0046	0.0064	0.0075	0.0086	0.0099
COV	1.25	1.22	1.10	1.15	1.07	1.07	1.02	0.85



B.1.2. Maximum drift determination								
(DR3 - DW1) / 3170								
	1xNCOE		2xNCOE		4xNCOE		6xNCOE	
	X dir.	Y dir.						
CEA&IRSN, France	0.0003	0.0004	0.0007	0.0009	0.0018	0.0017	0.0041	0.0154
EdF, France	0.0007	0.0012	0.0019	0.0026				
AREVA, Germany	0.0026	0.0025	0.0062	0.0062	0.0111	0.0167	0.0132	0.0301
VGB, Germany	0.0006	0.0008	0.0017	0.0024	0.0028	0.0036	0.0035	0.0044
SPI, Germany	0.0005	0.0009	0.0014	0.0022	0.0021	0.0039	0.0053	0.0062
AERB, India	0.0062	0.0084	0.0134	0.0146	0.0234	0.0266	0.0290	0.0313
ITER, Italy								
KINS, Korea	0.0010	0.0010	0.0018	0.0019	0.0031	0.0031	0.0047	0.0051
NRC, USA	0.0012	0.0016	0.0022	0.0029	0.0036	0.0039	0.0044	0.0039
Mean	0.0018	0.0024	0.0041	0.0047	0.0077	0.0096	0.0100	0.0135
SD	0.0020	0.0027	0.0044	0.0046	0.0084	0.0098	0.0099	0.0134
COV	1.13	1.15	1.08	0.99	1.09	1.02	0.99	0.99



3.3.4. Comparison of pushover analysis and dynamic analysis results

Participants’ dynamic analysis and pushover analysis results (base force – top displacement curves) for the fixed-base model in the X and Y directions are presented in Figs 49 and 50, respectively: eight participants presented the pushover analysis results and four participants presented the dynamic analysis results. Two participants provided results for both analyses.

Participants’ dynamic analysis and pushover analysis results (base force – top displacement curves) for the soil-structure model in the X and Y directions are presented in Figs 51 and 52: eight participants presented the pushover analysis results and three participants presented the dynamic analysis displacement results. One participant provided results for both analyses.

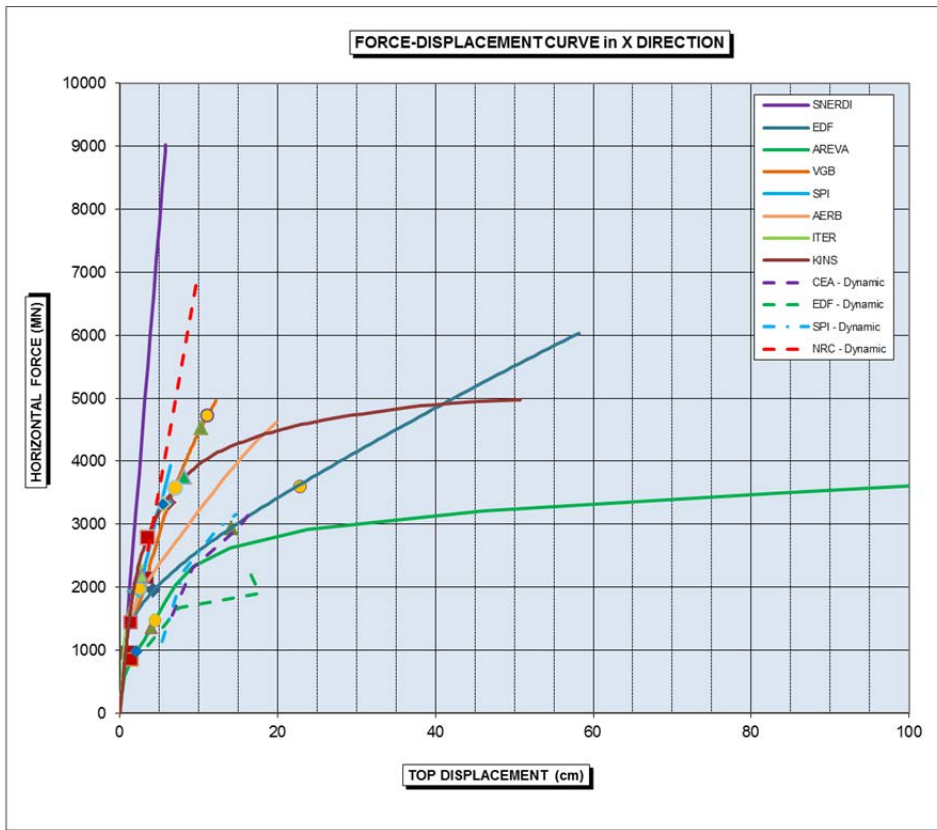


FIG. 49. Pushover and dynamic analysis curves in the X direction for the fixed-base structure model.

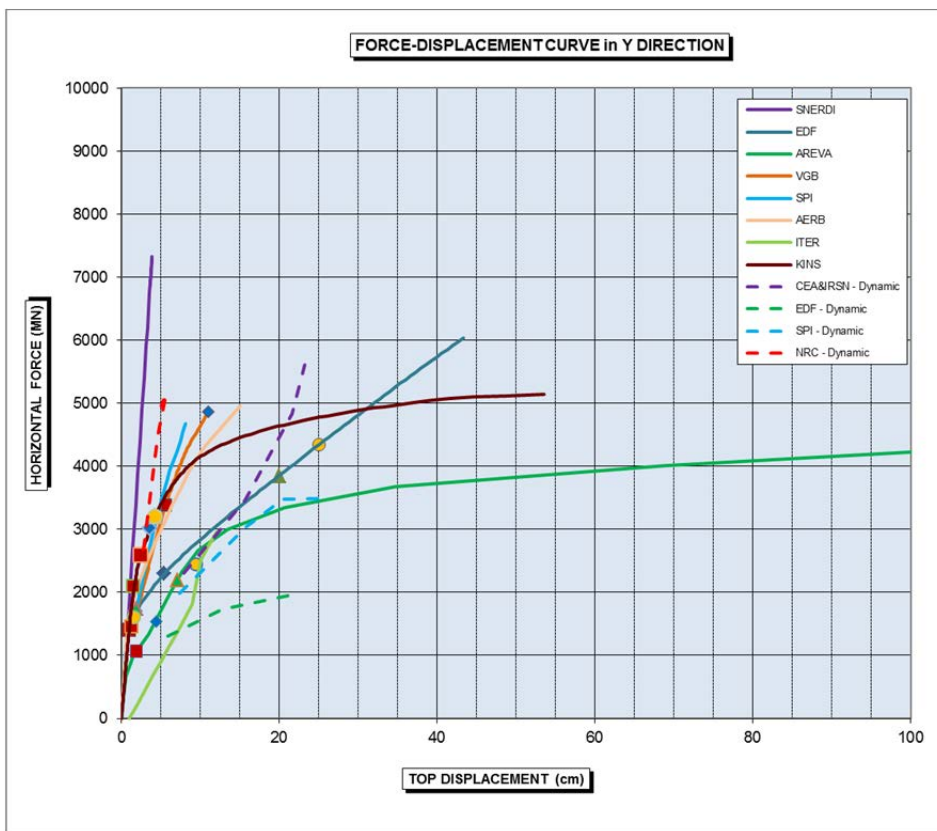


FIG. 50. Pushover and dynamic analysis curves in the Y direction for fixed-base structure model.

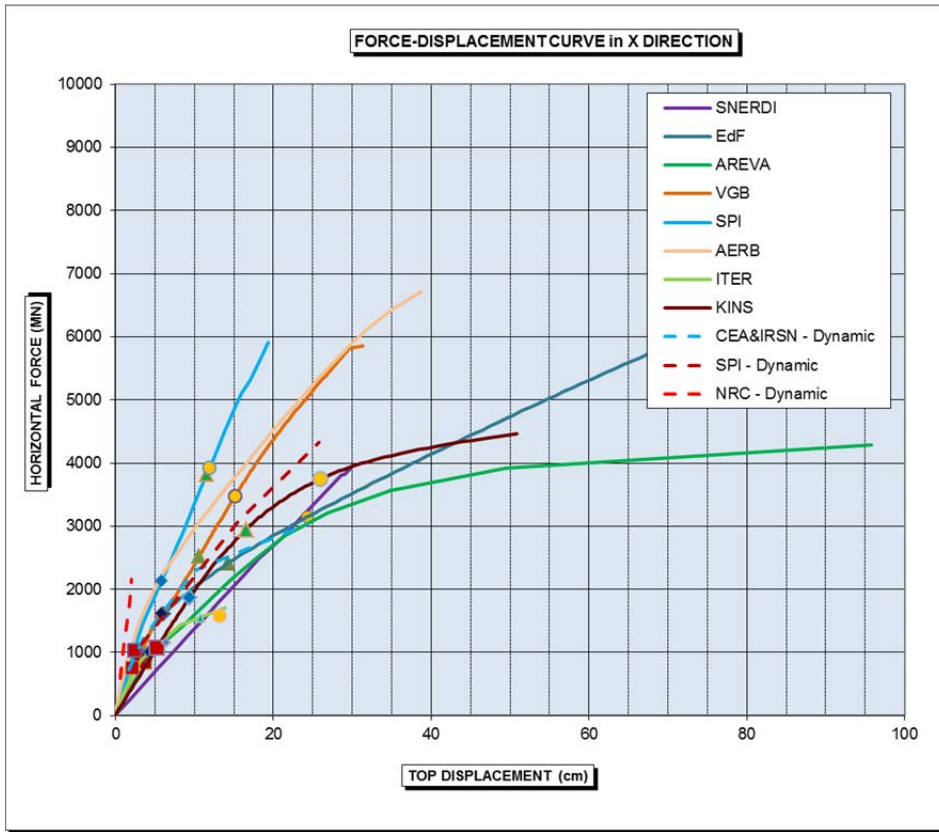


FIG. 51. Pushover and dynamic analysis curves in the X direction for the soil-structure interaction model.

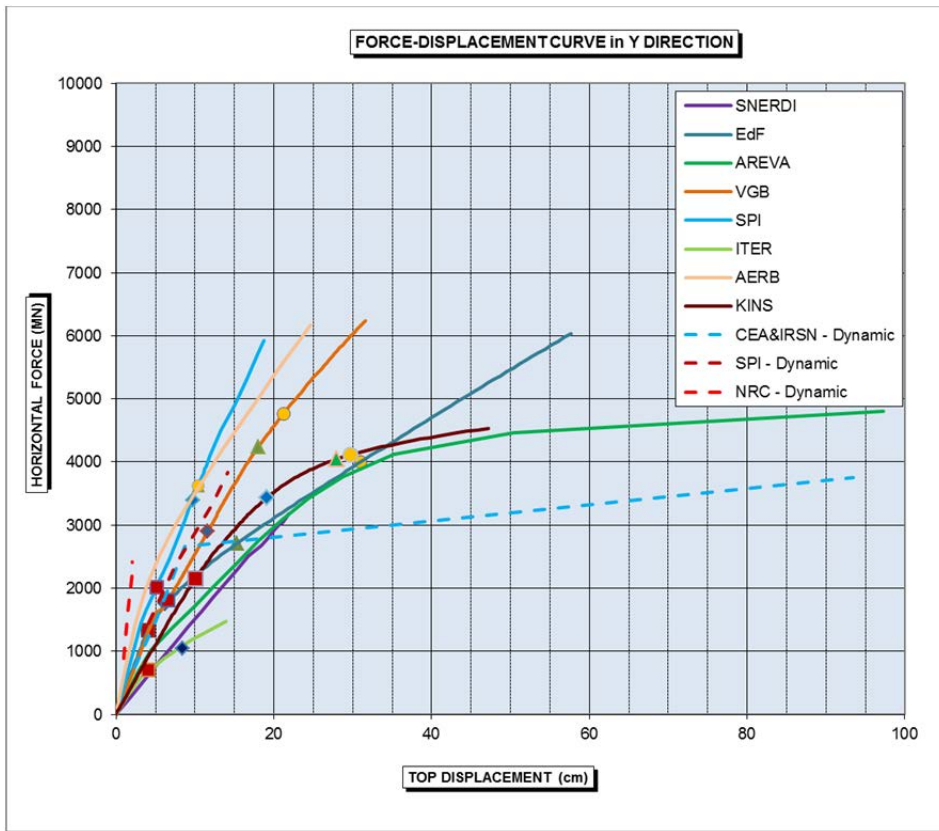


FIG. 52. Pushover and dynamic analysis curves in the Y direction for the soil-structure interaction model.

4. ANALYSES OF THE MAIN RESULTS OF THE BENCHMARKING EXERCISE FOR PART 2 EQUIPMENT

4.1. MAIN RESULTS FOR TASK 2.1 RHR PIPING SYSTEM

Benchmarking results for Part 2 “Equipment” for Phases I, II and III are presented in tables and figures with corresponding evaluation and comments. Representative comparisons are presented in the body of the document; all results are presented in Annex VI.

Statistical processing of the results was performed when it was appropriate: mean, standard deviation and COV (Coefficient of Variation) are presented in the tables. Maximum and minimum results were not included in mean, standard deviation and COV calculations in the tables with enough number of results.

4.1.1. Phase I and Phase II: Initial Analyses and Analyses with modified support conditions

4.1.1.1. Model presentation

Types of models, model characteristics, boundary conditions of model/supports modelling and calculation codes used by participants are presented in Table 34. All six participants used finite element models. Different computer codes were used by participants. The numbers of nodes used for developing the models vary from 120 to 299. Typical views of some participants’ models are shown in Fig. 53.

4.1.1.2. Static analyses under sustained loads and pressure

The first set of analyses was static analyses under sustained loads and pressure of the RHR piping system. Participants’ results for resultant stress under sustained loads and pressure, allowable stress according to national practice and ratio of resultant to allowable stresses at selected piping points at the RHR piping system (at elbow, tee, reducer and in pipe) are presented in Table 35. Allowable stresses used by each participants (depends on national practice) vary from 122 MPa to 205 MPa. Since the ratios of resultant to allowable stresses depend on allowable stresses, capacity of the RHR piping system under sustained loads and pressure provided by participants are quite different from each other. But, according to all participants’ results, stresses at selected piping points due to sustained loading and pressure in the RHR piping system are much lower than allowable ones except one piping point (at Node 95, Tee).

4.1.1.3. Modal analyses of the RHR piping system

Participants’ results are given in Table 36. Fundamental frequencies by three participants are around 5.5 Hz. But, two participants’ results for the fundamental frequencies are 3.1 Hz and 8.0 Hz.

4.1.1.4. Response spectrum analysis

Participants’ results for resultant stresses due to the NCOE loading, allowable stresses according to national practice and ratio of resultant to allowable stresses at selected piping points of the RHR piping system are presented in Table 37. Three participants assumed 2% damping ratio; two of them assumed 4% damping ratio.

Similarly, allowable stresses used by each participant vary from 162 MPa to 410 MPa. Since the ratios of resultant to allowable stresses depend on allowable stresses, estimated capacity of the RHR piping system under the NCOE loading are again quite different from each other.

According to two participants' results, stresses due to the NCOE at a few piping points in the RHR piping system are higher than allowable stresses. According the other four participants' results, stresses due to the NCOE at all piping points of the RHR piping system are lower than allowable stresses.

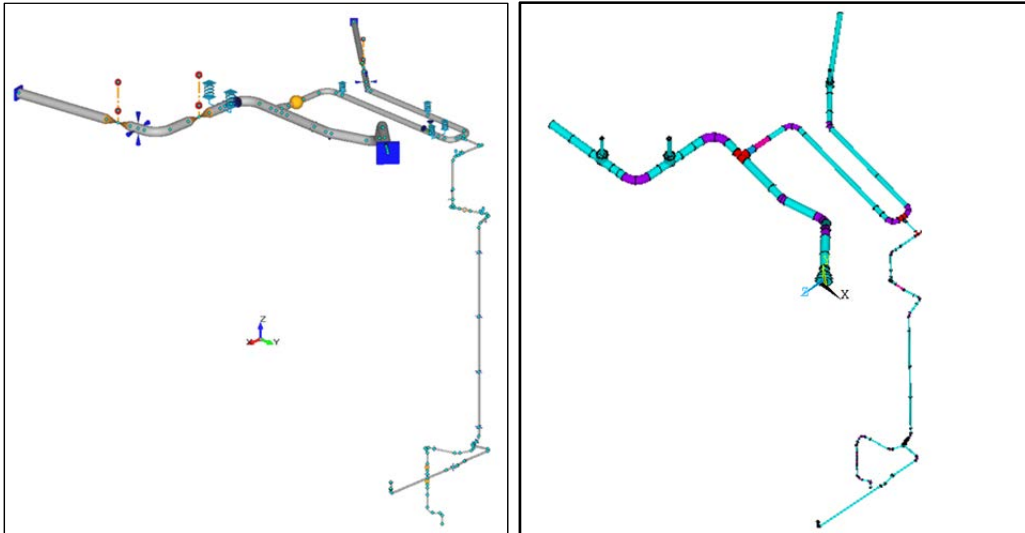


FIG. 53. Example of the participants' models for RHR piping system.

4.1.1.5. Time history analysis

Only two participants presented results for ratio of resultant stress to allowable stress at elbow, tee, and reducer and in pipe by time history analysis due to the NCOE loading (Table 38). Allowable stresses used by the participants are close to each other: varying 232.5 MPa to 272.4 MPa.

According to one participant results, stresses at all piping points in the RHR piping system are lower than allowable stresses. On the other hand, according to the other participants' results, stresses at two piping points (42 and 95 tee) in the RHR piping system are higher than allowable stresses.

Comparison of time history analysis results and response spectrum analysis results of these two participants shows that one participant's both analysis results (time history and response spectrum) are quite close. On the other hand, comparison of the other participant shows that time history analysis results give lower stresses comparing to response spectrum analysis results.

Response spectra for participants' time history analysis results at two representative points (valves) of the RHR piping system (Fig. 54: RHR piping system nodes where response spectrum presented) are presented in Fig. 55. Floor response spectra are good representative of the piping dynamic response. It should be noted that the spectrum frequency contents among participants are in good agreement.

TABLE 34. PARTICIPANTS' MODEL PRESENTATION

Part 2 Equipment: Taks 2.1 RHR Piping System Subtask 2.1.1- Initial Analyses and 2.1.2- Analyses with modified support conditions Model Presentation		
No	Participant Organization	Type of model
1	FNS, Finland	Pipe, spring and mass elements. The mass (point) elements are used to model valves.
2	VGB, Germany	For the static and dynamic calculation a spatially extended beam model is used. Static calculation is done with distributed mass, dynamic calculation with lumped mass. Spacing of the structure is depending on the cut-off-frequency (f _{Grenz}).
3	AERB, India	Lumped mass model using pipe elements in ANSYS
4	BARC, India	Lumped Mass
5	CVS, Russian Federation	Beam FE model with distributed weight characteristics and lumped masses for dynamic analysis.
6	CSN & IDOM, Spain	Bar model
No	Participant Organization	Model characteristics (Number of nodes, elements)
1	FNS, Finland	Number of Nodes = 299, Number of Pipe elements = 299. Total mass of the model is 35644 kg.
2	VGB, Germany	Number of Nodes: 212 (static calculation), typ of elements: beam elements. Automatic calculation of lumped mass points acc. $\Delta l \leq \frac{1}{3} \sqrt{\frac{\pi}{2 * f_{Grenz}}} * \left(\frac{E * J}{m} \right)^{1/4}$
3	AERB, India	No of nodes - 270; No of elements - 226
4	BARC, India	Number of elements = 120. Types of elements used: pipe, bend, tee
5	CVS, Russian Federation	Number of nodes: 177, Total piping length: 71.50 m, Number of branch: 11 Number of FE: 176 Piping weight: 64070 N Medium weight: 18858 N Insulation weight: 143869 N Lumped weights: 58360 N Total weight of pipeline: 285157 N
6	CSN & IDOM, Spain	Current model is carried out with 164 elements, nearly all of a piping nature and the others as valves, reducers and tees as rigid elements

Part 2 Equipment: Taks 2.1 RHR Piping System	
Subtask 2.1.1- Initial Analyses and 2.1.2- Analyses with modified support conditions	
Model Presentation	
No	Participant Organization
1	FNS, Finland
2	VGB, Germany
3	AERB, India
4	BARC, India
5	CVS, Russian Federation
6	CSN & IDOM, Spain
No	Participant Organization
1	FNS, Finland
2	VGB, Germany
3	AERB, India
4	BARC, India
5	CVS, Russian
6	CSN & IDOM, Spain
	Boundary conditions of the model/supports modelling
	Linear calculation without gaps and clearance. Material: linear isotrop (Hooke). The time history analysis is done with a THMA calculation (time history modal analysis).
	Spring hanger modeled using spring element (stiffness as given in guidance document). Restraints modeled as fixed supports
	All degrees of freedom Fixed at equipment connecting end (anchor locations)
	Boundary conditions for piping systems (spring hangers, restraints, snubbers and anchorage) were represented by the boundary and spring elements. For such pipe supports as hangers, the pendulum effect has been taken into account.
	Stiffness
	Calculation code
	Abaqus-69
	ROHR2, Version 30.3c
	ANSYS
	CAESAR Ver 5.00.2
	dPIPE 5
	Caesar II v. 4.4

TABLE 35. STATIC ANALYSIS RESULTS UNDER SUSTAINED LOAD AND PRESSURE: RESULTANT AND ALLOWABLE STRESS AT PIPING POINTS

TASK 2.1 - EQUIPMENT: RHR PIPING SYSTEM SUBTASK 2.1.1 - Initial Analyses and 2.1.2 - Analyses with modified support conditions																			
A. Static analysis under vertical loads (weight) + pressure																			
A.3. Resultant and allowable stress at piping points																			
Node No.	Elbow, tee, reducer and in pipe	FNS, Finland			VGB, Germany			AERB, India			BARC, India			CVS, Russian Federation			CSN & IDOM, Spain		
		Resultant Stress (MPa)	Allowable Stress ⁽¹⁾ (MPa)	Ratio Res./All. Stress (%)	Resultant Stress (MPa)	Allowable Stress ⁽¹⁾ (MPa)	Ratio Res./All. Stress (%)	Resultant Stress (MPa)	Allowable Stress ⁽¹⁾ (MPa)	Ratio Res./All. Stress (%)	Resultant Stress (MPa)	Allowable Stress ⁽¹⁾ (MPa)	Ratio Res./All. Stress (%)	Resultant Stress (MPa)	Allowable Stress ⁽¹⁾ (MPa)	Ratio Res./All. Stress (%)	Resultant Stress (MPa)	Allowable Stress ⁽¹⁾ (MPa)	Ratio Res./All. Stress (%)
7-8	Elbow				59.2	124.7	47	50.4	205.0	25	13.9	205.0	7	61.2	167.9	36	36.5	122.0	30
14-16	Elbow				45.2	124.7	36	56.3	205.0	27	12.0	205.0	6	60.5	167.9	36	46.2	122.0	38
22-23	Elbow				49.4	124.7	40	115.1	205.0	56	13.6	205.0	7	60.5	196.7	31	34.3	122.0	28
35-36	Elbow				53.9	128.4	42	47.5	205.0	23	15.0	205.0	7	58.7	167.9	35	30.8	122.0	25
43-44	Elbow				38.6	128.4	30	119.8	205.0	58	6.7	205.0	3	57.5	167.9	34	32.5	122.0	27
65-66	Elbow				35.6	128.4	28	117.3	205.0	57	12.5	205.0	6	31.4	167.9	19	25.3	122.0	21
75-76	Elbow				26.5	128.4	21	95.6	205.0	47	11.4	205.0	6	30.9	167.9	18	26.2	122.0	22
78-79	Elbow				29.1	128.4	23	128.2	205.0	63	11.6	205.0	6	30.5	167.9	18	30.2	122.0	25
99-100	Elbow				33.9	128.4	26	28.5	205.0	14	12.1	205.0	6	35.4	167.9	21	14.0	122.0	11
118-119	Elbow				41.3	128.4	32	36.9	205.0	18	18.7	205.0	9	47.0	167.9	28	12.5	122.0	10
10	In pipe							47.0	205.0	23	33.9	205.0	17	60.3	167.9	36	35.7	122.0	29
21-22	In pipe				39.3	124.7	32	52.7	205.0	26	34.1	205.0	17	60.5	196.7	31	32.4	122.0	27
38	In pipe							44.2	205.0	22	33.6	205.0	16	58.1	167.9	35	30.8	122.0	25
45	In pipe							58.7	205.0	29	31.6	205.0	15	57.4	167.9	34	32.5	122.0	27
63	In pipe				41.1	128.4	32	95.1	205.0	46	20.6	205.0	10	37.7	167.9	22	14.0	122.0	11
70	In pipe				26.5	128.4	21	128.7	205.0	63	19.2	205.0	9	31.1	167.9	18	17.2	122.0	14
84	In pipe				24.4	128.4	19	28.7	205.0	14	17.8	205.0	9	30.4	167.9	18	15.9	122.0	13
86	In pipe							14.0	205.0	7	17.8	205.0	9	30.4	167.9	18	14.7	122.0	12
102	In pipe				32.7	128.4	25	15.8	205.0	8	18.3	205.0	9	32.4	167.9	19	19.3	122.0	16
109	In pipe							36.9	205.0	18	20.8	205.0	10	31.8	167.9	19	28.5	122.0	23
120	In pipe							45.3	205.0	22	18.7	205.0	9	30.7	167.9	18	28.2	122.0	23
129	In pipe				19.7	128.4	15	19.2	205.0	9	16.2	205.0	8	26.0	167.9	15	16.4	122.0	13
12	Tee				48.4	124.7	39	49.6	205.0	24	31.2	205.0	15	97.1	167.9	58	32.6	122.0	27
42	Tee				54.2	128.4	42	78.1	205.0	38	32.2	205.0	16	91.2	167.9	54	26.4	122.0	22
95	Tee				103.5	128.4	81	69.1	205.0	34	22.0	205.0	11	170.1	167.9	101	27.1	122.0	22
32-33	Reducer				73.0	128.4	57	36.2	205.0	18	29.4	205.0	14	70.2	167.9	42	25.7	122.0	21
38-59	Reducer				57.6	128.4	45	85.4	205.0	42	18.0	205.0	9	33.9	167.9	20	21.1	122.0	17

⁽¹⁾ Allowable Stress is according to National Practice.

TABLE 36. MODAL ANALYSIS RESULTS: NATURAL FREQUENCIES

SUBTASK 2.1.1- Initial Analyses and 2.1.2- Analyses with modified support conditions						
Part 2 Equipment Task 2.1 RHR Piping System						
B. Modal analysis of the RHR piping system						
B.1. Frequencies						
Mode	FNS, Finland Frequency (Hz)	VGB, Germany Frequency (Hz)	AERB, India Frequency (Hz)	BARC, India Frequency (Hz)	CVS, Russian Frequency (Hz)	CSN & IDOM, Spain Frequency (Hz)
1	5.5	5.7	5.3	8.0	5.5	3.1
2	5.9	6.0	6.2	12.9	5.7	4.3
3	6.7	6.0	6.8	14.7	6.3	5.3
4	7.1	7.0	6.9	16.5	6.6	5.6
5	8.2	7.9	8.5	17.2	7.8	6.0
6	8.9	8.6	8.9	17.3	8.4	6.5
7	9.4	9.0	9.2	19.7	8.7	7.4
8	10.0	9.1	9.9	20.5	9.2	7.7
9	10.1	9.5	10.5	21.2	9.7	8.2
10	10.7	9.7	11.0	23.3	9.9	10.3
11	11.3	10.4	11.2	24.5	10.2	10.7
12	11.5	10.7	12.2	25.0	11.3	11.3
13	12.1	10.9	12.5	28.1	11.7	12.7
14	12.4	11.2	12.7	28.5	12.0	14.6
15	13.0	11.6	13.3	32.0	12.1	15.5
16	13.1	12.1	14.8	32.6	12.4	15.8
17	13.2	12.2	14.9	32.7	13.2	17.1
18	14.3	12.5	15.2	34.8	13.3	17.4
19	14.7	12.6	15.4	35.4	14.1	19.8
20	15.4	13.9	16.3	36.2	14.6	20.0
21	15.9	14.5	17.3	40.9	15.8	21.9
22	16.5	14.9	17.5	41.9	16.4	22.2
23	17.1	15.5	18.4	43.9	16.5	22.5
24	17.5	16.2	18.4	44.2	16.6	23.6
25	17.9	16.5	19.0	46.8	17.6	24.2
26	18.2	17.0	19.2	51.0	18.0	26.9
27	18.6	17.7	20.2	56.7	18.1	27.6
28	19.1	18.3	20.8	61.2	18.5	29.2
29	19.8	18.6	21.5	65.4	18.9	31.7
30	20.5	19.0	22.4	65.8	19.2	32.7

TABLE 37. RESPONSE SPECTRUM ANALYSIS RESULTS: RESULTANT AND ALLOWABLE STRESS AT PIPING POINTS

TASK 2.1 - EQUIPMENT: RHR PIPING SYSTEM SUBTASK 2.1.1 - Initial Analyses Subtask and 2.1.2 - Analyses with modified support conditions
C. Modal spectrum analysis

Node No.	C.4. Resultant and allowable stresses due to loading combination																	
	FNS, Finland			VGB, Germany			AERB, India			BARC, India			CVS, Russian Federation			CSN & IDOM, Spain		
	Resultant Stress (MPa)	Allowable Stress ⁽¹⁾ (MPa)	Ratio Res./All. Stress (%)	Resultant Stress (MPa)	Allowable Stress ⁽¹⁾ (MPa)	Ratio Res./All. Stress (%)	Resultant Stress (MPa)	Allowable Stress ⁽¹⁾ (MPa)	Ratio Res./All. Stress (%)	Resultant Stress (MPa)	Allowable Stress ⁽¹⁾ (MPa)	Ratio Res./All. Stress (%)	Resultant Stress (MPa)	Allowable Stress ⁽¹⁾ (MPa)	Ratio Res./All. Stress (%)	Resultant Stress (MPa)	Allowable Stress ⁽¹⁾ (MPa)	Ratio Res./All. Stress (%)
7-8	71.0	162.0	44	105.0	249.4	42	22.6	410.0	6	26.9	307.5	8.7	65.3	232.5	28	59.6	162.2	37
14-16	94.0	162.0	58	80.2	249.4	32	20.1	410.0	5	27.0	307.5	8.8	62.9	232.5	27	62.8	162.2	39
22-23	85.0	239.0	36	71.6	249.4	29	14.1	410.0	3	35.8	307.5	11.6	61.9	272.4	23	46.8	162.2	29
35-36	96.0	162.0	59	95.1	256.9	37	21.1	410.0	5	27.0	307.5	8.8	64.7	232.5	28	56.2	162.2	35
43-44	86.0	162.0	53	123.8	256.9	48	36.3	410.0	9	38.3	307.5	12.5	64.0	232.5	28	48.0	162.2	30
65-66	191.0	162.0	118	136.9	256.9	53	58.5	410.0	14	62.1	307.5	20.2	115.5	232.5	49	72.3	162.2	45
75-76	121.0	162.0	75	104.0	256.9	40	47.2	410.0	12	74.5	307.5	24.2	96.1	232.5	41	78.6	162.2	48
78-79	87.0	162.0	54	71.8	256.9	28	22.4	410.0	5	81.8	307.5	26.6	52.7	232.5	23	46.9	162.2	29
99-100	59.0	162.0	36	72.6	256.9	28	16.7	410.0	4	21.4	307.5	7.0	56.0	232.5	24	35.4	162.2	22
118-119	92.0	162.0	57	87.0	256.9	34	17.7	410.0	4	28.5	307.5	9.3	84.9	232.5	27	22.2	162.2	14
10	79.0	162.0	49	79.0	256.9	49	22.5	410.0	5	45.1	307.5	14.7	62.0	232.5	27	53.2	162.2	32
21-22	74.0	239.0	31	55.0	249.4	22	12.5	410.0	3	41.8	307.5	13.6	62.0	272.4	23	45.0	162.2	28
38	85.0	162.0	52	74.0	256.9	34	34.6	410.0	8	42.5	307.5	13.8	75.6	232.5	32	54.6	162.2	32
45	80.0	162.0	49	70.0	256.9	36	26.3	410.0	6	42.8	307.5	13.9	68.7	232.5	30	55.7	162.2	30
63	163.0	162.0	101	135.7	256.9	53	70.0	410.0	17	37.9	307.5	12.3	122.1	232.5	52	68.8	162.2	42
70	118.0	162.0	73	93.7	256.9	36	38.0	410.0	9	88.5	307.5	28.8	70.7	232.5	30	52.1	162.2	32
84	69.0	162.0	43	56.3	256.9	22	45.0	410.0	11	24.5	307.5	8.0	65.9	232.5	28	60.9	162.2	38
86	86.0	162.0	53	74.2	256.9	29	29.9	410.0	7	23.0	307.5	7.5	63.3	232.5	27	44.3	162.2	27
102	80.0	162.0	49	74.2	256.9	29	20.0	410.0	5	21.4	307.5	7.0	46.7	232.5	20	43.5	162.2	20
109	103.0	162.0	64	75.0	256.9	46	22.4	410.0	5	22.0	307.5	7.2	46.2	232.5	20	67.0	162.2	20
120	75.0	162.0	46	52.4	256.9	17	52.4	410.0	6	26.3	307.5	8.6	59.0	232.5	25	22.2	162.2	25
129	93.0	162.0	57	42.8	249.4	34	24.1	410.0	6	23.0	307.5	7.5	42.7	232.5	18	137.7	183.4	75
12	295.0	162.0	182	202.3	256.9	79	21.7	410.0	5	41.1	307.5	13.4	164.1	232.5	71	49.8	162.2	31
42	147.0	162.0	91	188.8	256.9	73	36.0	410.0	9	59.6	307.5	19.4	271.4	232.5	117	46.8	162.2	29
95	114.0	162.0	70	153.1	256.9	60	26.0	410.0	6	34.3	307.5	11.2	112.5	232.5	48	94.8	162.2	58
32-33	210.0	162.0	130	209.9	256.9	82	75.9	410.0	19	41.1	307.5	13.4	152.8	232.5	66	72.4	162.2	45
58-59	210.0	162.0	130	209.9	256.9	82	75.9	410.0	19	41.1	307.5	13.4	152.8	232.5	66	72.4	162.2	45

⁽¹⁾ Allowable Stress is according to National Practice.

TABLE 38. TIME HISTORY ANALYSIS RESULTS: RESULTANT AND ALLOWABLE STRESS AT PIPING POINTS

TASK 2.1 - EQUIPMENT: RHR PIPING SYSTEM SUBTASK 2.1.1 - Initial Analyses Subtask and 2.1.2 - Analyses with modified support conditions D.Time history analysis																				
C.4. Resultant and allowable stresses due to loading combination																				
Node No.	Elbow, tee, reducer and in pipe	FNS, Finland			VGB, Germany			AERB, India			BARC, India			CVS, Russian Federation			CSN & IDOM, Spain			
		Resultant Stress (MPa)	Allowable Stress ⁽¹⁾ (MPa)	Ratio Res./All. Stress (%)	Resultant Stress (MPa)	Allowable Stress ⁽¹⁾ (MPa)	Ratio Res./All. Stress (%)	Resultant Stress (MPa)	Allowable Stress ⁽¹⁾ (MPa)	Ratio Res./All. Stress (%)	Resultant Stress (MPa)	Allowable Stress ⁽¹⁾ (MPa)	Ratio Res./All. Stress (%)	Resultant Stress (MPa)	Allowable Stress ⁽¹⁾ (MPa)	Ratio Res./All. Stress (%)	Resultant Stress (MPa)	Allowable Stress ⁽¹⁾ (MPa)	Ratio Res./All. Stress (%)	
7-8	Elbow		75.4	249.4	30															
14-16	Elbow		62.7	249.4	25															
22-23	Elbow		62.3	249.4	25															
35-36	Elbow		75.0	256.9	29															
43-44	Elbow		72.8	256.9	28															
65-66	Elbow		87.5	256.9	34															
75-76	Elbow		71.3	256.9	28															
78-79	Elbow		61.5	256.9	24															
99-100	Elbow		67.1	256.9	26															
118-119	Elbow		67.0	256.9	26															
10	In pipe																			
21-22	In pipe		43.7	249.4	18															
38	In pipe																			
45	In pipe																			
63	In pipe		87.6	256.9	34															
70	In pipe		599	256.9	23															
84	In pipe		40.8	256.9	16															
86	In pipe																			
102	In pipe		580	256.9	23															
109	In pipe																			
120	In pipe																			
12	Tee		35.0	256.9	14															
129	In pipe		71.1	249.4	29															
42	Tee		148.7	256.9	58															
95	Tee		155.5	256.9	61															
32-33	Reducer		122.1	256.9	48															
58-59	Reducer		147.5	256.9	57															

(1) Allowable Stress is according to National Practice.

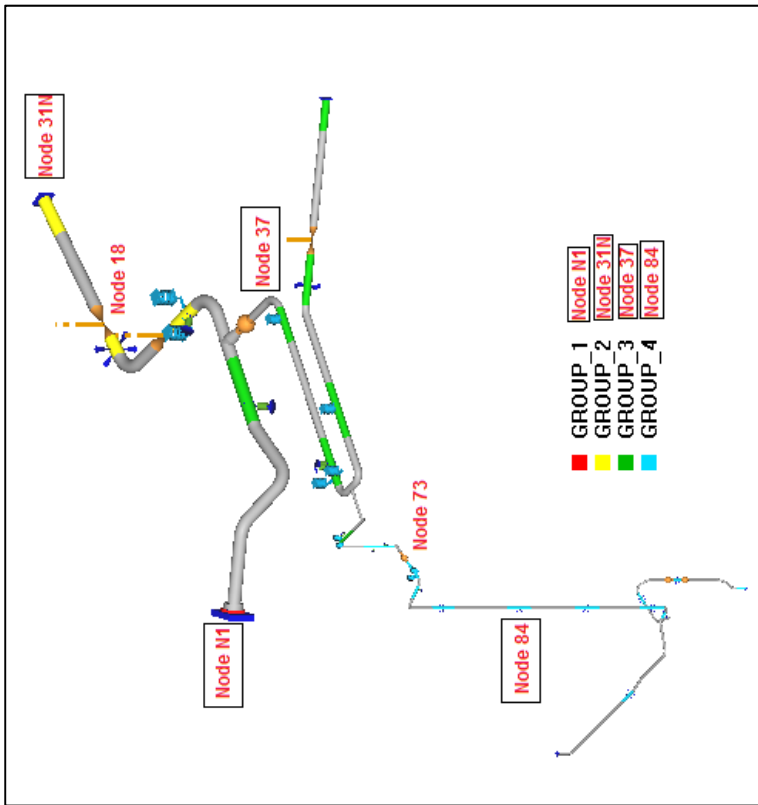


FIG. 54. RHR piping system nodes where response spectrum presented.

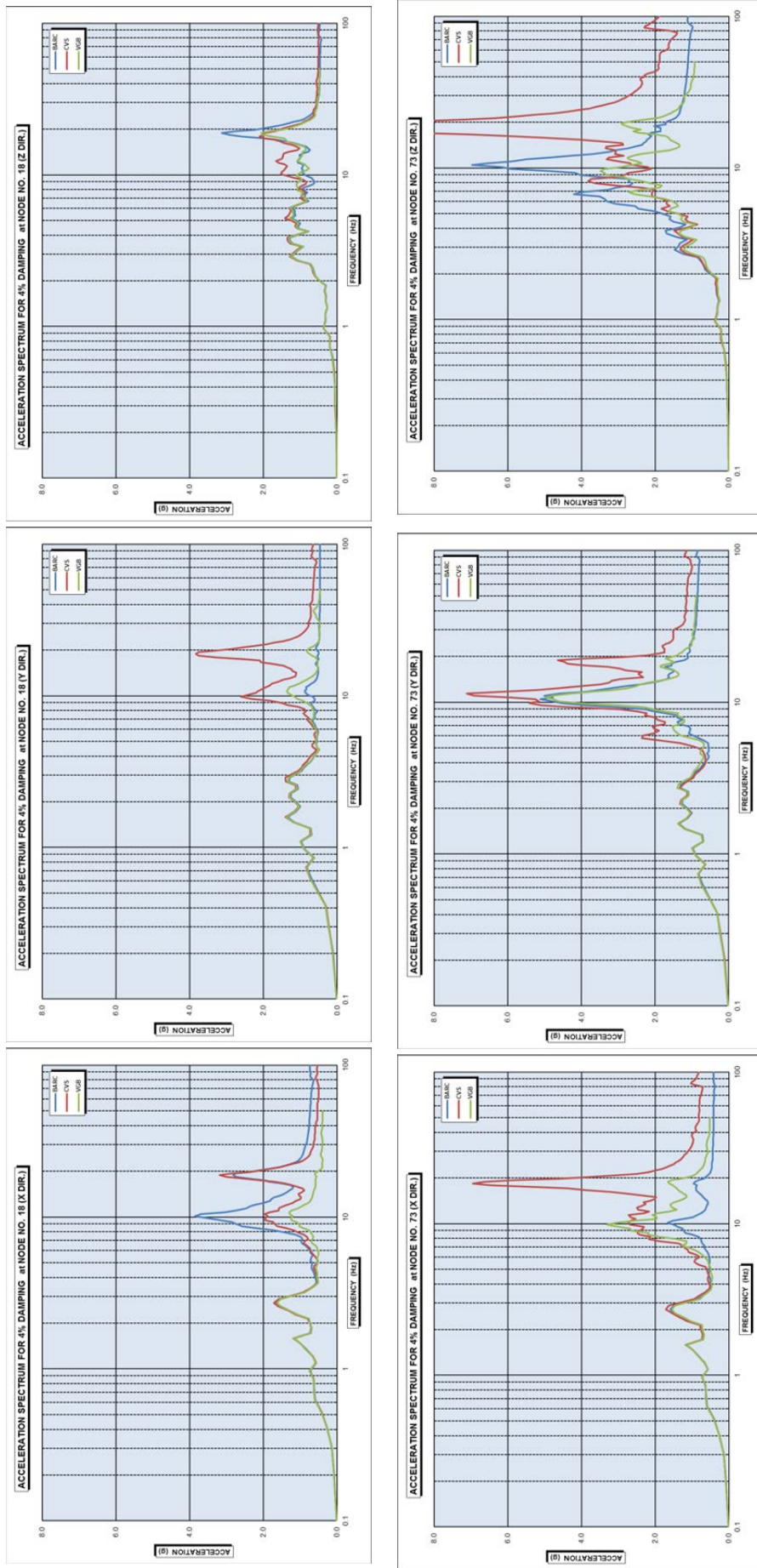


FIG. 55. Time history analysis results: response spectra at nodes 18 and 73 in the X, Z and Y directions.

4.1.2. Phase III: Multi-support Analysis

Descriptions of the multi-support analyses performed by participants in terms of combination of different support movements (See Section 2.5.1.2) are presented in Table 39. Only three participants performed this analysis.

TABLE 39. DESCRIPTION OF THE MULTI-SUPPORT ANALYSES

PART 2 EQUIPMENT Task2.1: RHR Piping System Subtask 2.1.3- Multisupport Analyses and Margin Assessment		
No	Participant Organization	Describe how the multisupport analyses performed: -Relative displacement -Combination of different support movements
1	FNS, Finland	
2	VGB, Germany	The task is the calculation of section quantities due to dynamic loads, given in form of multiple floor response spectra e.g. Earthquake. The calculation takes place according to the response spectra method following the KTA-rule 2201.4 section 4.3.3.2 and is based on the eigen value calculation. With the eigen frequencies, eigenforms and static load cases unit accelerations and the response spectra for support nodes to be described here, absolute thresholds for dynamic section quantities are determined. The calculation considers: - Different excitations of the support nodes and - directions - Condensation of supports to 'buildings', a 'building' is here characterized by similar excitation inside it, also in case of different response spectra. - Influence of the rigid-body acceleration through calculation of a 'Restmode-portion'. - Different possibilities for the superposition of the modal contributions. - Various possibilities for the superposition of the building contributions.
3	AERB, India	Model used was same as phase II. Modal Envelope response spectra analysis was carried out using four input motions was used for the analysis. Modal combination was done using SRSS method. Multi point response spectrum analysis was undertaken using ANSYS. The Multi Point Response Spectrum Option available in ANSYS was used. The steps involved are following: 1. Eigen Value Analysis: Eigen value analysis was done to obtain the frequencies and the mode shapes of the piping system. 2. Determination of Support Coefficients: This is done by giving unit displacement to that support in the direction of the degree of freedom, keeping all other supports as constrained. 3. Combination of Support Coefficients: ANSYS uses a default SRSS combination rule to combine the support coefficients. 4. Calculation of Modal Quantities: The mode shapes, mode stresses, etc. are multiplied by the support coefficients to compute modal quantities. 5. Modal Combination: SRSS was used. Multi-support time history analysis was carried out by applying the acceleration corresponding to each group at the supports. The output for this analysis are obtained in form of absolute acceleration and absolute displacement. To derive the relative displacement, the displacement time history corresponding to the acceleration time histories for each group in XYZ directions were derived. It was observed that the displacement time history for X Y and Z directions are almost same for all groups. The average displacement for each direction was used as the base and this was deducted from the absolute displacement to calculate the relative displacement.
4	BARC, India	
5	CVS, Russian Federation	dPIPE Version 5.21 was used. For multisupport THA additional modifications in the code were introduced: extracting of "rigid body" mode shapes from the total response to separate "inertial" and pseudo static parts of solution
6	CSN & IDOM, Spain	

4.1.2.1. Response spectrum analysis using enveloped response spectra developed from the four input motions

Participants' results for resultant and allowable stresses at elbow, tee, and reducer and in pipe for response spectrum analysis using enveloped response spectra developed from the four input motions are given in Table 40. Allowable stresses used by participants vary from 232.5 MPa to 410 MPa. Although, allowable stresses used by participants are different, according to participants' response spectrum analysis results using enveloped response spectrum, stresses at all piping points in the RHR piping system are lower than allowable stresses, except for two nodes (Node 42 and node 95, Tee).

4.1.2.2. Multi-support response spectrum analysis using four input motions

Participants' results for resultant and allowable stresses at elbow, tee, reducer and in pipe for response spectrum analysis using four input motions are given in Table 41. Again, according to participant response spectrum analysis results using four input motions, stresses at all piping points in the RHR piping system are lower than allowable stresses except for two nodes (Node 42 and node 95, Tee).

4.1.2.3. Multi-support time history analysis using four input motions

Participants' results for resultant and allowable stresses at elbow, tee, reducer and in pipe by time history analysis using four input motions are given in Table 42. According to participants' results using four input motions, stresses at all piping points in the RHR piping system are lower than allowable stresses, except for one node (Node 95, Tee).

In general, multi-support response spectrum analysis results using four input motions are lower than the ones using enveloped response spectra in terms of stress ratios in piping points. Moreover, multi support time history analysis results are lower than the ones for multi-support response spectrum analysis in terms of stress ratios in piping points.

Response spectra for participants' multi-support time history analysis results at two representative points (valves) of the RHR piping system are presented in Fig. 56. It should be noted that the spectrum frequency contents among participants are in good agreement.

TABLE 40. RESPONSE SPECTRUM ANALYSIS RESULTS FOR ENVELOPED RESPONSE SPECTRUM: RESULTANT TO ALLOWABLE STRESS RATIO

PART 2 EQUIPMENT Task2.1: RHR Piping System Subtask 2.1.3- Multisupport Analyses and Margin Assessment																			
A. Modal spectrum analysis using envelop response spectrum																			
A.4. Resultant and allowable stresses due to Combination																			
Node No.	Elbow, tee, reducer and in pipe	FNS, Finland			VCB, Germany			AERB, India			BARC, India			CVS, Russian Federation			CSN & IDOM, Spain		
		Resultant Stress (MPa)	Allowable Stress ⁽¹⁾ (MPa)	Ratio Res./All. Stress (%)	Resultant Stress (MPa)	Allowable Stress ⁽¹⁾ (MPa)	Ratio Res./All. Stress (%)	Resultant Stress (MPa)	Allowable Stress ⁽¹⁾ (MPa)	Ratio Res./All. Stress (%)	Resultant Stress (MPa)	Allowable Stress ⁽¹⁾ (MPa)	Ratio Res./All. Stress (%)	Resultant Stress (MPa)	Allowable Stress ⁽¹⁾ (MPa)	Ratio Res./All. Stress (%)	Resultant Stress (MPa)	Allowable Stress ⁽¹⁾ (MPa)	Ratio Res./All. Stress (%)
7-8	Elbow		249.4	51	128.1	249.4	51	92.3	410.0	23							72.7	232.5	31
14-16	Elbow		249.4	39	97.0	249.4	39	85.0	410.0	21							68.0	232.5	29
22-23	Elbow		249.4	32	78.9	249.4	32	45.5	410.0	11							61.8	272.4	23
35-36	Elbow		256.9	40	101.7	256.9	40	61.4	410.0	15							68.0	232.5	29
43-44	Elbow		256.9	64	164.4	256.9	64	139.8	410.0	34							83.0	232.5	36
65-66	Elbow		256.9	65	165.9	256.9	65	159.0	410.0	39							116.1	232.5	50
75-76	Elbow		256.9	46	119.2	256.9	46	87.8	410.0	21							74.2	232.5	32
78-79	Elbow		256.9	31	79.6	256.9	31	57.7	410.0	14							47.8	232.5	21
99-100	Elbow		256.9	28	71.1	256.9	28	60.6	410.0	15							53.9	232.5	23
118-119	Elbow		256.9	29	74.8	256.9	29	58.0	410.0	14							77.1	232.5	33
10	In pipe							61.5	410.0	15							64.0	232.5	28
21-22	In pipe							58.2	410.0	23							62.2	272.4	23
38	In pipe							78.8	410.0	19							93.7	232.5	40
45	In pipe							62.7	410.0	15							73.4	232.5	32
63	In pipe							158.3	256.9	62							136.1	232.5	59
70	In pipe							104.7	256.9	41							67.9	232.5	29
84	In pipe							56.0	256.9	22							51.2	232.5	22
86	In pipe							68.2	256.9	27							46.6	232.5	20
102	In pipe							68.2	256.9	27							46.6	232.5	20
109	In pipe							59.4	410.0	14							36.8	232.5	16
120	In pipe							67.2	410.0	16							53.6	232.5	23
129	In pipe							40.2	256.9	16							39.7	232.5	17
12	Tee							96.7	249.4	39							195.0	232.5	84
42	Tee							218.3	256.9	85							256.1	232.5	110
95	Tee							183.2	256.9	71							243.1	232.5	105
32-33	Reducer							151.3	256.9	59							130.6	232.5	56
58-59	Reducer							172.3	256.9	67							145.2	232.5	62

⁽¹⁾ Allowable Stress is according to National Practice.

TABLE 41. RESPONSE SPECTRUM ANALYSIS RESULTS USING FOUR INPUT MOTIONS: RESULTANT TO ALLOWABLE STRESS RATIO

PART 2 EQUIPMENT Task2.1: RHR Piping System Subtask 2.1.3- Multisupport Analyses and Margin Assessment B. Multisupport modal spectrum analysis																			
B.4. Resultant and allowable stresses due to Combination																			
Node No.	Elbow, tee, reducer and in pipe	FNS, Finland			VGB, Germany			A ERB, India			BARC, India			CVS, Russian Federation			CSN & IDOM, Spain		
		Resultant Stress (MPa)	Allowable Stress ⁽¹⁾ (MPa)	Ratio Res. / All. Stress (%)	Resultant Stress (MPa)	Allowable Stress ⁽¹⁾ (MPa)	Ratio Res. / All. Stress (%)	Resultant Stress (MPa)	Allowable Stress ⁽¹⁾ (MPa)	Ratio Res. / All. Stress (%)	Resultant Stress (MPa)	Allowable Stress ⁽¹⁾ (MPa)	Ratio Res. / All. Stress (%)	Resultant Stress (MPa)	Allowable Stress ⁽¹⁾ (MPa)	Ratio Res. / All. Stress (%)	Resultant Stress (MPa)	Allowable Stress ⁽¹⁾ (MPa)	Ratio Res. / All. Stress (%)
7-8	Elbow		117.0	249.4	47	73.1	410.0	18	83.9	232.5	36								
14-16	Elbow		88.3	249.4	35	67.3	410.0	16	76.0	232.5	33								
22-23	Elbow		75.4	249.4	30	36.4	410.0	9	62.5	272.4	23								
35-36	Elbow		86.9	256.9	34	45.1	410.0	11	67.4	232.5	29								
43-44	Elbow		143.2	256.9	56	108.8	410.0	27	108.6	232.5	47								
65-66	Elbow		140.6	256.9	55	119.4	410.0	29	133.0	232.5	57								
75-76	Elbow		104.3	256.9	41	67.5	410.0	16	89.3	232.5	38								
78-79	Elbow		72.5	256.9	28	51.6	410.0	13	65.3	232.5	28								
99-100	Elbow		71.5	256.9	28	65.7	410.0	16	79.7	232.5	34								
118-119	Elbow		70.3	256.9	27	54.8	410.0	13	108.5	232.5	47								
10	In pipe					48.8	410.0	12											
21-22	In pipe		66.0	249.4	26	24.7	410.0	6	63.7	272.4	23								
38	In pipe					60.1	410.0	15											
45	In pipe					48.9	410.0	12											
63	In pipe		140.5	256.9	55	104.3	410.0	25	158.8	232.5	68								
70	In pipe		88.6	256.9	34	48.9	410.0	12	79.9	232.5	34								
84	In pipe		49.8	256.9	19	52.8	410.0	13	59.4	232.5	26								
86	In pipe					32.4	410.0	8	56.3	232.5	24								
102	In pipe		64.3	256.9	25	70.9	410.0	17	54.6	232.5	23								
109	In pipe					64.1	410.0	16	46.1	232.5	20								
120	In pipe					58.7	410.0	14	69.6	232.5	30								
129	In pipe		38.0	256.9	15	27.2	410.0	7	48.6	232.5	21								
12	Tee		88.1	249.4	35	85.5	410.0	21	217.5	232.5	94								
42	Tee		185.6	256.9	72	144.7	410.0	35	291.9	232.5	126								
95	Tee		180.6	256.9	70	158.9	410.0	39	301.5	232.5	130								
32-33	Reducer		134.8	256.9	52	78.3	410.0	19	142.1	232.5	61								
58-59	Reducer		146.1	256.9	57	91.9	410.0	22	172.5	232.5	74								

(1) Allowable Stress is according to National Practice.

TABLE 42. TIME HISTORY ANALYSIS RESULTS USING FOUR INPUT MOTIONS: RESULTANT TO ALLOWABLE STRESS RATIO

PART 2 EQUIPMENT Task2.1: RHR Piping System Subtask 2.1.3: Multisupport Analyses and Margin Assessment C. Multi-support Time history analysis																			
C.5. Resultant and allowable stresses due to Combination																			
Node No.	Elbow, tee, reducer and in pipe	FNS, Finland			VGB, Germany			AERB, India			BARC, India			CVS, Russian Federation			CSN & IDOM, Spain		
		Resultant Stress (MPa)	Allowable Stress ⁽¹⁾ (MPa)	Ratio Res./ All. Stress (%)	Resultant Stress (MPa)	Allowable Stress ⁽¹⁾ (MPa)	Ratio Res./ All. Stress (%)	Resultant Stress (MPa)	Allowable Stress ⁽¹⁾ (MPa)	Ratio Res./ All. Stress (%)	Resultant Stress (MPa)	Allowable Stress ⁽¹⁾ (MPa)	Ratio Res./ All. Stress (%)	Resultant Stress (MPa)	Allowable Stress ⁽¹⁾ (MPa)	Ratio Res./ All. Stress (%)	Resultant Stress (MPa)	Allowable Stress ⁽¹⁾ (MPa)	Ratio Res./ All. Stress (%)
7-8	Elbow				109.2	249.4	44	44.6	410.0	11							65.5	232.5	28
14-16	Elbow				74.9	249.4	30	49.7	410.0	12							63.0	232.5	27
22-23	Elbow				76.1	249.4	31	35.4	410.0	9							61.0	272.4	22
35-36	Elbow				88.3	256.9	34	35.8	410.0	9							61.6	232.5	26
43-44	Elbow				117.2	256.9	46	45.2	410.0	11							69.8	232.5	30
65-66	Elbow				137.5	256.9	54	33.0	410.0	8							78.7	232.5	34
75-76	Elbow				87.3	256.9	34	16.6	410.0	4							43.9	232.5	19
78-79	Elbow				113.1	256.9	44	17.0	410.0	4							36.1	232.5	16
99-100	Elbow				87.9	256.9	34	16.6	410.0	4							48.1	232.5	21
118-119	Elbow				114.7	256.9	45	14.6	410.0	4							75.7	232.5	33
10	In pipe							33.5	410.0	8							60.6	232.5	26
21-22	In pipe							59.2	249.4	24							61.2	272.4	22
38	In pipe							21.4	410.0	5							72.1	232.5	31
45	In pipe							20.7	410.0	5							60.9	232.5	26
63	In pipe							126.2	256.9	49							104.4	232.5	45
70	In pipe							73.4	256.9	29							41.8	232.5	18
84	In pipe							53.3	256.9	21							37.2	232.5	16
86	In pipe								4.6	410.0	1						34.5	232.5	15
102	In pipe							76.2	256.9	30							36.7	232.5	16
109	In pipe								51.6	410.0	13						33.1	232.5	14
120	In pipe								16.0	410.0	4						44.2	232.5	19
129	In pipe							68.9	256.9	27							30.9	232.5	13
12	Tee							93.4	249.4	37							148.6	232.5	64
42	Tee							163.4	256.9	64							156.9	232.5	67
95	Tee							214.2	256.9	83							250.8	232.5	108
32-33	Reducer							130.3	256.9	51							98.0	232.5	42
58-59	Reducer							148.1	256.9	58							88.2	232.5	38

⁽¹⁾ Allowable Stress is according to National Practice.

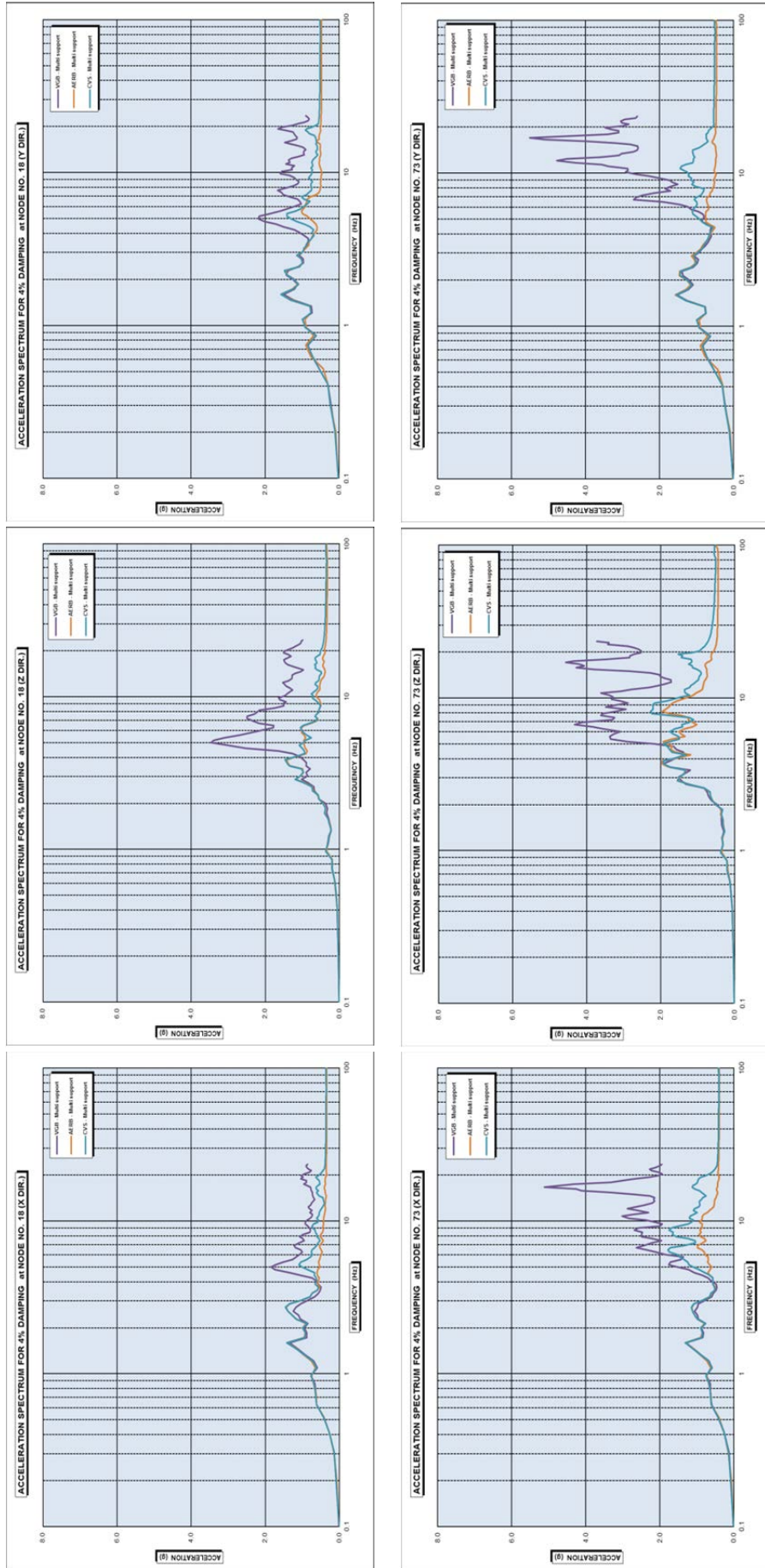


FIG. 56. Time history analysis results for multi-support excitations; response spectra at nodes 18 and 73 in the X, Z and Y directions.

4.2. MAIN RESULTS FOR THE TASK 2.2 SLOSHING OF THE SPENT FUEL POOL

4.2.1. Phase I and Phase II: Initial and Complete Analyses

4.2.1.1. Model presentation

Types of models, methodologies of analyses and calculation codes used by participants for the analysis of the Unit 7 spent fuel pool are presented in Table 43. One participant presented two-dimensional finite element analysis and all others presented three-dimensional finite element analyses. In order to investigate the sloshing characteristics of the spent fuel pool, one participant conducted experimental tests on a 1/20 scaled pool model made of glass plates, using a three dimensional shaking table. Different computer codes were used by the participants. Typical views of some participants' models are shown in Fig. 57.

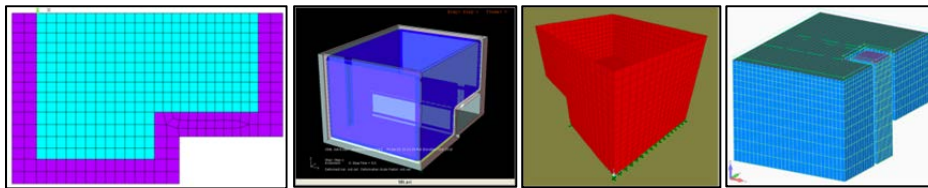


FIG. 57. Examples for participants' modelling of the spent fuel pool.

TABLE 43. METHODOLOGY OF ANALYSIS USED BY PARTICIPANTS

PART 2. EQUIPMENT: TASK 2.2 Sloshing of the Spent Fuel Pool Subtask 2.2.2 Complete analysis of spilled water: Model Presentation				
No	Participant Organization	Type of model	Methodology of analysis	Calculation code
1	CNEA&UNCU, Argentina -1	3D FEM - Implicit	Four-node shell elements with six degrees of freedom per node were used to model the pool. Eight-node solid-fluid elements (size 55cm) with three degrees of freedom per node were used to model the inviscid liquid without net flow rate. The finite element formulation allows acceleration effects such as sloshing. In order to satisfy the continuity conditions between the fluid and solid shell at the wall boundary, the "coincident" nodes of the fluid and shell elements are constrained to be coupled in the direction normal to the interface, while relative motions are allowed to occur in the tangential directions. In order to investigate the sloshing characteristics of the spent fuel pool, experimental tests were conducted on a 1/20 scaled pool model made of glass plates, using a three dimensional shaking table. The following tests were performed: a) sine wave sweep tests in NS and EW directions (evaluation of natural frequencies and mode shapes), b) seismic tests (estimation of maximum wave height, spilled water amount and free surface evolution). The tests were designed according to the following fundamental scales: length 1/20, time 1/4.47, density 1/1, acceleration 1/1. The natural frequencies of the sloshing waves were determined by the Fourier spectrum of the signals from instrumented buoys. In order to obtain the spilled water the observed seismic record at T.M.S.L.23500 level floor was used considering the most significant 15 sec. All records (NS, EW and UD) were applied simultaneously at the base of the pool.	ANSYS v.12.01
2	FNS, Finland	3D FEM	We used explicit time integration with coupled Euler-Lagrange method available in Abaqus-6.9. 17 second acceleration histories were constructed from given +23.5 level histories. The loading was applied as an inertial load. Accelerations all directions were applied simultaneously.	ABAQUS-6.9
3	AERB, India	2D FEM	A 2 dimensional analysis is attempted. The tank walls are modelled using plain stress elements and water 2-d fluid elements. The current analysis does not consider any fuel bundles inside the tank. The natural frequency as well the behaviour of the fluid will change if this is considered and a separate analysis is planned for that. Along the boundary of the wall, the fluid elements are allowed to move parallel to the wall and not perpendicular to the wall. The degree of freedom of fluid and wall perpendicular wall is coupled so that any movement of wall is seen on the fluid and vice versa.	
4	KINS, Korea	3D FEM	Three-dimensional fluid elements (FLUID80), which is a modification of the 3-D structural solid element, are used. The fluid element is used to model fluids contained within vessels having no net flow rate. The element is defined by eight nodes having three transitional degrees of freedom at each node.	ANSYS v. 12.0.1
5	KOPEC, Korea	3D FEM	Mode-Superposition Transient Dynamic Analysis (Modal Analysis : Reduced Mode-extraction Method)	ANSYS
6	PAEC, Pakistan	3D FEM	No. of nodes: 30174, No. of 8-Noded solid elements: 27152 Type of elements: FLUID80 for Water and SOLID45 for RCC Structure Transient Dynamic Analysis was performed for the given set of simulated time histories.	ANSYS Release 11.0.1
7	CVS, Russian Federation	3D FEM	Potential flow fluid 3D analysis , Time History Analysis only , Rayleigh Damping: 0.3Hz - 0.5%, 10Hz - 0.5%	SOLVIA v. 03.0.9

4.2.1.2. Modal analyses of the sloshing

Participants' results for the first sloshing frequencies in the X and Y directions and modal mass participation ratios are presented in Table 44. Mean values for the first sloshing frequencies in the X and Y directions are 0.22 Hz and 0.20Hz, respectively; COV of the results is 0.08 in the X and Y directions.

TABLE 44. SLOSHING FREQUENCIES, MODAL MASSES PARTICIPATION RATIO

PART 2. EQUIPMENT: TASK 2.2 Sloshing of the Spent Fuel Pool									
Subtask 2.2.2 Complete analysis of spilled water A. Modal analysis of the sloshing									
A.1. Sloshing frequencies, modal masses, participation factors									
No	Participant Organization	Natural Frequency (Hz)		Damping Ratio %	Modal participating mass ratios (%)		Total mass (ton)	Total mass in each direction (%)	
		in X	in Y		U _X	U _Y		M _{total}	M _x
1	CNEA&UNCU, Argentina - Model 1	0.23	0.20						
	CNEA&UNCU, Argentina - Model 2	0.22	0.18						
2	FNS, Finland								
3	AERB, India		0.20	0.50		32			
4	KINS, Korea	0.22	0.19	0.50	45	54	1764	47	57
5	KOPEC, Korea	0.19	0.23	0.50	96	98	1859	100	100
6	PAEC, Pakistan	0.24	0.20	0.50					
7	CVS, Russian Federation								
Mean		0.22	0.20		71	61	1812	73	78
Standard deviation		0.02	0.02		36	34	67	38	31
Coefficient of variation		0.08	0.08		0.51	0.55	0.04	0.52	0.39

4.2.1.3. Estimation of maximum wave height assuming

Participants' results for the maximum wave height at the spent fuel pool in the X and Y directions are given in Table 45. Mean values for the maximum wave height in the X and Y directions are 83cm and 104m, respectively. COVs in the X and Y directions are 0.14 and 0.38, respectively.

TABLE 45. MAXIMUM WAVE HEIGHT

PART 2. EQUIPMENT: TASK 2.2 Sloshing of the Spent Fuel Pool			
Subtask 2.2.2 Complete analysis of spilled water			
No	Participant Organization	B.1. Maximum wave height	
		Max wave height in x direction (cm)	Max wave height in y direction (cm)
1	CNEA&UNCU, Argentina - Model 1		165
	CNEA&UNCU, Argentina - Model 2		102
2	FNS, Finland		
3	AERB, India		48
4	KINS, Korea	82	83
5	KOPEC, Korea		138
6	PAEC, Pakistan	72	79
7	CVS, Russian Federation	193	193
Mean		115	115
Standard deviation		67	52
Coefficient of variation		0.58	0.45

4.2.1.4. Estimation of spilled water amount during the NCO earthquake

Participants' results for the estimation of spilled water amount from the Unit 7 spent fuel pool during the NCOE are given in Table 46. A few participants presented methodologies used for the spilled water amount estimation and the spilled amount of water. There is discrepancy between participants' results varying from 66 m³ to 376m³.

TABLE 46. ESTIMATION OF SPILLED WATER AMOUNT DURING THE NCOE

PART 2. EQUIPMENT: TASK 2.2 Sloshing of the Spent Fuel Pool Subtask 2.2.2 Complete analysis of spilled water C. Estimation of spilled water amount during NCOE and D. Free surface evolution (if available)			
No	Participant Organization	C. Estimation of spilled water amount during NCOE	
		C.1. Methodology used for spilled water amount estimation	C.2. Spilled water amount (m ³)
1	CNEA&UNCU, Argentina - Model 1	From each instant of time in which the overflow occurred during the motion (i.e. when the liquid surface level exceeds the operating floor level), the number of elements with a chance to spill was estimated. From total number of elements, the volume of spilled water was approximately estimated.	133
	CNEA&UNCU, Argentina - Model 2	The volume of spilled water was determined from difference between the heights of the free surface measured before and after of the ground motion	90
2	FNS, Finland	Vertical reaction force time-history was smoothed (moving average) and the end value of the reaction force subtracted from the initial value. Two smoothing parameters were considered. Smooth 1000 shows clear convergence at the end.	376
3	AERB, India		
4	KINS, Korea		
5	KOPEC, Korea		
6	PAEC, Pakistan	Average of slosh height above free board of 31.0 cm is calculated for X and Y directions. Assuming that 10 % of the surface area is spilling out for the averaged heights in X and Y direction, the amount of spilled water is calculated for two directions and added to find the amount of spilled water.	77
7	CVS, Russian Federation	H - maximum wave height above curb in pool corner, LxB are pool dimensions, h is curb height; $V=(H-h)^3*L*B/H^2/6$	55
Mean			146
Standard deviation			132
Coefficient of variation			0.90

4.3. MAIN RESULTS FOR TASK 2.3 PURE WATER TANK BUCKLING

4.3.1. Phase I: Initial Analyses

Participants presented results only for Phase I which was the analysis of pure water tank buckling under the NCOE for the fixed-base model. No results were presented by participants for Phase II which was analysis of pure water tank buckling under the NCOE including soil.

4.3.1.1. Model presentation

Types of models, model characteristics (the number of nodes and the number and types of elements), damping values used for the structure and water and calculation codes used by participants for the pure water tank buckling analyses are given in Table 47. All participants generated 3D FEMs. The numbers of nodes for 3D models vary from 2211 to 13018. Different computer codes were used by participants. Typical views of some participants' models are presented in Fig. 58.

TABLE 47. MODEL PRESENTATION FOR THE PURE WATER TANK

TASK 2.3 Equipment: Pure Water Tank Buckling Subtask 2.3.1 Initial Analyses						
No	Participant Organization	Type of model	Model characteristics (Number of nodes, elements)	Damping value (%) for structure	Damping value (%) for water	Calculation Code or Software used
1	FNS, Finland	Shell element model. Wind girder modeled with beam elements	Total number of nodes: 2958 Total number of elements: 3077 80 linear line elements of type B31; 2-node Timoshenko beam elements used for wind girder 2915 linear quadrilateral elements of type S4R; 4-node reduced integration general purpose shell elements 82 linear triangular elements of type S3; 3-node general purpose shell elements.	Rayleigh damping with $\alpha=0.123$ and $\beta=0.0003105$ (values based on ASCE-98 code specification)		Abacus/Standard-6.9 and Fpipe
2	EdF, France - Model1	Plate elements (4 nodes) (Discret Kirchhoff elements)	8417 nodes, 9959 elements	4	0.5	Code Aster V 9.06
	EdF, France - Model2	Lumped mass, beam elements (Timoshenko elements)	85 nodes, 168 elements	4	0.5	Code Aster V 9.06
3	AERB, India	Tank modelled by SHELL, Fluid modelled by 3D element	Total No. of elements: 6166; Total no. of nodes 6830; Tank element :SHELL63; Fluid element : FLUID80; Wind girder and roof rafter: BEAM188	5	0.5	ANSYS
4	KOPEC, Korea	Shell element model w/ added mass and stiffened frame	10325 nodes for structure and 3888 nodes for added mass			ABAQUS 6.5 and some house codes for data processing
5	AMEC, NNC, Romania Model1	Model1 is for modal analysis. Model1 uses shell elements (SHELL63) for steel structure and solid elements (FLUID80) for water.	Model 1: 6297 nodes; 4200 FLUID80 elements; 1480 SHELL63 elements	5	0.5	ANSYS v11.0
	AMEC, NNC, Romania Model2	Model2 for transient analysis. Model2 uses point to point contact elements (CONTAC52) for the interface between tank bottom and foundation, BEAM4 elements for wind girder, and spar elements (LINK180) for the bolts; the tank elements are SHELL181.	Model 2: 2211 nodes; 1188 FLUID80 elements; 624 SHELL181 elements; 121 CONTAC52 elements; 12 LINK 180 elements; 24 BEAM4 elements	5	0.5	ANSYS v11.0
6	CVS, Russian Federation	Time history potential flow model, no modal analysis available. Soil modeled by springs	12203 nodes; 10032 FLUID3d elements; 2040 SHELL elements, 748 BEAM elements, 5 SPRING elements	5	0.5	SOLVIA v. 03.0.9

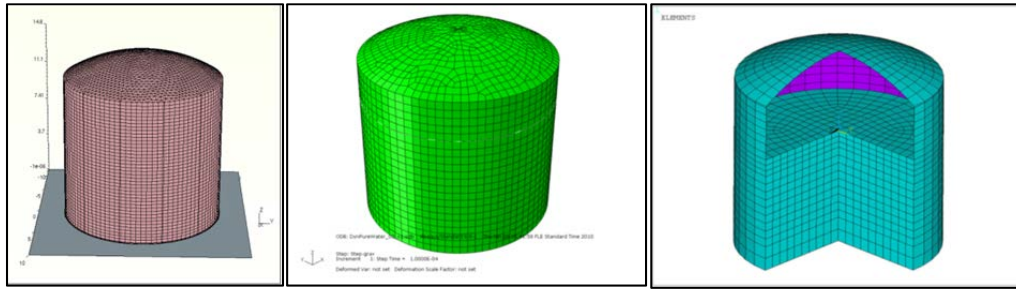


FIG. 58. Example of participants' models of the the pure water tank.

4.3.1.2. Modal analyses of the pure water tank

Participants' results are given in Table 48. All participants presented the same sloshing frequency result: 0.24 Hz. Participants' results for the first frequency of the tank vary from 1.62 Hz to 10.72 Hz.

TABLE 48. MODAL ANALYSIS RESULTS: SLOSHING AND STRUCTURE FREQUENCIES

TASK 2.3 Equipment: Pure Water Tank Buckling						
Subtask 2.3.1 Initial Analyses - A. Modal analysis of the pure water tank						
No	Participant Organization	A.1. Frequencies, modal masses, participation factors and A.3 Total mass participating in each direction (X, Y and Z)				
		Natural Frequency (Hz)				
		Sloshing in X	Sloshing in Y	Structure in X	Structure in Y	Structure in Z
1	FNS, Finland			5.00	5.00	9.40
2	EdF, France - Model 1	0.24		9.13	9.13	10.24
	EdF, France - Model 2	0.24		10.72	10.72	
3	AERB, India	0.24		7.95		8.21
4	KOPEC, Korea			1.62		
5	AMEC, NNC, Romania - Model 1	0.24	0.24	8.10	8.10	8.25
6	CVS, Russian Federation					

4.3.1.3. Response spectrum and time history analyses of the pure water tank: displacement, resultant force and stress

Since only a few participants presented results, COV of participants' results has not been calculated.

Participants' response spectrum analysis and time history analysis results of the pure water tank for the maximum displacement at the centre of the roof are given in Table 49. Participants' results for the maximum top displacement of the tank are not consistent.

Participants' response spectrum analysis and time history analysis results of the pure water tank for the maximum resultant forces below the bottom plate are given in Table 50. Participants' response spectrum analysis and time history analyses results for the maximum resultant force are quite close to each other.

Participants' response spectrum analysis and time history analysis results of the pure water tank for vertical, hoop and shear stresses are given in Table 51. Again participants' results for stresses are not in good agreement. Only one participant presented results for the stresses for both types of analyses.

TABLE 49. RESPONSE SPECTRUM AND TIME HISTORY ANALYSES: TOP DISPLACEMENT

TASK 2.3 Equipment: Pure Water Tank Buckling							
Subtask 2.3.1 Initial Analyses							
No	Participant Organization	B. Modal spectrum analysis of the pure water tank Maximum displacements due to combination; at center of Roof			C. Time history analysis of the pure water tank Maximum displacement due to combination at center of roof		
		Displ. Combination (mm)			Displ. Combination (mm)		
		Δx	Δy	Δz	Δx	Δy	Δz
1	FNS, Finland				53	108	18
2	EdF, France - Model 1	35	108	2			
	EdF, France - Model 2				4	1	0
3	AERB, India						
4	KOPEC, Korea	40	63	1	66	82	260
5	AMEC, NNC, Romania - Model 1	7	8	2			
	AMEC, NNC, Romania - Model 2				45	190	87
6	CVS, Russian Federation				10	16	4

TABLE 50. RESPONSE SPECTRUM AND TIME HISTORY ANALYSES: MAXIMUM RESULTANT FORCES BELOW BOTTOM PLATE

TASK 2.3 Equipment: Pure Water Tank Buckling							
Subtask 2.3.1 Initial Analyses							
No	Participant Organization	B. Modal spectrum analysis of the pure water tank Maximum resultant forces <u>below</u> bottom plate for the loading in X, Y, Z direction and Combination			C. Time history analysis of the pure water tank Maximum resultant forces <u>below</u> bottom plate for the loading in X, Y, Z direction and Combination		
		Force Combination (MN)			Force Combination (MN)		
		Fx	Fy	Fz	Fx	Fy	Fz
1	FNS, Finland						
2	EdF, France - Model 1	6	19	31	9	12	15
3	AERB, India						
4	KOPEC, Korea						
5	AMEC, NNC, Romania - Model 1	15	16	7	9	17	42
6	CVS, Russian Federation				9	14	33

TABLE 51. RESPONSE SPECTRUM AND TIME HISTORY ANALYSES: VERTICAL, HOOP AND SHEAR STRESSES

TASK 2.3 Equipment: Pure Water Tank Buckling							
Subtask 2.3.1 Initial Analyses							
No	Participant Organization	B. Modal spectrum analysis of the pure water tank Maximum combined stresses at points: Level 1 Point 6			C. Time history analysis of the pure water tank Maximum combined stresses at points: Level 1 Point 6		
		Total (Dead load + Seismic load)			Total (Dead load + Seismic load)		
		Vertical stress (MPa)	Hoop stress (MPa)	Shear stress (MPa)	Vertical stress (MPa)	Hoop stress (MPa)	Shear stress (MPa)
1	FNS, Finland						
2	EdF, France - Model 1	116	49	22			
3	AERB, India						
4	KOPEC, Korea	19	101	30			
5	AMEC, NNC, Romania - Model 1	57	250	64	142	151	83
6	CVS, Russian Federation				29	43	69

4.3.1.4. Buckling estimation

Participants' results for buckling types and locations in the case of local criteria at level 1 and level 3 at eight points of the pure water tank are given in Table 52. Two participants reported elephant foot buckling at level 1 points and one team reported elephant foot buckling at level 3 points.

Participants' results for buckling types and locations in the case of global criteria at eight points of the pure water tank are also given in Table 52. Only one participant reported elephant foot buckling at level 3 and two participants reported diamond buckling at level 5 and 6. It is possible that sloshing of the water may have contributed to this failure mode.

TABLE 52. BUCKLING TYPES AND LOCATIONS IN THE CASE OF LOCAL CRITERIA: LEVEL 1 AND LEVEL 3 AND IN THE CASE OF GLOBAL CRITERIA

TASK 2.3 Equipment: Pure Water Tank Buckling Subtask 2.3.1 Initial Analyses - D Buckling estimation									
No	Participant Organization	D.2. Buckling type and location in case of local criterion : Level 1							
		Point 1	Point 2	Point 3	Point 4	Point 5	Point 6	Point 7	Point 8
1	FNS, Finland								
2	EdF, France - Model 1	Low margin for EFB	Low margin for EFB	Low margin for EFB	Low margin for EFB	Low margin for EFB	Low margin for EFB	Low margin for EFB	Low margin for EFB
3	AERB, India								
4	KOPEC, Korea								
5	AMEC, NNC, Romania - Model 1	EFB	EFB	EFB	EFB			EFB	
6	CVS, Russian Federation								
EFB : Elephant Foot Buckling									
TASK 2.3 Equipment: Pure Water Tank Buckling Subtask 2.3.1 Initial Analyses - D Buckling Prediction									
No	Participant Organization	D.3. Buckling type and location in case of global criterion							
		Level 1	Level 2	Level 3	Level 4	Level 5	Level 6	Level 7	Level 8
1	FNS, Finland								
2	EdF, France - Model 1			EFB		DB - External pressure			
3	AERB, India								
4	KOPEC, Korea								
5	AMEC, NNC, Romania - Model 1								
6	CVS, Russian Federation					DB	DB		
EFB : Elephant Foot Buckling DB : Diamond Buckling									
TASK 2.3 Equipment: Pure Water Tank Buckling Subtask 2.3.1 Initial Analyses - D Buckling estimation									
No	Participant Organization	D.2. Buckling type and location in case of local criterion : Level 3							
		Point 1	Point 2	Point 3	Point 4	Point 5	Point 6	Point 7	Point 8
1	FNS, Finland								
2	EdF, France - Model 1	EFB	EFB	EFB	EFB	EFB	EFB	EFB	EFB
3	AERB, India								
4	KOPEC, Korea								
5	AMEC, NNC, Romania - Model 1								
6	CVS, Russian Federation								
EFB : Elephant Foot Buckling									

5. OBSERVATIONS AND CONCLUSIONS

5.1. OBSERVATIONS

5.1.1. Part 1 Structure

5.1.1.1. Observations on key modelling assumptions

i. Input signal

Signals derived at the Outcrop of the Engineering Bedrock (OEB) elevation (TMSL -155m) compatible with NCOE main shock records were used in Phase II (Fig. 19). Signals derived at the Outcrop of the Raft elevation (ORE) (TMSL -13.7m) and at the OEB elevation corresponding to 1*NCOE, 2*NCOE, 4*NCOE, 6*NCOE were provided to the participants in Phase III (Fig. 21). Corresponding response spectra were also provided (Figs 20 and 22).

Participants' assumptions for the location of a control point are presented in Table 54 in Appendix. Most of the participants used the raft elevation (TMSL -13.7m) as a control point, as outcrop motions or as in-column motions. One participant used free surface of the soil as a control point.

ii. Soil

- *Modelling of SSI model and non-linear behaviour of soil*

Participants' assumptions for modelling of SSI and non-linear behaviour of soil are given in Table 55 in Appendix for Task 1.3. For those participants that explicitly modelled nonlinear behaviour of the structure, simplified treatment of SSI modelling was used. Most of these participants calculated impedance functions and based on this computation, they modelled the soil using the spring and dashpot elements representing the soil medium for the SSI analysis.

One participant used the direct time domain finite element method with full contact between soil and outer walls and viscous absorbing boundary to represent the far-field soil (lateral sides and bottom).

Some of the participants modelled the soil by linear springs. Some others took into account the soil nonlinearity using the equivalent linear method. One participant modelled the soil by nonlinear soil springs.

Global impedance discretization/distribution in the model is given in Table 56 in Appendix. Most of the participants distributed the soil impedances over all basemat nodal points. One participant performed the time domain integration directly on the coupled soil-structure system. There is no need to compute the soil impedance in this method.

- *Damping modelling for soil and SSI model (equivalent damping / Rayleigh damping)*

Participants' assumptions for damping modelling for soil and SSI model are given in Table 57 in Appendix. Some of the participants used the Rayleigh damping and others used the SSI equivalent damping.

- *Consideration of embedment*

Participants' assumptions for consideration of embedment in the SSI model are given in Table 58 in Appendix. Most of the participants considered the embedment effect in the SSI model

through impedances and scattering functions using non-linear spring and gap element between soil and structure or including effect of embedment in the soil impedances. One participant ignored the effect of the embedment. One participant considered the effect of the embedment by a realistic finite element modelling of the near field soil and the structure. One participant took into account the embedment effect by considering the de-convoluted signal at the raft of the structure. In this model, there is no contact between the soil and the lateral walls in contact with the soil.

- *Basemat (rigid or flexible with discrete springs and dampers)*

Most of the participants modelled the basemat using solid elements with elastic material behaviour. One participant modelled the basemat as rigid (Table 55 in Appendix).

iii. Structural system

- *Structural modelling*

Types of structural modelling and model characteristics (e.g. the number of nodes, types of elements, the number of elements, etc.) used by participants are given in Table 25 and Table 26, respectively.

Most of the participants used 3D Finite Element Model (FEM) with shell elements for walls and floors, beam elements for beams and columns, and solid elements for basemat. One participant used 3D FEM with solid elements for walls, floors, beams, columns and basemat and truss elements for the steel roof structure. The number of nodes for 3D models spread from 1463 to 74780, almost a factor of 50.

- *Damping modelling for structural elements*

Participants' assumptions for damping of structural elements are given in Table 59 in Appendix. Most of the participants used the Rayleigh damping for structural elements. One participant used modal damping.

- *Linear / Non-linear structural members*

Participants' assumptions for modelling the structural elements in linear or nonlinear behaviours are given in Table 60 in Appendix. All participants assumed non-linear material behaviour for main walls and RCCV wall except one participant who assumed all structural elements as equivalent linear. Some of the participants assumed also non-linear material behaviour for columns, beams and floors and auxiliary walls. Some of the participants did not consider the auxiliary walls in their models.

- *Modelling assumptions for non-linear behaviour of structure (e.g. material and element constitutive laws, capability of prediction of crack distribution)*

Material properties for concrete and reinforcing steel were proposed to the participants [5]. Most participants used the proposed properties. In one case, the effect of aging was included in the derivation of concrete material properties. Participants' assumptions for modelling linear and non-linear behaviour of the structure (e.g. material and element constitutive laws, capability of prediction of crack distribution) are given in Table 61 in Appendix. Some of the participants included consideration of capability of prediction of crack distribution.

- *Non-linear dynamic analysis assumptions*

Participants' assumptions for non-linear dynamic analysis are given in Table 62 in Appendix.

- *Pushover analysis assumptions, shape of loading function*

Participants' pushover analysis assumptions are given in Table 63 in Appendix. The load functions were generated by uniform distribution of horizontal accelerations. Uniform horizontal load should have been applied from lower level of the raft elevation to the roof (top). Most of the participants used the given load function in the pushover analysis. One participant used the generated load function based on the first mode distribution which was applied and increased until the ultimate load or a sufficient large displacement has been reached.

- *Determination of performance point (smoothing demand spectrum)*

Participants' assumptions for determining performance points on pushover curves are given in Table 64 in Appendix. Participants had difficulties in determination of performance points for an unsmoothed ADRS (Acceleration Displacement Response Spectrum). Some of the participants used smoothed spectra obtained from the given response spectra.

- *Overall evaluation for ultimate capacity of the structure:*

Performance criteria for structural elements and overall structure used by participants are given in Table 65. Story drift (e.g. 0.0075 for significant damage), concrete compressive strain (e.g. $\geq 0.4\%$), cracking of concrete were used by participants for performance criteria for structural elements and overall structure.

Some of the participants considered geometric nonlinearity in the soil-structure interface using non-linear spring and gap elements to take into account uplift, sliding and rocking of the foundation and non-linear response of the lateral soil (Table 55 in Appendix).

None of the participants considered the geometric non-linearity of the structure in terms of P- Δ effect due to significant drift. They considered only material non-linearity.

- *Structure Soil Structure Interaction (SSSI)*

SSSI is not considered in the analyses.

5.1.1.2. *Observations on results of analyses*

i. Results from Phase I

Most of the participants developed 3D finite element structural models (15 out of 18) and used commercial computer codes for the seismic analysis. The degree of refinement of the finite element mesh varied from models with approximately 2,600 to 75,000 nodes (average 20,000 nodes).

To check completeness and coherence of input data and soundness of the models, the resultant force of a fixed-base model at the bottom of the basemat under static dead weight and uniformly distributed load due to 1 g acceleration applied in the X and Y directions was calculated and compared. The results from vertical (Z direction) and horizontal loads in the X and Y directions are well comparable and the scatter small (COV = 8 %). Notably, due to

small eccentricities (resulting eccentricities (M/F) less than 1 m), the COV of the resulting moments due to the vertical loads is high (e.g. 50 % for M_y). The corresponding displacements at the 3rd floor (T.M.S.L. +23.5) and roof top (T.M.S.L. +49.7) for locations on the main reinforced load-bearing structure show relatively small scatter. The calculated displacements in all three directions at the roof centre show strong scatter (COV = 60% - 100 %), indicating modelling uncertainty in the roof structure. Obviously, participants did not spend much effort on modelling the roof structure, due to its secondary role in the benchmark exercise.

The results from the modal analysis of the fixed-base model indicate a very small scatter (COV = 9 %) in the frequency values of the fundamental horizontal modes. It is recalled that the COV of the calculated fundamental frequencies for the simple test structure in the IAEA CAMUS benchmark [15] was 10 %.

All participants used one-dimensional soil column model with vertically propagating shear waves. This is considered to be the most reasonable assumption in view of the data available for the benchmark. The numerical code SHAKE91 was used by most of the participants. SHAKE91 performs successive iterations on the soil characteristics until convergence is achieved within each sub layer between the average induced shear strain, shear modulus and damping ratio.

For Aftershock I, depending on the choice of a control point in the analysis, COV varies from 9 to 19 % for the maximum accelerations at the 6 observation points in the X direction. A comparison of the calculated and recorded response spectra reveals that most participants predicted the resonant frequencies of the soil profile with high accuracy with a slight shift towards the lower frequencies. A review of the calculated data for the soil shear modulus reduction, damping ratio and maximum shear strain along the depth indicates that results are more consistent for maximum shear strain than for shear modulus reduction and damping ratio.

For the Main shock, COV of the maximum accelerations at different observation points varies between 11 and 38 %. COVs for the Main shock are higher than those for Aftershock I due to stronger non-linear response of the softer top soil. A comparison of the calculated and recorded response spectra indicates that most participants predicted almost the same resonant frequencies of the soil profile. A few results show a shift towards higher frequencies with depth. Results at different soil depths cannot be compared with the corresponding recorded motions in borehole G5 since these are unavailable.

A comparison of the calculated fundamental frequencies in both horizontal directions from modal analysis for fixed-base and coupled soil-structure interaction (SSI) models indicates COV = 9 % for the fixed-base model and COV = 9 % in the X direction and 12 % in Y direction for the SSI model.

As expected, the SSI has a significant effect on the response by decreasing the fundamental frequency. In the horizontal direction, the decrease is by a factor of about 2 and in the vertical direction of about 2.5.

As a conclusion of Phase I, the analytical models developed by the participants give coherent global results and are considered suitable for the next phases of the benchmark.

ii. Results from Phase II

As a conclusion of Phase II, although some variation exists among the participants' results, they show a general tendency towards over-prediction of the recorded data. Variation in the "best-estimate analysis" results is higher in comparison to the variation observed in the "reference analysis" results. Notably, some outliers are observed. SSI plays a key role in the response of the structure and thus the freedom of choice of the control point location for SSI analysis within the "best-estimate analysis" contributes to the scatter in the results (e.g. relative displacement) significantly. This effect is less pronounced on the calculated absolute accelerations which exhibit lower COVs and fit relatively well the recorded data. In general, computed spectral accelerations at the basemat and at the 3rd floor are higher than the recorded data throughout the whole frequency range. However, a few participants predicted quite well the observed response spectra at both levels.

The SSI analysis results show that acceleration response spectra have two major peaks around 1.5-2Hz and 4-5Hz, where the first peak frequency corresponds to the system frequency and the second one to the dominant frequency of seismic input ground motions, which can be observed from the ratios of in-structure response spectra and input response spectra. In general participants failed to represent correctly FRS for frequencies above 2-3 Hz, giving significantly higher result than observed results.

The effect of embedment is two-fold: on the effective input motion into the foundation (kinematic interaction); and the effect on combined dynamic response characteristics of the soil-structure system (inertial interaction). The former is represented by scattering functions the effect of which is denoted foundation input motion in the literature. Therefore, the foundation input motion is significantly affected by embedment. Results of the effect of embedment on the impedances show significant variations with erratic behaviour of the real part for frequencies above about 5Hz . Surface founded vs embedded foundation impedances presented differences of about 30-40% depending on the frequency of interest. The effect of these differences on predicted seismic responses of the K-K Reactor Building were not quantified, however, it is expected that the differences would lead to response differences in the 10-20 % range.

iii. Results from Phase III

Material properties for concrete and reinforcing steel (e.g. constitutive laws) were proposed to the participants and most participants used these properties. The participants made many assumptions, as e.g. on modelling linear and non-linear behaviour of the soil and structure; on the soil global impedance discretization/distribution under the basemat of the structural model; on consideration of embedment effect; on damping in the structural elements and in the soil (including SSI effects); on static nonlinear (pushover) analysis and on determination of the performance point; on dynamic nonlinear analysis and on performance criteria for structural elements and overall structure. All these assumptions, which are expected to represent the current state-of-the-practice, are compared in a tabular form.

Pushover analysis of the reactor building was carried out for fixed-base and coupled soil-structure interaction models.

Pushover analysis results are pushover curves (top displacement versus applied base shear force) and performance points corresponding to seismic input motions scaled to 1*NCOE, 2*NCOE, 4*NCOE and 6*NCOE. For both the fixed-base and coupled SSI models, results are not in a good agreement. Some pushover curves indicate a significantly higher capacity.

Although it is expected that the structure will exhibit non-linear behaviour, some results show linear behaviour.

In the scope of the dynamic analysis, results are maximum relative displacement, maximum absolute acceleration and floor response spectra of absolute acceleration at the location (FP2) of the accelerometer device installed on the 3rd floor (T.M.S.L +23.5m) which recorded the event.

For the fixed-base structural model, the COV of the maximum relative displacement due to seismic input time-histories scaled to 1*NCOE, 2*NCOE, 4*NCOE and 6*NCOE vary from 11 to 52 %. COVs of the displacement results in the X direction are significantly lower than in the Y and Z directions. The COVs of the maximum absolute acceleration results vary from 15 to 43 %. Some results indicate a maximum displacement and acceleration decrease with increasing seismic demand. In comparison to the results from pushover analyses, dynamic analyses indicate a lower seismic capacity. Calculated floor response spectra of absolute acceleration in the X direction for 1*NCOE do not fit well to the observed response spectra. Most of participants' results show significant over-estimation of the spectral acceleration for frequencies beyond 3 Hz. The higher the scaling factor of the input time-histories the bigger the scatter of the results due to strong nonlinear effects in the behaviour. The spectral peaks do not shift notably to lower frequencies due to anticipated stiffness degradation effects, which may be due to the fact that the spectral peak frequency comes from the dominant frequency of the input seismic motion.

For the coupled soil-structure interaction model, the COV of the maximum relative displacement due to seismic input time-histories scaled to 1*NCOE, 2*NCOE, 4*NCOE and 6*NCOE vary from 27 to 55%. In comparison to the results from pushover analyses, dynamic analyses indicate a lower seismic capacity. As mentioned earlier, the ability of nonlinear static analysis is limited in capturing the transient dynamic behaviour with cyclic loading and corresponding degradation, and in taking into account high soil damping. In comparison to the results from the fixed-base model, the calculated displacements from the coupled soil-structure interaction model are bigger. The COVs of the maximum absolute acceleration results vary from 19 to 42 %. Some results indicate a maximum acceleration decrease with increasing seismic demand. In comparison to the results from the fixed-base model, the calculated accelerations from the coupled soil-structure interaction model are smaller. Calculated floor response spectra of absolute acceleration in the X direction for 1*NCOE do not fit well to the observed response spectra. Most of participants' results show significant over-estimation of the spectral acceleration for frequencies beyond 3 Hz. The higher the scaling factor of the input time-histories the bigger the scatter of the results due to strong nonlinear effects in the behaviour. The spectral peaks do not shift notably to lower frequencies due to anticipated stiffness degradation effects, which may be due to the fact that the spectral peak frequency comes from the dominant frequency of the input seismic motion.

It is observed that differences between structural responses from the nonlinear dynamic analyses are reduced, with increase of excitation levels such as seismic input motions scaled to 1*NCOE, 2*NCOE, 4*NCOE and 6*NCOE.

Inter-story drift ratios of the reactor building obtained from nonlinear dynamic analysis of fixed-base models due to seismic input time-histories scaled to 1*NCOE and 6*NCOE are 0.0024 to 0.0081, respectively (COVs of the results vary 65 to 117%). Inter-story drift ratios of the reactor building obtained from nonlinear dynamic analysis of SSI models due to seismic input time-histories scaled to 1*NCOE and 6*NCOE are 0.0024 to 0.0135, respectively (COVs of the results vary 99 to 115%). Inter-story drift ratio results from

nonlinear dynamic analysis of fixed-base and coupled SSI models due to seismic input time-histories scaled to 1*NCOE, 2*NCOE, 4*NCOE and 6*NCOE indicate that results show an increased story drift due to the effect of soil-structure interaction.

5.1.2. Part 2 Equipment

5.1.2.1. Observations on key modelling assumptions and results of analyses

i. RHR Piping System

Deviations in participants' results and corresponding possible sources of discrepancies are explained in Table 53.

TABLE 53. FINDINGS FROM PARTICIPANTS' RESULTS AND POSSIBLE SOURCES FOR DISCREPANCIES

Findings from participants' results	Possible sources for discrepancies
Total mass of piping system varies in the range from 28.5 tons to 35.6 tons	Engineering practice
Different modelling of spring hanger supports	Engineering practice, Software
Different flexibility factors for bends	National Codes, Software
Temperature dependence of Young's modulus	National Codes, Software
Non-linear behavior of piping supports for static analysis (friction in sliding and guide supports, pendulum effect for hangers)	Engineering practice, Software
Time step used for time history analysis	Engineering practice
Different methods of time history analyses: modal or direct integration	Software, Engineering practice
Interpretation of damping for time history analyses (modal or Rayleigh damping)	Software
Different modal damping values (2% or 4%)	National Codes
Different rules for modal superposition (SRSS, CQC, etc.)	Engineering practice, Software
Use of missing mass correction	National Codes, Software
Rules for dynamic and pseudo static response combination for multi support excitation	Engineering practice, Software
Seismic Anchor Motion to be combined or not with dynamic response	National Codes, Engineering practice
Different stress intensification factors for piping elements (bends, tees, reducers)	National Codes, Software
Different safety classification	National Codes
Different values for allowable stresses for different service limits	National Codes

Notes: "Engineering practice" reflects experience of analyst and traditional approaches used in the industry.

"Software" means an ability of the FE Computer Programs to address relevant issues.

"National Codes" means prescribed rules in the national Codes and Standards.

ii. Spent fuel pool sloshing

Reviewing participants' models and results the following issues have been observed:

- Different modelling techniques for liquid: analytical formulation (Housner formula), 2D or 3D fluid elements, experiment;

- Different approaches to model the geometry of the pool: 2D vertical cross-sectional shape, model with equivalent 3D rectangular shape, 3D models reflecting main dimensions of the pool without details, detailed geometry of the pool including the pit and scaled model of the pool used for experiment;
- Uniform approach for dynamic response analysis: time history analysis;
- Different seismic input: acceleration time histories at different levels (TMSL +18.1 m – simulated and TMSL +23.5 – recorded). No rocking was considered;
- Different analysis techniques: explicit solvers with Lagrange – Euler viscous fluid formulation or implicit solver with non-compressible perfect fluid;
- Different approaches for estimation of sloshing frequency: modal analysis or Housner formula. Different approaches for spilled water: directly from explicit solution or engineering estimation;
- Participants' results show good agreement for those parameters that could be predicted analytically: sloshing frequency (COV = 0.08) and total wave height (COV = 0.2). However, spilled water results have a big variation: from 66 tons to 376 tons. Recorded movie during the earthquake provided by TEPCO showed quite complex free surface wave form and results of some teams confirmed that tendency;
- Scaled experiment was very valuable for this benchmark, but it was not analysed in detail.

iii. Tank Analysis

Reviewing participants' models and results the following issues have been observed:

- All participants used shell FE models for analysis. One team used an additional beam element model to get seismic loads in time history analysis;
- The representation of the liquid differed from team to team: some participants used explicit modelling of water, other added water weight to the structural model, other applied an equivalent hydrostatic pressure for quasi-static analysis;
- Models of materials differ as well: some used nonlinear elasto-plastic models, other used only elastic one;
- Some participants considered possibility of lift-off in boundary conditions;
- Some models explicitly included anchor bolts in different degree of details;
- Response spectrum and time history analyses were used to predict seismic response;
- In the frame of modal analysis participants achieved a good agreement in estimation of sloshing frequency, but the fundamental structural frequency was estimated with higher variability;
- All participants reported diamond buckling, elephant foot buckling and anchor bolts failure;
- Those teams who considered anchor bolts coincided in prediction of the loads;
- Reporting of the diamond buckling was based either on observation of tank's wall deformation, or assessment of stress values in comparison with allowable installed by Codes;
- The governing mechanism of the elephant foot buckling is tensile hoop stress in conjunction with compressive axial stress, but nobody from participants simulated this effect directly;

5.2. CONCLUSIONS

5.2.1. Part 1 Structure

The participants' one-dimensional soil-column models with vertically propagating waves in horizontally layered soil system, which are adopted in many computer codes for site response

analysis with an equivalent-linearization concept such as SHAKE, provided resonance frequencies of soil profile with a slight shift towards the lower frequencies under the NCOE aftershock, although they yielded somewhat scattered results. However, the analysis did not predict well the recorded soil responses in the borehole due to the uncertainty and the non-uniformity of the soil, three-dimensional wave propagation effects, etc. The analysis results by participants were more consistent for maximum shear strain than for shear modulus reduction and damping ratio of soil along the depth in the borehole.

In general, the nonlinear static analysis procedure based on the displacement-based approach utilizing a pushover curve, works well for low-rise square buildings with symmetrical regular configurations. However, sometimes it is difficult to find single, correct performance point from the acceleration-displacement response spectra (ADRS) in the case of real earthquake events due to zigzag shapes of the spectra. Smoothing of the ADRS in order to avoid this difficulty may lead to errors.

The nonlinear static analysis predicted larger nonlinear structural response than the dynamic response analysis, especially for the SSI models, under seismic input motions scaled to 1*NCOE, 2*NCOE, 4*NCOE and 6*NCOE. The ability of the nonlinear static analysis is limited in capturing the transient dynamic behaviour with cyclic loading and corresponding degradation, and in taking into account high soil damping. Nevertheless, nonlinear static analysis is a convenient procedure that provides reliable results for structures whose dynamic response is governed by the first-mode sway motions.

Inter-story drift ratios obtained from the nonlinear dynamic analysis with the fixed-base and the SSI models under seismic input motions scaled to 1*NCOE, 2*NCOE, 4*NCOE and 6*NCOE indicated that the structure has larger capacity than three times of the NCOE, based on an allowable drift limit (i.e., essentially elastic behaviour, no damage, Limit State-A) as a function of limit state of structural systems provided in ASCE 43-05, which is consistent with an elastic design concept applied to the most countries' NPP design. They also indicated that the structure has larger ultimate capacity than five times of the NCOE, based on an allowable drift limit (i.e., moderate permanent distortion, generally repairable damage, Limit State-B) as provided in ASCE 43-05. It appears that the reactor building of K-K Unit 7 has much higher seismic capacity than design one.

The SSI analysis is carried out in the time domain or the frequency domain. Generally, the time domain approaches are simplified methods, which can account for localized nonlinearities, and the frequency-dependent approaches typically include the CLASSI and SASSI approaches, which treat the SSI problem linearly (soil and structure are modelled as behaving linearly) and solve the problem in the frequency domain to permit treatment of the frequency-dependent characteristics (stiffness and damping) of the supporting soil media. In some cases, infinite elements are utilized for modelling far-field soil media in the frequency domain in order to improve the accuracy of the analysis and reduce computing time for the analysis.

The general tendency towards over-prediction of the recorded structural response may be due to uncertainty and non-uniformity of the soil profile and properties, three-dimensional wave propagation effects, the ways how to take into account embedment effect of the structure and soil damping, etc.

5.2.2. Part 2 Equipment

5.2.2.1. RHR Piping System

i. Modelling

The following parameters are considered to be significant for creating the analysis model:

- geometry of piping system;
- material properties;
- total mass of the piping system (deadweight, insulation, medium) and its spatial distribution;
- representation of the boundary conditions with appropriate stiffness: fixed points, sliding or guide supports, restraints, spring or rod hangers, snubbers, etc.;
- operational conditions consistent with an earthquake (usually Normal Operational Conditions);
- establishing of the flexibility coefficients and stress intensification factors for piping fittings;
- size of the finite-element mesh to capture the highest natural frequency to be assessed.

A piping system is subjected to a broad set of loads that can be classified according to their nature as:

- sustained loads (such as deadweight and pressure);
- thermal expansion loads;
- inertial seismic loads in terms of floor response spectra or time history accelerations;
- loads due to seismic anchor movements (deformation loads).

ii. Analysis technique

Analysis technique is to be consistent with Code Requirements: conventional analysis is performed with the beam FE model assuming linear material behavior in the elastic range. Other analysis approaches (shell or volume finite elements, nonlinear material behavior, etc.) can be used only in conjunction with appropriate criteria to meet Code requirements. Assembling of the stiffness matrix is to be done with use of elastic modulus (Hot or Cold) according to the Code requirements.

In static analysis credit could be taken from the nonlinear behavior of piping supports (friction, uplift, pendulum effect for hangers). In the case of linear dynamic analysis a response spectrum method is normally used. To address nonlinearities for piping boundary conditions, time history analysis is more appropriate; care is needed to consider higher values of damping if the associated effects (e.g. friction) are included in analysis explicitly.

In the frame of the response spectrum method the most commonly used rule for modal combination is SRSS (Square Root of the Sum of the Squares). More general rule for the modal combination is CQC (Complete Quadratic Combination) that addresses closely spaced modes. An important thing in the modal analysis, modes with frequencies higher than the cut-off frequency (missing mass effect) needs to be taken into account.

Time step used in time history analysis is to be consistent with a cut-off frequency value and provide convergence in case of nonlinearities. Modal damping is used in the case of modal time history analysis. Direct integration methods require assembling a damping matrix. In the case of Rayleigh damping attention is needed that damping values are in the expected range over the concerned frequencies.

Multi-support excitation technique allows considering of seismic inputs at different supports in more realistic way. In multi-support analysis combining relative support motion and

motion due to inertia loads are important. Multi-support time history analysis is not common practice in piping engineering. There are two methods for accounting for different support motions in the time domain: explicitly apply displacements for each support or to reproduce desired seismic motion with use of “seismic mass” and forcing function.

In the case of multi-support time history analysis the main concern is a consistency of the signals: e.g. artificial acceleration time histories are needed to be baseline corrected. Inertial load creates mainly primary stress and seismic anchor motion being deformation load in nature creates secondary stress.

iii. Interpretation of results

Interpretation of results should be consistent with Code Requirements. Since the philosophy of the main Piping Codes is linear elastic analysis, the calculated stresses as well as allowable stresses could be beyond yield stress.

Following the code procedure calculated stresses for seismic loading are distinguished between primary and secondary stresses corresponding to each specific allowable value.

Failure modes of piping system according to the Code requirements are:

- integrity of pipe pressure boundary → stress;
- operability and integrity of inline components → accelerations or displacements or nozzle loads;
- strength of piping support → reaction forces and moments;
- piping supports functionality (spring and constant hangers, snubbers, etc.) → not exceeding allowable loads.

iv. Margin Assessment

In margin assessment, some major considerations are as follows:

- There is a mutual understanding that seismic margin of pipes should be expressed in terms of strains rather than stresses. In that case analysis taking into account material nonlinear behavior (plasticity) should be applied;
- Alternative and practical procedure for seismic margin assessment is Conservative Deterministic Failure Mode (CDFM) approach;
- This approach is based on the Code requirements and considers possibility to apply ductility factor and 5% damping for analysis;
- Most seismic margin research does not consider the piping collapse due to inertial loads as credible failure mode. According to the recent tests and investigations cyclic progressive failure mode governs mechanism for piping;
- It is more likely that pipes would fail due to seismic anchor motion or significant earth settlements as it happened during the NCOE;
- It is recalled that reliable seismic margin assessment can be performed only in conjunction with a detailed on-site seismic walkdown undertaken by a group of qualified specialists.

5.2.2.2. Spent fuel pool sloshing

- Currently there is not an established state-of-the-art technique for assessment of spilled water due to sloshing which could be required for beyond design basis earthquake evaluations.

5.2.2.3. Tank Analysis

- Elephant foot buckling failure mode could be addressed in the frame of material and geometry non-linear approach when appropriate criteria for strain is assumed;

- In some circumstances soil-structure interaction could play a significant role for seismic assessment of the ground based water tanks;
- Implementation of pushover analysis technique could be alternative to time history analysis for seismic evaluation of thin-walled tanks.

6. OUTLOOK AND SUGGESTIONS

6.1. GENERAL OUTLOOK AND SUGGESTIONS

The NCO earthquake of 2007 was the first major seismic event to affect a nuclear power plant and the IAEA was invited to Japan with the purpose of collecting and disseminating the lessons learned from this event. One of the issues related to the behaviour of the plant SSCs was their apparent robustness when faced with loads far exceeding the design bases. The KARISMA project had the aim to understand the root causes of this behaviour and share this information with the nuclear safety community worldwide. The exchange of information and discussions among the participants during project were considered very useful and they lead to a common understanding of complex topics. Since the occurrence of the NCO event, other major external hazards have affected NPPs. For example, in 2011 several NPPs on the East coast of Japan; the Fukushima Daiichi, Fukushima Daini, Tokai and Onagawa NPPs were affected by the Great Tohoku Earthquake and Tsunami to varying degrees of severity.

The results of the Benchmark exercise that are reported in this document represent only a fraction of the information for the K-K plant and its behaviour during the NCO. The accompanying database (provided in the enclosed CD) should be explored further to look into other relevant issues. This database comprises results obtained by different participants and they can be used for reference, for training or as a basis for subsequent developments on methodologies, modelling approaches, margins assessment and criteria derivation.

As already mentioned above, one of the major objectives of the Benchmark exercise was related to the evaluation of the findings when a recorded target value was not available and a prediction was not relevant. In this case, it is possible to make observations regarding the overall methodologies (e.g. pushover analysis versus dynamic modelling) and the variability involved in this. The latter provides a useful indication of the epistemic uncertainties that may be encountered in seismic structural analyses in general. This area should be further explored for both within methods (i.e. variability between participants using the same method) and also across methods.

The value of seismic records from instruments placed in the free field, in boreholes, on structures and components is well understood especially during a project such as KARISMA. It is suggested to encourage plant operators to deploy such instrumentation in their facilities, ensure operability through regular testing under simulated earthquake conditions, and to ensure the easy retrieval of the records after a seismic event. This is especially the case for NPPs located in seismically active regions of the world.

6.2. SPECIFIC SUGGESTIONS

In the Benchmark exercise, story drift was used as the damage indicator in determining margins. It is suggested that further studies should be conducted for developing other engineering damage indicators than the above (story drift) for seismic margin assessment, such as local stress or strain, or global indicators such as velocity, CAV, JMA intensity, etc.

The SSI analysis should be performed so as to take into account the effects of the potential variability in the soil properties at the site in seismic design: that is, at least three soil profiles such as a best estimate, a lower bound and an upper bound profile. It indicates that the range of the lower and upper bound profiles should be wide enough.

Nonlinear static analysis is a convenient procedure that provides reliable results for structures whose dynamic response is governed by the first-mode sway motions.

In comparison to the results from pushover analyses, dynamic analyses indicate a higher seismic capacity. The ability of nonlinear static analysis is limited in capturing the transient dynamic behaviour with cyclic loading and corresponding degradation, and in taking into account high soil damping. Therefore appropriate methods should be chosen according to the needs of the project.

One of the main parameters influencing the response is “energy dissipation” of the soil-structure system. Energy dissipation is comprised of radiation damping, material damping in the soil, and material damping in the structure. The relative importance of the three elements of energy dissipation is a function of the frequency content of the excitation, the soil material properties, the characteristics of the foundation, and the stress level in the structure. For the K-K reactor building, it is expected that radiation damping was an important contributor with structure damping next in importance. As a consequence, the way how the equivalent damping (Rayleigh damping) was effectively determined, plays a very important role in the analysis. This point may be the most significant source of discrepancies. When radiation damping is significant, material damping in the soil or structure is of much less importance. If nonlinear structure behaviour is sought and SSI is important, then more sophisticated nonlinear analyses may need to be performed and/or hybrid methods, where SSI response of the soil-structure system is calculated for linear structure behaviour – the output being foundation response, and then that foundation response, including rotations are input to the nonlinear analyses of the structure.

For the reactor building, there are no obvious differences in results from the different simulation methodologies used by participants. Clearly, stick models are not able to represent local effects, such as roof bending. The exercise shows that 3D finite element model constitute a pertinent state of the art approach. The main differences come from soil modelling. The choice of the methodology to be used should depend on the purpose of the analysis.

One important point is the robust seismic design of the reactor building: regular, compact, without significant mass and stiffness eccentricities, presence of thick reinforced shear walls and RCCV. This may explain the limited variability of fixed-base frequencies obtained by participants and, in addition, this is also a reason for the large structural margins obtained by the analyses, approximately four times NCOE level.

For piping analyses, additional studies should be performed for the following topics:

- Investigate friction versus damping in dynamic analysis;
- Develop more precise procedures for multi-support input motions time history analysis;
- Extend the dynamic analysis to nonlinear material behavior;
- Develop criteria for allowable strain in the case of material nonlinearities;
- Investigate credible piping failure modes that should be considered for margin assessment.

For spent fuel pool sloshing, techniques for assessment of spilled water due to sloshing should be developed since it could be required for beyond design basis earthquake evaluations. Scaled experiments may be valuable for a better understanding of sloshing effects.

For tank buckling analysis, failure of a single anchor bolt could not be considered as a global failure mechanism. But it should be understood that loss of several anchor bolts could lead to the partial uplift with consequent local deformation. In this case appropriate criteria for strain should be considered. Additional research is needed for a better calibration of nonlinear approaches with available formulations from Codes and Standards.

APPENDIX

SUMMARY OF PARTICIPANTS' MODELLING ASSUMPTIONS

TABLE 54. MODELLING ASSUMPTIONS: LOCATIONS OF CONTROL POINTS

PART 1. STRUCTURE: TASK 1.3- Margin Assessment : Modeling Assumption	
No	Participant Organization
1	SNERDI-SNPTC, China
2	CEA&IRSN, France
3	EdF, France
4	AREVA, Germany
5	VGB, Germany
6	SPI, Germany
7	AERB, India
8	ITER, Italy
9	KINS, Korea
10	NRC, USA

Control point in team's analysis

The control point in the analysis is supposed to be on the free surface of the soil.

The structure is not considered as embedded. Thus, the seismic inputs are defined at the raft elevation level. The accelerograms are from the guidance document.

Outcropping Raft Elevation at TMSL -13.7 m

Basemat level

Base of the structure

In the soil column analysis, the control points for input ground motions are located at the elevation of T.M.S.L -155m.

In the structural analyses for the fixed base and SSI models, the control points are located at the elevation of T.M.S.L -13.7m (The soil deposit above T.M.S.L -13.7m were neglected.)

For all analyses, the control point was defined at elevation -13.7m and the motion was in-column motion.

TABLE 55. MODELLING ASSUMPTIONS: MODELLING OF SSI AND NON-LINEAR BEHAVIOUR OF SOIL

PART 1. STRUCTURE: TASK 1.3- Margin Assessment : Model Presentation	
No	Participant Organization
	Modeling of SSI and non-linear behaviour of soil
1	SNERDI-SNPTC, China
	Soil springs are added to consider the soil effect to the whole soil-structure system in static pushover analysis . Nonlinear soil springs are used. This kind of spring elements have the capability of turning on and off during an analysis. When force in the spring become positive (tension), the spring will be "off". The stiffness of soil springs are calculated with Table 3.3-3 and Figure 3.3-3 of ASCE 4-98, 1998.
2	CEA&IRSN, France
	Direct time domain finite elements method: - 3D finite elements modelling for the structure and the near-field soil, - Full contact between soil and outer walls, - Viscous absorbing boundary to represent the far-field soil (lateral sides and bottom). Soil nonlinearity is taken into account by the linear equivalent method - Reference soil models for 1*NCOE, 2*NCOE, 4*NCOE, 6*NCOE given by the consultant are used.
3	EdF, France
	Soil is not meshed. Only interface between the not embedded structure and soil layers is represented to compute impedance functions. Structure is not embedded and there are not contact between ground and lateral walls. We performed our SSI calculations using Ground Springs methods. The raft elevation is considered for the input spectra. Non linearities are represented by linear-equivalent method using stratigraphy defined in the guidance document. Young Modulus and damping are determined as a function of computed strains into the soil (except for the push-over analysis).
4	AREVA, Germany
	The present soil structure interaction analysis assumes a surface founded reactor building at elevation T.M.S.L. -13.70m. Impedance functions are calculated with strain-compatible soil profile in frequency domain in order to account for frequency dependency of the radiation damping. Based on these impedance functions 6 global springs and dampers representing the 6 DOF of the rigid foundation are evaluated for modal analysis. The global springs are distributed under foundation mat and Rayleigh damping values are tuned to the main frequencies of the coupled soil-structure system. The nonlinear dynamic analysis of the coupled soil-structure system is performed in the time domain. The provided reference signals in all three directions at outcropping "raft elevation" (TMSL-13.7m) are applied as control motion to the SSI model. The signals for key locations within the building structure are calculated as time histories.
5	VGB, Germany
	Soil is modeled by distributed (discrete) springs and dampers; only linear soil behaviour assumed -> linear springs (corresponding to 1xNCOE-impedances)
6	SPI, Germany
	The soil is modelled by soil springs, which have been adopted from phase II of the study and from studies of our partner Basler & Hofmann, distinguished between excitation levels 1*NCOE up to 4*NCOE (same springs for these 3 excitation levels), and 6*NCOE (reduced springs due to higher soil strains).

7	AERB, India	<p>Grade level of structure is at TMSL+12.0 below which effect of soil is considered. Though soil is not explicitly modelled but is effect on the behavior of structure is modelled by providing frequency independent spring elements at nodes below the grade level. Stiffness of the soil spring is taken from the stick model of the R/B structure as given in Guidance document (Appendix B) and is appropriately distributed to the nodes. Axial stiffness is divided equally to all nodes at a floor level to an effective area equal to half the storey height above and below of the floor level. Two separate models are developed for nonlinear static and dynamic analysis. For pushover analysis raft is modelled with 8-noded solid elements, so to apply the rotational soil springs to the solid elements, constraint equations are used to couple the effective rotation of the raft to the rotational spring. As these constraint equations caused convergence problem in nonlinear dynamic analysis, for dynamic analysis raft is modelled with shell elements and rotational d.o.f are directly coupled to soil springs. All the springs are provided with linear behavior.</p> <p>The SSI analysis has been developed using a 3D time domain model of a soil island including the reactor building.</p> <p>The model size is 300x300 m in plan (about five times the size of the reactor building) and 167 m in depth, down to the assumed bedrock in the soil response analysis.</p> <p>The soil island model is strictly linear. It has the main purpose of propagating the motion to the building foundation taking into account both kinematic and inertial interaction.</p> <p>The first step of the analysis is the development and the calibration of a 3D model that yields approximately the same free field response of the ID frequency domain analysis developed for the benchmark with an equivalent linear approach (SHAKE or EERA).</p> <p>The size of the finite elements has been chosen having in mind the objective to keep the computational burden within a reasonable limit and to describe adequately the spectral content of the motion at the building foundation at the expected frequencies of the nonlinear stick models with base springs (about 1Hz).</p>
8	ITER, Italy	<ol style="list-style-type: none"> 1. The soil layer at T.M.S.L -13.7 m has been assumed as ground surface, and soil layers between T.M.S.L 12.3 m and -13.7 m have been neglected in the analysis. 2. The earthquake signal measured at outcrop of engineering bedrock (T.M.S.L -155m) has been used as the input ground motion for the all simulations in Subtask 1.3.1.B and 1.3.2.B. 3. The transfer function at the request points with respect to the control point located at the elevation T.M.S.L -155 m have been computed. 4. Modified nonlinear curves of sand and clay (Table G.3 and Figure G.7) as the soil property has been adopted for Subtask 1.3.1.B and 1.3.2.B. 5. Soil response analysis of Unit 7 soil column of Table G.4 as the standard soil characteristics have been used for Subtask 1.3.1.B and 1.3.2.B. 6. The soil has been represented by the spring and dashpot elements representing the soil medium for the SSI analysis. For doing this, the stiffness and dashpot (soil impedance obtained by ACS SASSI analysis) corresponding to the dominant frequency of the soil-structure model were selected as the spring and dashpot constants. <p>Structure and soil were treated as equivalent linear.</p>
10	NRC, USA	

TABLE 56. MODELLING ASSUMPTIONS: GLOBAL IMPEDANCE DISCRETIZATION/DISTRIBUTION AND CONSIDERATION OF EMBEDMENT

PART 1. STRUCTURE: TASK 1.3- Margin Assessment : Modeling Assumption	
No	Participant Organization
1	SNERDI-SNPTC, China
2	CEA&IRSN, France
3	EdF, France
4	AREVA, Germany
5	VGB, Germany
6	SPI, Germany
7	AERB, India
8	ITER, Italy
9	KINS, Korea
10	NRC, USA

How soil impedance distributed in the model

Time domain integration is performed directly on the coupled soil-structure system. There is no need to compute the soil impedance in this method.

Impedance functions were computed by ProMISS3D. Then soil springs are chosen by using iterative modal analysis :

- For each direction, the global stiffness of springs is the impedance value at the frequency of main ISS eigen modes in the same direction.
- Then, the global stiffness is distributed at each node under the basemat (translation stiffness and rotating stiffness are modeled)
- A new modal analysis is done with the new soil springs and
- the same process is done until the ISS eigen modes convergence.

Impedance functions are calculated with strain-compatible soil profile in frequency domain in order to account for frequency dependency of the radiation damping. Based on these impedance functions 6 global springs and dampers representing the 6 DOF of the rigid foundation are evaluated for modal analysis. The global springs are distributed under foundation mat and Rayleigh damping values are tuned to the main frequencies of the coupled soil-structure system.

Distributed springs based on impedance functions, springs distributed on all faces embedded in the soil

Soil impedances were distributed over all basemat nodal points

Damping is specified by introducing damping factors to soil springs values of which are taken from the stick model of the R/B structure as given in Guidance document (Appendix B) and is appropriately distributed to the nodes. Damping factors for soil springs is divided equally to all nodes at a floor level to an effective area equal to half the storey height above and below of the floor level.

A direct time integratin scheme has been used in the analysis, using a F.E. model that takes into account the surrounding soil as previously described. In this model, the building structure has been modeled using equivalent SDF in x and y direction, to simulate first and second vibration modes.

The translational spring and dashpot elements were distributed to all of the interaction nodes between basemat and soil deposit (169 nodes) and the rotational spring and dashpot elements were attached at the only center node.

The spring and dashpot constants were obtained from the impedance analysis by ACS-SASSI.

Frequency-dependent, complex-valued impedances and scattering functions were used.

Fully three-dimensional representation. Impedances and scattering functions generated about the foundation reference point at the center of the interface between the bottom of the foundation and the soil.

TABLE 57. MODELLING ASSUMPTIONS: DAMPING MODELLING FOR SOIL AND SSI MODEL (EQUIVALENT DAMPING / RAYLEIGH DAMPING)

PART 1. STRUCTURE: TASK 1.3- Margin Assessment : Modeling Assumption	
No	Participant Organization
1	SNERDI-SNPTC, China
2	CEA & IRSN, France
3	EdF, France
4	AREVA, Germany
5	VGB, Germany
6	SPI, Germany
7	AERB, India
8	ITER, Italy
9	KINS, Korea
10	NRC, USA

SSI Equivalent damping or Rayleigh dampings

Rayleigh damping for soil elements.

Provided in "Non-linear dynamic analysis assumptions" (Table 5.9).

No SSI equivalent damping

For soil springs equivalent damping derived from the imaginary parts of the impedance functions at the fundamental modes were introduced in terms of Rayleigh parameters β .

Based on damping factor specified for soil springs in guidance document

The soil properties used in the time domain model are those obtained by iteration in the 1D equivalent linear model. The damping model is different, because in the time domain analysis Rayleigh damping has to be used, while constant hysteretic damping is used in the equivalent linear model. The damping matrix C is assumed to be proportional to mass matrix M and stiffness matrix K according to the equation $C = \alpha M + \beta K$

The Rayleigh damping coefficients have been evaluated to match the iterated damping values in the frequency range of interest.

In structural analysis for the SSI model, the translational and rotational soil dashpot constants determined from soil impedance analysis were applied to the interaction nodes between basemat and soil deposit in the K-K NPP model.

Energy dissipation of soil/structure explicitly included in the impedance functions for the SSI phenomena and in the structure model (represented by fixed-base modes and modal damping).

TABLE 58. MODELLING ASSUMPTIONS: CONSIDERATION OF EMBEDMENT

PART 1. STRUCTURE: TASK 1.3- Margin Assessment : Modeling Assumption		
No	Participant Organization	How embedment effect taken into account.
1	SNERDI-SNPTC, China	
2	CEA&IRSN, France	Reactor building embedment is taken into account by the realistic finite element modelling of the near field soil and the structure.
3	EdF, France	The embedment effect is taken into account by considering the deconvoluted signal at the raft of the structure. There are non contact modeled between the soil and the lateral walls in contact with the soil.
4	AREVA, Germany	The soil structure interaction analysis assumes a surface founded reactor building at elevation T.M.S.L. -13.70. Hence, embedment effect is neglected.
5	VGB, Germany	Full embedment taken into account.
6	SPI, Germany	Influence of embedment is included in the soil impedances.
7	AERB, India	Embedment effect is taken into account by providing lateral and rotational soil springs in both the direction upto the grade level (TMSL 12.0). The soil spring values are taken from stick model of R/B structure as given in guidance document.
8	ITER, Italy	The embedded effect have been directly taken into account. At the soil-structure interface non linear spring and gaps element have been used.
9	KINS, Korea	In this analysis, the soil embedment effect was not considered.
10	NRC, USA	Through impedances and scattering functions.

TABLE 59. MODELLING ASSUMPTIONS: DAMPING MODELLING FOR STRUCTURAL ELEMENTS

PART 1. STRUCTURE: TASK 1.3- Margin Assessment : Modeling Assumption	
No	Participant Organization
1	SNERDI-SNPTC, China
2	CEA&IRSN, France
3	EdF, France
4	AREVA, Germany
5	VGB, Germany
6	SPI, Germany
7	AERB, India
8	ITER, Italy
9	KINS, Korea
10	NRC, USA

Damping modeling for structural elements	
1	Rayleigh damping for structural elements.
2	For fixed base-model: Rayleigh damping is used. 2% is chosen for non linear elements. The alpha and Beta parameters are determined for 2% of damping and a frequency range of 1-10 Hz (non linear elements); 5% is chosen for linear element in the freq range of 5-15 Hz
3	For soil structure model : We use modal damping consistent with RCC-G. The principle of computation is based on weighting by rates of potential energy (compared to total energy) of the reduced damping affected by constitutive mesh groups and of the radiative damping in the ground, by degree of freedom, functions of the frequency. 2% is chosen for non linear structural elements and 5% for others elements.
4	Nonlinear Static Analysis: No damping to the structural elements is assigned due to the static approach. Nonlinear Dynamic Analysis: Provided in "Non-linear dynamic analysis assumptions" (Table 5.9).
5	Rayleigh-damping 5% (a = 1.204, b = 0.002)
6	The damping was introduced by Rayleigh parameters α and β adjusted to 2 % damping for fundamental frequencies and 5 % damping for 20 Hz for non-linear elements and 5 % damping for all frequencies for linear elements.
7	Material Damping for concrete = 2% , Steel = 2% in the nonlinear analysis furthermore hysteretic damping is expected to occur due to nonlinear material behavior
8	The damping matrix C is assumed to be proportional to mass matrix M and stiffness matrix K according to the equation $C = \alpha M + \beta K$
9	Rayleigh damping corresponding to 5% modal damping was applied to the structural elements.
10	Modal damping.

TABLE 60. MODELLING ASSUMPTION: MODELLING OF THE STRUCTURAL ELEMENTS (LINEAR / NONLINEAR)

Modelling of the Structural elements in linear or nonlinear?	SNERDI-SNPTC	CEA&IRSN	EdF	AREVA	VGB	SPI	AERB	ITER	KINS	NRC
Main walls		Non linear	Non linear	Non linear	Non linear	Non linear	Non linear	Non linear	Non linear	Equivalent linear
RCCV wall		Non linear	Non linear	Non linear	Non linear	Non linear	Non linear	Non linear	Non linear	Equivalent linear
Columns		Linear	Linear	Linear with 50 % Reduction of Stiffness	Linear	Linear	Linear	Non linear	Non linear	Equivalent linear
Beams		Linear	Linear	Linear with 50 % Reduction of Stiffness	Linear	Linear	Linear	Linear	Non linear	Equivalent linear
Floors		Linear	Non linear	Non linear	linear; thick floors: non linear	Linear	Non linear for dynamic analysis, Linear for static pushover analysis	Linear	Non linear	Equivalent linear
Auxiliary walls		Not considered in the model	Non linear	Non linear	Not considered in the model	predominantly non linear		Non linear	Non linear	Equivalent linear

TABLE 61. MODELLING ASSUMPTIONS: NON-LINEAR BEHAVIOUR OF STRUCTURE E.G. MATERIAL AND ELEMENTS CONSTITUTIVE LAWS

PART 1. STRUCTURE: TASK 1.3- Margin Assessment : Modeling Assumption	
No	Participant Organization
	Modeling assumptions for non-linear behaviour of structure e.g. material and elements constitutive laws
1	<p>Concrete material is assumed as ideal elastic-plastic and simulated with bilinear curve as shown in the picture below. 33MPa is used as the concrete compressive strength.</p> <p>Reinforce concrete wall and slab are simulated by layered shell element. This shell element has three layers, two outside layers are for reinforcement, and the middle layer is for concrete. Multilinear curve is used as the elastic and plastic modulus property of reinforcement.</p> <p>Multilinear curve as shown in the picture is for the elastic and plastic modulus of steel.</p> <p>Non linear behaviours are assumed for the main shear walls and the RCCV.</p> <p>Multilayer shell elements are used :</p> <ul style="list-style-type: none"> - Reinforcement bars (2x2 embedded layers) : unidirectional material with perfect elas-to-plastic law, - Concrete (5 layers) : smeared crack (Ottosen) model under tension forces, assumed elastic under compression forces. <p>The rest of the structure is assumed to be elastic.</p>
2	CEA&IRSN, France
3	<p>Only main shear walls and main floors have been modeled through nonlinear model. Constitutive laws of shell elements are modeled by homogenized reinforced concrete law (GLRC_DM). The other elements of the structures remain linear elastic.</p> <p>GLRC_DM (Generalized Law for Reinforced Concrete) implanted in Code_Aster. This constitutive law is modeling the damage under membrane stress and bending stress using « homogenized » parameters. It belongs to the models known as “total” used for thin structures (beams, plates and shells). In addition, plasticity phenomena in steel bars has been taken into account for the main shear walls and main floors.</p>
4	AREVA, Germany
	According to Chapter "2.7 Proposed Normalized Parameters" of the Guidance Document.
5	<p>Material laws for concrete and reinforcing steel according to DIN 1045/Eurocode (German Standard);</p> <p>reinforcing steel:</p> <p>$f_y = 350 \text{ MPa}$, $e_y = 0,17\%$</p> <p>$f_t = 550 \text{ MPa}$, $e_{max} = 5,00 \%$</p> <p>concrete:</p> <p>$f_c = 48 \text{ MPa}$, $e_{min} = -0,40\%$</p> <p>$f_t = 3,5 \text{ MPa}$, $e_{max} = 0,02\%$</p>
6	<p>The following members of the building have been introduced as non-linear element groups: main shear walls, pool walls, RCCV, auxiliary shear walls. All other members (floors, basemat slab of RCCV, beams and columns, steel structures) have been introduced with linear-elastic material behaviour.</p> <p>The non-linear behaviour is restricted to reinforced concrete shell elements. The non-linear behaviour of r/c shell elements is treated by a layered shell model including the arrangement of reinforcement layers. The model includes consideration of tension softening of concrete dependent of fracture energy, tension stiffening of reinforcement in the cracked condition, trilinear stress-strain laws for reinforcing steel including kinematic hardening. The material constitutive laws for concrete and reinforcing steel are plotted in the results templates.</p>
	SPI, Germany

7	AERB, India	<p>Concrete: Stress-strain curve of concrete under compression is taken as given in guidance document, the maximum compressive strength being 40 Mpa & compressive strain at failure being 0.0035. Tension stiffening model based on fracture energy concept as per JSCE guidelines for concrete (No. 15 – Standard Specifications for Concrete Structures-2007) is used, in this model tension stiffening is introduced by providing crack width (depends on fracture energy) as a function of tensile strength of concrete. Behavior of concrete under multiaxial state of stress is modeled by defining yield surface, non associative flow rule, and failure surface in 3-dimensional stress space. The failure surface used in the analysis is a bulged triangular shape on deviatoric plane and has pressure dependence. Definition of failure surface in 3-dimensional stress space in the software used for analysis needs definition of some key input parameters (apart from stress-strain curve) which are not available. Optimum value of these parameters are arrived for the present case through numerical modelling and parametric studies on experimentally tested shear wall specimens. Degradation and recovery of stiffness during load reversal is modelled by specifying different damage parameters under tension and compression and stiffness recovery factors. Steel: For reinforcing steel, elastic-strain hardening plastic bilinear stress-strain curve as given in guidance document is considered, yield strength being 345 Mpa & ultimate tensile strength being 450 Mpa, and ultimate strain equal to 5% is taken. Structural steel is assumed to be elastic.</p>
8	ITER, Italy	<p>Reinforced concrete walls modeled using 3-4 elements through the thickness and 3 elements along the height. Reinforced concrete column have 4 elements in the cross sections and 3 elements along the height. Also the vessel has been modeled in a simplified way, using 3D solid elements for the steel structure and 3D trusses to connect it to the surrounding reinforced concrete walls. Roof structure has been modeled using steel 3D truss elements and solid elements to represent the concrete slab. Additional masses have been included by means of ID MASS elements. In some cases, 2D QUAD elements, with no stiffness but only mass, have been used to take into account live and equipments loads. Auxiliary walls are not included in the model. About boundary conditions of the fixed base model, fixed nodes have been assumed at the bottom of the basement. Rebars have been modeled using a superimposed finite element mesh, having values for the stiffness odulus proportiona to the percentage of the present steel rebars.</p>
9	KINS, Korea	<p>Nonlinear Material Model for Uncracked Concrete : Elasto-plastic and fracture model (Maekawa and Okamura) Nonlinear Material Model for Cracked Concrete : Tension Stiffness model + Compressive Stiffness model + Shear Transfer Model Nonlinear Material Model for Steel : Bilinear model considering bond characteristics in concrete Modeling the post-yield behavior of reinforcing bars in concrete.</p>
10	NRC, USA	<p>Only soil-structure interaction (SSI) analyses were performed for NCOE*1, NCOE*2, NCOE*4, and NCOE*6 cases. Structure and soil were treated as equivalent linear.</p>

TABLE 62. NON-LINEAR DYNAMIC ANALYSIS ASSUMPTIONS

PART 1. STRUCTURE: TASK 1.3- Margin Assessment : Modeling Assumption	
No	Participant Organization
1	SNERDI-SNPTC, China
2	CEA&IRSN, France
3	EdF, France
4	AREVA, Germany

PART 1. STRUCTURE: TASK 1.3- Margin Assessment : Modeling Assumption		
No	Participant Organization	Non-linear dynamic analysis assumptions
1	SNERDI-SNPTC, China	Time domain resolution is performed using Newmark's integration algorithm with time step of 0.005 second.
2	CEA&IRSN, France	For fixed base-model: Rayleigh damping is used. 2% is chosen for non linear elements in the frequency range of 1-10 Hz; 5% is chosen for linear element in the freq range of 5-15 Hz For soil structure model : Damping choice is consistent with RCC-Grules by using modal damping. This method implicitly takes into account the damping into the soil. 2% is chosen for non linear structural elements and 5% for others elements.
3	EdF, France	• Four calculations with a single fixed base FE structural model are performed for the 4 seismic excitation levels - 1.0*NCOE, 2.0*NCOE, 4.0*NCOE and 6.0*NCOE. • Four calculations with 4 different soil-structure FE models are performed for the 4 seismic excitation levels. The soil stiffness and damping of the models is compatible to the corresponding strain level induced in the soil by the 4 seismic excitation levels - 1.0*NCOE, 2.0*NCOE, 4.0*NCOE and 6.0*NCOE. Rayleigh damping for fixed base model analyses: - Structure: D = 2% for non-linear elements at frequencies 4.7Hz and 35.0Hz and D = 4% for linear elements at frequencies 7.4Hz and 25Hz; Rayleigh damping for soil-structure model analyses: - Structure (all 4 models): D = 1% for non-linear elements at frequencies 0Hz and 5.8Hz (only stiffness-proportional) and D = 4% for linear elements at frequencies 0Hz and 12Hz (only stiffness-proportional) - Soil: > 1.0*NCOE: • horizontal: D = 16.2% at frequencies 0.6Hz and 4.6 Hz • vertical: D = 35.0% at frequencies 0Hz and 3.9 Hz > 2.0*NCOE: • horizontal: D = 17.7% at frequencies 0.3Hz and 4.5 Hz • vertical: D = 36.0% at frequencies 0Hz and 3.9 Hz > 4.0*NCOE: • horizontal: D = 20.7% at frequencies 0.3Hz and 4.3 Hz • vertical: D = 40.0% at frequencies 0Hz and 3.6 Hz > 6.0*NCOE: • horizontal: D = 19.1% at frequencies 0Hz and 3.1 Hz • vertical: D = 46.0% at frequencies 0Hz and 3.0 Hz
4	AREVA, Germany	

5	VGB, Germany	Rayleigh-damping 5% ($a = 1.204$, $b = 0.002$)
6	SPL, Germany	The non-linear dynamic analysis was performed by an implicit step-by-step integration using a modified Newmark method.
7	AERB, India	Raft is modelled as shell elements with an offset of half of raft thickness and is connected to the wall edges using rigid link. Stick model of RPV is connected to the 3D model of reactor building using beam elements, spring elements and dashpots with properties as specified in guidance document (Annexure F). All live loads (piping, crane, etc.) are lumped at corresponding nodes within specified area as inertial masses.
8	ITER, Italy	To perform the non linear dynamic analyses, a simplified finite element model has been constructed. The superstructure has been modeled using an Equivalent Single Degree Of Freedom Oscillator, corresponding to the first and the second vibration mode of the structure. The soil structure interaction has been modeled representing a significant part of the soil underneath the basemat. At soil-structure interface snon linear spring and gaps elements have been used to take into account uplift of the foundation and non linear response of the lateral soil.
9	KINS, Korea	Non-linear dynamic analysis was performed by the HHT- α method which had been developed based on the Newmark method, i.e an implicit step-by-step integration method.
10	NRC, USA	Not performed.

TABLE 63. PUSHOVER ANALYSIS ASSUMPTIONS

PART 1. STRUCTURE: TASK 1.3- Margin Assessment : Modeling Assumption	
No	Participant Organization
	Pushover analysis assumptions
1	SNERDI-SNPTC, China
2	CEA&IRSN, France
3	EdF, France
4	AREVA, Germany
5	VGB, Germany
6	SPI, Germany
7	AERB, India
8	ITER, Italy
9	KINS, Korea
10	NRC, USA

Only material nonlinear is considered. Geometry nonlinear is ignored.

Pushover analysis not performed.

One set of ground springs is used. It assumes linear characteristics of the ground.

Horizontal uniform load is applied to all the structure taking into account the dead load.

The generated load function based on first mode distribution is applied and increased until the ultimate load or a sufficient large displacement has been reached. The resulting "Push-Over" curve is representing the total base shear force as a function of the displacement at a given point CP2 at +23.5m.

Uniform horizontal loading as is specified in Guidance Document;

Additional: weighted loading according to fundamental eigenmode;

The pushover analysis was performed under the above described assumptions concerning the nonlinear elements. The horizontal loads were applied uniformly along the height of the structure.

Lateral load applied at each floor proportional to the floor masses. Floors are assumed to behave elastically for pushover analysis. RPV is not modelled for pushover analysis.

The pushover analyses have been conducted using two different horizontal load distribution. In the first approximated analyses an horizontal uniform load distribution has been assumed according to the questions of IAEA secretariat. To evaluate the equivalent non linear model, used to perform the dynamic non linear analyses, the pushover curves of global finite element model have been evaluated applying the first and the second eigenvectors, in direction X and Y respectively.

Pushover analysis for each X and Y direction

Uniform distribution of horizontal force (not, acceleration)

Against main columns (R1~R7, RA~RG) from T.M.S.L. -8.2m (3rd Basement) to +31.7m (4th Floor)

Not performed.

TABLE 64. ASSUMPTION FOR DETERMINATION OF PERFORMANCE POINT: NON-LINEAR SPECTRA

PART 1. STRUCTURE: TASK 1.3- Margin Assessment : Modeling Assumption	
No	Participant Organization
1	SNERDI-SNPTC, China
2	CEA&IRSN, France
3	EdF, France
4	AREVA, Germany
5	VGB, Germany
6	SPI, Germany
7	AERB, India
8	ITER, Italy
9	KINS, Korea
10	NRC, USA

PART 1. STRUCTURE: TASK 1.3- Margin Assessment : Modeling Assumption		
No	Participant Organization	Assumption for construction of performance point: non-linear spectra
1	SNERDI-SNPTC, China	
2	CEA&IRSN, France	Pushover analysis not performed
3	EdF, France	The capacity curve is consistent with the method described in the reference (BETBEDER-MA TIBET J., "Prévention parasismique", Hermès Science publications, Paris, 2003) The input acceleration-frequency spectra (INCOE to 6NCOE) are converted successively into acceleration-displacement curves and force-displacement curves (by multiplying the acceleration by the structure weight - curve A). The displacement of CP2 point is computed as function of increasing uniform load (curve B). The intersection between the curves A and B is the performance point.
4	AREVA, Germany	The performance point is constructed with the help of the software SOFISTIK 25. The procedure used for determination of performance point is based on Capacity Spectrum Method's Procedure A from ATC-40. For linear demand spectrum the smoothing is performed conservatively, i.e. the outer smoothed spectra of the appropriate given response spectra are used. For this procedure, the demand spectra are together with the obtained "Push-Over" curve converted into ADRS format.
5	VGB, Germany	Development of the demand spectrum by reducing the NCOE-5%-response spectra. Therefore, estimation of the corresponding hysteretic damping represented as equivalent viscous damping (acc.to ATC40/Chopra; assuming a structural behaviour type B) and with it derivation of reduction factors for NCOE-response spectra. The Performance Point is determined as the intersection point of the reduced demand spectrum and the bilinear representation of the capacity spectrum (= Pushover-Curve in ADRS-format).
6	SPI, Germany	The capacity curves were derived from the Pushover curves by transforming in ADRS format based on an equivalent one-degree-of-freedom system. The elastic earthquake input response spectra are converted in ADRS format, too. The performance points are constructed based on nonlinear ADRS earthquake response spectra with different ductility factors according to the method described by Chopra and Goel (1999)
7	AERB, India	Performance point of the structure is taken as the maximum displacement at the specified point obtained from nonlinear dynamic analysis of structure for corresponding time histories.
8	ITER, Italy	The performance points can be defined as the equilibrium point between the capacity of the structure and the earthquake. In the first part of the analysis the performance points have been identified according to the approximated procedure described in ATC 40. With the non linear dynamic analysis, however, performance points have been directly and more precisely evaluated. Using the displacements of the control point in correspondence of the performance point, it has been possible to identify the damage distribution in the structure using the results of the pushover analysis.
9	KINS, Korea	In order to determine the inelastic acceleration-displacement response spectra (ADRS), we considered the ductility reduction factor(Ru). The ductility reduction factor(Ru), inelastic spectral acceleration(Sa), and inelastic spectral displacement(Sd) are calculated from below equations. (Sae and Sde are elastic spectral acceleration and elastic spectral displacements, respectively) [Chopra and Goel, Earthquake Spectra, 15(4), 1999]
10	NRC, USA	Not performed.

TABLE 65. PERFORMANCE CRITERIA FOR STRUCTURAL ELEMENTS AND OVERALL STRUCTURE (E.G. CONCRETE COMPRESSIVE STRESS, REBAR TENSILE STRESS, CRACK WIDTH, STORY DRIFT ETC.)

PART 1. STRUCTURE: TASK 1.3- Margin Assessment : Model Presentation	
No	Participant Organization
1	SNERDI-SNPTC, China
2	CEA&IRSN, France
3	EdF, France
4	AREVA, Germany
5	VGB, Germany
6	SPI, Germany
7	AERB, India
8	ITER, Italy
9	KINS, Korea
10	NRC, USA
Performance criteria for structural elements (story drift, concrete compressive stress, crack width etc.)	
1	Story drift
2	Story drift, concrete compressive stress, rebar tensile stress and crack width
3	Concrete compression strain $>0.4\%$
4	For structural elements the performance criteria are the concrete compression stresses (limit value -3.5%).
5	Cracking of concrete is directly modeled by ADINA code, with sufficient modelization of the actual behaviour of the material. After a crack, normal stress is released, in proportion of the strain in the normal direction with respect to the crack plane. Until 3 cracks for each integration point is allowed by the Code
6	Story Drift (ASCE 43-05 : Table 5-2. Allowable Drift Limits as a Function of Limit State and Structural Systems)
7	- For the RC shear controlled walls, the allowable drift limits with limit states are as follows. -- LS-A (Significant damage) : 0.0075 -- LS-B (Generally repairable damage) : 0.006 -- LS-C (Minimal damage) : 0.004 -- LS-D (No damage) : 0.004
8	Not performed.
Performance criteria for overall structure (story drift, concrete compressive stress, crack width etc.)	
1	Story drift
2	Story drift, concrete compressive stress, rebar tensile stress and crack width
3	Overall collapse when exceedances of concrete compression strain in a wide area (or in sensible areas e.g. close to RCCV)
4	For the overall structure the performance criteria are defined by the story drift between TMSL +23.5 m and TMSL -8.2 m. The limit states of story drifts are taken to 0.006 according to ASCE-SEI 43-05 (LS-B for shear controlled reinforced concrete walls)
5	No performance criteria for overall structure have been adopted. The capacity of the structure has been evaluated looking at the global behaviour as described in the following point.
6	Not performed.

REFERENCES

- [1] <http://earthquake.usgs.gov/earthquakes/eqinthenews/2007/us2007ewac/#summary>, viewed on January 2013.
- [2] NUREG/CR-6241, BNL-NUREG-52422, Technical Guidelines for Aseismic Design of Nuclear Power Plants, Translation of JEAG 4601 (1987).
- [3] INTERNATIONAL ATOMIC ENERGY AGENCY, Preliminary Findings and Lessons Learned from the 16 July 2007 Earthquake at Kashiwazaki Kariwa NPP, Kashiwazaki Kariwa NPP and Tokyo, Mission Report Volume I, Vienna (2007).
- [4] INTERNATIONAL ATOMIC ENERGY AGENCY, General specification for the KARISMA Benchmark, Vienna (2009), (Document is available in attached CD).
- [5] INTERNATIONAL ATOMIC ENERGY AGENCY, KARISMA Benchmark Guidance Document Part 1: K-K Unit 7 R/B Structure – Phase I, II and III, Vienna (2012), (Document is available in attached CD).
- [6] INTERNATIONAL ATOMIC ENERGY AGENCY, KARISMA Benchmark Guidance Document Part 2 Task 2.1: K-K Unit 7 RHR Piping System – Phase I, II and III, Vienna (2011), (Document is available in attached CD).
- [7] INTERNATIONAL ATOMIC ENERGY AGENCY, KARISMA Benchmark Guidance Document Part 2 Task 2.2: K-K Unit 7 Sloshing of Spent Fuel Pool – Phase I and II, Vienna (2010), (Document is available in attached CD).
- [8] INTERNATIONAL ATOMIC ENERGY AGENCY, KARISMA Benchmark Guidance Document Part 2 Task 2.3: K-K Unit 7 Pure Water Tank Analyses – Phase I and II, Vienna (2009), (Document is available in attached CD).
- [9] INTERNATIONAL ATOMIC ENERGY AGENCY, Evaluation of Seismic Safety for Existing Nuclear Installations, IAEA Safety Standards Series No. NS-G-2.13, IAEA, Vienna (2009).
- [10] INTERNATIONAL ATOMIC ENERGY AGENCY, Seismic Design and Qualification for Nuclear Power Plants, IAEA Safety Standards Series No. NS-G-1.6, IAEA, Vienna (2003).
- [11] INTERNATIONAL ATOMIC ENERGY AGENCY, KARISMA Benchmark Minutes of 1st Review Meeting, Vienna (2010), (Document is available in attached CD).
- [12] INTERNATIONAL ATOMIC ENERGY AGENCY, KARISMA Benchmark Minutes of 2nd RM Meeting, Vienna (2011), (Document is available in attached CD).
- [13] INTERNATIONAL ATOMIC ENERGY AGENCY, KARISMA Benchmark Minutes of 3rd RM Meeting, Vienna (2011), (Document is available in attached CD).
- [14] INTERNATIONAL ATOMIC ENERGY AGENCY, KARISMA Benchmark Minutes of 1st OC Meeting, Vienna (2009), (Document is available in attached CD).
- [15] INTERNATIONAL ATOMIC ENERGY AGENCY, Non-linear response to a type of seismic input motion, TECDOC 1655, Vienna (2011).

ABBREVIATIONS

ABWR	Advanced boiling water reactor
BWR	Boiling water reactor
CQC	Complete quadratic combination
COV	Coefficient of variation
DBEGM	Design base earthquake ground motion
DEPSS	Drywell equipment and pipe support structure
EBP	Extrabudgetary programme
E-W dir.	East-West direction
FRS	Floor response spectra
ISSC	International Seismic Safety Centre
JMA	Japan Meteorological Agency
JNES	Japan Nuclear Energy Safety Organization
KARISMA	Kashiwazaki-Kariwa Research Initiative for Seismic Margin Assessment
K-K NPP	Kashiwazaki- Kariwa Nuclear Power Plant
NCOE	Niigataken-chuetsu-oki earthquake
NCO	Niigataken-chuetsu-oki
NPP	Nuclear power plant
N-S dir.	North-South direction
OC	Organizing committee
OEB	Outcrop of the Engineering Bedrock elevation
ORE	Outcrop of the Raft Elevation
PN	Plant North
RC	Reinforced concrete
RCCV	Reinforced concrete containment vessel
RHR	Residual heat removal
RM	Review meeting
RPV	Reactor pressure vessel
RSW	Reactor shield wall
SSCs	Structures, systems and components
SSI	Soil structure interaction
SRSS	Square-root-of-sum-of-squares
TMSL	Tokyo Mean Sea Level
U-D dir.	Up-Down direction
1-G1	Seismic observation shed for Unit 1
5-G1	Seismic observation shed for Unit 5

LIST OF THE KARISMA BENCHMARK PARTICIPANTS

No	Name and Surname of the participant	Participating Organization	PART 1 Structure			PART 2 Equipments		
			Phase I Task 1.1	Phase II Task 1.2	Phase III Task 1.3	Task 2.1	Task 2.2	Task 2.3
1	Enrique CINAT, José Luis FREIJO Daniel Ambrosini (UNCU)	CNEA, Argentina	√				√	
2	Zhong-cheng LI	CNPDC, China	√	√				
3	Rong PAN	NNSA, China	√					
4	Mao CHEN Mingdan WANG	SNERDI-SNPTC, China	√	√	√			
5	Pentti VARPASUO	FNS, Finland	√			√	√	√
6	Fan WANG Mathieu RAMBACH	CEA, France IRSN, France	√	√	√			
7	Elie PETRE-LAZAR Salim ABOURI Frederic TURPIN	EdF, France	√	√	√			√
8	Peter RANGELOW	AREVA, Germany	√	√	√			
9	Fritz-Otto HENKEL	VGB, Germany	√	√	√	√		
10	Rainer ZINN	SPI, Germany	√	√	√			
11	A.D. ROSHAN Ajai S PISHARADY	AERB, India	√	√	√	√	√	√
12	A.K.GHOSH	BARC, India	√	√		√		
13	Giampiero ORSINI	ITER, Italy	√	√	√			
14	Chang-Hun HYUN	KINS, Republic of Korea	√	√	√		√	
15	Sang-Hoon LEE	KOPEC, Republic of Korea	√				√	√
16	Muhammad A. S. KHAN Abdul WAHID	PAEC, Pakistan					√	
17	Nicolae Zemtev	AMEC NUCLEAR, Romania						√
18	Alexey BERKOVSKY Alexander KULTSEP Oleg KIREEV	CVS, Russian Federation				√	√	√
19	Antonio JIMENEZ Antonio MORENO	CSN & IDOM, Spain	√			√		
20	Pierre WÖRNDLE Jan MOORE	HSK, Switzerland	√	√				
21	Andrew MURPHY Annie KAMMERER James J. JOHNSON (Consultant)	NRC, USA	√	√	√			
Number of team			18	13	10	6	7	6

CONTRIBUTORS TO DRAFTING AND REVIEW

Altinyollar, A.	International Atomic Energy Agency
Berkovsky, A.	Russian Federation
Gurpinar, A	Independent expert, Turkey
Henkel, F.	WOELFEL Beratende Ingenieure GmbH + Co. KG, Germany
Hyun, C.	Korea Institute of Nuclear Safety, Republic of Korea
Rangelow, P.	Areva NP GmbH, Germany
Samaddar, S.	International Atomic Energy Agency
Sollogoub, P.	Independent expert, France

Consultants Meetings

Vienna, Austria: 27-31 August 2012, 19-23 November 2012, 7-11 January 2013



IAEA

International Atomic Energy Agency

No. 23

ORDERING LOCALLY

In the following countries, IAEA priced publications may be purchased from the sources listed below, or from major local booksellers.

Orders for unpriced publications should be made directly to the IAEA. The contact details are given at the end of this list.

AUSTRALIA

DA Information Services

648 Whitehorse Road, Mitcham, VIC 3132, AUSTRALIA

Telephone: +61 3 9210 7777 • Fax: +61 3 9210 7788

Email: books@dadirect.com.au • Web site: <http://www.dadirect.com.au>

BELGIUM

Jean de Lannoy

Avenue du Roi 202, 1190 Brussels, BELGIUM

Telephone: +32 2 5384 308 • Fax: +32 2 5380 841

Email: jean.de.lannoy@euronet.be • Web site: <http://www.jean-de-lannoy.be>

CANADA

Renouf Publishing Co. Ltd.

Telephone: +1 613 745 2665 • Fax: +1 643 745 7660

5369 Canotek Road, Ottawa, ON K1J 9J3, CANADA

Email: order@renoufbooks.com • Web site: <http://www.renoufbooks.com>

Bernan Associates

4501 Forbes Blvd., Suite 200, Lanham, MD 20706-4391, USA

Telephone: +1 800 865 3457 • Fax: +1 800 865 3450

Email: orders@bernan.com • Web site: <http://www.bernan.com>

CZECH REPUBLIC

Suweco CZ, spol. S.r.o.

Klecakova 347, 180 21 Prague 9, CZECH REPUBLIC

Telephone: +420 242 459 202 • Fax: +420 242 459 203

Email: nakup@suweco.cz • Web site: <http://www.suweco.cz>

FINLAND

Akateeminen Kirjakauppa

PO Box 128 (Keskuskatu 1), 00101 Helsinki, FINLAND

Telephone: +358 9 121 41 • Fax: +358 9 121 4450

Email: akatilaus@akateeminen.com • Web site: <http://www.akateeminen.com>

FRANCE

Form-Edit

5, rue Janssen, PO Box 25, 75921 Paris CEDEX, FRANCE

Telephone: +33 1 42 01 49 49 • Fax: +33 1 42 01 90 90

Email: fabien.boucard@formedit.fr • Web site: <http://www.formedit.fr>

Lavoisier SAS

14, rue de Provigny, 94236 Cachan CEDEX, FRANCE

Telephone: +33 1 47 40 67 00 • Fax: +33 1 47 40 67 02

Email: livres@lavoisier.fr • Web site: <http://www.lavoisier.fr>

L'Appel du livre

99, rue de Charonne, 75011 Paris, FRANCE

Telephone: +33 1 43 07 50 80 • Fax: +33 1 43 07 50 80

Email: livres@appeldulivre.fr • Web site: <http://www.appeldulivre.fr>

GERMANY

Goethe Buchhandlung Teubig GmbH

Schweitzer Fachinformationen

Willstaetterstrasse 15, 40549 Duesseldorf, GERMANY

Telephone: +49 (0) 211 49 8740 • Fax: +49 (0) 211 49

Email: s.dehaan@schweitzer-online.de • Web site: <http://www.goethebuch.de/>

HUNGARY

Librotade Ltd., Book Import

PF 126, 1656 Budapest, HUNGARY

Telephone: +36 1 257 7777 • Fax: +36 1 257 7472

Email: books@librotade.hu • Web site: <http://www.librotade.hu>

INDIA

Allied Publishers Pvt. Ltd.

1st Floor, Dubash House, 15, J.N. Heredi Marg
Ballard Estate, Mumbai 400001, INDIA
Telephone: +91 22 42126969/31 • Fax: +91 22 2261 7928
Email: arjunsachdev@alliedpublishers.com • Web site: <http://www.alliedpublishers.com>

Bookwell

3/79 Nirankari, Dehli 110009, INDIA
Tel.: +91 11 2760 1283 • +91 11 27604536
Email: bkwell@nde.vsnl.net.in • Web site: <http://www.bookwellindia.com/>

ITALY

Libreria Scientifica "AEIOU"

Via Vincenzo Maria Coronelli 6, 20146 Milan, ITALY
Tel.: +39 02 48 95 45 52 • Fax: +39 02 48 95 45 48
Email: info@libreriaaeiou.eu • Web site: <http://www.libreriaaeiou.eu/>

JAPAN

Maruzen Co., Ltd.

1-9-18 Kaigan, Minato-ku, Tokyo 105-0022, JAPAN
Tel.: +81 3 6367 6047 • Fax: +81 3 6367 6160
Email: journal@maruzen.co.jp • Web site: <http://maruzen.co.jp>

NETHERLANDS

Martinus Nijhoff International

Koraalrood 50, Postbus 1853, 2700 CZ Zoetermeer, NETHERLANDS
Tel.: +31 793 684 400 • Fax: +31 793 615 698
Email: info@nijhoff.nl • Web site: <http://www.nijhoff.nl>

Swets

PO Box 26, 2300 AA Leiden
Dellaertweg 9b, 2316 WZ Leiden, NETHERLANDS
Telephone: +31 88 4679 263 • Fax: +31 88 4679 388
Email: tbeysens@nl.swets.com • Web site: www.swets.com

SLOVENIA

Cankarjeva Založba dd

Kopitarjeva 2, 1515 Ljubljana, SLOVENIA
Tel.: +386 1 432 31 44 • Fax: +386 1 230 14 35
Email: import.books@cankarjeva-z.si • Web site: http://www.mladinska.com/cankarjeva_zalozba

SPAIN

Diaz de Santos, S.A.

Librerias Bookshop • Departamento de pedidos
Calle Albasanz 2, esquina Hermanos Garcia Noblejas 21, 28037 Madrid, SPAIN
Telephone: +34 917 43 48 90
Email: compras@diazdesantos.es • Web site: <http://www.diazdesantos.es/>

UNITED KINGDOM

The Stationery Office Ltd. (TSO)

PO Box 29, Norwich, Norfolk, NR3 1PD, UNITED KINGDOM
Telephone: +44 870 600 5552
Email (orders): books.orders@tso.co.uk • (enquiries): book.enquiries@tso.co.uk • Web site: <http://www.tso.co.uk>

On-line orders:

DELTA International Ltd.

39, Alexandra Road, Addlestone, Surrey, KT15 2PQ, UNITED KINGDOM
Email: info@profbooks.com • Web site: <http://www.profbooks.com>

United Nations (UN)

300 East 42nd Street, IN-919J, New York, NY 1001, USA
Telephone: +1 212 963 8302 • Fax: +1 212 963 3489
Email: publications@un.org • Web site: <http://www.unp.un.org>

UNITED STATES OF AMERICA

Bernan Associates

4501 Forbes Blvd., Suite 200, Lanham, MD 20706-4391, USA
Tel.: +1 800 865 3457 • Fax: +1 800 865 3450
Email: orders@bernan.com • Web site: <http://www.bernan.com>

Renouf Publishing Co. Ltd.

812 Proctor Avenue, Ogdensburg, NY 13669, USA
Tel.: +800 551 7470 (toll free) • +800 568 8546 (toll free)
Email: orders@renoufbooks.com • Web site: <http://www.renoufbooks.com>

Orders for both priced and unpriced publications may be addressed directly to:

IAEA Publishing Section, Marketing and Sales Unit, International Atomic Energy Agency
Vienna International Centre, PO Box 100, 1400 Vienna, Austria
Telephone: +43 1 2600 22529 or 22488 • Fax: +43 1 2600 29302
Email: sales.publications@iaea.org • Web site: <http://www.iaea.org/books>

International Atomic Energy Agency
Vienna
ISBN 978-92-0-114913-8
ISSN 1011-4289